

WP8 Detailed Blade Modelling Implemented in Aero-Elastic load simulation

Larsen, Torben J.; Blasques, José Pedro Albergaria Amaral; Hansen, Anders Melchior; Berring, Peter

Published in:

Torsional Stiffening of Wind Turbine Blades – Mitigating leading edge damages

Publication date:

2016

Document Version

Publisher's PDF, also known as Version of record

[Link back to DTU Orbit](#)

Citation (APA):

Larsen, T. J., Blasques, J. P. A. A., Hansen, A. M., & Berring, P. (2016). WP8 Detailed Blade Modelling Implemented in Aero-Elastic load simulation. In Torsional Stiffening of Wind Turbine Blades – Mitigating leading edge damages: EUDP project 64013-0115 – Final report (pp. 80-106). Bladena.

DTU Library

Technical Information Center of Denmark

General rights

Copyright and moral rights for the publications made accessible in the public portal are retained by the authors and/or other copyright owners and it is a condition of accessing publications that users recognise and abide by the legal requirements associated with these rights.

- Users may download and print one copy of any publication from the public portal for the purpose of private study or research.
- You may not further distribute the material or use it for any profit-making activity or commercial gain
- You may freely distribute the URL identifying the publication in the public portal

If you believe that this document breaches copyright please contact us providing details, and we will remove access to the work immediately and investigate your claim.

Torsional Stiffening of Wind Turbine Blades – Mitigating leading edge damages

EUDP project 64013-0115 – Final report

Authors: Find M. Jensen, John D. Sørensen, Malcolm McGugan, Johnny Plauborg, Christian Berggreen, Andrei Buliga, Lars Damkilde, Torben J. Larsen, Lars J. Nissen, Søren H. Petersen, Rune Kirt, Pedro Muñoz de Felipe

Date: 13 September 2016



Contributors:

The following additional persons have contributed to the project and their contributions are highly appreciated.

Bladena: Mikkel Lagerbon, Signe L. Olsson, Margrethe Werk, Mathias Reding.

DTU MEK: Jacob Paamund Waldbjørn, Maurizio Sala

DTU WIND: Anders M. Hansen, Luis A. G. Seabra

AAU Esbjerg : Martin Dalgård

AAU Aalborg : Mihai Florian

Vattenfall: Rikke J. Balle

E.ON: Birgit Junker

DONG Energy: Jakob Kronborg

Total Wind Blades: Niels C. Therkildsen, Simon Sunesen

Rope Partner: Eric Stanfield

DEWI OCC: Sebastian Flores

Aeroblade: Oscar L. Vidal, Francisco M. Marato

ECC: Christian Løjtved

DIS Engineering: Steven Alfheim, Laurids E. Kirchhoff

Kirt-Thomsen: Mads Thomsen

Contents

Introduction	3
WP1 Development of New Standardization Process.....	13
WP2 Damage Assessment and Measurement Techniques	26
WP3 Field Measurement and Testing	32
WP4 Full-Scale Fatigue Testing.....	44
WP5 Sub-Component and Sub-Structure Fatigue Testing.....	45
WP6 Finite Element Simulation.....	58
WP7 Design Tools for Wind Turbine Blades	70
WP8 Detailed Blade Modelling Implemented in Aero-Elastic	80
WP9 Product Development.....	107
WP10 Market Entrance Barriers.....	111
WP11 Visualization and Logging	129
WP12 Design of new blade	147
Summary of the Project results.....	163
References.....	168
Appendix A: Additional findings and papers	169
Appendix B: Workshops and seminars during the LEX project	170
Appendix C: FEM modelling and analysis.....	171
Appendix D: Data from WP5	173
Appendix E: Data from WP5 part 2	181

Introduction

This report is the end of project reporting for the project titled “Torsional Stiffening of Wind Turbine Blades – Mitigating leading edge damages”, the project was supported by the Danish Energy Agency EUDP program “Development and Demonstration” EUDP project file number 64013-0115 also called “LEX Project”. The project was a three-year project, which started July 2013 and finished September 2016. The project was carried out in collaboration with a large group of industrial and university partners. The partners of the project are:

- Bladena
- DTU - Technical University of Denmark
- AAU - Aalborg University
- Vattenfall
- E.ON
- DONG Energy
- Total Wind Blades
- RWE
- RopePartner
- DEWI OCC
- Aeroblade
- ECC
- DIS Engineering
- Kirt-Thomsen
- Boving-Horn

The overall scope of this project was to develop, prepare for market and demonstrate an applicable method for regaining operational life of installed wind turbine blades with structural defects based on Bladena’s patented technology, the X-Stiffener.

Furthermore, the project includes the collaboration between the industry partners in particular the Nordic Blade Group pertaining to the standardization of the inspection of wind turbine blades, the “Next generation inspection reports” (NGIR). The new inspection reports form the basis for the collection of inspection reports added into the Guide2Defect database. Guide2Defect database is a large collection of inspection reports showing the numerous blade failures on existing turbines. Based on the statistical data on blade failures a cost model was generated in order to calculate the return on investment as well as time to repair on a given turbine. The prediction of failure

rates provides the potential to schedule repair based on data thus reducing cost for maintenance. In the end of the project the database has been spun out in a separate company called Guide2Defect ApS. More information can be found at www.guide2defect.com.

Motivation

Wind turbine blades are during operation exposed to high stresses which have shown after few years of operation to result in damages, visible or not from the surface. The blades are subjected to gravity forces in the edgewise direction regardless of the wind condition. The total load on the blade is comprised of the edgewise loading, mainly gravity and aerodynamic loading caused by the wind, a so called “combined loading scenario” that will force the blades to deflect as seen in Figure 1.

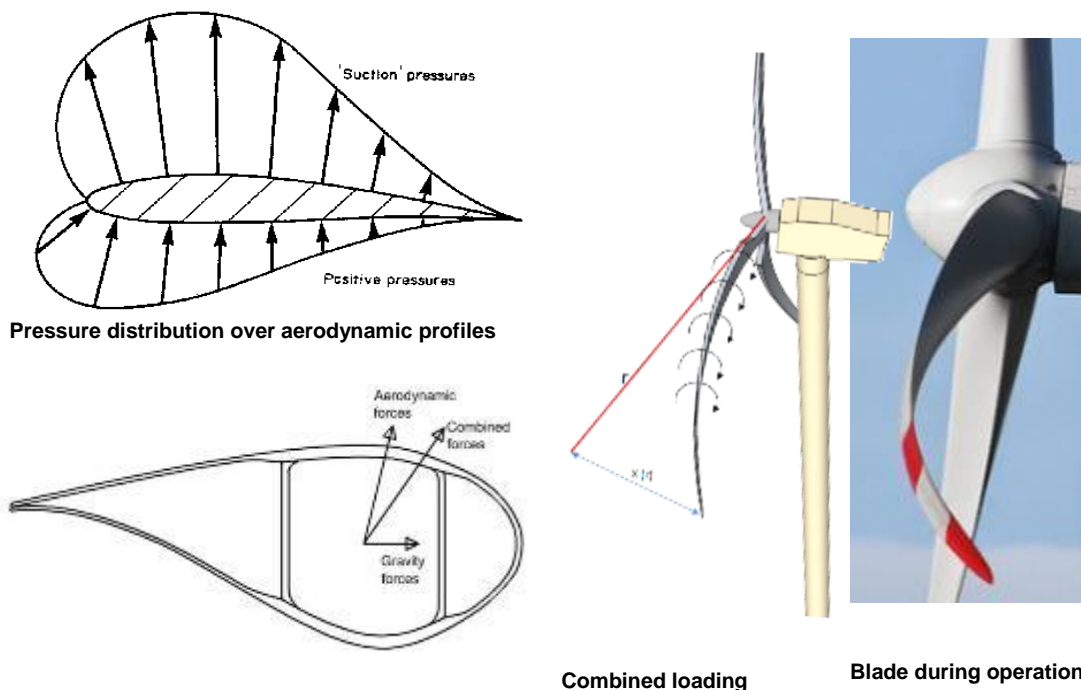


Figure 1: Combined loading scenario explained - The pressure distribution creates the aerodynamic load on the blade added to the gravity loading. The blade is therefore bent and a torsional moment due to the tip deflection is created.

The loading of the blade creates a fatigue movement that affect all adhesive bondlines within the blade. This is due to changing load direction from gravity and varying aerodynamic forces, see Figure 2.

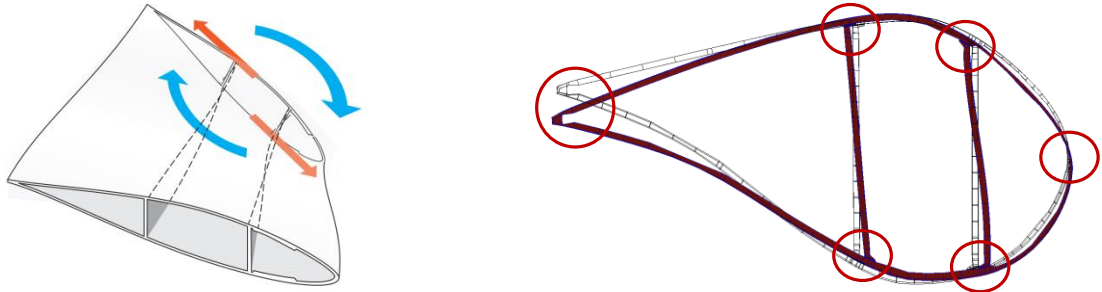


Figure 2: Sketch showing the cross-sectional shear distortion phenomenon. Left: 3D view of the blade deformation. Right: Cross-sectional shear deformation (CSSD) seen on a cross-section. Red circles point out where the adhesive bond-lines are found.

This phenomenon is of interest for large blades only (60m+) as it was shown during the project. Stiff blades and blades with a box bar construction are not prone for damages coming from the CSSD. The FEM simulations performed within the project by both Bladena and Aeroblade have confirmed that when the blades scale up, the cross-sectional shear distortion becomes important. Furthermore, on blades with a large flat-back, the magnitude of the cross-sectional shear deformation is increased due to the lack of support in the trailing edge.

Due to the high technical level, good communication within the project was essential. This process was supported by utilizing professional communication tools such as explicit 3D movies. Some of the videos available online illustrates blade behaviour during operation and the CSSD:

1. <https://youtu.be/78EUCG5A6Xs> – Cross-sectional view of FEM blade model deforming during normal operation.
2. https://youtu.be/2_vDqgm9opl – Sketch of video showing the blade behaviour during operation from a blade perspective.

There is a direct connection between the CSSD and peeling stresses in the adhesive bondlines: the higher the magnitude of the CSSD, the higher the peeling stresses are.

Since adhesive bondlines have similar bonding properties for all blade sizes, the risk for failure in the adhesive joints are significantly increased when the peeling stresses are high.

The X-Stiffener Technology

The X-Stiffener patented technology prevents the CSSD in cross-section areas by increasing the cross-sectional strength of the blade, see Figure 3.

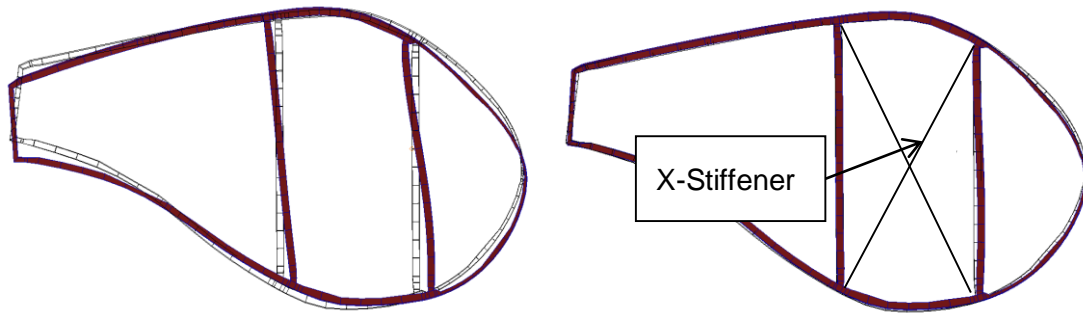


Figure 3: Effect of the X-Stiffener technology. Left: FEM blade model without reinforcements. Right: Reduction of CSSD when the X-Stiffener is installed. Plot scale factor 10. With shaded red deformed profile, with wireframe black original profile shape.

The X-Stiffener is a structural enhancement mounted between the shear webs in a diagonal direction, see Figure 4.

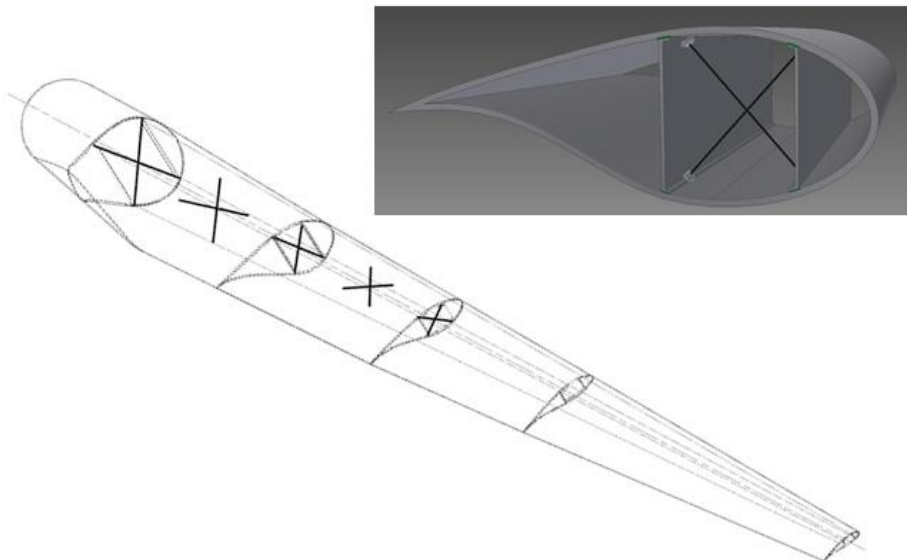


Figure 4: X-Stiffeners mounted in the 68m FEM-blade model.

The X-Stiffener can consist of either one or two diagonals, depending on the blade type.

The effect of X-Stiffener installation in a blade with traditional design or one with a flat-back design is that the CSSD magnitude reduces with app. 80-85%. This has a direct

impact on the peeling stresses in the adhesive bond-lines, leading to significant increase of the blade lifetime.

In the flat-back blade design, the X-Stiffener can be installed both in the rear and main boxes, see Figure 5.

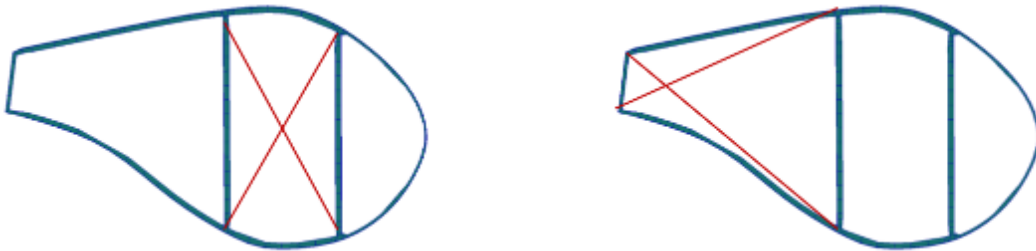


Figure 5: Possible solutions for X-Stiffeners enhancements in a flat-back blade design. Left: X-Stiffener installed in the main box. Right: X-Stiffener installed in the rear box.

Design and implementation

The X-Stiffener was further developed during the LEX project reaching a technological readiness level of five. Thus the X-Stiffener has been tested in a representative environment i.e. a large-scale blade test at DTU in Lyngby. Furthermore, several sub-component tests have been performed to verify the product design.

The development process has included several iterations between numerical studies, prototyping and testing in sub-component tests. Different versions of the product were statically tested during the development of the product.

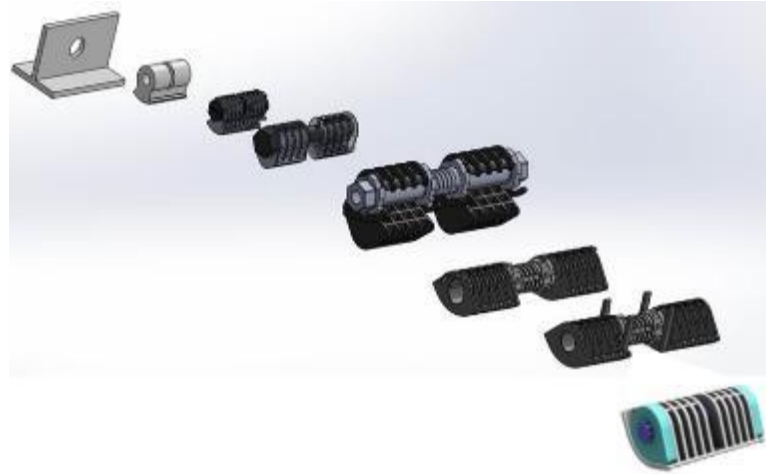


Figure 6: X-Stiffener product development

The prototype incorporates a pre-tension mechanism to ensure the part is sufficient to take the loads during turbine operation. The X-Stiffener load requirement is 1500kg. The test setup can be seen below in Figure 7.



Figure 7: Mechanical test of the X-Stiffener at DTU Mechanical.

The initial prototypes were printed, which in test was too brittle and held too low strength. The second generation prototypes were milled in ABS, which proved to take the required

load during testing. Next steps for the development is to develop an injection moulded prototype.

A large scale blade test has been performed on a SSP34m blade, and field measurements have been carried out on a V80 blade and a NM80 blade from LM-Windpower.

Communication and tools

One of the main focus within the LEX project was to create a link between academia and industry. A number of students and academic personnel was involved in meetings and workshops together with the industry partners. They were able to get an insight on the industry demands and requirements and helped them to further understand the needs of the industry. Similarly, the industry was able to get an insight where the academia is heading and what to expect in the coming years.

As a result, a handbook with terms and definitions was compiled where relevant topics are explained on an easy to understand technical level.

The LEX project challenged some of the available simulation software, E.g. within the project DTU Wind made a major improvement in the aero elastic commercially available code HAWC2 which is now capable of using a more advanced structural blade model in a time simulation, namely *super element* approach. This means that the accuracy of the simulations has increased and more reliable results can be achieved.

Furthermore, in order to cover the shortages of the available simulation tools, a method of coupling different tools together was developed. The technical team comprising of 2 universities, Danish Technical University and Aalborg University, together with Bladena has managed to summarize practical way on how to connect the tools used in the wind turbine blade design process: Aero elastic calculations and FEM structural analysis.

Bladena was trained by DTU Wind in using the HAWC2-code and simulations were carried out on a case study.

NGIR

Next Generation Inspection Reports (NGIR) is a number of documents covering instructions on how to do blade inspections and classify blade damages into categories. NGIR has focus on how to document both inspected damages and repair processes in order to be able to ask a standardized minimum requirement from service companies, especially in regard to documenting findings and reporting in a uniform way.

NGIR is working in close collaboration with Guide2Defects to make the transition of data from the field, to inspection reports and then to the Guide2Defect database as smooth as possible. The damages found and documented in NGIR will be a foundation for the statistical data in the Guide2Defect database.

Description of project

The project was organized in 12 different work packages; the scope of each of the work packages is briefly described in the following. Each of the sections in the report presents an extensive summary of the work performed in each of the work packages.

WP1 - Development of New Standardization Process: In this work package the existing standardization procedure will be reviewed with focus on recommendations / rules for avoiding leading edge cracks. A new standardization process will be proposed focusing on leading edge cracks.

WP2 - Damage Assessment and Measurement Techniques: This work package coordinate the application of various inspection and monitoring technologies to provide adequate detail regarding the structural response and damage condition around the leading edge panels during operation, during full-scale testing, and when undergoing dynamic fatigue sub-component testing. This work package will also deliver a structural assessment of the wind turbine blades and structural sections made available to the consortium for testing.

WP3 - Field Measurement and Testing: This work package covers tests of a Vestas 2.0 MW and a NM80 wind turbine both owned by Vattenfall. The full-scale tests performed in this project will include comprehensive monitoring technology to measure local and global deformation during operation. By using advanced measurement equipment, torsional and bending deformation can be predicted in blades both with and without the X-cross retrofit reinforcements.

WP4 - Full-Scale Fatigue Testing: The purpose of this work package was to investigate the fatigue resistance of the blade using an approach which is different from conventional fatigue testing of wind turbine blades. The conventional way of fatigue testing of blades is to calculate the equivalent 20 years load for the blade in the flap- and edgewise directions. The blade is tested with these loads and if the blade does not show any significant damage the blade is approved for use on wind turbines. This work package is closed and the task is taken over by DTU Mech in agreement with EUDP.

WP5 – Sub-component and sub-structure fatigue testing: The objective of this part of the work were to build a custom-made test rig in order to perform static and fatigue tests on 15m test blade section. These tests had to prove the benefits obtainable in

terms of structural resistance to torsional loading, anchoring the specimen with X-Stiffeners inside the blade girder box.

WP6 - Finite Element Simulation: The function of this work package has several purpose: (i) to achieve a thorough understanding of the importance of the twisting loads caused by the combination of the flapwise bending and edgewise loading, (ii) support the product development in WP9 and (iii) the effect of including dampers. Furthermore, WP6 will heavily support WP5.

WP7 - Design Tools for Wind Turbine Blades: The purpose of this work package is to develop a simplified method for analysis of the wind turbine blades including the so-called “cross-sectional shear distortion” effect and the stresses from local loading (e.g. wind-pressure). The method will be based on an extended beam theory which will contrary to the standard beam theory be able to include deformations of the cross-section in its own plane.

WP8 - WP8 Detailed Blade Modelling Implemented in Aero-Elastic Analyses: The purpose of this WP is to enable a direct coupling between detailed FEM modelling of wind turbine blades and the aero elastic simulations using the code HAWC2 for this 2 advanced methods will be developed. Furthermore, using the aero elastic tool HAWC2 load simulations can be performed early in the project and used as direct input for WP5, 6 and 7.

WP9 – Product development: The purpose of this work package is to develop cost efficient, relevant and marketable products based on the underlying patented technologies and the findings and conclusion during the present project. Two prototypes are planned in this WP one X-Stiffener without damper and one with.

WP10 - Market Entrance Barriers: The introduction of the developed retrofit stiffener and later the retrofit damper to the market place will be very challenging, predominantly because both solutions will be implemented inside the blade up-tower in a non-optimum installation situation and will be attached to the load carrying spar – a very critical component of the blade structure. A lot of relevant concerns and reservations among the future customers must thus be expected and need to be answered in a qualified way.

WP11 - Visualization and Logging: To meet the challenges of having various partners with different backgrounds, using different technical nomenclatures and terms, and having different focus areas this work package will add a new “tool” to the development process by creating a visual platform for logging of ideas, conclusions and challenges.

WP12 - Design of a New Blade: This WP deals with the development of two numerical blade models, a 39m and 60m one, where the technology will be implemented. Furthermore, the design will be carried out using a new design criteria agreed between Aeroblade and Bladena.

WP1 Development of New Standardization Process

WP responsible: John D. Sørensen - Aalborg University

The purpose of this work package can be divided into two main areas:

1. Review of existing standardization procedures with focus on leading edge fatigue cracks and recommendations / rules for avoiding leading edge cracks.
2. Development of a new standardization process focusing on leading edge cracks. The process must include a practical approach which can be implemented as an add-on to the recent certification procedure.

In addition to these main areas focus is also on cost models related to the costs of blade defects, inspections, repair and maintenance needed as a consequence of the (limited) requirements in the standards.

The background for this work package can be described by the following questions:

- Leading blade manufacturers claim a life time of 20-25 years for blades. However, wind turbine owners' experiences conclude that there are problems after only 5 years of operation. How should you as an owner proceed in order to have a fair estimation?
- Where in the Life Cycle Cost (LCC) curve lays the profit for the owner and the manufacturer?
- Which uncertainties/risks do we have in the LCC models and how do we identify, mitigate and manage the risks?
- If the estimate for blade's life differs with 10 years, depending on whether you ask the manufacturer or operator – how could we create a LCC?
- How can the blade experts who are trying to find the root-cause know whether it is due to poor manufacturing, poor design or too high loads under operation? Is there a procedure developed for this?

A generic cost model is developed which is linked to the information in the Guide 2 Defect (G2D) database used to formulate a damage model with 6 categories. A Markov model is used to represent the uncertainties. This model can be applied to answer the above basic questions.

1.1 Standardization

A number of meetings have been arranged with wind turbine owners (incl. Vattenfall, E.ON, DONG Energy, Statkraft and Arise), standardization bodies (incl. DNV-GL, DEWI-OCC) and research institutes (incl. Fraunhofer). In June 2015 a standardization and test

seminar was held with 24 companies attending representing the whole value chain. See also Appendix B:.

The industry is facing a huge challenge regarding O&M costs on blades in the future and especially for offshore installed turbines. The aim of the meetings was to identify the 'challenges' and learn from the experiences, and then to make the necessary improvements, in order to avoid damages which could have been avoided by taking preliminary actions such as additional testing, simulations etc.

Current standards for the design and testing of wind turbine blades require the assessment through a series of safety factors to knock down the material properties in order to compensate for the uncertainties related to the fabrication and degradation of composites, in combination with safety factors that increase the loads generated by the wind in order to compensate for the related uncertainties. Under this scheme the rotor blade is evaluated in a combination of extreme structural weakness and extreme external loading with the main objective to guarantee structural integrity and safety during the life span of the wind turbine.

In the wind industry, certification business plays a very important role since most wind turbines and its components are designed and manufactured to meet certain level of reliability. This means that the wind turbines shall be design to a minimum lifetime of 20 years. In the revision of the IEC 61400-1 ed.4 standard which at present is available in a CD version, a nominal target reliability level is indicated corresponding to an annual reliability index of 3.3 which means an annual probability of failure of 5×10^{-4} , among other requirements. It is through the scheme of type and component certification that an independent third party evaluates that these requirements are fulfilled and that the wind turbine is safe to operate during its design lifetime. This evaluation includes the design assessment of most components and systems, tests at coupon and component level as well as prototype testing and manufacturing evaluations. A wind turbine with a type certificate proves that the independent third party evaluation has been successfully fulfilled and meets the requirements established by the different recognized guidelines.

Wind Turbine Owners (WTO) in Scandinavia have established small blade expert groups, since it has been realised that blades have more issues than expected by taking into account that in general the blades are designed to last for 20-25 years. Furthermore, blade specialists from E.ON, Vattenfall, Dong Energy, Statkraft and Arise have in 2013 established the Blade ERFA group, where technical topics are discussed. They are interested to know more about the future possibilities for certification of blades, testing and future requirements which could be set up in order to reduce repair cost in the future. This growth has now increased to 20 European WTOs. The founding Nordic group is still close connected and the group name is renamed Nordic Blade Group. Bladena has

been asked by the WTO's whether it could facilitate meetings with DNV GL, DEWI-OCC and Fraunhofer. Bladena (and others) trust that many of the failures which are observed today could have been avoided by having better design and test criteria's. Often the observed failures are due to errors in the manufacturing process. However, when dealing with large cheap composite structures, there must be room that allows for some tolerances. It is therefore recommended that a scheme for this should be developed. In general the blades should be designed with more damage tolerance in mind, meaning that for instance the critical stresses should be kept "away" from the bond lines or the tension forces transverse to the fibres should be minimized.

Further, the aim of the meetings is to share views on the future challenges the wind turbine owners have on their blades. The overall purpose is to minimize the CoE and not only the initial cost price for buying the wind turbine (blades).

The main obstacle to overcome for the introduction of additional evaluations, would be the documentation and traceability linked to the type certification. Modifications in the design evaluation of the blade and/or testing evaluation reports could lead to the invalidation of current type certificates as conformity statements are usually linked to a specific certification report, where the scope of the evaluation is defined, the results are documented and it is stated whether the wind turbine/component fulfils the defined requirements. If the results of the additional evaluations were to be documented in additional evaluation reports, the same problem would occur as these would need to be documented in conformity statements and an update to the type certification would be needed, becoming this process very costly for stakeholders involved.

According to the IEC 61400-22 standard, type certification scheme is as described in Figure 8 below:

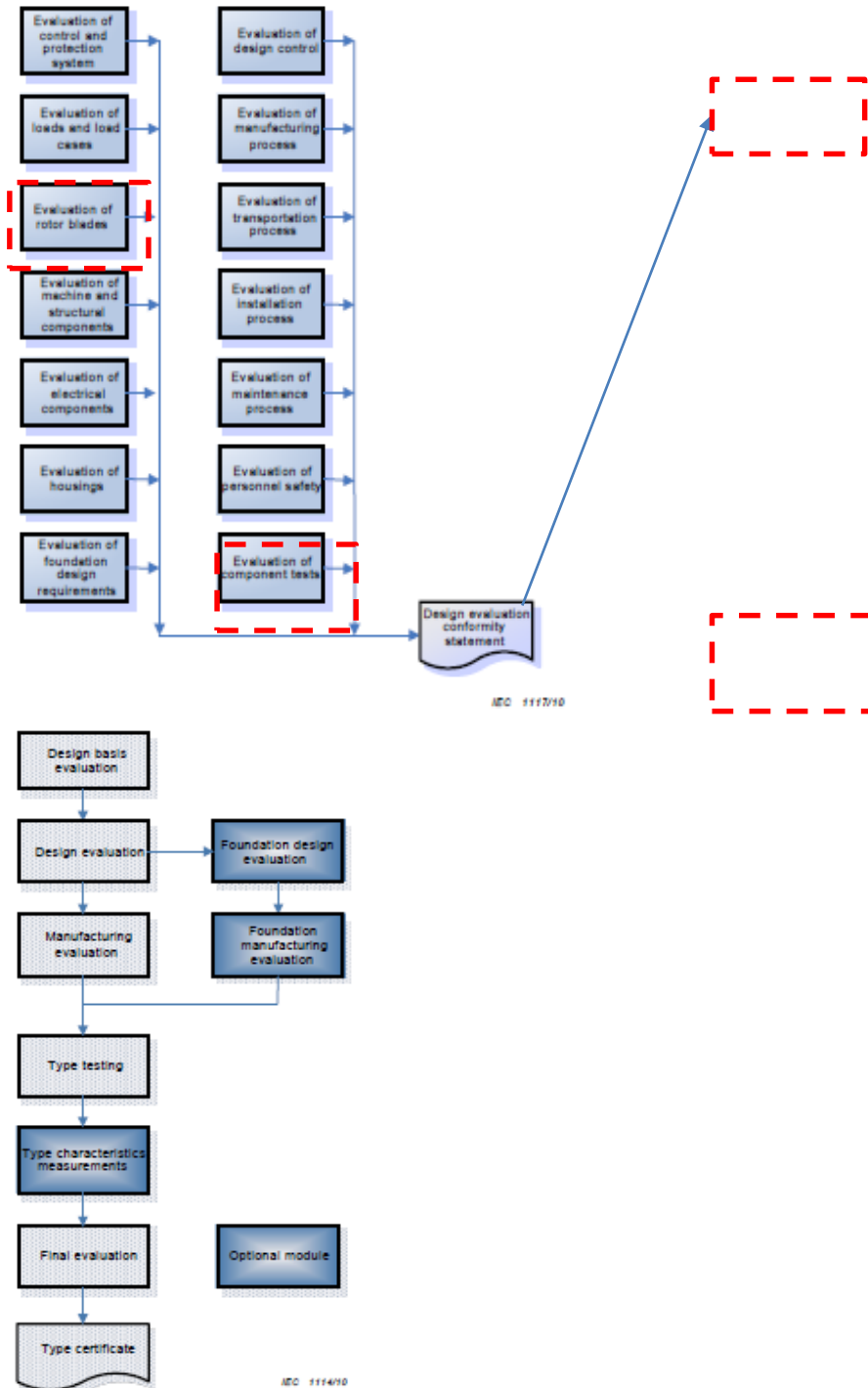


Figure 8: Type certification scheme

For wind turbine manufactures this approach would lead to an important effort since type certified wind turbines would then require to be updated in order to include the additional evaluation criteria.

DEWI-OCC has participated since the start of this project, mainly contributing with inputs regarding certification but has also independently carried out non-linear FEM analysis in order to understand and document the additional criteria proposed in this project, from the certification point of view. As a solution, DEWI-OCC proposed the “DEWI-OCC +” concept which would allow add-on additional criteria to be included without compromising the validity of existing type certificates.

These additional evaluation criteria could then be treated as “site-specific” (as defined in the IEC 61400-22) and would then leave space to submit and document the additional evaluations carried out. As a result, these additional criteria would be added in the certification of wind turbines/blades in a way that already valid component and type certificates would not be affected by these additional requirements.

The inclusion of the before mentioned failure modes represents a step towards the analysis of wind turbine blades based on local deformation and distortion which could be a cause, among others, for the functional failures seen by wind farm operators that lead to increased OPEX. It represents a step into certification schemes that respond to the immediate industry feedback and that not only focuses on structural integrity and safety, but also on parameters that are relevant to certain stake holders in the industry.

The additional criteria should include e.g. combined load scenarios, non-linear FEM, peeling test of bond lines as an add-on to existing standards and guidelines for wind turbine blades.

Bladena suggests a similar add-on to the existing standards the additional criteria are listed below:

1. **Combination of loads**
 - 1a) *Combination of edge-and flapwise loads are analyzed in FEM.*
 - 1b) *Combination of edge- and flapwise loads are tested by using a blade rotation method. Traditionally load clamps are replaced by anchor plates.*
 - 1c) *A torsional load case is tested that addresses the torsional stiffness and it is used to validate/calibrate the FEM-model.*
2. **Non-linear FEM + Trv. SG-measurements on the spar caps**
3. **Focus on peeling in bond lines**
 - 3a) *Dynamic full-scale test with combined edge-and flapwise loads and*

without traditionally load clamps which prevent breathing/pumping.

3b) Sub component testing – Mode 1 (Peeling). It is important that the quality of the adhesive and the adhesion is representative.

4. **Parked load scenarios and flutter with correct twisting stiffness represented**

In order to have the right torsional stiffness, a simple torsional test should be performed, simply by adding a torsional load in the tip region. The torsional twist which is measured is used to validate and calibrate the 3D-FE-model. When this is done the cross-sectional stiffness can be extracted and used in the load/stability 3D beam analyses.

1.2 Cost modelling in relation to Operation & Maintenance

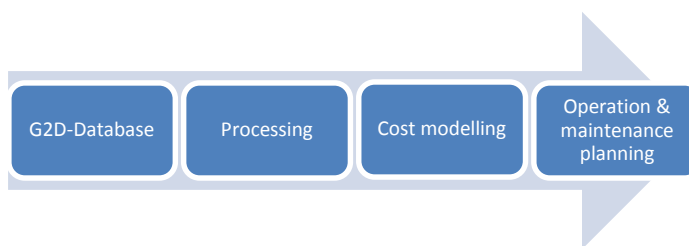


Figure 9: Cost modelling related to G2D

Generic cost models have been developed to be used for cost optimal decisions on planning of inspections and operation & maintenance for blades with defects. The cost models are connected to the statistics to be obtained on blade defects and failures from the Guide to Defect (G2D) database being developed in Task 10.4. The aim is to couple the cost models to the effect of improved requirements for standardization, see Figure 9: Cost modelling related to G2D.

The failure statistics in G2D contain information on failure rates and defects related to failure modes such as:

- Erosion on shells
- Cracking on main spar
- Debonding of glue joints
- Delamination of composite fiber
- Cracking of composite fiber
- Lightning

Further, the information in G2D is applied to model the damage accumulation and related uncertainty for e.g. leading edge cracks. The following description follows the papers:

- Mihai Florian & John Dalsgaard Sørensen: Case study for impact of D-strings on levelised cost of energy for offshore wind turbine blades. Submitted to the journal IJOPE, 2016.
- Mihai Florian & John Dalsgaard Sørensen: Risk-based planning of O&M for wind turbines using physics of failure models. International Journal of Prognostics and Health Management, 2016.
- Florian, M. & J.D. Sørensen: Wind Turbine Blade Life-Time Assessment Model for Preventive Planning of Operation and Maintenance. Journal of Marine Science and Engineering, Vol. 3, 2015, pp.1027-1040.

With the rapid growth of the offshore wind industry over the past two decade, and the implicit growth in the size of wind turbines, Operation & Maintenance (O&M) has become a major focus point in the attempt to lower cost of wind energy to market competitive prices. It is in general estimated that O&M operations account for around 25-30 [%] of the levelised cost of energy.

Aside from perfecting maintenance strategies and optimizing the placement of maintenance effort, several research projects and industry development are focusing on improving the structural performance of the wind turbine blades in an attempt to lower failure frequencies. One such example is the D-string concept, developed to stop edgewise crack development in the trailing edge for existing and future installed wind turbines. As shown in Figure 10, [11], this type of failure can account for 35% of blade defects, thus having considerable impact on maintenance cost.

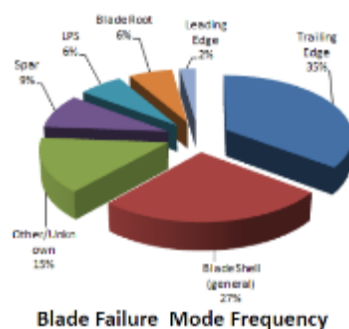


Figure 10: Blade defects

In the following a general maintenance model is set up using condition based maintenance for blades and corrective maintenance for the rest of the components in a

wind farm. A degradation model is set up for the blades, where the failure frequency output is dependent, among others, on the installation of the D-string device. A discrete event simulator is then used to estimate cost of energy with and without installing D-strings.

Damage modelling

Where preventive maintenance is concerned, current practices in maintenance planning imply performing regular inspections either at fixed time intervals, or depending on the result of the last inspection. Based on the inspection result, a number of repairs can be called for, making it necessary for a classification of the size of damage, as shown in Figure 11.

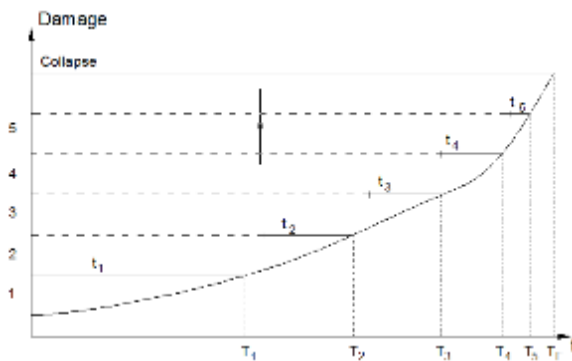


Figure 11: Damage growth with time, t.

It is important to mention that degradation can take a number of forms in the case of composite components like blades, most notably cracking on the shell and spar, erosion of the outer skin, delamination of the carbon fiber sheets or debonding in various joints. Due to a lack of information on the failure frequencies for each type of degradation, the model is considered to cover all types of damage.

A Markov state model is built, where the degradation process is divided in a finite number of states, as illustrated in Figure 12.

A state “ l ” is defined by a corresponding damage level and the amount of time T_i that the system spends in it. T_i is randomly generated using a transition rate.

The following assumptions are implied by using the Markov model:

- A blade starts its lifetime with 100% probability of having no defect, thus introducing a Category 0

- A defect goes consecutively through each category, with no possibility of jumping more than 1 state
- Defects cannot go to previous states without intervention/repair

The model is memoryless, implying that a probability to jump to a higher state is not influenced by the previous state

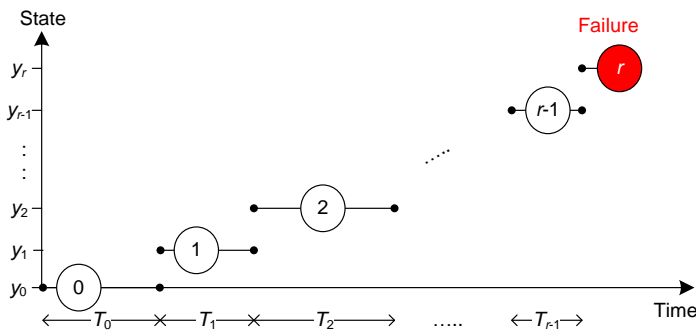


Figure 12: Markov state model for damage growth.

Table 1: Damage categories – example.

State / Category	Damage
1	No damage
2	Cosmetic
3	Minor damage, below tear and wear
4	Minor damage, above tear and wear
5	Serious damage
6	Critical damage / failure

The Markov model is calibrated to data in the G2D database using 6 states, see Table 1. The target number of observations for each state is calculated based on example annual failure frequencies from G2D, see example in Table 2.

Table 2: Annual failure rates

State	1	2	3	4	5	6
Markov model [%]	4.01	12.92	20.08	9.81	0.91	0.57
G2D [%]	4	13	20	10	0.9	0.6

In order to illustrate the application of the Markov damage model an application to an offshore wind farm is considered. The maintenance strategy applied in the following is partly based on corrective and partly based on condition based maintenance planning. Condition based maintenance is applied for the blade, implying a regular inspection

scheduling and a decision model for repair/maintenance, while corrective maintenance is used for all other wind turbine components.

Table 3: Blade maintenance model.

Category	Annual Rate [%]	Cost of Repair [€]	Repair Down Time [hours]	Technicians	Vessel	Continue operation	Wind limit [m/s]	Priority
1	4	2000	6	3	CTV	Yes	-	11
2	13	4000	10	3	CTV	Yes	-	10
3	20	10000	24	3	CTV	Yes	8	9
4	10	15000	40	3	CTV	Yes	8	8
5	0.9	25000	80	6	CTV	No	8	7
6	0.6	400000	80	6	HLV	No	-	2
Inspection	1	1000	6	3	CTV	Yes	-	6
D-String install	-	15000	12	3	CTV	Yes	12	12

Table 3 shows the activities that are planned for blade maintenance, along with the required resources as function of blade damage. Aside from repair activities, inspections and installation of D-strings are considered part of the blade maintenance model. It is important to note that the failure rates given in Table 2 are prior to installation of the D-string, which is considered to mitigate 20% of all developing damage.

Each of the 6 damage states has specific characteristics in terms of cost, time and work force (vessels and technicians). The policy is to perform the repairs as soon as possible, given that the weather conditions are favourable and the appropriate vessel and technicians are available. Depending on the required vessel, a maximum wave/wind limit is included, aside from the wind limit given in Table 3. Specifications on vessels are shown in Table 4.

In case there are not sufficient vessels to carry out all necessary actions at the same time, a priority system is used, as shown in Table 3. The order has been chosen so that the downtime is reduced, hence turbines that need to be taken out of operation due to failure or high damage will be prioritized.

Table 4: Vessels.

	Crew Transfer Vessel (CTV)	Heavy-Lift Vessel (HLV)
Number	8	1
Limiting weather criteria	Wave 1.5 [m]	Wind / Wave 20 [m/s] / 2[m]
Mobilisation time	0	30 [days]
Mobilisation cost	0	250.000 [€]

Speed	20 [knots]	11 [knots]
Technician capacity	12	100
Day rate	1000 [€]	100000 [€]
Maximum offshore time	1 shift	Unlimited

Table 5 shows the model for general maintenance. This model is partly based on [12]. The occurring frequency is given in number of failures per turbine per year, and is meant to cover failures for all components other than blades. Weather limitations are only dependent on vessels, and similar to the blade maintenance model, repairs are made as soon as possible, with respect to weather conditions, work force availability and priority order.

It is considered that technicians work in one daily 12 hour shift, from 07:00AM until 19:00PM. An exception is when replacement activities are carried out. In this case, to make maximum use of the heavy lift vessel, two 12 hour shifts will be used.

Table 5: General maintenance.

Category	Annual Frequency	Cost of Repair [€]	Repair Down Time [hours]	Technicians	Vessel	Continue operation	Priority
Minor repair	2	20000	6	3	CTV	No	3
Major repair	0.6	180000	18	3	CTV	No	4
Major replacement	0.1	1000000	48	6	HLV	No	1
Annual service	1	140000	35	3	CTV	Yes	5

Finally, for the cost modelling to be applied in connection with inspections probabilities of detections are needed, see Table 6.

Table 6: Probability of detection by blade inspections.

State	1	2	3	4	5
Probability of detection	0.4	0.8	0.9	0.98	1

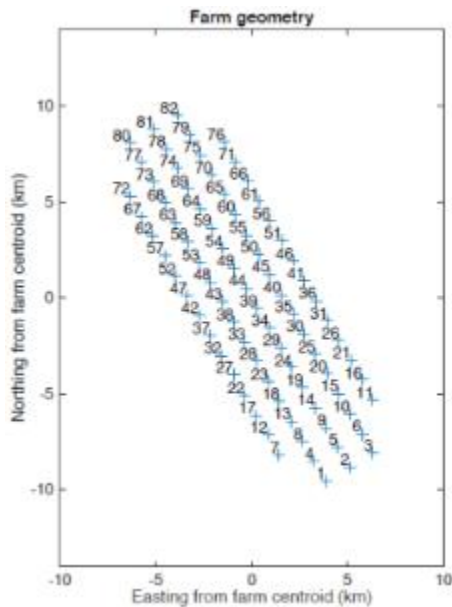


Figure 13: NORCOWE wind farm layout.

For optimal decision making, a simulation based approach is used where lifetime (25 years) simulations are performed. For illustration the NORCOWE wind farm layout [13] is used, with the specification that 3MW turbines are considered, see Figure 13.

A base case inspection plan is set at the beginning of the simulation. Inspections are carried out at the appropriate moment, when resources are available according to the priority order. Further, it is considered that installation of the D-strings can be scheduled at a pre-decided point in the wind farm lifetime. When the installation is finished, it is for illustration assumed that 20% of the damage development in the blades will be stopped. It is assumed that the D-strings are installed in year 5. Figure 14 illustrates the expected cumulative expenses for the blade maintenance.

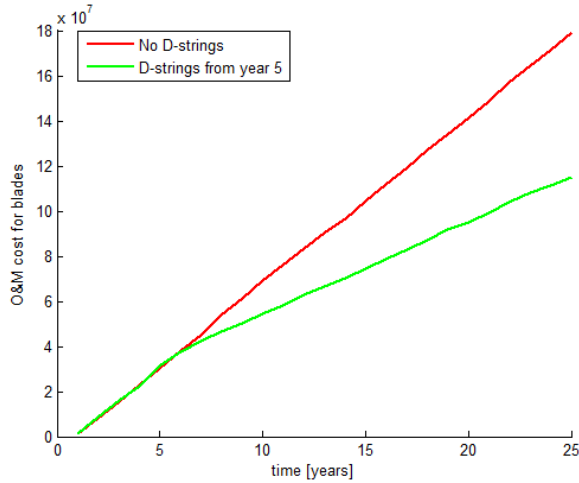


Figure 14: Mean cumulative cost for blade maintenance with and without D-strings installed.

The investment cost for installing the strings is seen to result in an increase of the accumulated maintenance cost at year 5, followed by a reduction of the slope due to the blade defect mitigating effect of the D-strings. Given that installation of the strings takes on average 4 months to complete, the return of investment is obtained at approximately year 6. Further, the results show that the downtime is also lowered with 5%. This, together with the reduction in OPEX, translates into a reduction of LCoE by around 1.6% in this illustrative case study.

More results in the above papers.

WP2 Damage Assessment and Measurement Techniques

WP responsible: Malcolm McGugan - Technical University of Denmark Wind Energy Department

Summary of WP2.2 - Instrumentation for measurement of operational response

Purpose

In this task all the WP2 partners agreed on the details of an instrumentation plan for measuring the structural response of an operational wind turbine. DTU Wind Energy assembled and tested the required hardware and developed the instrumentation plan with Total Wind Blades who were responsible for the on-site work.

The following on-site measurements were completed at Østerbyvej 70, Tjærborg.

V80 turbine blade internal beam shear (20 sets)	16-19 Feb 2014
NM80 turbine blade internal beam shear (8 sets)	16-18 Mar 2015
NM80 rotor imbalance (2 nacelle mounted accelerometers)	Mar-Jul 2015
NM80 turbine blade root strain (8 fibre Bragg gratings)	Mar-Oct 2015

Figure 15: Operational turbine measurements taken in WP2.2.

The initial idea behind the WP2.2 measurements was to determine the effect that reinforcing the blade would have on the beam shear during operation. But little to no shear displacement was measured on either the V80 or NM80 blades in their normal condition. For this reason, the instrumentation task was re-scoped and came to include an investigation of a possible rotor imbalance, and a demonstration of a commercially available fibre optic root strain measurement system.

Conclusions

The WINDAQ blade shear measurements between radius R5m-R18,5m on the V80 and R6m-R15m on the NM80 showed little to no displacement (+/- 1mm) during normal operation in wind speeds of between 10 and 13 ms⁻¹.

The NACELLE accelerometer measurements on the NM80 turbine uncovered a rotor imbalance of around 130kg and an aerodynamic asymmetry on blade number 3.

The WindMETER system installed on the NM80 turbine provided details of the complex, dynamic strain field active in the root section of the blade. Dynamic strain change at the

root section (R5.0m) during normal operation was a relatively symmetric 0.04% for the longitudinal strain sensors at the pressure and suction faces. For the longitudinal strain sensors at the leading and trailing edges the response was less symmetric and included dynamic strain changes of up to 0,1% and 0,05% respectively, although these were rare peaks and ranges of 0.03% and 0.01% were standard. All the circumferential root strain gauges measured a low and symmetric dynamic strain range of between 0.01% and 0.03%.

Measurement reports for WP2.2

- *“Investigation of rotor imbalance on a NEG-Micon 80 Wind Turbine”*, Christos Galianos and Torben Juul Larsen, DTU Wind Energy Reprot-I-0386, October 2015
- *“V80 Measurement report LEX EUDP”*, Malcolm McGugan, DTU Wind Energy Report-I-0442, January 2016
- *“NM80 Measurement report LEX EUDP”*, Malcolm McGugan, DTU Wind Energy Report-I-0443, January 2016

These reports describe the planning and implementation of the V80 and NM80 instrumentations; including the discussions regarding re-scoping the on-turbine measurement effort, the details of the hardware acquisition and specifications, the on-site instrumentation procedures and a presentation of the data.

Description of the WINDAQ system

The WINDAQ hub system consisted of a robust computer logger, a P2858 DAU (Data Acquisition Unit), a Strain gauge amplifier, a power unit, ten displacement (posiwire) sensors and mounting fittings, one inclinometer, and assorted USB memory sticks, cabling, attachment equipment, and a portable screen and keyboard for system set-up.

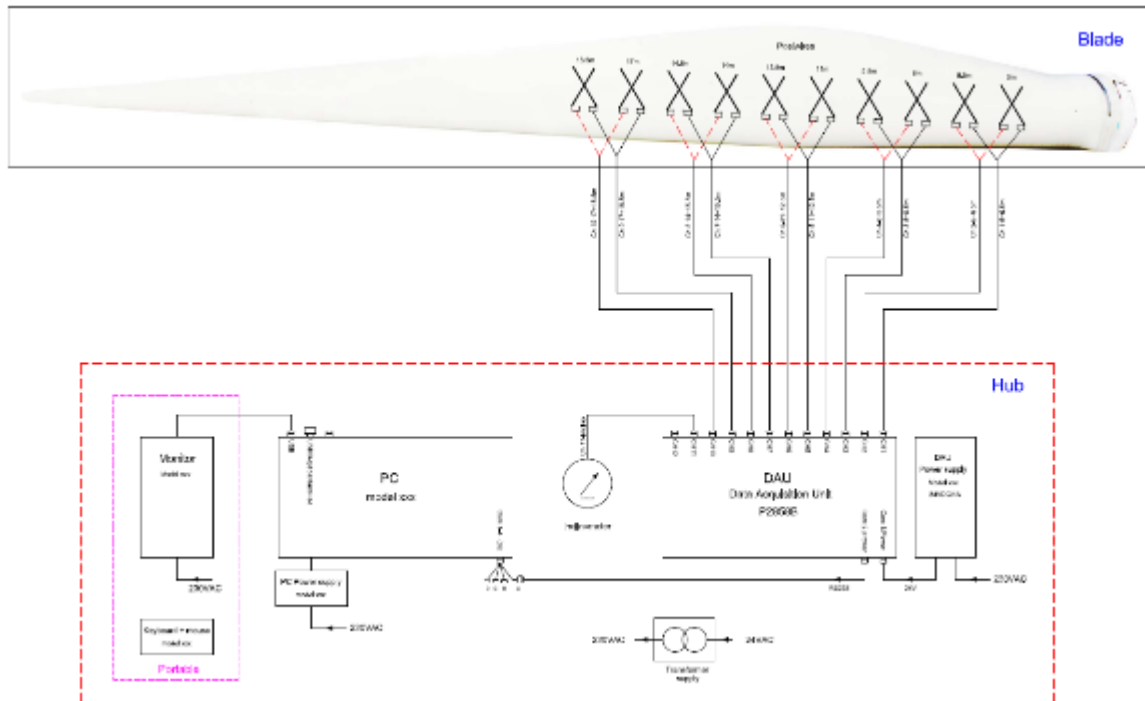


Figure 16: V80 instrumentation plan for the WINDAQ (posiwire) system.

The acquisition, control, and power units (plus the inclinometer) were mounted on a plate attached in the rotor hub. Cabling was installed from here into the blade where the posiwire pairs measured from corner to corner at the agreed blade beam radii.

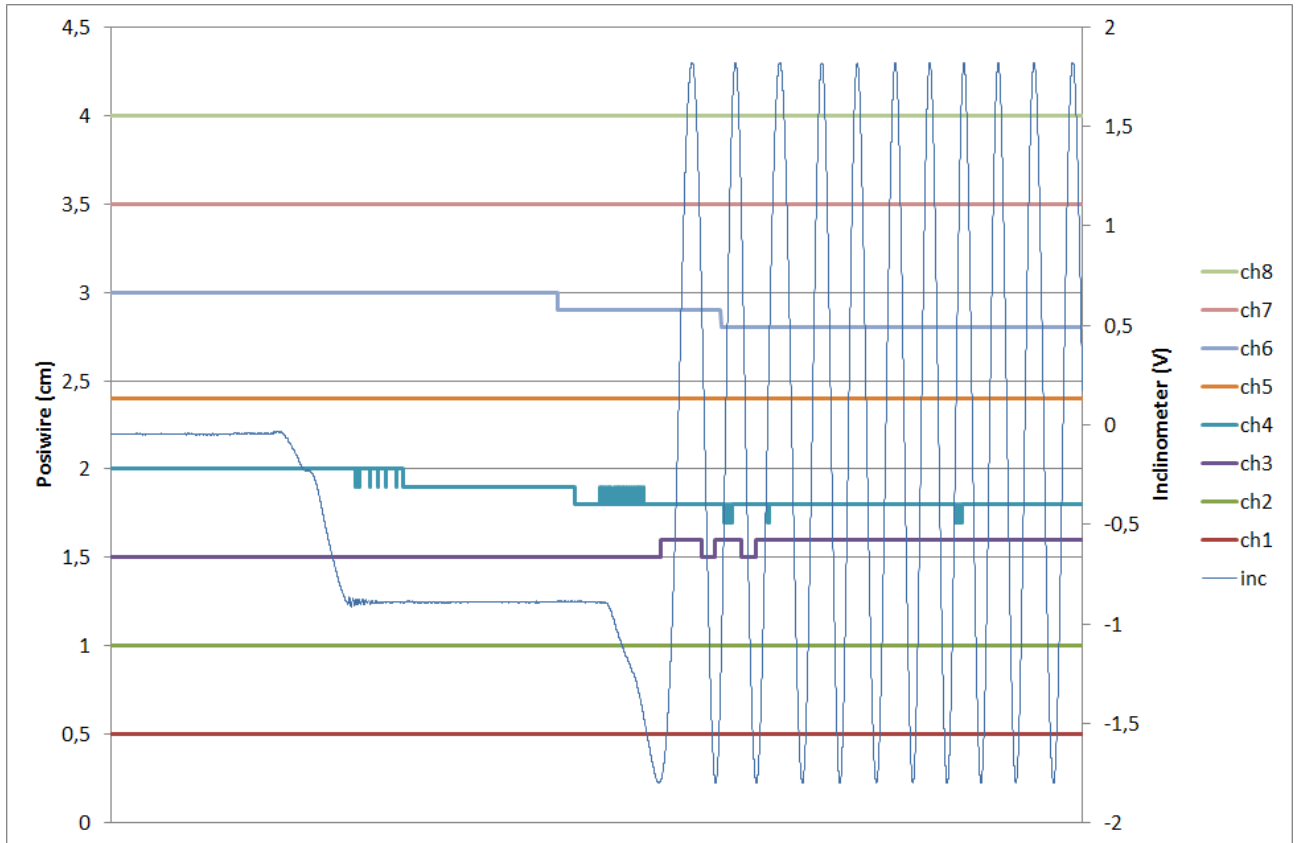


Figure 17: WINDAQ data output from NM80 showing inclinometer response as the rotor is held with the instrumented blade at one horizontal position, then round to the next horizontal and held again, before being put into a slow autorun rotation

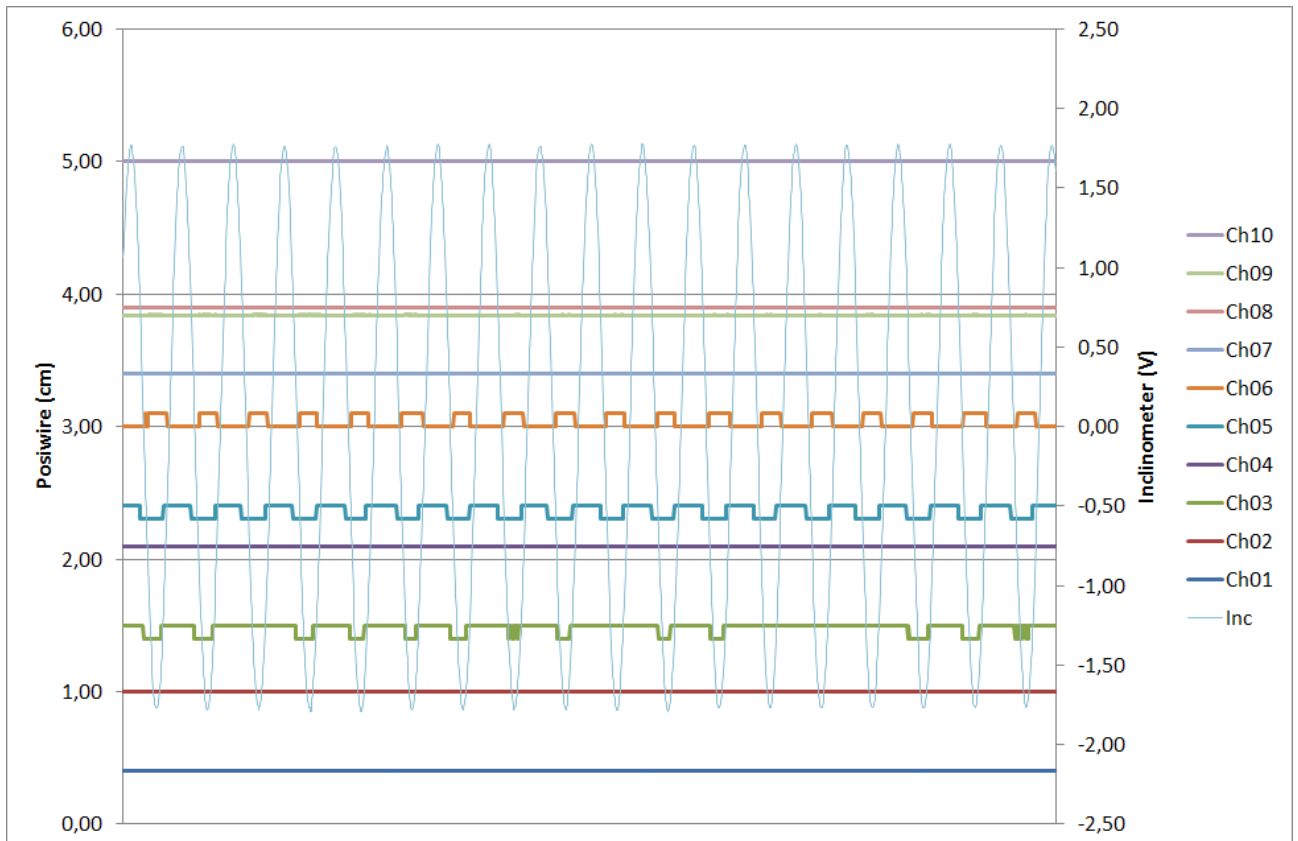


Figure 18: WINDAQ data output from V80 showing minimal response from the posiwire shear displacement channels during full operation.

Description of the NACELLE system

The NACELLE system consisted of a pair of triaxial accelerometers installed in the NM80 nacelle (one on the tower centre line, and the second 472cm behind) with an azimuth rotor position providing 10-minute time series data. Fast Fourier Transform analysis was used to identify peaks in acceleration spectra and extract the rotor imbalance information.

Description of the WindMETER system

The WindMETER system is a commercial product from HBM Fibersensing and consisted of a hub mounted data acquisition system and two fibre optic cables going into the root of the blade (R5.0m) and measuring point strain at 0°, 90°, 180°, and 270° around the root section in the longitudinal and circumferential directions. A data router/receiver system was used to wirelessly transmit the WindMETER data from the hub to a data acquisition laptop running in the nacelle.



Figure 19: The WindMETER system mounted centrally in the hub with the power unit on the left, and data transmitter on the right.

Corrected strain (%) maximum range		
Long	Press	0,05 aveage about 0,04
	Trail	0,10 (rare peaks, av approx. 0,03)
	Suct	0,06 average about 0,04
	Lead	0,05 (rare peaks, av approx. 0,01)
Circ	Press	0,02
	Trail	0,01
	Suct	0,03
	Lead	0,02

Figure 20: Compiled data from the WindMETER system showing maximum dynamic strain range recorded during the instrumentation period.

WP3 Field Measurement and Testing

WP responsible: Johnny Plauborg – Total Wind Blades

Field test on Vestas V80 with 39m blades

Description of work

1. Work info
2. Turbine info
3. Access to turbine, Nacelle, Hub and Blade.
4. Measuring positions
5. Mounting instruments
6. Running the test with posiwires along the spar, to measure deformation
7. Data collected on memory card and delivered to DTU wind energy

Work info

In 2013/2014 we have had several work and planning meetings in Brande, with Bladena and DTU wind energy. To prepare us, as much as possible, for Field and measurement test in Tjæreborg. We have extra test blades lying in Brande, so everything is tried and tested, before the real blade test, at the turbine. Week 8, 2014 we made field and measurement test in Tjæreborg, with Bladena and DTU wind energy.

Turbine info

The field test and measuring was done in Tjæreborg, on a V80 Vestas turbine, and the blades is 39M. Vestas blade.

Turbine owner is Vattenfall.



Figure 21. Vestas test turbine

Access to Turbine, Nacelle, Hub and Blade

Access to the turbine bottom platform. For going to the Nacelle, there is a long ladder or service lift as you can see on the picture.



Figure 22. entrance to the turbine and service lift

The working area in the nacelle for preparation of the instruments before going to the hub and blade.



Figure 23. Working area in the nacelle.

After the rotor has been locked, the turbine is ready for accessing Hub and Blades. The red line shows the difficult path from Nacelle to hub.

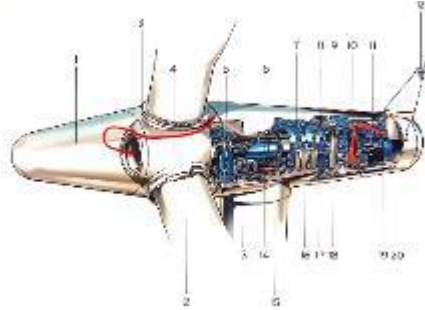


Figure 24. entrance path from the nacelle to the hub.

Finally, the entrance to the blade where the installation of instruments can start. A wind fan is mounted to give fresh air at all time in the blade.



Figure 25. Entrance to the blade.

Measurement positions

There is measured in a total of 10 positions and 5 positions at the time. It starts 5 meters from the root end and for every 1.5 meters, so the 10th measurement is 18.5 meters from the root end. All positions are targeted with laser equipment.



Figure 26. Inside of the blade mounted with measurement equipment.

Mounting instruments

The posiwire and aluminum plates was mounted with double sided tape and sealed with gaffa tape. The same method was used in all positions.



Figure 27. Mounting of instruments

Running the test with posiwires along the spar, to measure deformation

After all instruments was installed in position, different pitch and break positions was tested including run and production.



Figure 28. Running of the turbine while measuring the deformations.

Data collected on memory card and delivered to DTU wind energy

All data was collected with DTU wind energy instruments, which was have mounted inside the hub. The data is stored on a memory stick and handed over to DTU for further analysis.



Figure 29. Data acquisition unit installed inside the hub.

Field test on NM80 turbine with 38.8m blades

Description of work

1. Work info
2. Turbine info
3. Access to turbine, Nacelle, Hub and Blade.
4. Measuring positions
5. Mounting instruments
6. Running the test with posiwires along the spar, to measure deformation
7. Data collected on memory card and delivered to DTU wind energy

Work info

In 2014/2015 we have had several work and planning meetings in Brande, with Bladena and DTU wind energy. To prepare us, as much as possible, for Field and measurement test in Tjæreborg. Week 12, 2015 we made field and measurement test in Tjæreborg, with Bladena and DTU wind energy.

Turbine info

The field test and measuring was done in Tjæreborg, on a NM80 NEG Micon turbine, and the blades is 38,8M. LM blade.

Turbine owner is Vattenfall.



Figure 30. NM80 test turbine.

Access to turbine, Nacelle, Hub and Blade

Access to the Turbine bottom platform. For going to the Nacelle, there is a long ladder or service lift as you can see on the picture.

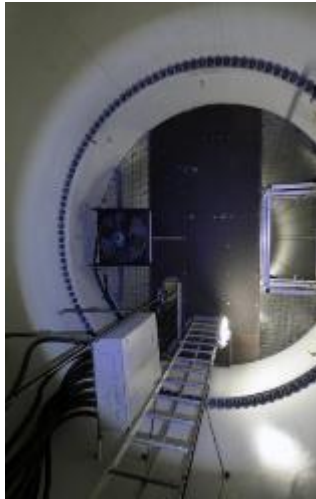


Figure 31. Entrance to the turbine and service lift.



The working area in the nacelle for preparation of the instruments before going to the hub and blade.



Figure 32. Working area in the nacelle

After the rotor has been locked, the turbine is ready for accessing Hub and Blades.



Figure 33. entrance hole to the hub from the nacelle.

Entrance to the hub, seen from inside the hub.



Figure 34. Entrance to the hub.

Finally the entrance from hub to the blade, seen from inside the blade. Where the installation of instruments can start.



Figure 35. Inside the blade.

Measurement positions

There is measured in a total of 4 positions. It starts 6 meters from the root end and for every 3 meters, so the 4th measurement is 15 meters from the root end. All positions are targeted with laser equipment.



Figure 36. Inside of the blade mounted with measurement equipment.

Mounting instruments

The posiwire and aluminum plates was mounted with double sided tape and sealed with gaffa tape. The same method was used in all positions.



Figure 37. Mounting of instruments

Running the test with posiwires along the spar, to measure deformation

After all instruments was installed in position, different pitch and break positions was tested including run and production.



Figure 38. Running of the turbine while measuring the deformations.

Data collected on memory card and delivered to DTU wind energy

All data was collected with DTU wind energy instruments, which was have mounted inside the hub. The data is stored on a memory stick and handed over to DTU for further analysis.



Figure 39. Data acquisition unit installed inside the hub.

EUDP-LEX Glass fiber cut outs in the field

From 2013-2016 Total wind blade have made and delivered several glass-fibre cut outs from actual blades located in Brande to DTU and Bladena. The specimens have been used to do different tests on the LEX prototypes and glues.



Figure 40. Cutting out of different blade specimens.

WP4 Full-Scale Fatigue Testing

WP cancelled.

WP5 Sub-Component and Sub-Structure Fatigue Testing

Test setup

Structural assessment of the inner 15m root section of an SSP34m wind turbine blade is conducted through a fatigue rated test rig. In the following the test setup is presented in two sections including: load train and clamped support.

The load train is designed capable of applying a discrete load at the free end of the substructure comprising two dofs: translation in the edgewise direction along with torsion. The load is generated through a single and double actuator configuration which are illustrated in Figure 41a and Figure 41b respectively. The load is transferred to the free end of the wind turbine blade through a bulkhead which is installed in the load carrying box girder cf. Figure 41.

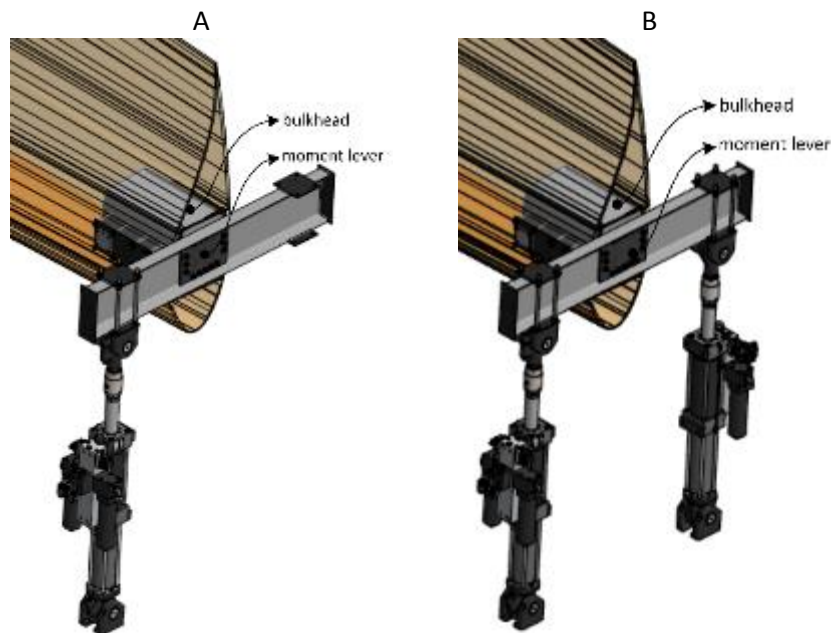


Figure 41: Actuator configuration: a) single and b) double

Attached to the bulkhead is a moment lever which accommodates the swivel head of the servo hydraulic actuator with an eccentricity of 904mm relative to the center of the bulkhead. The location and specification of the servo hydraulic actuator is presented in Figure 42a. The bulkhead is extending 750mm into the free end of the load carrying box girder and is fixed to the inner surface of both spar caps using glue and thread bars.

From the outside the thread bars are pretensioned and the loads transferred into the aerodynamic skin through installation plates.

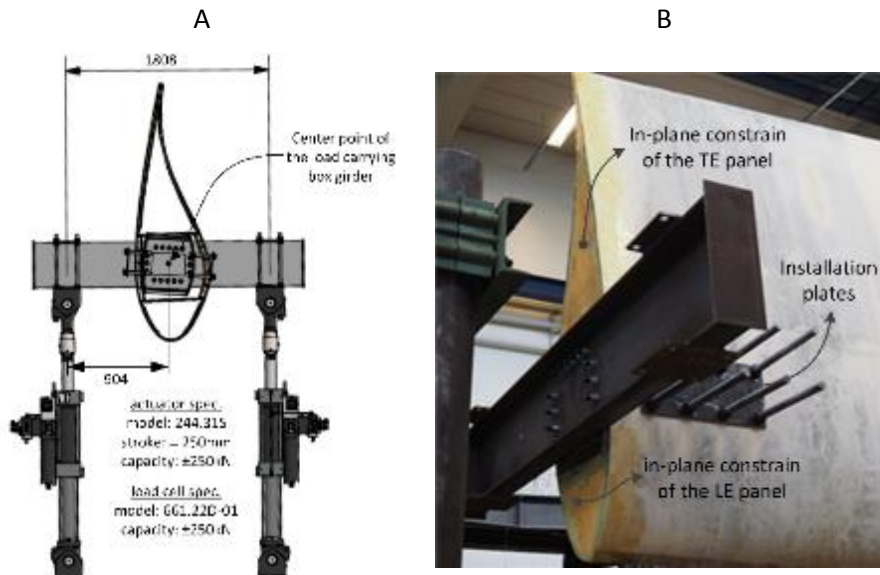


Figure 42: Load train including: a) cross section and b) photography representation

To avoid critical peeling stresses in the adhesive bond line connecting the trailing edge (TE) and leading edge (LE) panels with the spar caps, the free end of the wind turbine blade is fully constrained against in-plane distortion. This is achieved by closing the cross section by installing plywood plates which are over laminated with G-RP fabrics cf. Figure 42b.

A

B

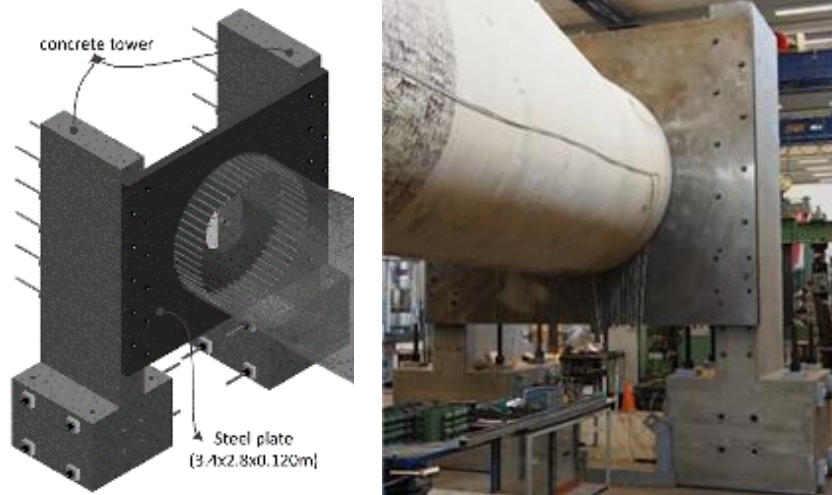
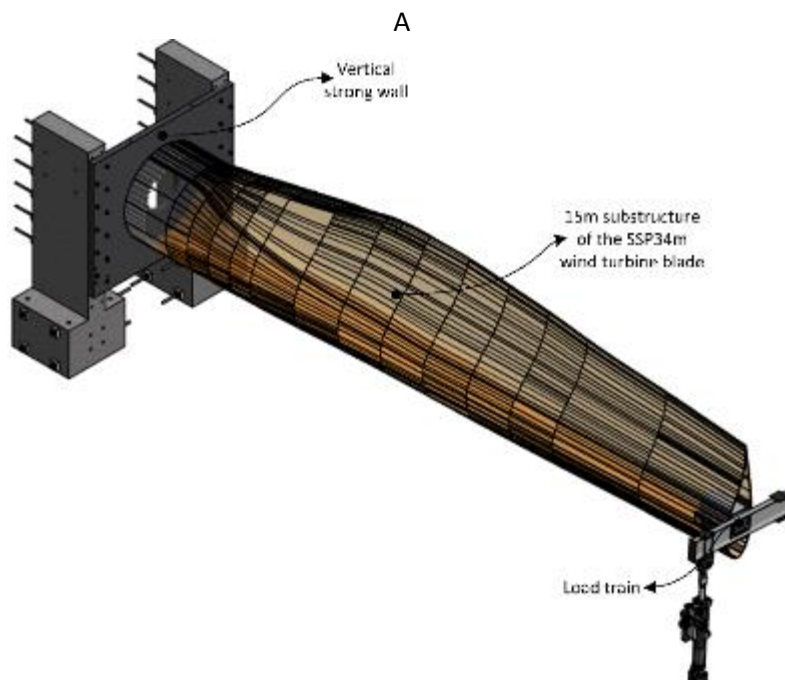


Figure 43: Clamped support including: a) detailed 3D illustration and b) photography representation

The clamped support of the root joint is achieved through a mobile vertical strong wall cf. Figure 43. This vertical strong wall consists of two concrete towers which are mounted to the horizontal strong floor using pretensioned thread bars. A steel plate with a width, height and thickness of 3.4m, 2.8m and 0.120m respectively is mounted to the concrete towers using pretensioned thread bars. The SSP34m wind turbine blade is connected to the center of the steel plate using 54 pretensioned thread bars.



B



Figure 44: Full test setup for handling of the 15m inner root section of the SSP34m blade: a) 3D illustration and b) photography representation

In the single actuator configuration, the load is applied in the trailing towards leading edge (TTL) direction through the deformation controlled servo hydraulic actuator in a ramped pattern ranging from 0-75kN. A full period is conducted within a duration of 6 min. The global stiffness obtained by the actuator in the given configuration is presented in Figure 45. Here a linear behavior is identified in the full loading range of the SSP34m blade. The stiffness is constant in both the loading and unloading sequence.

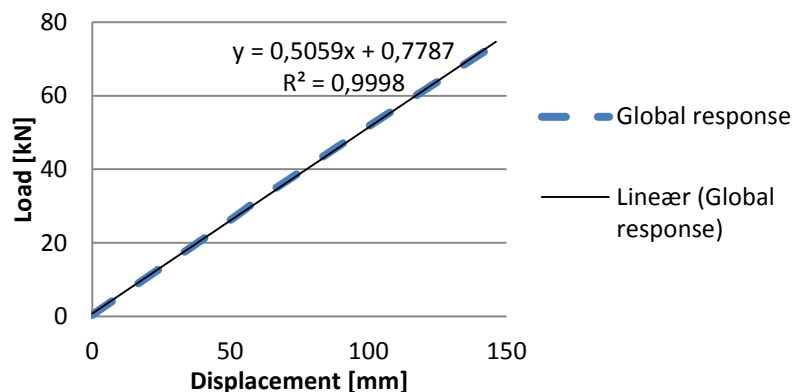


Figure 45: Global stiffness of the of the 15m inner root section in the single actuator configuration

In the double actuator configuration, a pure clockwise torsion is applied through the two deformation controlled servo hydraulic actuators in a ramped pattern ranging from 0-90kNm. A full period is conducted within a duration of 6 min. The global stiffness obtained by the actuator in the given configuration is presented in Figure 46.

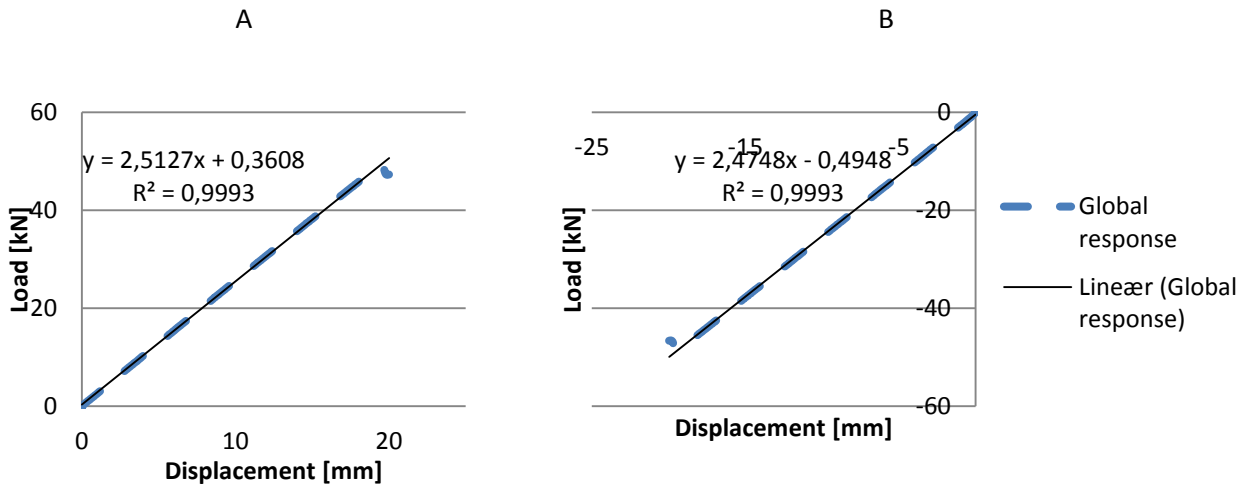


Figure 46: Global stiffness of the 15m inner root section in the double actuator configuration: a) act. A and b) act. b

In the following the actuator forces outlined in Figure 46 are converted to an equivalent torsional moment with the positive direction of rotation defined by the right hand rule.

Data acquisition

Wire potentiometer measurements

The wire potentiometer is implemented to quantify the cross sectional shear distortion of the blade as outlined in figure x (refer to a representative figure in the introduction or previews wp). The relative change of distance in the two diagonals labelled: D1 and D2 will be measured at the following distance from the root of the blade: 5.5m, 7.0m, 8.5m, 10.0m and 11.5m. The readings with and without the stiffener is outlined in figure 7-11 for the single actuator configuration. The corresponding peak deformation and relative deviation with and without the X-Stiffener is outlined in Table 7.

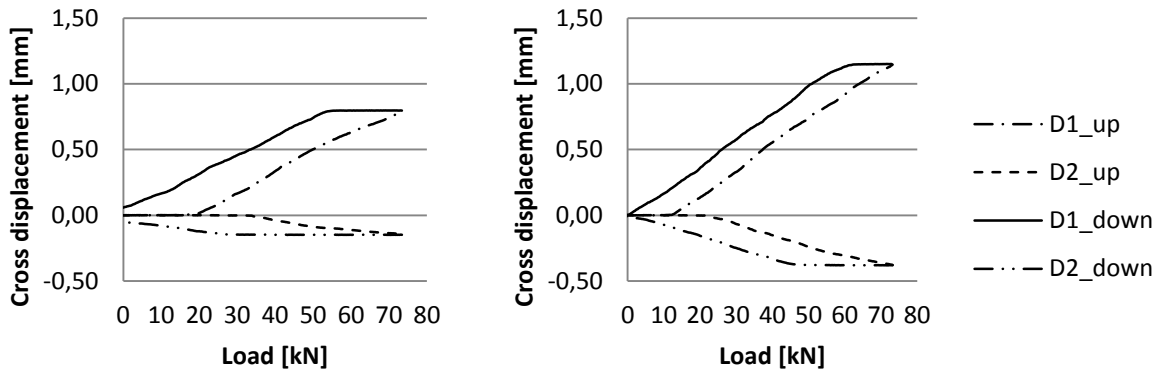


Figure 47: Cross sectional shear distortion in the 5.5m section: a) without X-Stiffener and b) with X-Stiffener

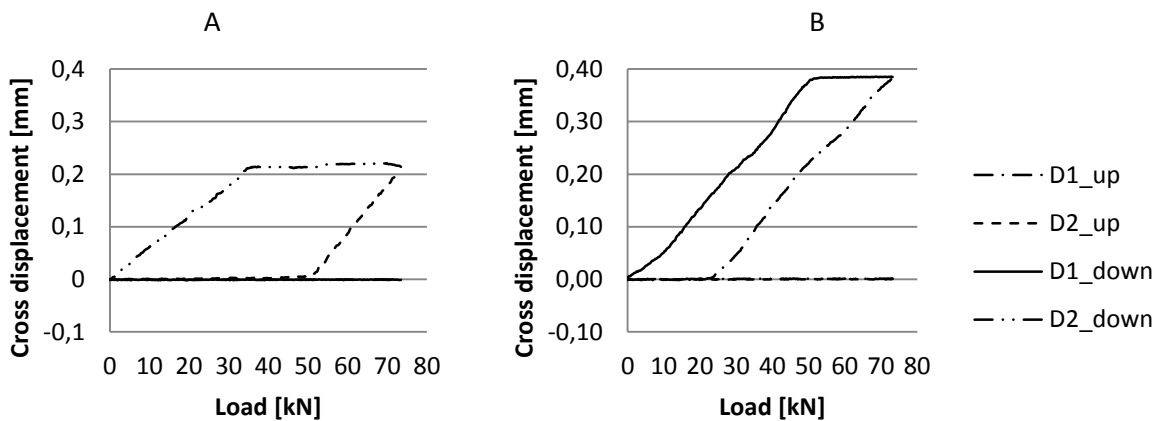


Figure 48: Cross sectional shear distortion in the 7.0m section: a) without X-Stiffener and b) with X-Stiffener

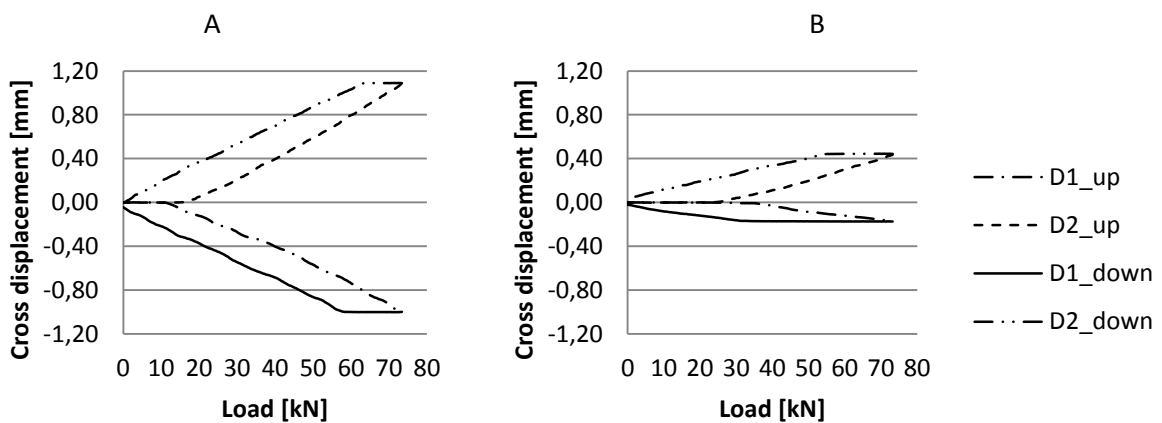


Figure 49: Cross sectional shear distortion in the 8.5m section: a) without X-Stiffener and b) with X-Stiffener

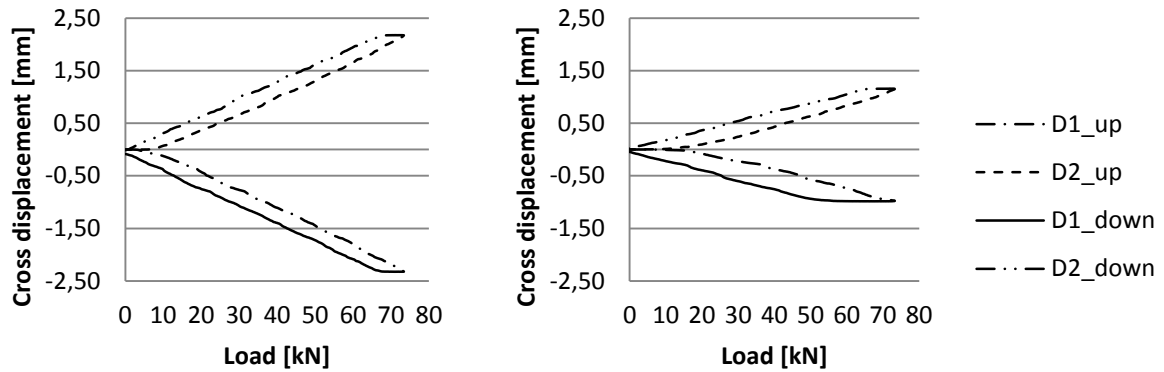


Figure 50: Cross sectional shear distortion in the 10.0m section: a) without X-Stiffener and b) with X-Stiffener

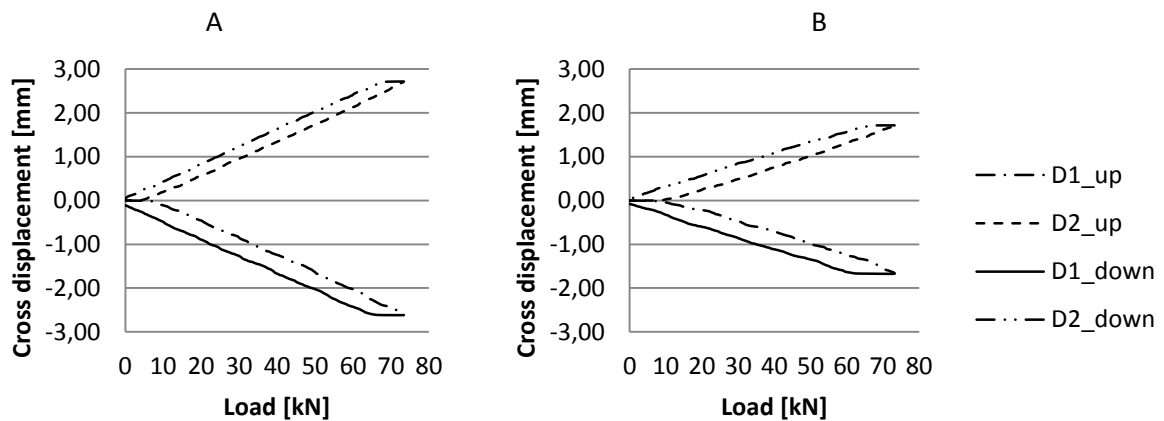


Figure 51: Cross sectional shear distortion in the 11.5m section: a) without X-Stiffener and b) with X-Stiffener

Table 7: Peak cross sectional shear distortion in the single actuator configuration

		Without X-Stiffener [mm]	With X-Stiffener [mm]	Div. [%]
5.5m	D1	0.790	1.145	-44.88
	D2	-0.145	-0.378	-159.7
7.0m	D1	-0.002	0.382	-100.5
	D2	0.207	0.001	99.34
8.5m	D1	-0.994	-0.172	82.70
	D2	1.081	0.435	59.77
10.0m	D1	-2.311	-0.972	57.91
	D2	2.155	1.143	46.94
11.5m	D1	-2.599	-1.659	36.15
	D2	2.705	1.699	37.18

In the double actuator configuration, the readings of the cross sectional shear distortion as a function of the torsional moment is presented in Figure 52 - Figure 56.

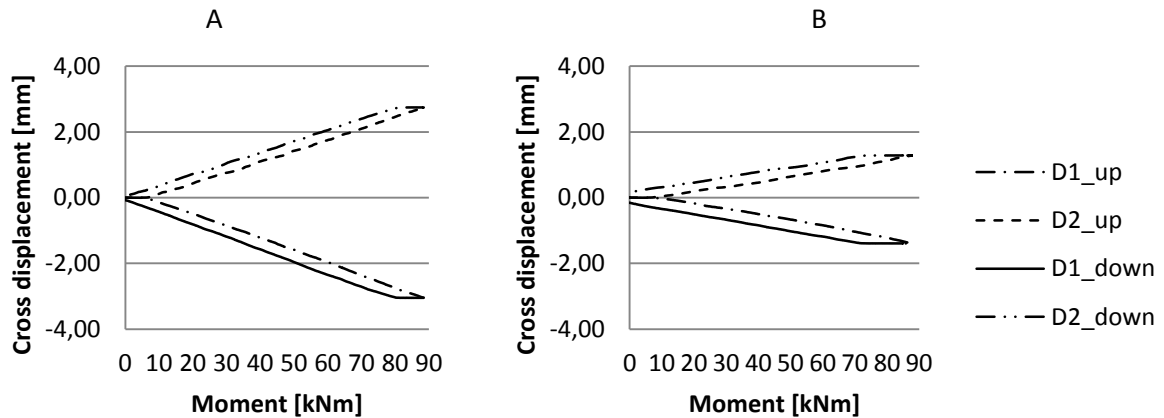


Figure 52: Cross sectional shear distortion in the 5.5m section: a) without X-Stiffener and b) with X-Stiffener

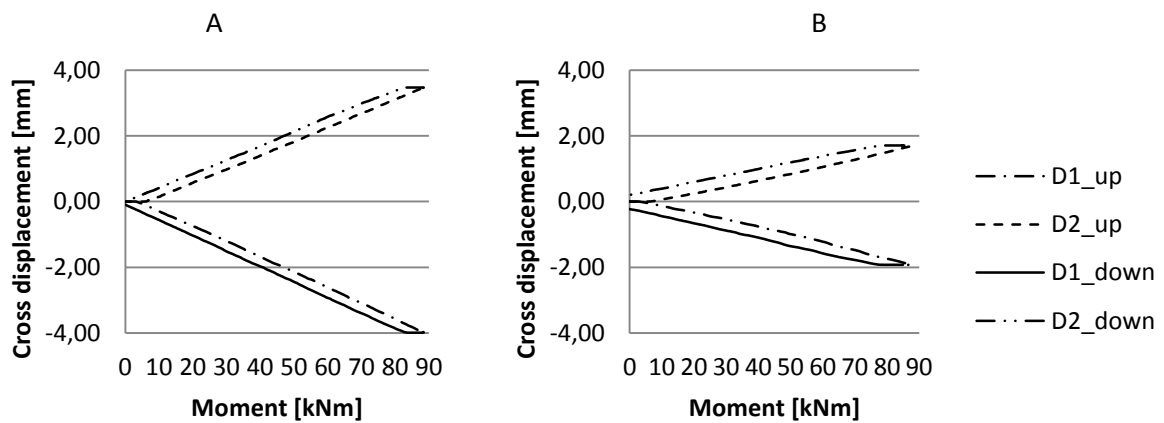


Figure 53: Cross sectional shear distortion in the 7.0m section: a) without X-Stiffener and b) with X-Stiffener

A

B

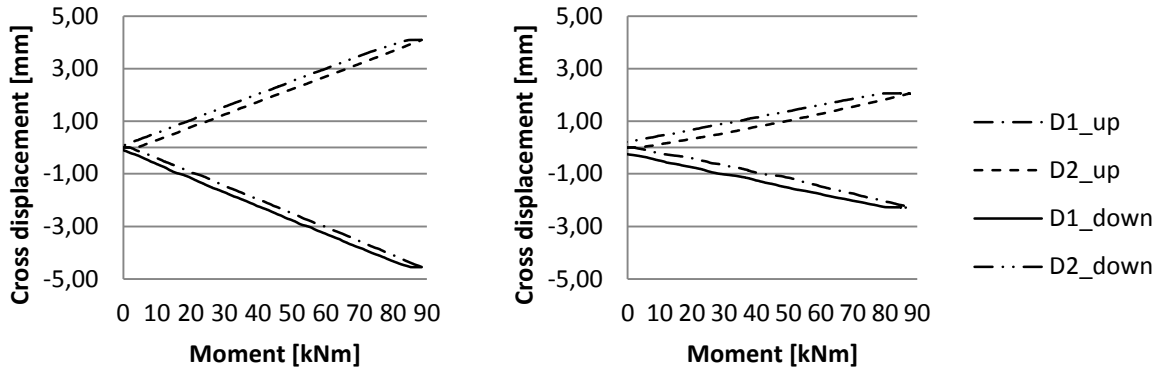


Figure 54: Cross sectional shear distortion in the 8.5m section: a) without X-Stiffener and b) with X-Stiffener

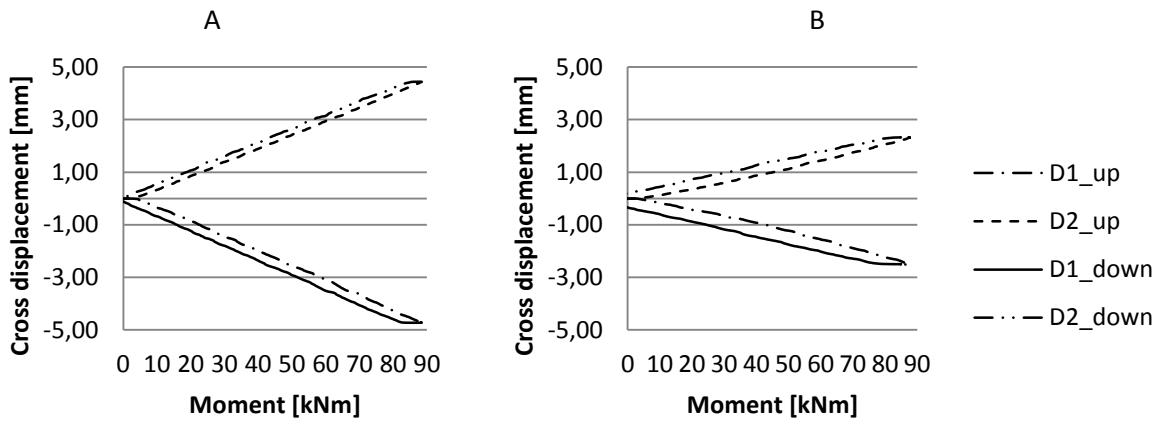


Figure 55: Cross sectional shear distortion in the 10.0m section: a) without gftyrX-Stiffener and b) with X-Stiffener

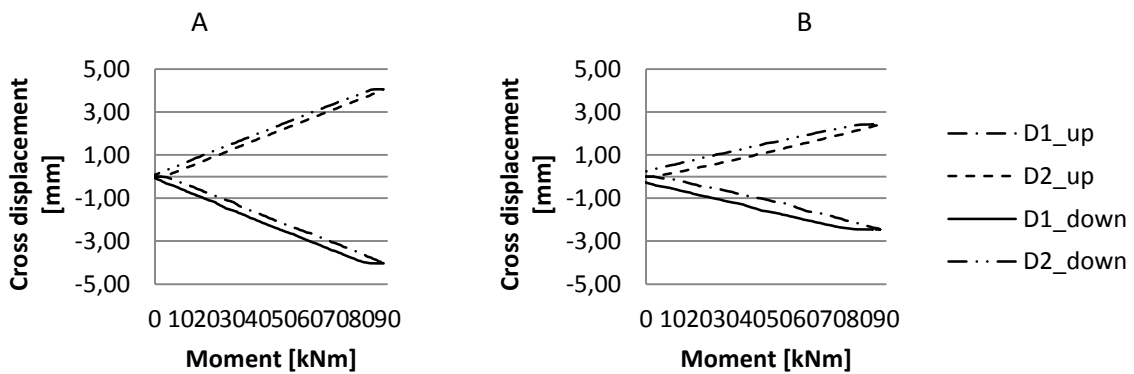


Figure 56: Cross sectional shear distortion in the 11.5m section: a) without X-Stiffener and b) with X-Stiffener

Table 8: Peak cross sectional shear distortion in the double actuator configuration

		Without X-Stiffener [mm]	With X-Stiffener [mm]	Div. [%]
5.5m	D1	-3.028	-1.398	53.83
	D2	2.727	1.283	52.93
7.0m	D1	-3.947	-1.925	105.0
	D2	3.445	1.709	50.39
8.5m	D1	-4.516	-2.282	49.48
	D2	4.059	2.064	49.16
10.0m	D1	-4.698	-2.506	46.67
	D2	4.404	2.327	47.16
11.5m	D1	-3.995	-2.458	38.48
	D2	4.029	2.416	40.04

Strain gauge measurements

To evaluate the structural response of the aerodynamic skin at certain location a number of strain gauges are applied on the outer skin of the SSP34m blade. Location and labelling of each strain gauge mounted on the outer skin of the SSP blade is identified in Figure 57.

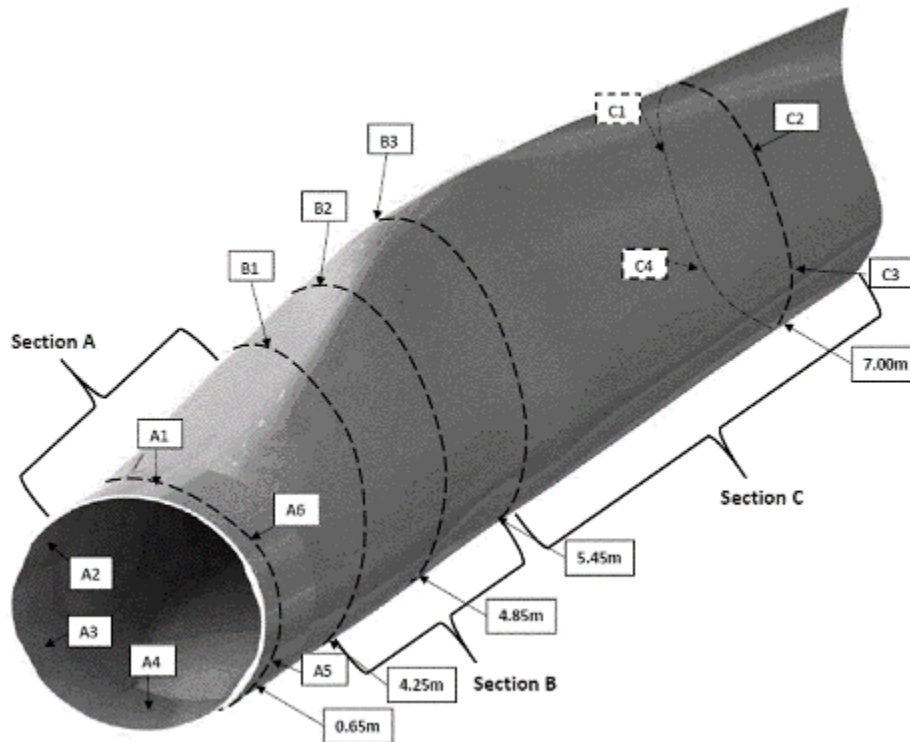


Figure 57: Location and labelling of the strain gauges mounted on the SSP blade

In section A and C the strain gauges are of the type: rectangular rosette. In section B bi-axial strain gauges are implemented. The 0 degree direction are defined in the longitudinal direction of the blade. An illustration of a strain gauge rosette mounted to the outer skin of the SSP blade is outlined in Figure 58.

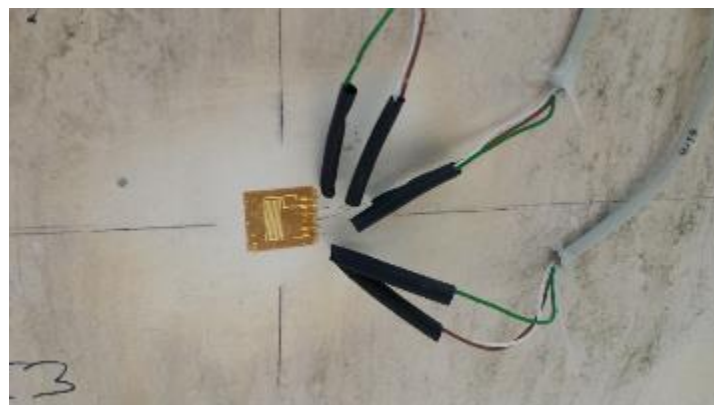


Figure 58: Illustration of a rectangular rosette which is mounted in the outer skin of the SSP blade

The strain gauge readings with and without the retrofitted X-Stiffeners in section A are given in in Appendix D:.

Digital Image Correlation measurements

To acquire a detailed picture of the structural behavior of the max chord section, 4 zones are evaluated through full field DIC measurements covering both the PS and SS panels cf. Figure 59a and Figure 59b respectively. In the trailing edge area (zone 3 and 4) the max chord area is evaluated, located $7.0\text{m} \pm 1.0\text{m}$ from the root. The leading edge area (zone 1 and 2) is located $6.5\text{m} \pm 1.0\text{m}$ from the root. For further details, see Figure 59.

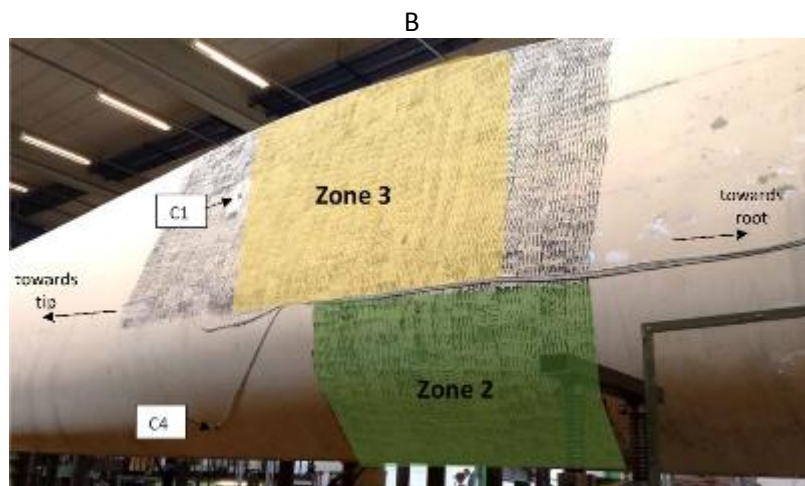
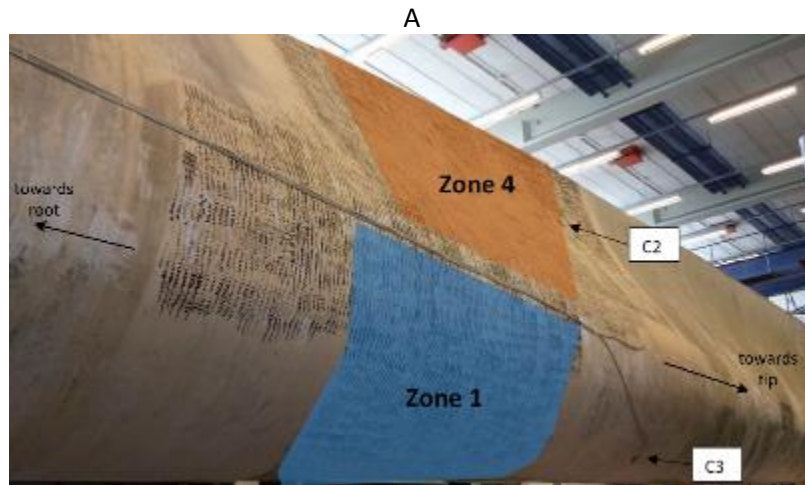


Figure 59: Location and labelling of the full field measurements on the SSP blade: a) PS panels and b) SS panels

In Appendix D: the data obtained for each zone are presented including out-of-plane displacements and strains.

WP6 Finite Element Simulation

WP responsible: Andrei Buliga – Bladena

Introduction

New improvements within the wind turbine industry, such as the development of longer blades and the use of large flat-backs, dramatically increase the stress levels on the adhesive bondlines of the blades. Unfortunately, the adhesive strength of the glue used within the industry have remained more or less constant during the last 10 years, thus exacerbating the problem of peeling in the adhesive bondlines. These challenges are further accentuated in blades with large flat-backs.

The Finite Element Method(FEM) is used in order to study different blade types and shapes by means of parameter study. Furthermore, with FEM it is possible to assess stress level, a quantity that in practice cannot be measured.

Another point why one should use FEM is that is considerably more cost effective than testing and certain things can be asses e.g. different blade parts that usually are not accessible for inspection (blade interiors). This aspect is of major importance due to the fact that damages caused by the excessive twisting of blades appear initially on the inside of the blades and are discoverable only by internal blade inspections, which today is not part of a standard blade inspection. Blades with a weakened main structure are prone to catastrophic failures.

For further information on the finite element analysis, see Appendix C:.

Scope

Finite element models of different blade designs are tested with and without X-Stiffeners installed. The effect of X-Stiffeners installed in blades are thereby tested. In order to investigate the need for a solution like the X-Stiffeners when blades grow larger or when blades are given a large flat-back profile, several FE blade models were developed and tested. A list of the models referred to in this report can be seen in Table 9.

Table 9: A list of blade FEM models referred to in this report.

Name of FEM model	Model description	Blade length
RM1	Reference blade model: Straight parallel shear webs.	34 m
RM3	Reference blade model: Straight parallel shear webs.	68 m
RM3_newFB	Reference blade model with a large flat-back design.	68 m

Challenges

When rotating, the blades are subjected to gravity forces in the edgewise direction regardless of the wind condition. Aerodynamic pressure from the wind contributes to the total load on the blade, creating the combined loading scenario. This loading forces the blades to deflect as seen in Figure 60.

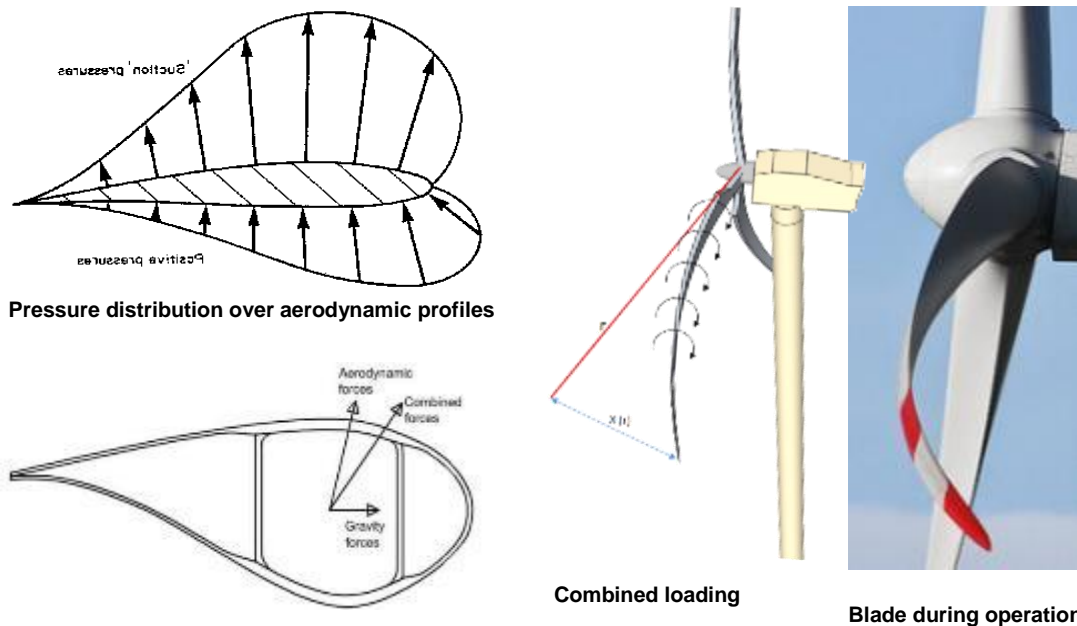


Figure 60: Combined loading scenario explained - The pressure distribution creates the aerodynamic load on the blade added to the gravity loading. The blade is therefore bent and a torsional moment due to the tip deflection is created.

The loading of the blade creates a fatigue movement that affect all adhesive bondlines within the blade. This is due to changing load direction from gravity and varying aerodynamic forces, see Figure 61.

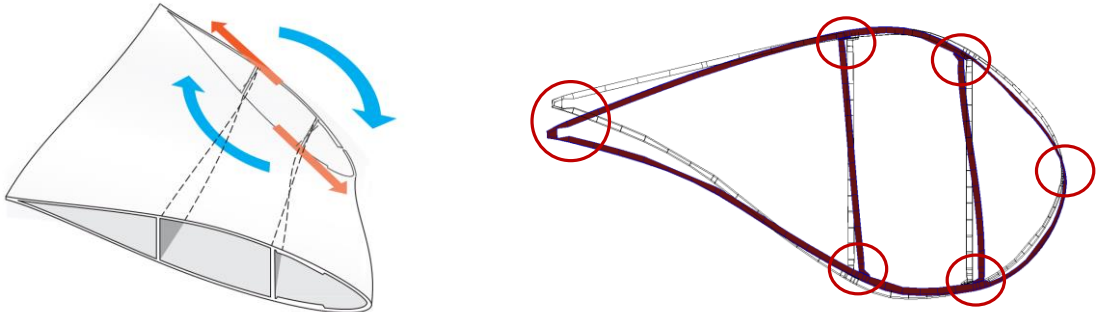


Figure 61: Sketch showing the twisting phenomenon. Left: 3D view of the blade deformation. Right: Cross-Sectional Shear Deformation CSSD seen on a cross-section. Red circles point out where the adhesive bond-lines are found.

These phenomena are further illustrated in the following videos available online:

3. <https://youtu.be/78EUCG5A6Xs> – Cross-sectional view of FEM blade model deforming during normal operation.
4. https://youtu.be/2_vDqgm9opl – Sketch of video showing the blade behaviour during operation from a blade perspective.

The phenomenon is also described in ref. [14].

Cross-sectional shear distortion effect when blades grow larger

The cross-sectional shear distortion (CSSD) becomes much more pronounced as blades increase in size. A simple comparison between a 34m and 68m blade revealed an increase of more than 250% of the CSSD magnitude, see Figure 62.

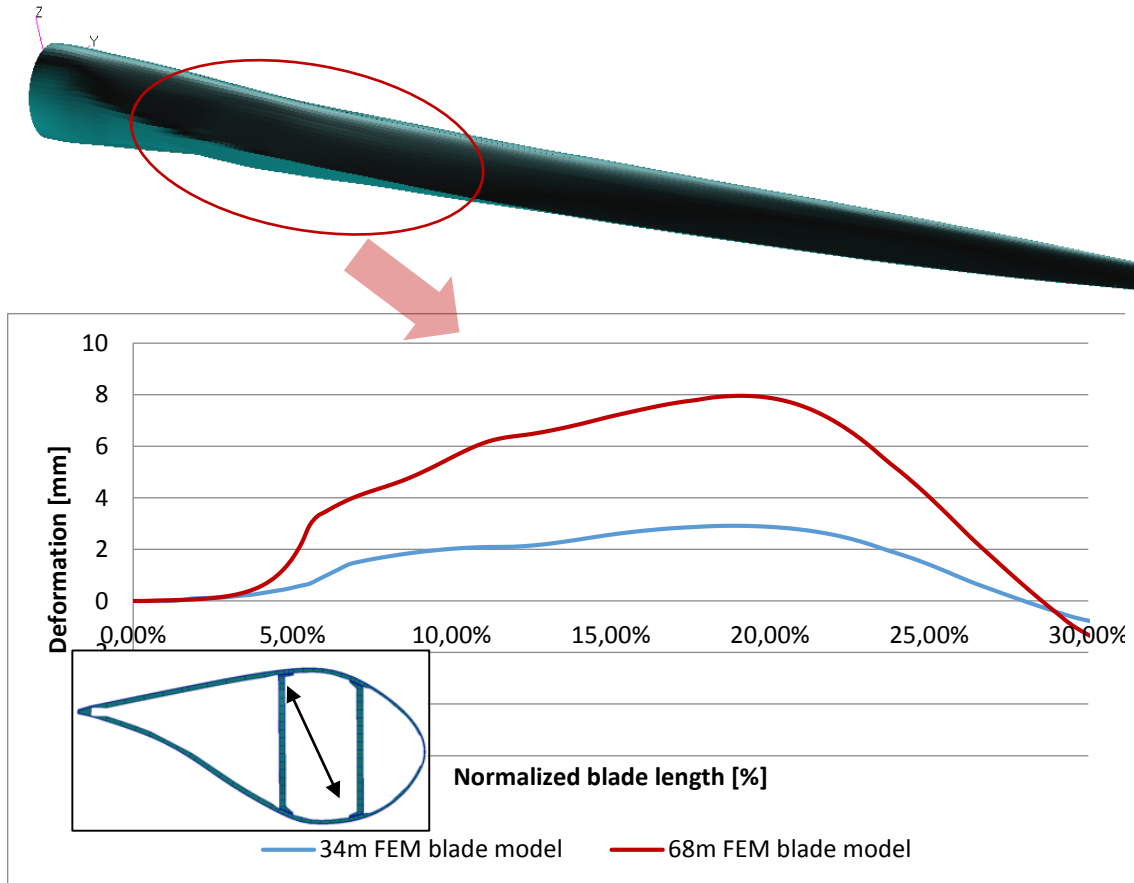


Figure 62: CSSD magnitude increase when blade size increase. The results on the graph are from the first third of the blade as shown on the top figure. Blue line: CSSD magnitude of the 34m FEM blade model. Red line: CSSD of the 68m FEM blade model.

In Figure 62 the relative diagonal displacement is used in order to compare the two 34 and 68 blade FEM blade models. Post-processing is performed on a normalized blade length scale in order to accommodate results in the same length scale.

Results indicate that at an area measured at approx. 1/5 of the blades length, where the max chord is situated, the CSSD maximum magnitude is found for both the 34m and 68m FEM-blade models.

There is a direct connection between the CSSD and peeling stresses in the adhesive bondlines: the higher the magnitude of the CSSD, the higher the peeling stresses are, see Table 10 below.

	34m FEM-blade model	68m FEM-blade model	Increase in percentage
CSSD magnitude	3mm	8mm	260%
Stress level	1.7 MPa	5.1 MPa	290%

Table 10: Comparison of peeling stress magnitude between the 34m and the 68m FEM blade models.

Table 10 indicates the direct link between the CSSD and the peeling stresses in the adhesive bondlines seen as a function of the blade length. The results indicate that when the blades increase in size the stress levels increase as well.

Since adhesive bondlines have similar bonding properties for all blade sizes, the risk for failure in the adhesive joints are significantly increased when the peeling stresses are high.

The peeling stresses are post-processed in the adhesive bondlines using as indicated below in Figure 63.

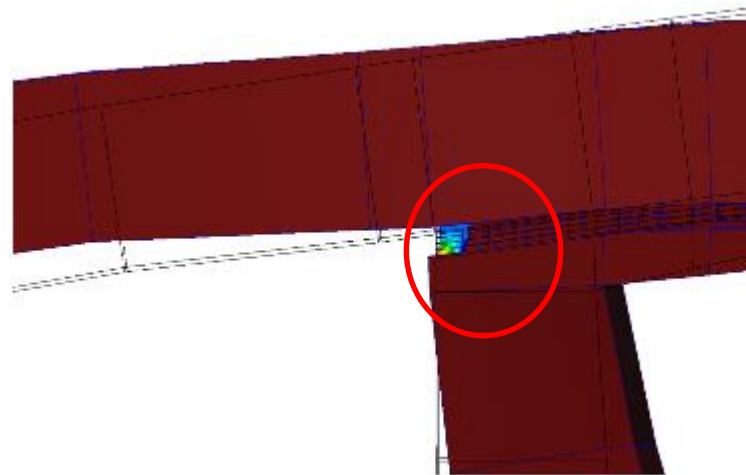


Figure 63: Cross-sectional shear deformation creates peeling stress levels in the adhesive bondlines. With black wireframe undeformed structure. With dark red-deformed structure (scaled plot). The colours represent peeling stress levels in the adhesive bondlines.

The area where the stress is post processed is fine meshed, this ensuring that the deformations are captured in a correct way, see Figure 64.

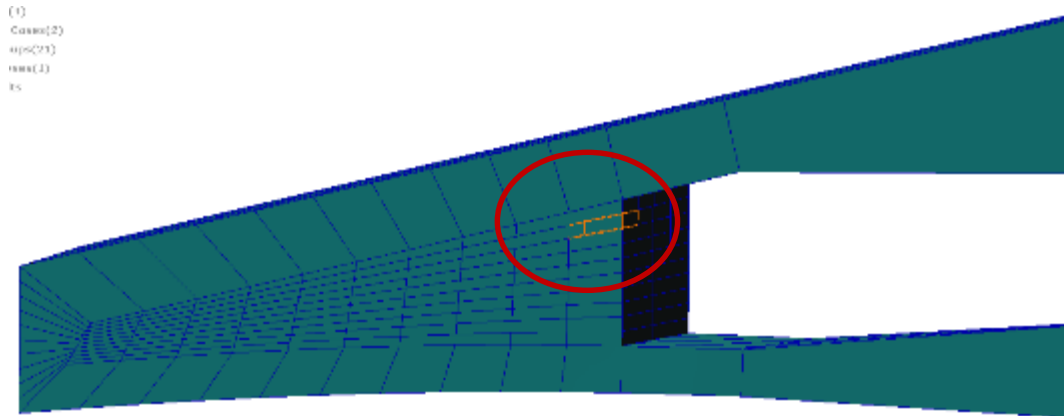


Figure 64: Detail on meshing of adhesive bondline. The highlighted element is used for stress post-processing.

Using this methodology ensures that correct results are obtained and the influence of adjacent elements consisting of different materials is avoided.

CSSD effect for "normal" and flat-back profile design

On blades with a large flat-back, the magnitude of CSSD is increased, see Figure 65.

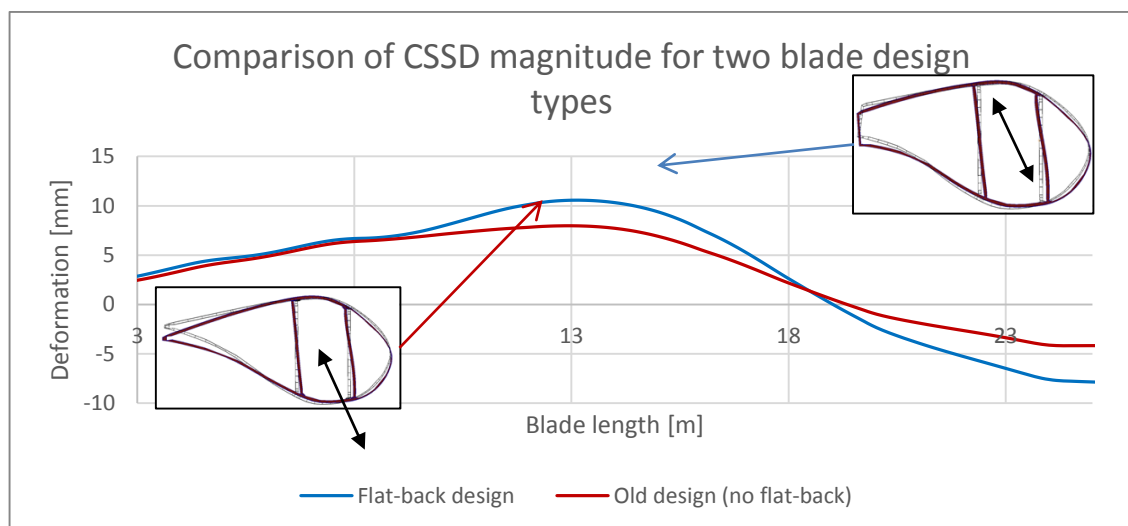


Figure 65: CSSD on normal blade design and flat-back design. Conventional design (no flat-back)

The graph in Figure 65 illustrates the magnitude of the CSSD, post-processed directly on the diagonal between the opposite corners of the main structural box within the FEM blade model. The main difference between a blade profile with and without a flat-back is the lack of structural support in the trailing edge in the flat-back case. This will further

increase the magnitude of the CSSD and adds even more stresses in the adhesive bondlines within the blade, see Figure 66.

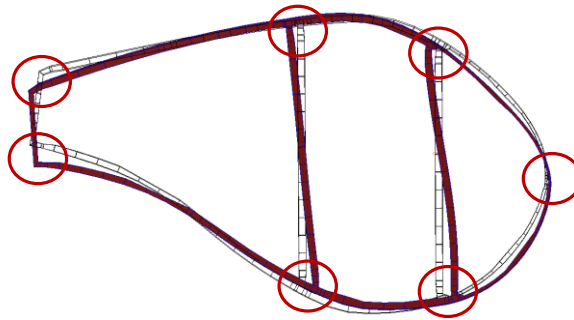


Figure 66: CSSD seen on a FEM blade model with a flat-back cross-section. Red circles point out where the adhesive bond-lines are usually found.

In the flat-back blade design, the X-Stiffener can be installed both in the rear and main boxes, see Figure 67.

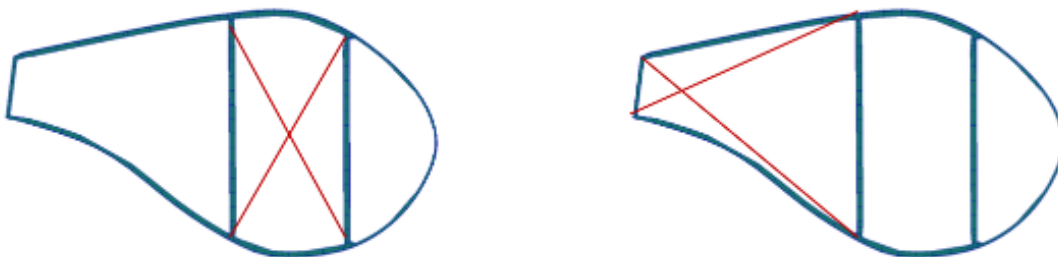


Figure 67: Possible solutions for X-Stiffeners enhancements in a flat-back blade design. Left: X-Stiffener installed in the main box. Right: X-Stiffener installed in the rear box.

CSSD comparison with and without D-Stiffeners installed

As already shown, the problem of CSSD and resulting stresses in bondlines increases for larger blades. For blades designed with a flat-back profile the stress levels get even more critical. The effect of inserting X-Stiffeners in a 68m FEM-blade model with a large flat-back is shown in Figure 68.

CSSD magnitude with the X-Stiffener installed

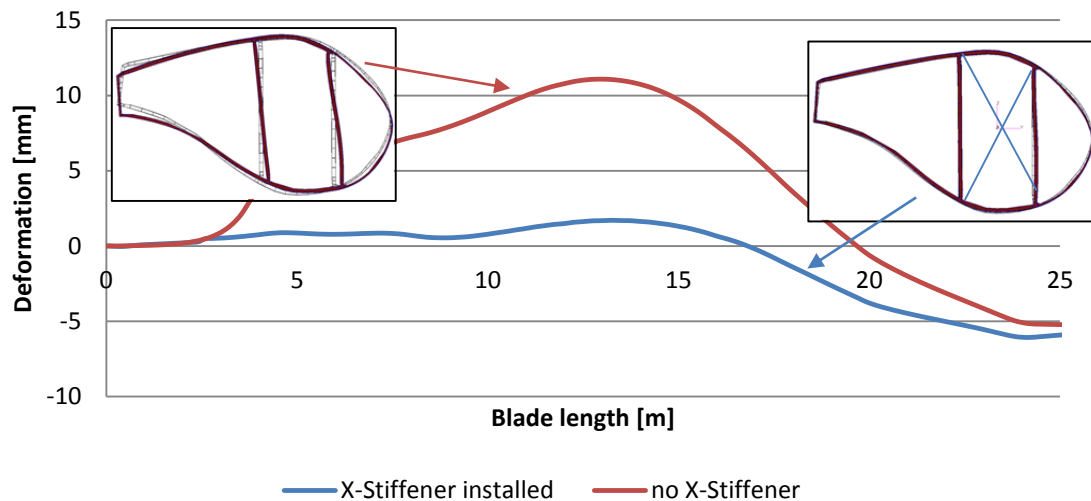
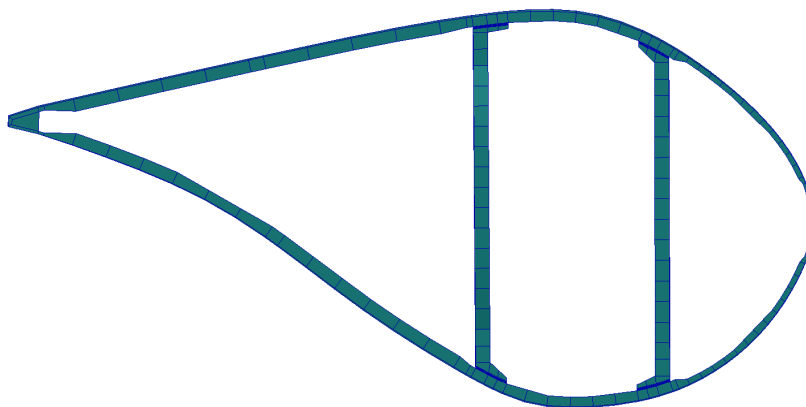


Figure 68: CSSD post-processed from a 68m FEM blade with a large flat-back design. Red: no X-Stiffeners installed; Blue: Deformations significantly reduced after the X-Stiffener technology has been used.

After installation of the X-Stiffener in the blade FEM model, CSSD reduces 80-85%. This has a direct impact on the peeling stresses in the adhesive bond-lines, leading to significant increase of the lifetime.

In Figure 69 the colours represent the magnitude of the peeling stresses: with red showing high stress levels and green and blue low stress level. In practice, a factor 2 reduction of the peeling stresses is observed. Such a reduction results in a significant increase in blade lifetime due to the nature of composite/adhesives and fatigue life properties.



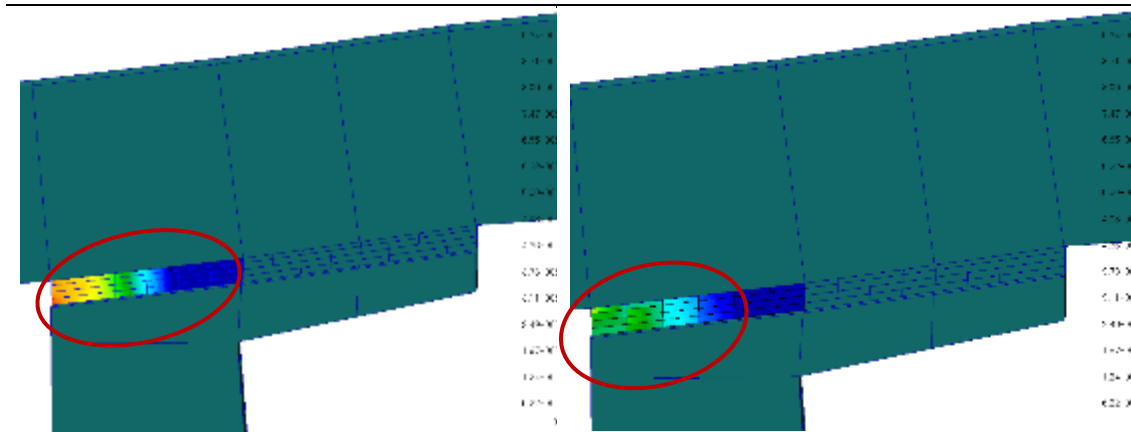


Figure 69: Reduction of peeling-stresses in adhesive bondlines. Top: post-processed position of the shown peeling stresses. Bottom Left: peeling stress level without the use of X-Stiffener technology. Bottom Right: Reduced peeling stress level when the X-Stiffener technology is implemented. The colors represent stress level using the same scale. Red color shows high stresses and green color shows low stresses.

Input for WP5

Another important usage of FEM within the LEX project was support for other WP's, both experimental WP's and analytical WP's.

In order to create the right boundary conditions for testing, WP6 was heavily involved in WP5 where the large subcomponent test was carried out.

The SSP34 FEM blade model was used to create the input for the large sub-component testing. The methodology was:

- Divide the SSP34 FEM blade model in two so that the section from blade root to 15m radius is available, similar to what is used in WP5. The necessary blade dimensions were supplied based on the FEM model.
- A number of load scenarios were carried out in order to generate the same behaviour of the 15m FEM blade model as it would have in real world if combined loading would be used.
- It was ensured that the boundary conditions can be applied in practice (lab limitations) and also pinpointed areas where the blade needs to be reinforced so that the test can be carried out in a safe manner, see ref. [16] for full details on the test input.
- A measurement plan was created and the measurement locations were pinpointed where different measurement equipment needs to be installed. (posiwires and strain gauges), see ref. [17] for full details on the measurement plan.

Once the 15m blade was tested, a validation of the FEM blade model was possible, see Figure 70.

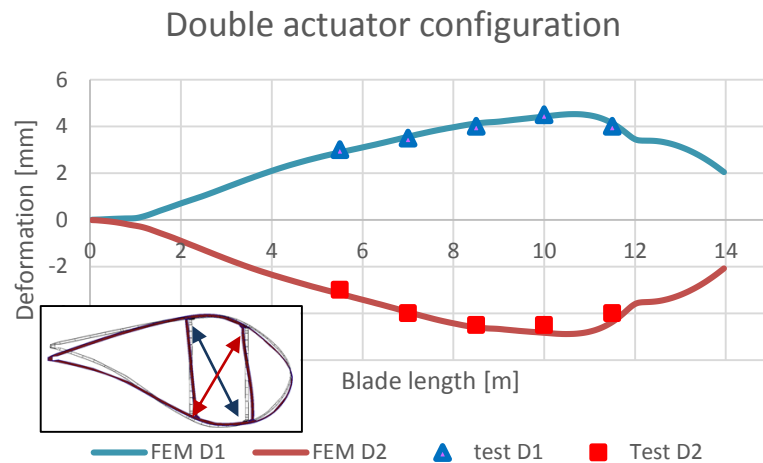


Figure 70: Comparison of FEM results and large testing results

The graph in Figure 70 show the cross-sectional shear distortion in the first 14m of a SSP34m blade tested in torsion. Comparison of FEM and experimental results show good correlation after having made the blade “softer”. This is a classical problem that FEM results are more “stiff” than measured experimental results.

Field testing and FEM

Within the LEX project two individual field tests were carried out on small blades (40m range) with stiff internal main carrying structures. The cross-sectional shear distortion was measured and the results compared with the ones obtained by FEM simulations. The results were in good agreement even though the measured deformations were relatively low, as shown earlier for the comparison of a small FEM blade model with a large one.

There are two main reasons for obtaining small deformations:

- Low wind conditions were recorded during the measurement campaign days, meaning low flapwise loading on the blades. A parameter FEM study carried out in the project has revealed that the main driver of the cross-sectional shear distortion is the flapwise loading, see Figure 71.

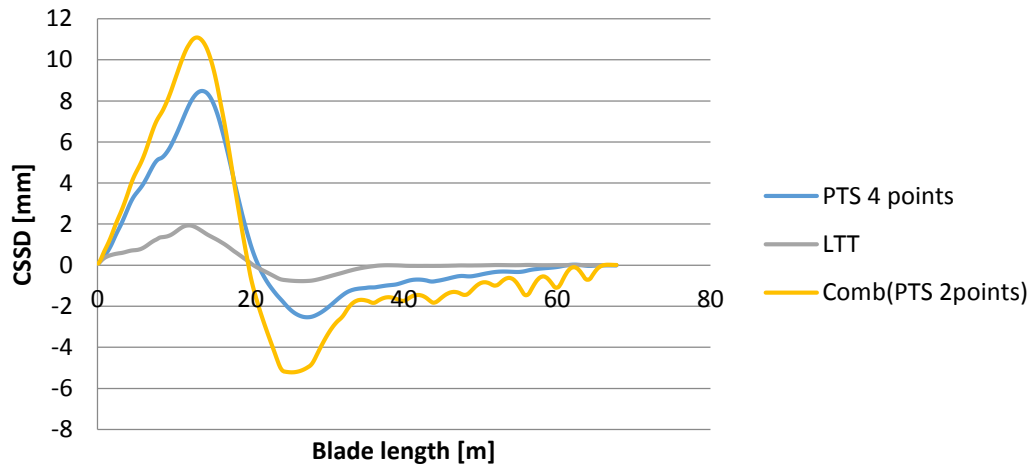


Figure 71: Cross-sectional shear distortion magnitude for three different loading configurations.

In Figure 71, different loading configurations create different cross-sectional shear distortion magnitudes. It is noted the flapwise influence over the edgewise loading being significantly higher, therefore in the combined loading scenario, which is the loading scenario blades experience while operating on the field, the flapwise loads determine the magnitude of the cross-sectional shear deformation.

- The tested blades are built around a stiff main carrying box (the V80 has a box bar construction which is extremely stiff and the NM80 blade is one of the stiffest blades LM has developed).

Conclusion

Three separate FEM generic blade models were developed based on the SSP34 FEM blade model.

A number of comparison were carried out involving different generic FEM blade model sizes by using non-linear geometric simulations. The results indicate that as blade increase in length, the cross-sectional shear distortion magnitude increases as well.

Different blades of the same length have different characteristics, e.g. flat-back design. A parameter study revealed that blades with a large flat back construction have a higher cross-sectional shear distortion magnitude than of those with a more conventional design, thus making them more prone to structural damages.

The studies revealed that when the cross-sectional shear distortion is decreased due to the use of the X-Stiffener technology, the stress level in the adhesive bondlines is reduced, thus the blade lifetime is prolonged.

A comprehensive work was carried out in close collaboration with WP5 where full support for the large testing was supplied. The FEM simulations were the base for providing the right boundary conditions for testing. Later in the project, results from the large scale testing were in good agreement with the prior obtained FEM results.

A comparison between measurements carried out in the field on two small stiff blades (WP3) and numeric FEM simulations using a model of similar size was carried out. The results confirmed the initial FEM findings where the cross-sectional shear deformation magnitude on small blades is relative low.

WP7 Design Tools for Wind Turbine Blades

WP responsible: Lars Damkilde - Aalborg University

The main goal for the WP7 was to bridge the gap between the wind load simulations (WP8) and the detailed structural FEM models used in design (WP6).

Simulation of operating wind turbine blades is a non-linear mechanical problem involving large displacements, dynamics and buckling. Modelling of a wind turbine blade can be made at different levels of accuracy depending on the use of the results. In detailed structural, FEM-based analysis of, e.g., stresses at a joint, there is a need for using solid or shell elements in order to capture an accurate stress level to be utilized in, e.g., fatigue analysis of the composite elements. This ends in an FEM-model where the number of degrees of freedom typically will be of the order of 10^6 , and this result in a time consuming analysis.

In simulation of the wind loads, the key issue is dynamic analysis of the blade taking into account large displacements/rotations of the blade. The wind simulations result in time series of the displacements/rotations, and each time step involves recalculating the mechanical properties as the blade changes its spatial form, i.e., accounting for the large displacements/rotations. For the wind simulations, it is mandatory that the number of degrees of freedom is kept low, and at present a realistic value would be of the order 10^3 . The wind simulations are therefore made with beams or beam-like elements. The beam-type elements ensure a sufficient accuracy of the wind load as they describe the overall stiffness of the blade rather accurately.

In the wind calculations, most of the structural non-linear effects are handled, i.e., the analysis takes into account that the blade is both twisted and rotated and therefore carries the load in a different way compared to a pure linear analysis. However, there are non-linear effects of more local nature that are not accounted for. The most prominent is known as the Brazier effect, and its importance in design of wind turbine blades has previously been identified. The Brazier effect is also called ovalization; a term that very well describes the deformation of bended tubes. The effect is due to bending moments in the beam, and it grows with the square of the bending moment, hence a non-linear geometric effect. In the Figure below, the Brazier effect on a hollow section is illustrated.

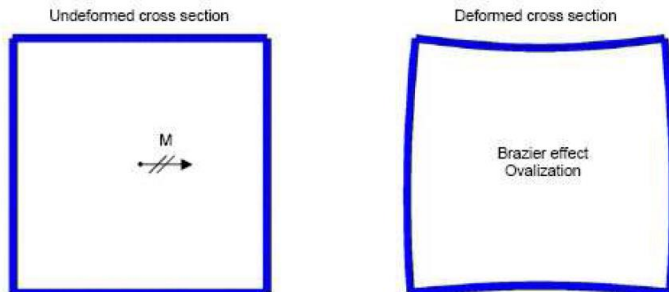


Figure 72 The Brazier or ovalization effect.

The deformations have been scaled (enlarged) and the actual change – at least at the present level of wind calculation – has no significance. However, the change of shape will introduce additional stresses, which have to be quantified.

In the present project, an additional effect of torsional moments has been identified, and to our knowledge no others have done that before. We consider this as an important finding, and we have, as such, denoted it the Generalized Brazier effect. In the Figure below, the torsional effect has been illustrated. As with the previous effect, the effect on the wind calculation is negligible; however, the deformations will introduce additional stresses.

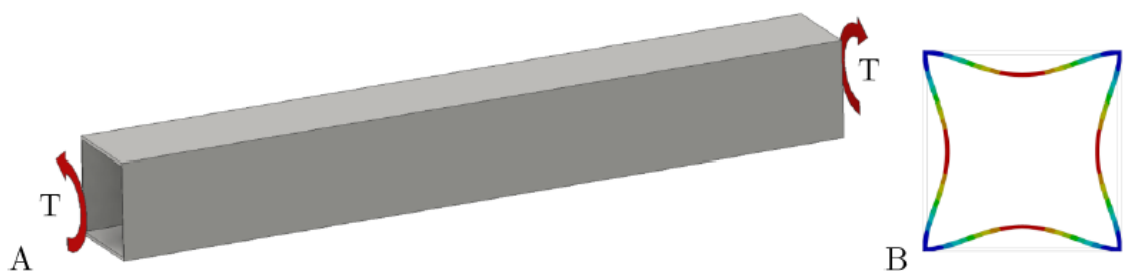


Figure 73 Torsion of beam in large displacements – Generalized Brazier effect. A) The structural model B) cross-sectional deformations enlarged.

Wind simulations were earlier mostly done by use of beam element, namely, Timoshenko elements taking into account the shear flexibility. The beam theory builds on some basic assumptions, and in this context the assumption that in-plane cross-sectional deformations are not possible is the most important. This assumption will, for instance, not allow for the deformations illustrated in the Figure above. Beam theory is

applied in many technical aspects, and it is usual a very good approximation. However, for very slender cross-sections, the assumption may lead to serious underestimation of the stresses and a too optimistic evaluation of the overall stiffness of the beam. In composite structures, this is even more pronounced as the material stiffness typically change significantly in different directions. Traditionally, beam theory cannot model the so-called shear distortion phenomenon, and this has, both in previous projects and the Lex-project, been identified as a prominent component.

Nowadays, the wind simulations have been improved, and by using either extended beam elements, see, e.g., BECAS or Super Element technique (described in the WP8 section), the shear distortion phenomenon can be described. The extended beam element has not the same accuracy as a Super Element due to the more limited number of unknowns. None of the methods are able to describe the extended Brazier effect, and the nature of the elements is basically linear, i.e., the loads and the associated stresses are proportional. The elements can handle some non-linear geometric effects by rotation the elements during the load process.

In the WP7, it was originally planned to develop a more advanced beam element that takes into account the full non-linear effects. This method has previously been used successfully in stability problems for slender steel frames. However, during the research process, we found an even more effective procedure, which would have at least the same accuracy and be far easier to implement in the existing software for wind turbine design. Before entering the technical description of the method, some arguments for a refined analysis will be mentioned.

The first issue is the composite material, which allows great freedom in the design process. In a design optimization, material will be removed from directions with low utility degree into more critical directions. This means that if the stresses either are neglected or inaccurately determined, the design may have too little strength in some directions. The second issue is that accurate stress determination is very important in joints where fatigue may occur. The third issue is on the challenges in modern design of wind turbine blades. Focus on weight, price and efficiency will rise in the future, and this means that designs will become much slenderer during the years to come, hence implying that some issues treated below may, at present, seem of more academic than practical importance. However, the history shows that more and more refined methods enter in design and analysis of wind turbine blades.

Generalized Brazier effect

The Brazier effect is illustrated in the Figures below. The Brazier effect arises due to the bending moment, which gives the beam a curvature. The normal stresses in each end

are rotated, and that results in an inward stress, which, in some papers, are denoted crushing pressure, see Figure 74 and Figure 75 below.

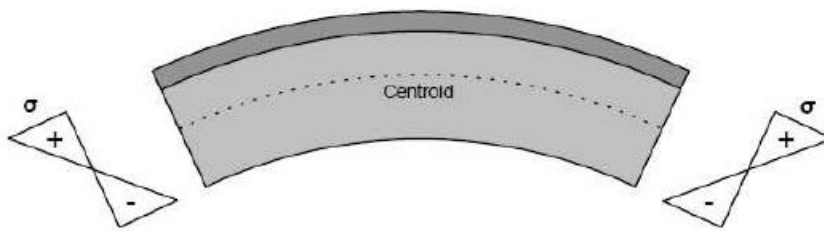


Figure 74 Distribution of the stresses from bending moment

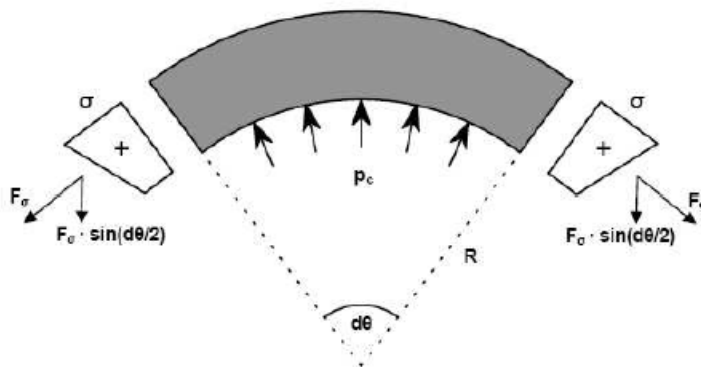


Figure 75 Resulting pressure due to bending of the beam,

The effect is geometrical nonlinear, and the crushing pressure will be proportional to the square of the bending moment. Brazier was, in his original work, focusing on the ultimate load capacity, and he calculated the maximum moment capacity. He did take into account that the geometry of the cross-section changed (ovalization). In the context of wind turbine blades, there will not be significant changes in the geometry; however, the influence of the stresses perpendicular to the beam axis (Crushing pressure) can be of high interest as the strength in this direction typically is low.

The torsional moment will also have a similar effect, but it is somewhat more difficult to illustrate and explain physically. In the Figure below, we have shown a hollow quadratic cross-section subjected to pure torsion. The deformations are scaled in order to pinpoint the effect. The shear stresses on each side are rotated, and this will result in a twisting moment of the cross-section. This can be compared to the so-called crushing pressure, and we have therefore denoted the combined non-linear effect of bending and torsion

as the Generalized Brazier effect. Introducing the non-linear effects will give a deformation figure similar to that depicted in Figure 76.

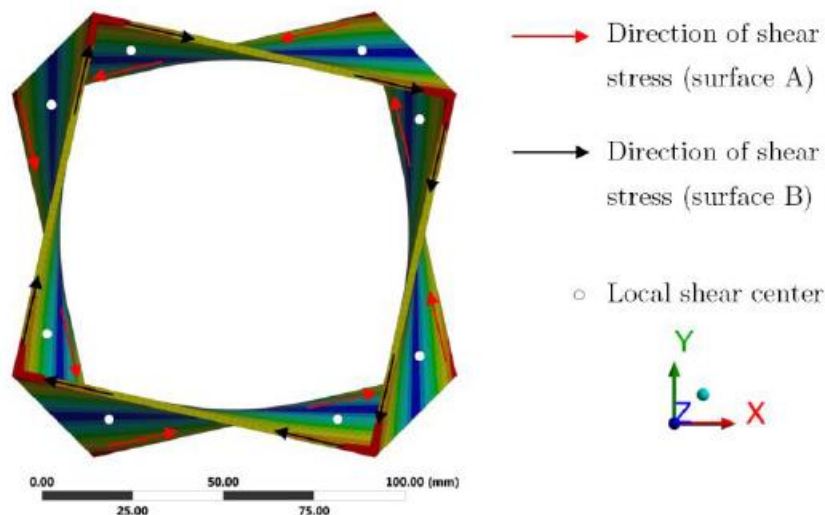


Figure 76 Generalized Brazier effect on a hollow section

The Generalized Brazier effect is illustrated on simple geometrical cross-sections, but it should be stressed that the effect also applies on more complicated geometries. Especially the torsional part is very important in slender, asymmetric profiles, which is found in wind turbine blades. The underlying theory will be published in an international journal.

The author has previously published a numerical method for calculating the Brazier effect in a Finite Element context. The method is very effective and can be seen as a postprocessing of a linear calculation, followed by calculating the load from the crushing pressure and finding the resulting stresses, as illustrated in the Figure below. It should be noted that the crushing pressure typically will lead to bending/shear in the individual parts of the cross-section. The shear forces are typically largest at the corners, and it has been shown experimentally that profiles fail in these regions.

The numerical method is very suited for Finite Elements, and the second-order effects are calculated in an element-by-element fashion. In the WP, we have extended the method to the Generalized Brazier effect, and basically it is only an extra part that has to be added to the load. The method has been implemented in Ansys as a so-called APDL (Ansys Parametric Design Language). It means that the calculations are done automatically based on a model of the wind turbine blade and a linear load case. Later examples will be shown on the effectiveness.

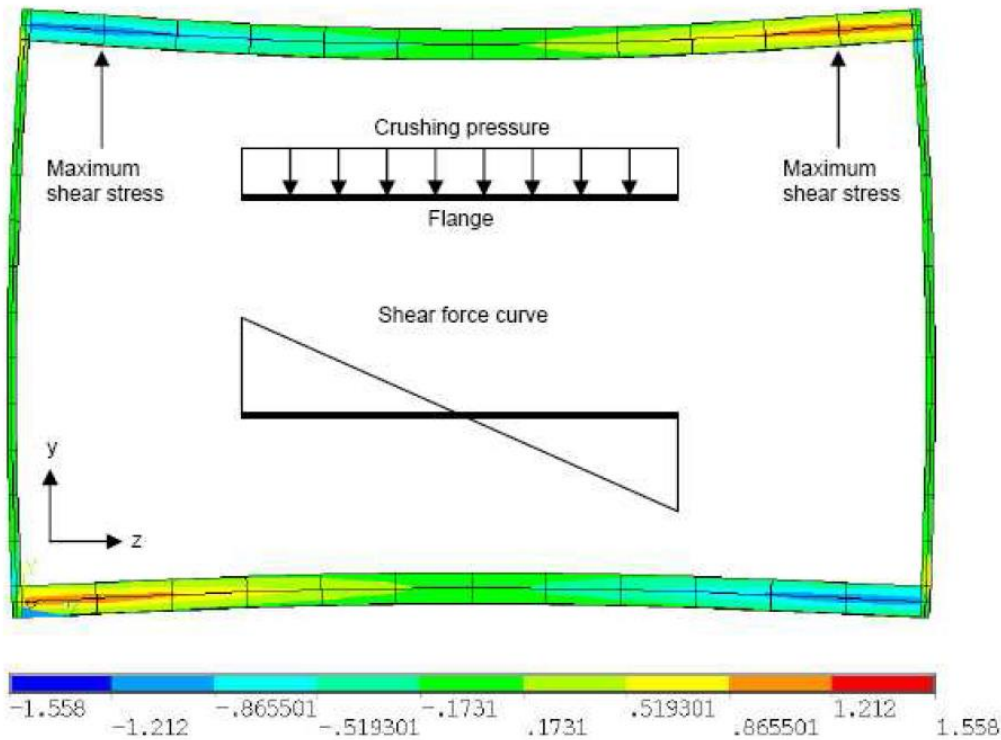


Figure 77 Brazier effect on a cross-section.

Generalized Brazier versus linear/non-linear analysis

Applying a full non-linear geometric analysis will be the most precise method; however, it should be noted that proper analysis of buckling/postbuckling phenomena would demand modelling of imperfections. This is highly complicated due to the stochastic nature of imperfections. There are some ad hoc methods which generally gives good results, but they are, to the author's knowledge, not used in analysis of wind turbine blades.

The major differences between the full-nonlinear analysis and the Generalized Brazier effect are

- Buckling is not dealt with in the Generalized Brazier effect as it by nature is a linear calculation. There could be added a linear buckling check based on the linear and the non-linear load.

- Changes of the cross-sectional profile, e.g., tapering. The effect is treated indirectly in the Generalized Brazier approach.

We have made calculations on an SSP 34 m blade from SSP Technology A/S, for which we had the geometry and material properties. The load cases are somewhat simplified, and is similar to some of tests in the Lex project.

The first effect is shown in Figure 78 below.

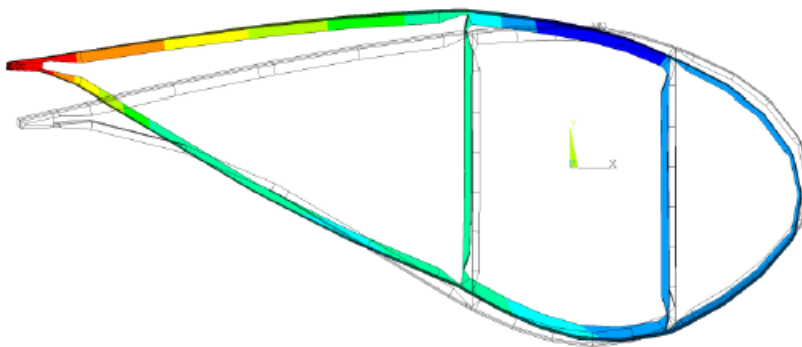


Figure 78 Deformations due to Brazier effect. Scaled 30:1.

The result of the Generalized Brazier effect is isolated, and it is seen that there is significant shear distortion. The in-plane cross-sectional deformations are most prominent in the trailing edge due to its low stiffness.

It also leads to the conclusion that shear distortion can be due to both the linear part (mentioned earlier) and the non-linear part.

In the Figure below, the normal stress perpendicular to the blade axis is illustrated.

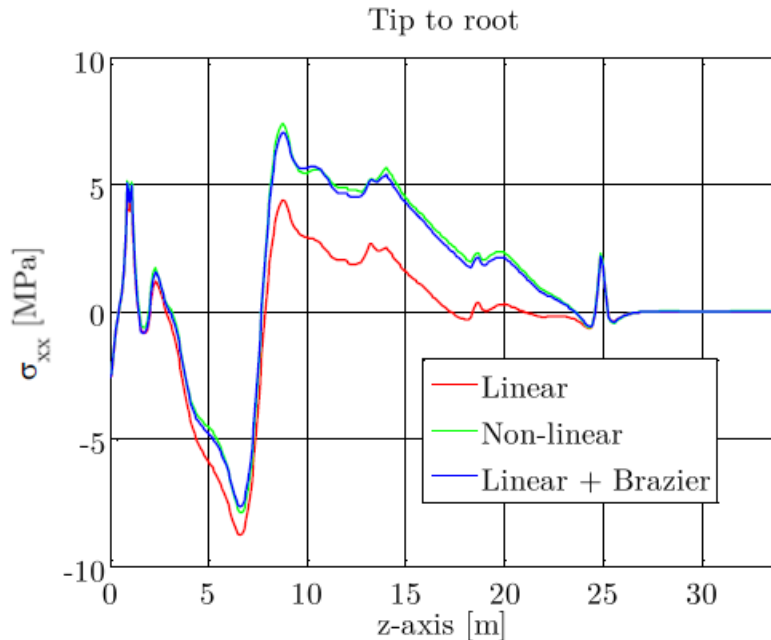


Figure 79 Variation of normal stress perpendicular to the blade axis.

It is clear that a linear calculation will be misleading. Even though that the stress level might be low the influence on fatigue/strength calculation can be much more pronounced in composite structures. It is also seen that the non-linear and the Generalized Brazier effect are very close. Numerous different comparisons have been conducted, and they all demonstrate the same tendency.

The Finite Element approach, the APDL and the results will be presented/published at a conference in October. The APDL code is available from the authors.

Influence of wind load and gravity

During the meetings between WP6, 7 and 8, the wind load was discussed. In the simulations, the distributed wind pressures are converted into 4 forces acting directly at the core of the blade. The 4 forces are determined in a way that ensures statical equivalence.

To the author's opinion, the wind turbine blade would experience a difference between the distributed and the concentrated loading. On a global scale, there would be no difference in, e.g., tip deflection. However, in local areas, there might be significant differences. In the Figure below, we have calculated the so-called influence surface for

the normal stress perpendicular to the blade axis. For completeness, there will also be areas where the influence is negative, but that has not been shown here.

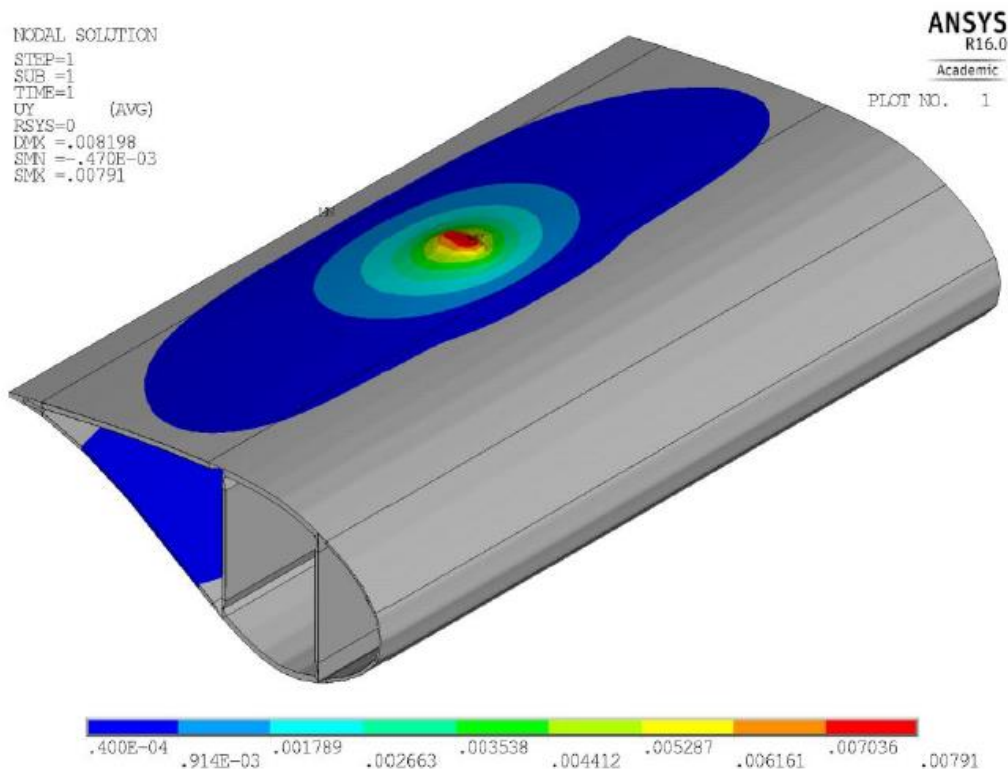


Figure 80 Positive influence surface for the normal stress perpendicular to the blade axis. The point A is in the red area.

The total stress in point A can be found by integrating the influence surface with the wind pressure. This will lead to resulting normal stresses perpendicular to the blade axis. This will not be the case if the wind loads attack directly in the webs. Definitely, this is not a conservative approach. Whether or not the simplified approach will have any significance can only be determined in specific cases. Unfortunately, we could not have access to the wind pressure. We plan to publish the observations of the effect of wind pressure, and, in this regard, we hope to find some reasonable wind pressure distributions.

Somewhat similar effect can be seen in the gravity load. In change of acceleration of the blade, the forces needed for acceleration will come from the forces in the web, which have to be transferred to the flanges by shear/bending; again resulting in normal stresses perpendicular to the blade axis.

Future Activities

The results obtained in the WP7 could be further exploited in different ways:

- Implementing the Generalized Brazier approach in optimization of the material layout of wind turbine blades. In this way, the non-linear geometric effect could be handled more effectively allowing for more design iterations.
- Implementing the Generalized Brazier approach as a postprocessor to the wind simulations results, e.g., the DTU-Risø Becas and Super Element approach.
- Investigating the influence of wind pressure and gravity. The influence will be more distinct in slender structures.

Other activities

The WP activity has also involved some other tasks not directly described in the purpose. The activities deal with 5 topics,

1. Several joint meetings with the WP6 and WP8. The original idea was to get a common understanding of the interface between the wind load calculation and the non-linear structural analysis. There were identified some limitations in the current procedure, which first of all deals with the information on the wind pressure distribution. This point has, in detail, been treated above. We also discussed non-linear versus linear calculations plus use of extended beam elements and superelement techniques. This issue has also been treated above, but not in detail as it is well-known techniques/theoretical results.
2. Several joint meetings with WP6 and WP7. Parts of the meetings dealt with dynamic analysis of the blade and stiffener, but Bladena changed focus, and therefore is this part not documented. On several occasions, Bladena had an employee in Esbjerg in order to improve his knowledge on Finite Element.
3. We recalibrated a Finite Element model developed by DTU, and we have send the result to Bladena. Our recalibrated model is able to describe both the static load case and the dynamic eigenfrequencies.
4. We also organized a workshop on finite element in Ringsted. The outcome of this is hard to judge as the audience had very different experiences.
5. We have also contributed to the Handbook.

WP8 Detailed Blade Modelling Implemented in Aero-Elastic

Torben Larsen, José Blasque, Anders Melchior Hansen, Peter Berring

Purpose

In the aeroelastic codes used today for load analysis of wind turbines, which is a crucial element of a wind turbine design procedure, the physical model of structure, aerodynamics, control is included. However, even though as the aeroelastic model is fundamentally based on the physical behaviour of the wind turbine, each sub model is reduced in complexity so that simulations are practically feasible to carry out for the large number of design load cases typically used. With simple wording, one can say that the models used shall be: *“as simple as possible, but still as complex as necessary”*. The complexity depends on the structure and the particular focus area, which, for research projects, can vary significantly with practically no upper limit on the complexity. In design situation the approach is more mainstream. In general, the validity of the models is based on validations from comparisons between simulated and measured load levels for previous generations of wind turbines. An example of such validation can be found in [1] and [2]. As the purpose of the aeroelastic simulations is to simulate the dynamic behaviour of the wind turbine and output sensor values as function of time. Such sensors could typically be cross sectional shear force or bending moments, rotor speed, pitch angle, blade tip deflection or acceleration levels used for the detailed stress and strain analysis of the wind turbine components. The simulated time series are post processed to find the equivalent 20year fatigue load levels as well as the 50year extreme loads.

HAWC2 – Timoshenko beam

The applied method today when it comes to how blades are modelled is based on technical beam properties. This means that the detailed information about fiber layout, resin, glue etc. is condensed into equivalent cross sectional information consisting of: Mass/length, areal and mass moment of inertias, torsional stiffness, Young’s modulus of elasticity, shear center location, elastic centre location, and orientation of principal bending axis. An important assumption is that the cross sectional properties are unaffected by the neighbouring areas of the blade, hence a pure 2D behaviour is assumed, see Figure 81. Furthermore, as the beam elements are prismatic it is assumed that the local properties remain constants for any deformation and displacement, which again requires that local geometric deformations in the cross section are very small.

One of the problematic issues with these data are how to extract the cross sectional data so the input corresponds to the real blade properties. Another issue is that the technical beams used in the aeroelastic code typically are prismatic. This means that for

the individual beam tapering and twisting is ignored. Only by having a not too coarse beam resolution, these effects of taper and twist are included by a stepwise change over the blade length, which then pose a minimum resolution of number of beams to model a full blade. A typical blade of 50m is modelled using 20+ beam elements.

The detailed theory for the Timoshenko beam element can be found in [4]**Fejl!** **Henvisningskilde ikke fundet.**, whereas the multibody coupling approach can be found in [6]. It should be noted that geometric nonlinear effects resulting from large deflections are including by a proper division of the blade into several sub bodies as the elements used by itself are linear. An example of such effect is eg. the blade radius which for a straight blade modelled as a linear structure remain constant no matter the flapwise deflection. For a model with the geometric nonlinear effects included (by a proper subdivision of the blade into several subbodies) the rotor diameter reduces when the blade deflects. These geometrically nonlinear couplings also affect the structural couplings between flap, edge and torsion as the blade deflects. Local deformation of the cross sectional geometry is however not included as this is not part of the Timoshenko beam model. In order to find the local blade stresses a FE model of the blade has to be used.

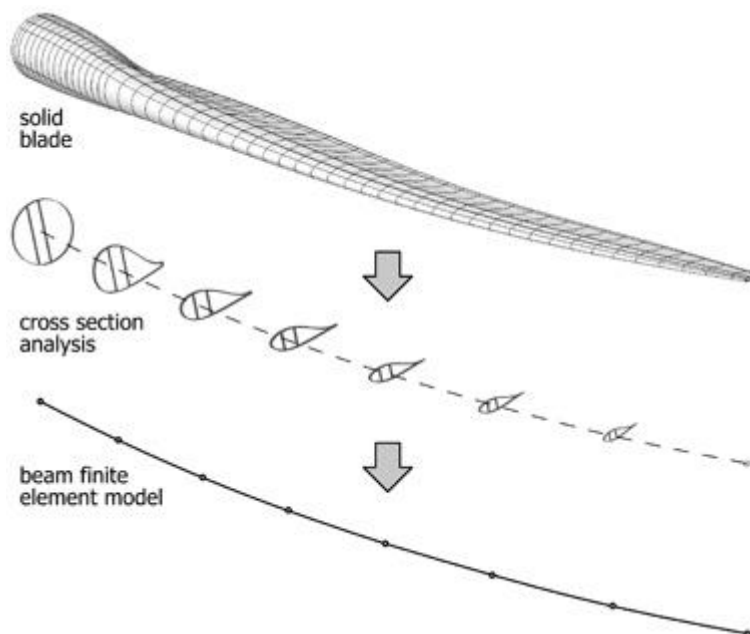


Figure 81. Principle of reducing information from a full blade into cross sectional data which is finally used for finite element beam model used in the aeroelastic analysis.

In the following a simple method to extract blade structural 2D properties for HAWC2 from a 3D Finite Element Model is presented. Details can be found in [3].

The different steps in the basic extraction method for computing the structural properties for HAWC2 are described in the following:

The bending stiffness denoted by the the product $E \cdot I_x$ for the flapwise stiffness is found from FE model by subjecting the blade model to a pure flapwise bending moment with respect to the global coordinate system. The longitudinal strain, at the outer layers, along two paths on the pressure and suction side are reported. The location of the two paths is the middle of the suction and pressure caps. A least squares method is applied to describe the strain response and reducing the noise caused by ply drops etc. The mean strain is computed along the blade and as the moment distribution and locations of the two paths are known, the flapwise stiffness can be determined as:

$$EI_{\text{flap}}(z) = \frac{M_{\text{flap}}(z) \cdot \frac{\text{Profile_height}(z)}{2}}{\varepsilon_{\text{mean}}(z)}$$

The method for computing the edgewise stiffness is similar to the method described for the flapwise stiffness. In this case the blade model is subjected to a pure edgewise bending moment with respect to the global coordinate system. The longitudinal strain at the outer layers along two paths is reported. The locations of the two paths are the trailing edge and the leading edge of the blade profiles. Again a least squares method is applied to describe the strain response and reducing the noise caused by ply drops etc. The mean strain is computed along the blade and as the moment distribution and locations of the two paths are known the edgewise stiffness can be determined as:

$$EI_{\text{edge}}(z) = \frac{M_{\text{edge}}(z) \cdot \frac{\text{Profile_height}(z)}{2}}{\varepsilon_{\text{mean}}(z)}$$

As a first order approximation the orientation of the principle axis and the structural pitch can be assumed to be identical.

A 2x2 stiffness matrix as depicted below was created:

$$EI(z) = \begin{pmatrix} EI_{\text{flap}}(z) & 0 \\ 0 & EI_{\text{edge}}(z) \end{pmatrix}$$

The stiffness matrix was transformed into the assumed principle axis via:

$$R(z) = \begin{pmatrix} \cos(\alpha) & -\sin(\alpha) \\ \sin(\alpha) & \cos(\alpha) \end{pmatrix} \quad EI_{local}(z) = R(z) \cdot EI(z) \cdot R(z)^T$$

Where α is the orientation of the chord along blade with respect to the global coordinate system (rotor plan). The angle α was found using a pure flapwise load situation where the 2D FE model resulted in both flap and edgewise deflections. The angle α was adjusted in order to obtain similar ratio of flap and edgewise deflection.

The following constitutive relation between moments and curvature can be given as below. For different load configurations the displacement field is computed by means of integration. This were performed and compared with the response of the detailed 3D FE-model. Miner fine tuning were performed to match the results.

$$\begin{pmatrix} \kappa_x(z) \\ \kappa_y(z) \end{pmatrix} = EI_{local}(z) \cdot \begin{pmatrix} M_{flap}(z) \\ M_{edge}(z) \end{pmatrix}$$

In order to find the torsional stiffness GJ, the FE-model of the blade was subjected to a torsional moment and the twist angles along blade were inserted via MPC-elements of the type RBE3, as these does not constrain the cross sections. The torsional stiffness can be determined as:

$$GJ(z) = \frac{T \cdot L_e}{\Delta r_z}$$

Were Δr_z is the relative twist angle between cross sections and L_e is the length between cross sections.

The axial stiffness was found by subjecting the blade model to an axial load and the displacements along blade were inserted via MPC-elements of the type RBE3. The axial stiffness was determined as:

$$AE(z) = \frac{F_z \cdot L_e}{\Delta u_z}$$

Were Δu_z is the relative displacement in the z-direction between cross sections and L_e is the length between cross sections.

In this simplified scheme the shear stiffness was assumed to be 0.5 in agreement with typical assumptions.

In this simplified scheme The location of the two elastic and shear center was assumed to be identical with the location of the half chord coordinates.

The mass properties for the structural input such as mass per length, center of gravity and radius of gyration was exported directly from the FE tool MSC.Patran.

For the SSP34 blade the resulting natural frequencies was found.

Table 11 Mode shapes and natural frequencies of a blade fixed to the root

Mode shape	Frequency [Hz]
1 st Blade flap	1.09
1 st Blade edge	1.60
2 nd Blade flap	3.00
2 nd Blade edge	5.53
3 rd Blade flap	6.13
3 rd Blade edge	10.66
4 th Blade flap	12.09
5 th Blade flap	14.23
1 st Blade torsion	16.37

Table 12. Structural damping based on the used Rayleigh damping coefficients

Mode shape	Structural damping [%]
1 st Tower bending	2.0
1 st Blade flap	3.0
1 st Blade edge	3.0
2 nd Blade flap	8.2
2 nd Blade edge	10.5
1 st Blade torsion	43.9

A turbine model was setup with typical properties from a 2MW turbine and a pitch regulated variable speed controller was tuned for the turbine. Finally, the IEC61400-1 load cases used for fatigue load simulation was simulated in HAWC2. Based on these simulations, the time series was postprocessed with respect to fatigue based on a typical Weibull distribution with $C = 9.6$ and $k = 2$. A summary of the 20year loads for the SSP4 with $m=12$ and $n=10^7$ is given in

Table 13.

Table 13. 20-year fatigue loads of the SSP34 blade extracted based on an equivalent number of cycles of 10⁷

Radius [m]	Mx (kNm)	My (kNm)	Mz (kNm)
0	2181	1661	20,7
2	1965	1437	17,3
4	1755	1238	36,6
6	1550	1057	52,1
8	1349	892	51,3
10	1160	743	47,1
12	977	607	44,2
14	813	485	39,1
16	651	377	34,9
18	516	284	29,4
20	392	206	24,1
22	287	143	19,3
24	197	92,4	15,1
26	125	54,8	10,7
28	68,8	28,5	5,92
30	29,8	11,7	3,7
32	9,3	2,8	1,4

As equivalent blade fatigue data is normally presented for a slightly higher number of load cycles than used in full scale blade fatigue test, the load in

Table 13 can be recalculated based on

$$R_{eq,new} = R_{eq,old} \left(\frac{n_{eq,old}}{n_{eq,new}} \right)^{1/m}$$

Where R_{eq} is the equivalent bending moment and n_{eq} is the associated number of loadcycles and m is the wöhler exponent.

HAWC2 – BECAS. Full populated stiffness matrix

Introduction

This section of the report presents a novel framework for the structural design and analysis of wind turbine blades and establishes its accuracy. The framework is based on the BEam Cross section Analysis Software – BECAS – a framework for structural analysis of wind turbine blades. BECAS can take into account the effects of material anisotropy (from, e.g., fiber orientation) and correctly estimate torsional stiffness, a feature previously deemed unimportant when analyzing shorter blades. These new features make it possible to incorporate new blade technologies like aeroelastic tailoring for load mitigation through material and geometrical design. The internal forces and moments at each section of the blade stemming from nonlinear aeroelastic analysis can be seamlessly transferred to the cross section analysis tool. It is then possible to accurately assess the structural performance of the blade with a high level of detail down to the material level with a very low computational effort. BECAS was used extensively for the design of the DTU 10MW reference wind turbine [9],[10]. The workflow devised using BECAS is described in Figure 82. The pre-processing step concerns the generation of input for the cross section analysis tool based on existing information of the blade. BECAS currently encompasses a number of solutions for automatic input generation based on, e.g., existing shell finite element models. The stiffness and mass properties are then computed by the cross section analysis tool and used as input for the wind turbine aeroelastic simulation tool (e.g., HAWC2 [8]). The internal cross section forces and moments resulting from wind turbine aeroelastic simulations are finally returned to BECAS, and used, e.g., for the analysis of the local strain and stress fields at a cross section level. The proposed framework is very efficient and therefore ideally suited for integration within wind turbine aeroelastic design and analysis tools. A number of benchmark examples are presented here comparing the results from the proposed beam model to 3D shell and solid finite element models. The examples considered include an entire wind turbine rotor blade and a detailed wind turbine blade cross section. The benchmark examples show excellent agreement suggesting that the proposed framework is a highly efficient alternative to 3D finite element models for structural analysis of wind turbine blades. All results presented here have been published and discussed in much further detail in [7].

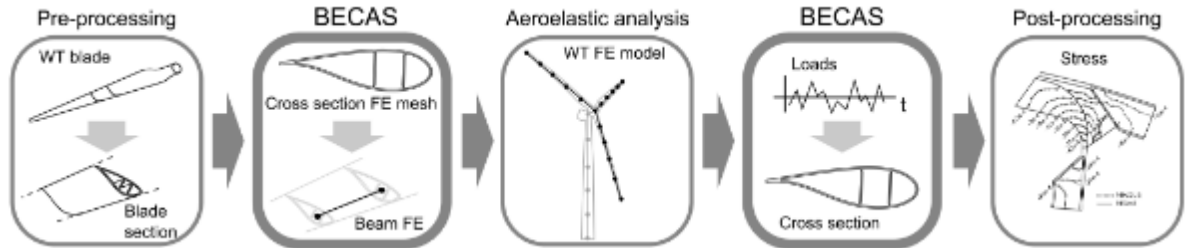


Figure 82 - Schematic description of the workflow used for the structural design and analysis of wind turbine blades based on the cross section analysis tool, BECAS.

Validation

The results obtained using the beam finite element framework based on the proposed cross section analysis tool are presented and validated in this section. Two different numerical examples were considered. The first example considers the DTU 10MW reference wind turbine rotor blade presented in [9],[10]. BECAS was extensively used in the design of this blade. Hence, the results presented here serve to further establish the accuracy of the proposed method when used within such wind turbine blade design frameworks. In the second example, the interest was on the detailed analysis of local phenomena at the cross section scale, namely, strains and stresses at the material level. In this example the geometry, materials distribution, and structural layout of a wind turbine cross section were defined in great detail. This example serves to establish the accuracy of the proposed method when working at later stages of the design process where a great level of detail has been reached. For all numerical experiments the displacements and rotations were assumed small and varying linearly with respect to the loads. The structural stiffness, frequency, and strength responses were analyzed using beam finite element models generated based on BECAS, henceforth referred to as BECAS models. The results were compared against detailed 3D finite element models discretized using shell and solid finite elements. The load cases for each of the validation examples are compiled in Table 14.

Table 14 - Load cases considered for each of the validation examples presented in Table I. Load case SLC1 is a vertical force applied at the tip of the square beams S1, S2, and S3. Load cases BLC1 and BLC2 are associated with the DTU10MW, where the load application point is the half-chord point of the respective cross section. The torsional moment m_z in BLC1 is applied only in the beam finite element model in order to compensate for the offset between the beam nodal positions and the half-chord position. Load case DLC1 and DLC2

associated with the DWT are internal cross section forces and moments defined according to the cross section coordinate system in Figure 12.

DTU 10MW RWT blade (DTU10MW)	BLC1	z	[m]	20.1	30.4	33.0	47.7	52.0	62.4	63.8	76.2	84.8
		f_x	[kN]	0.0	0.0	290.0	180.0	0.0	130.0	0.0	18.0	25.0
		f_y	[kN]	230.0	270.0	0.0	0.0	250.0	0.0	220.0	190.0	165.0
	m_z	[kNm]	-122.7	-226.5	-27.1	-8.0	-170.8	-0.6	-111.9	-74.0	-46.9	
	BLC2	z	[m]	89.166								
Detailed WT blade section (DWT)	DLC1	T_y	[MN]	1								
		M_x	[MNm]	-30								
	DLC2	M_x	[MNm]	1								

DTU 10 MW RWT

The 86.37m long rotor blade of the DTU 10 MW reference wind turbine (DTU10MW RWT) was considered here. A total of 51 cross sections along the blade length were defined as presented in Figure 83. The cross section coordinate system of each section was placed at the half-chord point with the axis parallel to the blade coordinate system shown in Figure 83. For the development of the BECAS based beam finite element model the stiffness and mass properties were analyzed at each of these sections. The cross section finite element mesh was generated automatically based on the shell finite element model as shown in Figure 84. The beam finite element model of the blade was then obtained by integration of these properties. The results obtained using the BECAS model were compared against the ABAQUS 3D shell finite element model (3DFEM).



Figure 83 - Baseline cross sections and coordinate system of DTU 10 MW reference wind turbine rotor blade.

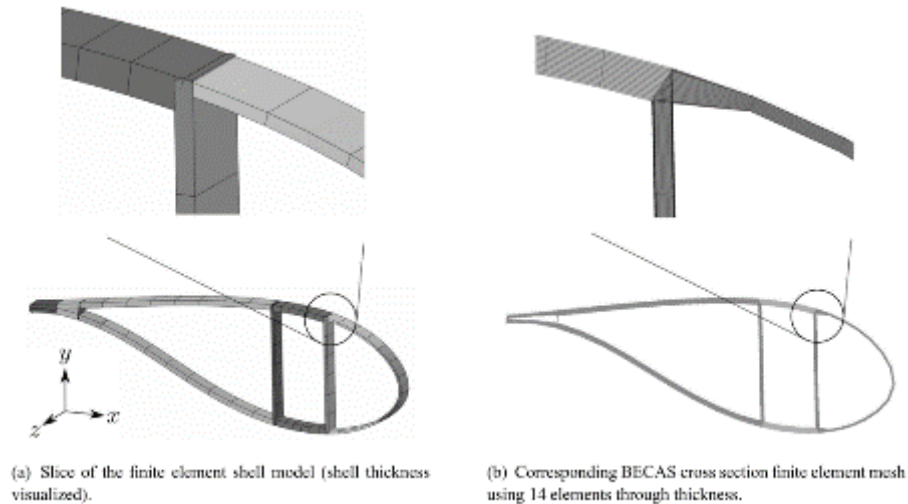


Figure 84 - The BECAS cross section finite element mesh (b) is generated automatically based on the shell finite element model (a).

Two load cases were considered – BLC1 and BLC2 as described in Table 14. In load case BLC1 the blade was loaded by 11 concentrated forces – 6 forces in the flapwise direction (f_y) and 5 forces in the edgewise direction (f_x). The forces were defined in such a way that the resulting distribution of bending moments closely approximates the distribution of the ultimate bending moments resulting from the aeroelastic computations as described in [9],[10]. In load case BLC2 a torsional moment was applied at the tip of the blade. The ability to correctly estimate the torsion response was one of the main motivations for the development of BECAS. Hence this load case was introduced so that the accuracy of the torsional response of the wind turbine blade could be assessed individually. The most relevant components of displacements and rotations at each of the 51 sections calculated using both BECAS and the 3D shell finite element model are compared in Figure 85 for both load cases. The strains were measured along three different paths defined along the length of the blade as indicated in Figure 86. The relevant components of the strain are compared in Figure 87 for both load cases. Finally, the six lowest natural frequencies are compared in Table 15.

Table 15 - Six lowest eigenfrequencies for DTU 10 MW RWT rotor blade calculated using BECAS and ABAQUS shell finite element model (3D FEM). The labels flapwise (flap), edgewise (edge) and torsional (torsion) are indicative of the predominant motion observed for each of the eigenmodes.

Freqs. [Hz]	f_1 (flap)	f_2 (edge)	f_3 (flap)	f_4 (edge)	f_5 (flap)	f_6 (torsion)
BECAS	0.62	0.95	1.75	2.80	3.57	5.69
3DFEM	0.61	0.95	1.75	2.84	3.58	5.69
Rel. Diff. [%]	-0.72	0.61	0.25	1.54	0.37	-0.04

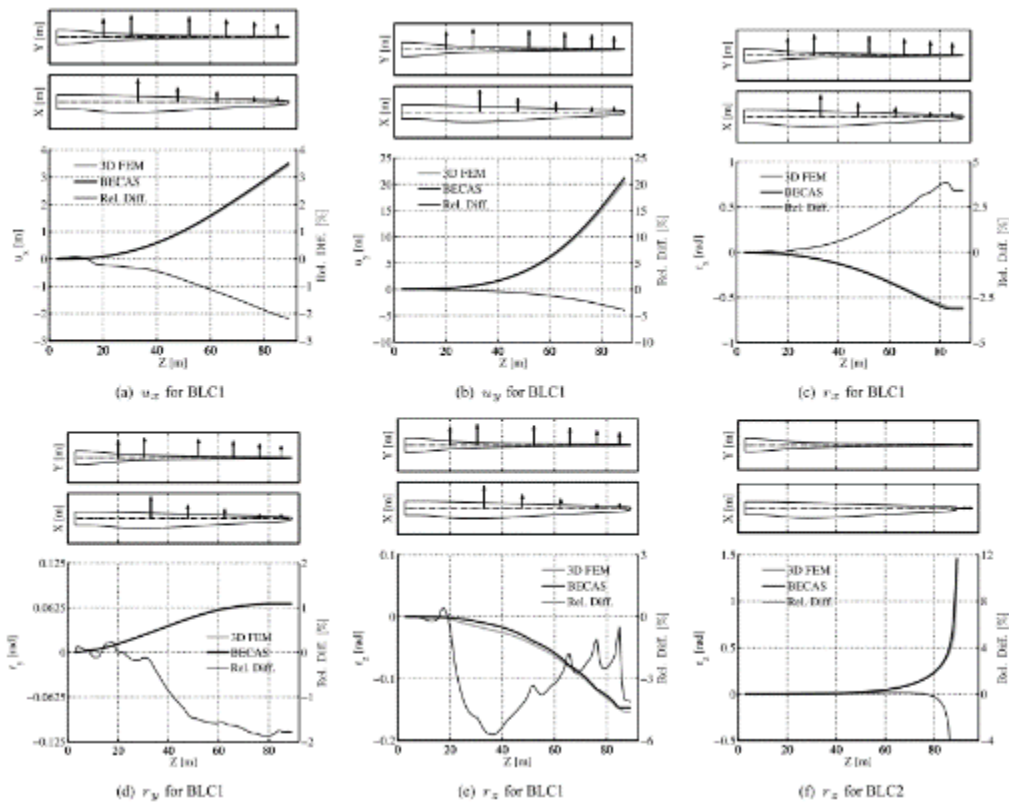


Figure 85 - Comparison of displacements in the DTU 10 MW reference wind turbine blade determined using BECAS and a shell finite element model in ABAQUS (3DFEM). Results for load case BLC1 (flap and edgewise bending) and BLC2 (torsion), cf. Table 14.

Detailed wind turbine blade cross section

In this validation example we focused on the analysis of the strains and stresses on a generic wind turbine blade cross section where the structural lay-out was defined with great detail. The cross section geometry, finite element mesh, coordinate system, and location of reference, shear, mass, and elastic centers along with the elastic axes as determined by BECAS are presented in Figure 88. The outer shell consisted of a sandwich structure with an inner core material (Core) and faces composed of a tri-axial laminate (TRIAX). The suction and pressure side shells were bonded to each other and to the load carrying spar by an adhesive (Adhesive). The spar caps consisted mainly of uni-directional fibers (UD) while the shear webs were sandwich structures with a core material (Core) and layers of a bi-axial laminate (BIAX) in the faces. The material distribution at a detail of the junction between shear web and the cap is presented in Figure 91(a). Two load cases were considered in this validation example – DLC1 and DLC2 as defined in Table 14. In load case DLC1 the cross section was subjected to a transverse force $T_y = 1 \times 10^6$ N and a bending moment $M_x = -30 \times 10^6$ Nm. This is similar to subjecting the blade to a flapwise load. In load case DLC2 the cross section was subjected to a torsional moment $M_z = 1 \times 10^6$ Nm.

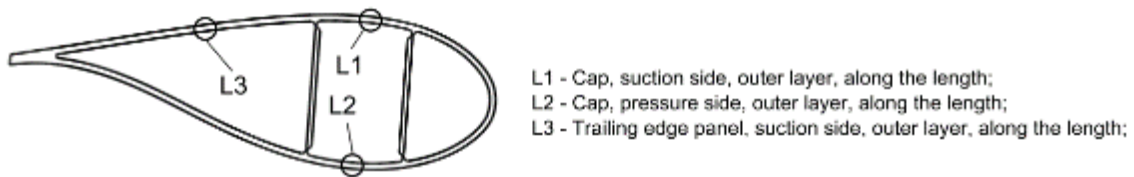


Figure 86 - Schematic wind turbine blade section indicating the location of the longitudinal paths used in the analysis of the strains in the DTU10MWRWT rotor blade. Strains along these paths are presented in Figure 87.

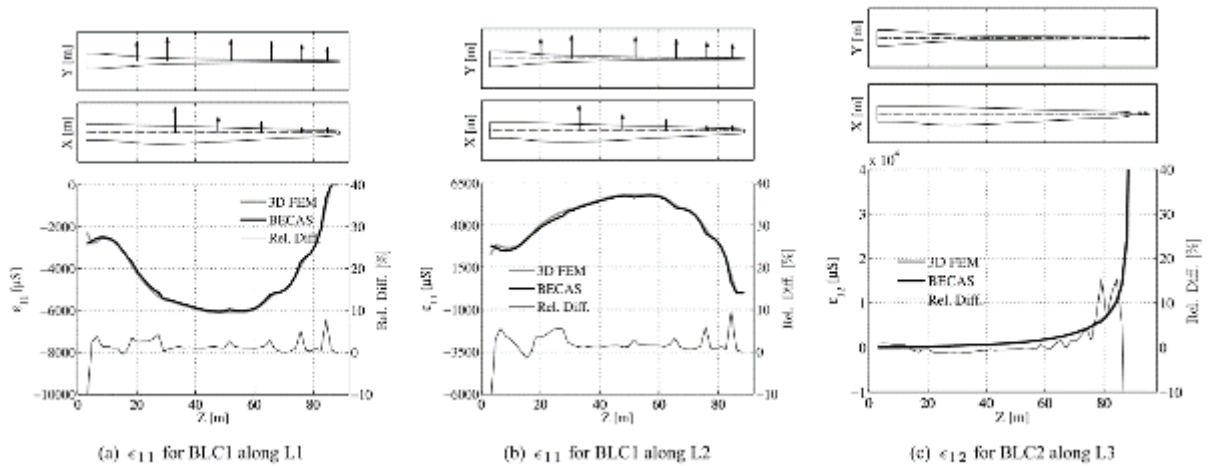


Figure 87 - Strains in the DTU 10 MW reference wind turbine blade determined using BECAS and a shell finite element model in ABAQUS. The location of the longitudinal paths are indicated in Figure 86. Results for load case BLC1 (flap and edgewise bending) and BLC2 (torsion), cf. Table 14. (a) and (b) Axial strains ϵ_{11} for load case BLC1. (b) In-plane shear strains ϵ_{12} for BLC2.

The results from BECAS were compared against a 3D solid finite element model in ABAQUS. The finite element mesh was generated through extrusion of the cross section mesh presented in Figure 88. The result was a 60m long solid finite element model of a beam of constant cross section meshed with 20 node layered solid finite elements (ABAQUS element type C3D20). The model was clamped at one end while tip forces and moments were applied at the opposite end. The loading was chosen such that it induces the same internal forces and moments as in DLC1 and DLC2 at the cross section of interest, i.e., at the central section of the beam, 30m from the ends, where the strains and stresses were analyzed. The length was chosen to ensure that the effect of the boundary conditions does not affect the results. The strains and stresses estimated by both numerical models were finally compared. The six stress components were evaluated along paths defined in Figure 89. The results obtained from each model for different paths, load cases, and stress components are presented in Figure 90. Finally, the six components of the strains at a detail of the connection between the shear web and the cap were analyzed. The shear strain ϵ_{12} in the material coordinate system resulting from the DLC1 load case is compared in Figure 91(b).

Discussion

Regarding the validation results obtained based on the DTU10MW RWT blade. The eigenfrequencies obtained using the BECAS based beam finite element model and 3D shell finite element model (3DFEM) are in very good agreement, the largest deviation being 1.54%. Note that these frequencies match well also with those reported in [10] obtained using BECAS for the analysis of the cross section properties but relying on a different beam finite element formulation implemented in HAWC2 [8]. Overall the blade deformation results presented in Figure 85 are in good agreement for both load cases. The results suggest that the BECAS model is generally more compliant than the 3DFEM model. This may partly be due to the mesh generation procedure illustrated in Figure 84. This procedure may generate small discrepancies in the material distribution between the BECAS and shell finite element model which then affects the stiffness and mass properties and ultimately can be observed in the structural response of the models. The irregularities in the lengthwise variation of the torsional rotation given by the 3DFEM model suggest that these moments induce significant local deformation. The local effect of the loads is only partly captured by the beam model and is perhaps the reason for the deviation between the two models. These local effects are negligible for the other blade deformation results obtained for the same load case. The effect of the loads is also visible in the strain results presented in Figure 87. For both load cases there is a very good match between the strains obtained by BECAS and the 3DFEM model. Note that, in accordance with the blade deformation results, the strain results for load case BLC1 also indicate that the BECAS model is generally more compliant than the 3DFEM model for both load cases. The strains from BECAS are offset by approximately 1% everywhere except in the vicinity of the load application points where the deviation is larger. For the torsional load case BLC2 the deviation is practically negligible although increasing significantly close to the tip where the moment is applied, as expected. Finally, note that the strains obtained by BECAS do not account for tapering, twist and spanwise curvature which is naturally accounted for in the 3DFEM model. However, in the inner part of the blade where these geometrical features are more pronounced the deviations are not larger, suggesting that their effect on the strains is of minor importance in the regions where the strains were measured.

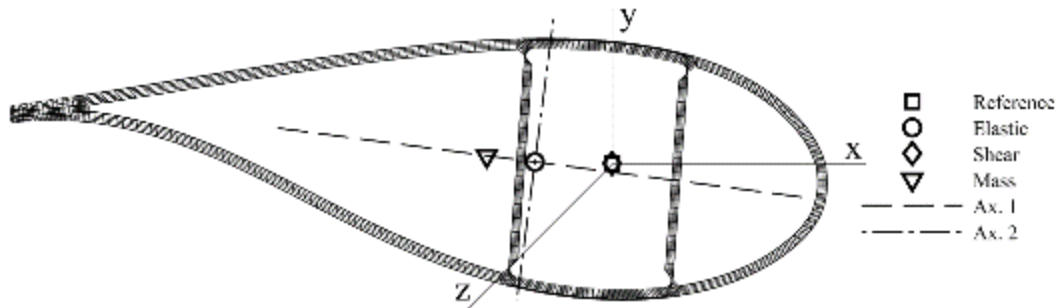


Figure 88 - Detailed wind turbine blade cross section (DWT) finite element mesh and coordinate system. Reference, elastic, shear, and mass center positions, and elastic axis orientation as calculated by BECAS.

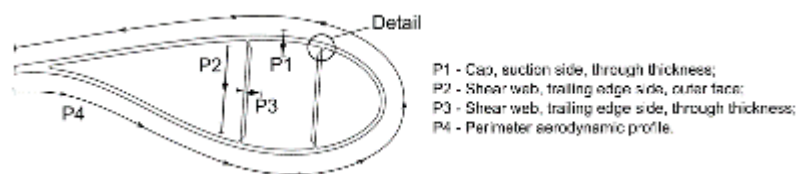


Figure 89 – Schematic wind turbine blade section indicating the location of the paths used in the analysis of the stresses in the detailed wind turbine blade cross section (DWT). Stresses along these paths are presented in Figure 90.

The last example concerns the analysis of the strains and stresses in a detailed wind turbine blade cross section. The stresses presented in Figure 90 analyzed along the different paths match very closely for all load cases and stress components, the largest deviation being less than 1%. The last results concern the stresses at a the connection between the shear web, cap, and leading edge panel as presented in Figure 91. The analysis of the stresses in this region is specially challenging since it is composed of many different materials (e.g., uniaxial and triaxial laminates, core material, and adhesive) and joins different types of panels (e.g., the monolythic laminates in the caps with the sandwich panels of the leading edge and shear web). The BECAS and the 3DFEM model results show a very good match thus attesting the ability of BECAS to correctly account for different material effects and accurately predict complex 3D strain and stress fields. In general, the set of results presented in this paper suggests that the proposed framework is suitable for the structural analysis of wind turbine blades.

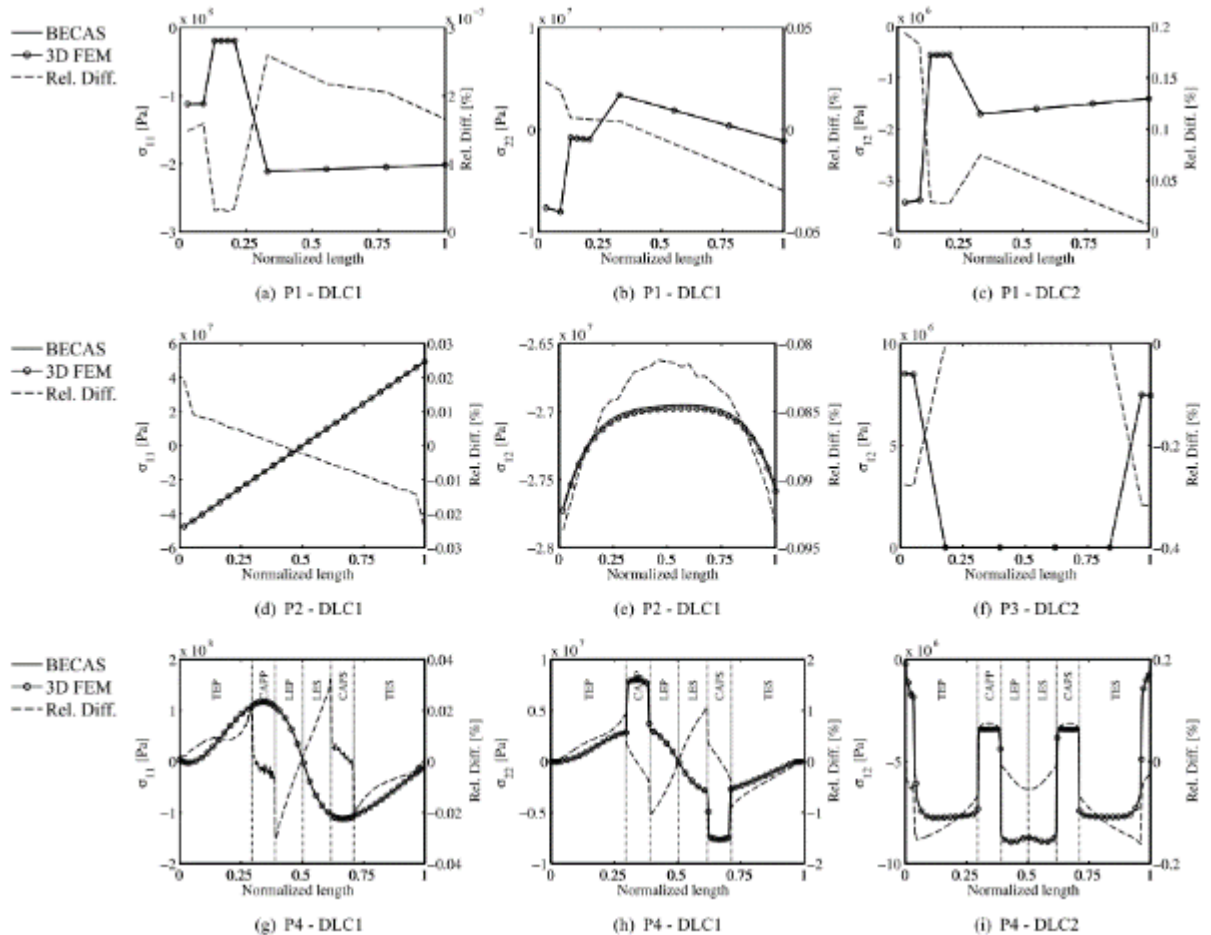


Figure 90 - Results by BECAS and 3D FEM for detailed wind turbine blade cross section. Cross section subjected to load cases DLC1 (flapwise bending) and DLC2 (torsion), cf. Table 14. Stress components σ_{11} , σ_{22} and σ_{12} evaluated at element centers along paths P1 (spar cap, suction side, through thickness), P2 (shear web, from suction side to pressure side), P3 (shear web, through thickness), P4 (around the perimeter of the aerodynamic profile), cf. Figure 89. For P4 each region is identified: TEP (trailing edge panel pressure side), CAPP (spar cap pressure side), LEP (leading edge panel pressure side), LES (leading edge panel suction side), CAPS (spar cap suction side), TES (trailing edge panel suction side).

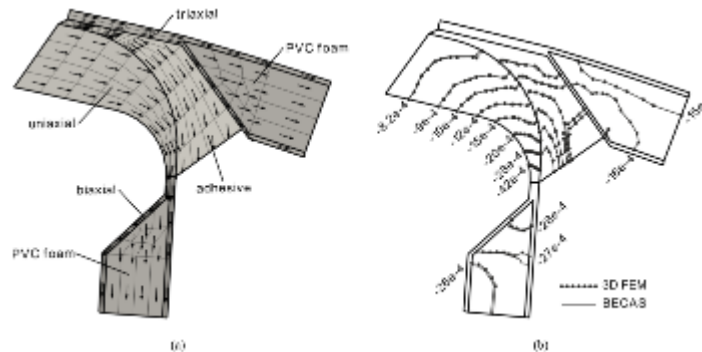


Figure 91 - Results at the junction between the caps, shear webs, and leading edge panels of the detailed cross-section (see Figure 88). Cross section subjected to load cases DLC1 (flapwise bending), cf. Table III. (a) Material distribution and principal fiber plane orientations. (b) Strains ϵ_{12} in material coordinate system analyzed at element centroids.

Conclusions

This work assesses the accuracy of the BEam Cross section Analysis Software – BECAS – a computational framework for structural analysis of wind turbine blades. Two validation examples were considered - an entire wind turbine blade and a detailed wind turbine blade cross section. The validation work focused on phenomena at the blade length scale (i.e., blade deformation and eigenfrequencies) and cross section length scale (i.e., material strains and stresses). Results generated by the BECAS based beam model were compared with 3D shell and solid finite element models generally showing a very good agreement. Yet, the ability of the BECAS framework to separate the 2D problem at the cross section scale from the blade length scale allows for much greater computational efficiency than that of 3D shell and solid finite element models. Finally, it is worth noting that the source code of the entire framework is distributed free of charge for academic use.

HAWC2 – 3D FEM super element

Introduction

The objective of the present work is to investigate if it is possible to base the blade model in the aeroelastic code, HAWC2, on a detailed 3D FEM model as an alternative to the beam elements presently used inside HAWC2. There are many good reasons for doing this in general, however, the main reason in the context of LEX is to enable handling of the structural add-ons in aerolastic calculations. These add-ons are located at discrete locations inside the blade and introduces large stress changes along the blade axis which will be difficult for the beam models to capture. In a 3D FEM model, the add-ons can be modelled in detail, and the effect of their prescence is directly captured.

A 3D FEM model of a blade can contain millions of degrees of freedom (DOFs) while the FEM model of a blade in HAWC2 normally has 40-100 DOFs. Time simulation with millions of DOFs is not realistic, so first challenge is to reduce the many DOFs of the 3D FEM model into the same number of DOFs presently used for blades in HAWC2. The result from such a reduction is called a super element (SE) in the next sections.

Another challenge is to capture the fictitious forces acting on the blade during operation; when blades rotate and vibrate, they are exposed to fictitious forces e.g. centrifugal forces. These force contributions must somehow be represented in the SE. Apart from the fictitious forces, the aerodynamic and gravity forces must also be applied to the SE blade.

This section presents a summary of the SE methodology (in words) and presents results related to eigenfrequencies and time simulation of the DTU 10MW reference wind turbine [9],[10].

Summary of work

This section describes the SE methodology in words. For details, see [18].

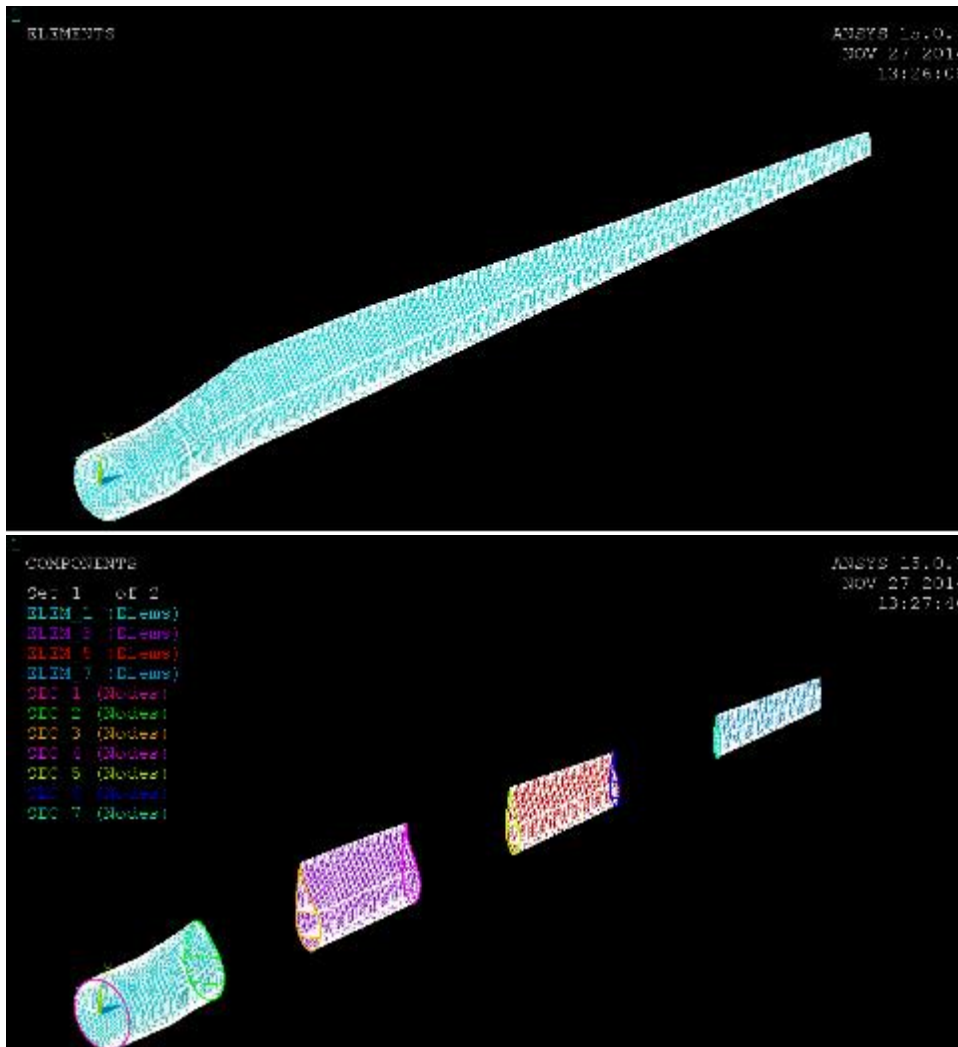


Figure 92: Ansys finite element model of the 10MW DTU blade

The first step going from a full 3D FEM model to a reduced model is the reduction step which is explained next; a user-specified number of sub-set of nodes in the 3D FEM model are selected and used as reference nodes for the same number of SE nodes, and all other nodes are statically condensed. The assumption behind the statically condensed nodes is that the nodes are not exposed to any external forces, which is of course not entirely true since the aerodynamic forces are applied to the blade. The assumption related to the SE nodes is that a force/moment vector load applied to the SE nodes is distributed among the related FEM nodes in a prescribed way dependent on the SE node type. So far, two distribution types can be selected, one which fixes the

3D FEM nodes so that they move rigidly relative to the related SE node, and one where the mean displacement and rotation of the 3D FEM nodes are equal to the displacement and rotation of the SE node.

To exemplify, a FEM model of a wind turbine blade is shown in Figure 92; the top figure shows the entire blade model (approx. 500.000 DOFs) and in the lower figure some of the elements are removed to show the sections. The 8 sections shown in the figure contain the sub-set of nodes which are related to the SE nodes – all the other nodes are statically condensed while the nodes in each section are condensed into 6 DOFs using one of the distribution of forces from the previous paragraph. In this particular case, the number of DOFs is reduced from several hundred thousand to 48 (8 sections times 6 DOFs/section).

Next step is to include the fictitious forces. This is done by fixing one of the SE nodes relative to a floating frame of reference so that all SE nodes displace and rotate relative to this frame. By formulating the equations of motion (EOMs) using the virtual work principle including the rigid body displacements and rotations related to the frame, the fictitious forces can be identified. It is shown in [19] that the EOMs of the SE, including fictitious forces and gravity, can be formulated based on the stiffness, damping, and mass matrices of the 3D FEM model, plus the 12 external force vectors corresponding to prescribed motion of the structure. These motions are; linear acceleration in the principal directions (3), rotational acceleration about principal directions (3), rotational velocity about principal directions, and rotational velocity about combinations of principal directions (3).

Note that this is a general result which means that any FEM programme which can make these outputs available to the user can be used to generate SEs. In the project, interfaces to the two commercial FEM programmes, ANSYS and ABAQUS, have been developed. In practice this means that a set of scripts have been developed which need to be run inside the FEM programmes in order to export the required matrices and the force vectors related to the (12) required load cases. These system matrices and force vectors are then read by another developed programme which does the actual reduction step and exports the SE EOMs to file.

Next step is to import the SE into HAWC2 and connect it to the existing HAWC2 structure (if present). This is done using the standard external system interface to HAWC2; this interface allows any dynamic system to be included, connected to, and simulated together with existing HAWC2 structures or other external systems, see [18],[20]. This requires that the EOMs of the external system are defined and that a set of constraint equations which describe how the kinematic relation between the states of the external

system and HAWC2 must be related. A DLL implementing the steps described above has been developed; it reads the exported SE EOMs and defines a set of constraint equations which can be used to connect SE nodes and HAWC2 beam nodes as well as connecting SE nodes of different SEs.

Last step is to apply external forces (e.g. from aerodynamics) on the structure. For now, this is only possible indirectly through the HAWC2 structure which means that in order to load the SE structure, a dummy HAWC2 structure is first connected to the SE structure (using the coupling constraint) and then this dummy HAWC2 structure is exposed to the external load. The same goes for aerodynamic forces; if we want aerodynamic loading on a SE blade, we have to model a HAWC2 blade without mass, damping and stiffness, and then connect the nodes of the two blades (node by node). All the aerodynamic forces are then passed from the HAWC2 nodes to the SE nodes through the constraint forces between the nodes.

One major challenge during this project has been to go from working with models with approx. 1000 DOFs to full 3D FEM models with >10,000,000 DOFs. This requires use of sparse matrix storage and sparse matrix solvers as well as 64-bit computer architecture to handle such problems.

Results

A large amount of test cases have been run during the project to test and validate the SEs. However, in this section the focus is on the results related to the DTU 10MW RWT, which is an artificial yet well-defined wind turbine. The blade for this wind turbine “was born” as a 3D FEM model and beam properties for BECAS and HAWC2 have also been extracted based on the full 3D FEM model.

Eigenfrequencies of the DTU 10 MW RWT blade

This section compares eigenfrequencies and modeshapes of the DTU 10 MW RWT blade modelled with SEs, BECAS beam elements, and HAWC2 beam elements. The properties for these different models are all based on the full 3D FEM model of the blade which was modelled using the ABAQUS commercial FEM programme.

The comparison is shown in Table 16; the eigenfrequencies and corresponding mode shape of the 3D FEM model are shown in column 2 and 1, respectively. It is seen that the SE matches fine up to the 2nd torsion mode around 9 Hz. The BECAS and the HAWC2 models both compare well up to the 1st torsion mode around 5.7 Hz, however, both beam models seem to miss one of the two coupled flap/torsion modes. For higher frequencies, there is some mismatch between mode shape and frequencies for the beam models.

Table 16: Eigenfrequencies [Hz] for different models of the DTU 10 MW RWT blade. The first column identify the mode of the ABAQUS (i.e. the 3D FEM model) , the next four columns show the eigenfrequencies of the individual models.

Mode	ABAQUS	SE	BECAS Fejl! Henvi- snings- skilde ikke fundet.	HAWC2 [10]
Flap	0.611	0.611	0.611	0.61
Edge	0.961	0.951	0.930	0.93
2. Flap	1.75	1.75	1.74	1.74
2. Edge	2.88	2.84	2.75	2.76
3. Flap	3.58	3.58	3.58	3.57
Flap/torsion	5.71	5.71	5.66(1 st tors.)	5.69(1 st tors.)
Flap/torsion	5.75	5.76	-	-
4. Flap	6.16	6.13	6.06	6.11
5. flap	8.57	8.59	6.13(3 rd edge)	6.66(3 rd edge)
2. Torsion	9.21	9.53	-	-

HAWC2 simulation of the DTU 10 MW RWT blade

This section presents a comparison between the time simulation of the regular HAWC2 blade and the SE blade for a wind ramp simulation. The SE model is generated from the 3D FEM model and imported into HAWC2 by the procedure described in section 0. Figure 93 shows the HAWC2 model using the SE blade. Each of the sections in the figure represents a SE node and these nodes are then connected to a mass-less and soft HAWC2 blade. Thus, the two models have the same aerodynamic properties but different structural properties, at least for the blades – the rest of the structure, wind input, controller etc. are identical.

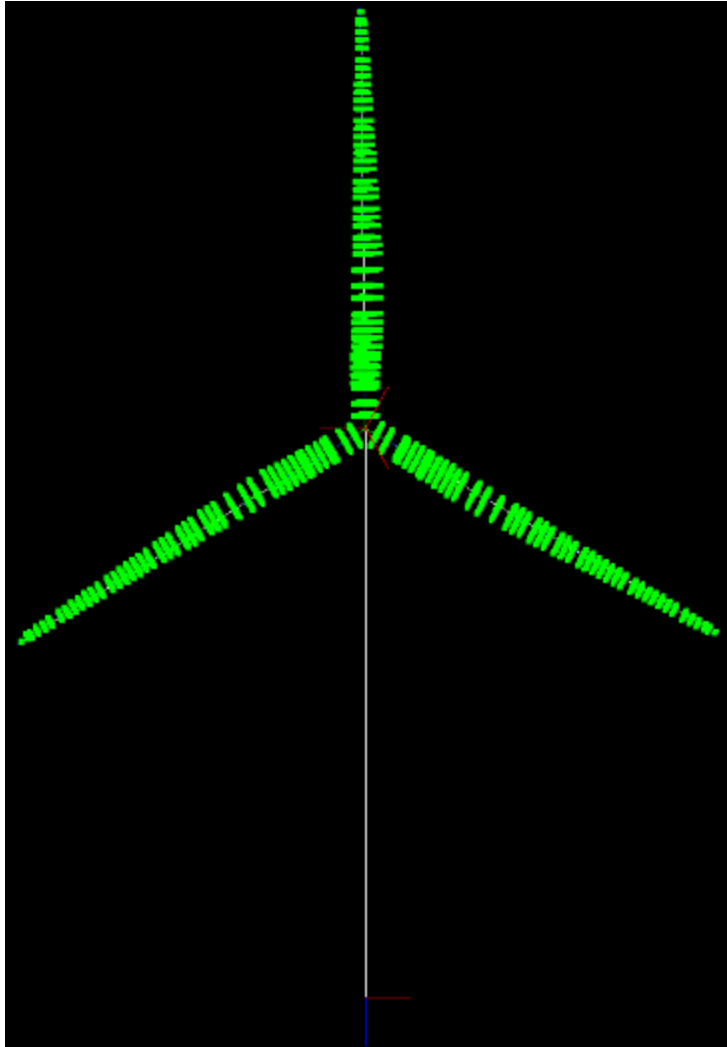


Figure 93: HAWC2 animation snap shot showing the nodes from the 3D FEM model on which the SE nodes are based.

Figure 94 show the comparison between the models. All the blue curves show results using the HAWC2 blade and the red curves show results from the SE blade. From the figures it is seen that the two models behave similarly, however, some differences are seen in the two figures in the last row (left shows the tower yaw moment and right shows the tip displacement in the wind direction). These differences are most likely due to the fact that the blades in fact are different. The stiffness of the blades when exposed to a static tip load show that, especially in the edge direction, are in fact different so a different response should also be expected in the simulated results.

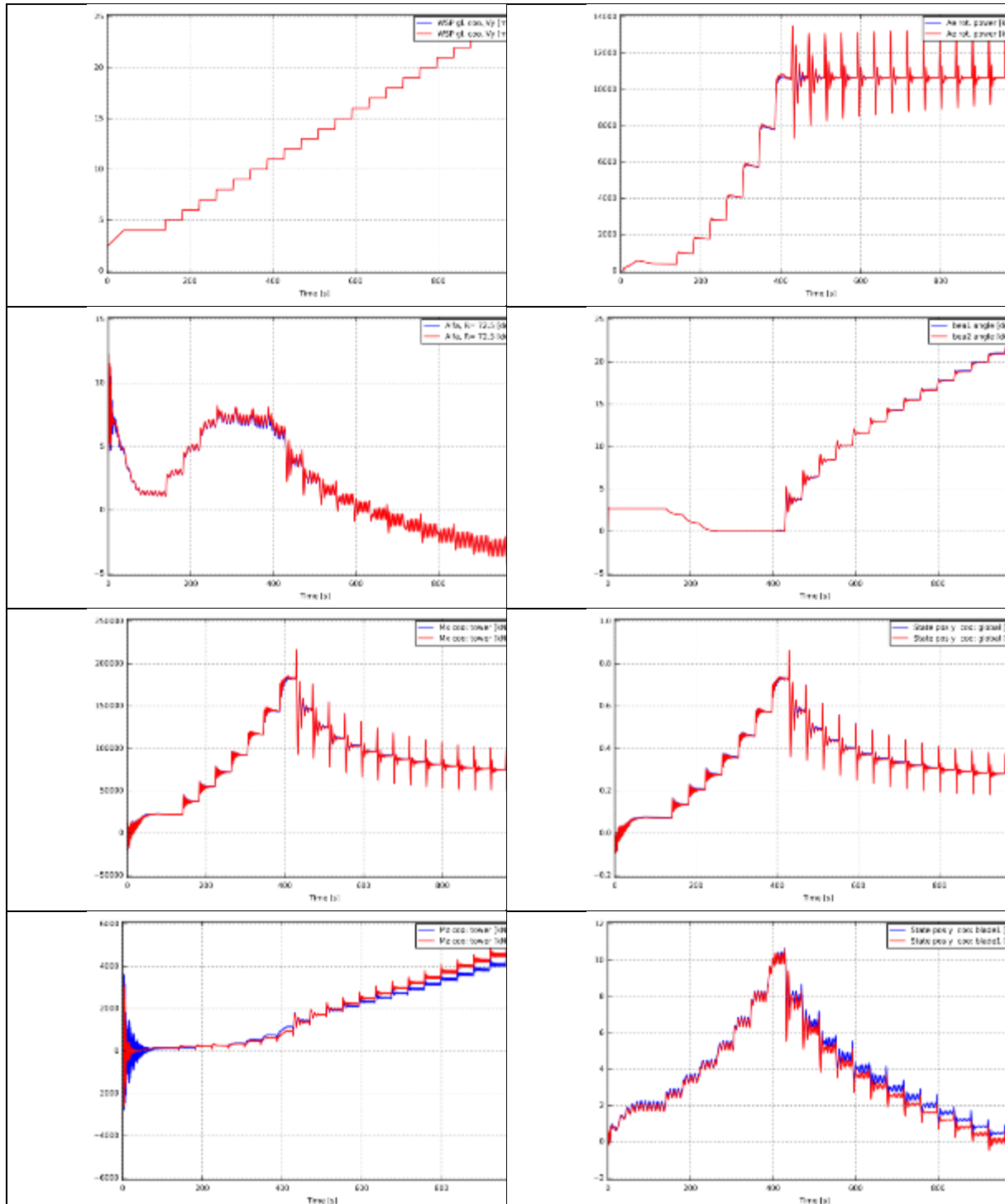


Figure 94: Comparison between HAWC2 simulation of wind ramp input using two different blade models, HAWC2 blade (blue) and SE blade (red). The figures in left column show; wind speed, AOA at 72 m, pitching moment in

tower bottom, and yaw moment in tower bottom. The right column show; power, pitch angle, tower top displacement fore/aft, and blade flap position.

Another result which can be post-processed from the simulated time series is how the individual DOFs in the nodes of the 3D FEM model vary as function of time. During the reduction step, a transfer matrix describing the relation between the SE nodes and the 3D FEM model DOFs is generated and stored in a recover file. From the simulated response, the SE node DOFs can be extracted and by multiplication with the transfer matrix, the 3D FEM model DOFs can be extracted. An example of this is shown in Figure 95; the figure shows an animation snap shot of the SE wind turbine model. The green section on the blade pointing towards the upper right corner is one on the SE sections, and this section is magnified and drawn at the bottom of the figure. The green dots show the node locations in the section, and the red dot show the displaced nodes magnified by a factor of 50, i.e. the red dots show how the section is deformed during operation.

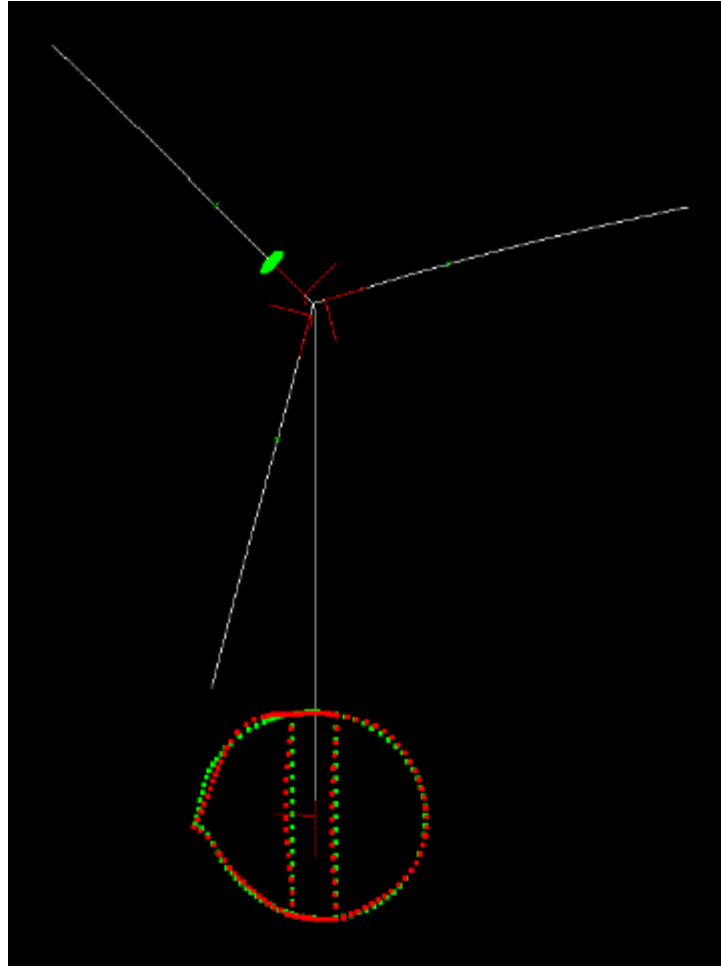


Figure 95

Being able to post-process the behaviour of the DOFs in the 3D FEM model opens up the possibility to go directly from simulated response of a reduced model to stresses anywhere in the detailed blade mode, however, this step has not yet been investigated further.

Conclusion

The present work has provided a method to go from a full 3D FEM model of a blade (or any other sub-structure) to a reduced model a with sufficiently low number of DOFs that

it can be used in aeroelastic simulations of wind turbines. The formulation includes the fictitious forces, e.g. centrifugal forces, due to rotation of the rotor and also gravity forces.

The method was demonstrated using the 10 MW DTU reference turbine. The comparison of eigenmodes between the full 3D model and the reduced model showed an excellent agreement both regarding eigenfrequencies and mode shapes, at least for the first 9 modes (up to approximately 9 Hz).

The use of the reduced blade model in an aeroelastic simulation was also demonstrated and compared with results from an existing HAWC2 model of the 10 MW RWT. In general, the comparison of various channels show excellent agreement, however, small differences in yaw moment and tip displacement were found. These differences are attributed the fact that the two blade models have different stiffness properties especially in the edge direction.

Another issue which is out-of-scope related to the LEX project, but still worth mentioning here, is that the SEs can be used for other wind turbine components than the blades. Many aeroelastic programmes model the structure as beam elements, and for the structural engineer it can be a challenge to interpret the detailed sub-structures of a wind turbine (e.g. the bedframe of the nacelle or various joints in a jacket foundation) into simple beam properties. By applying SEs, this task is easy and it will enhance the quality of the aeroelastic models.

WP9 Product Development

WP responsible: Lars Jøker Nissen – DIS Innovative Engineering

The purpose of this work point is to develop cost efficient, relevant and marketable products based on the underlying patented technologies and the findings and conclusion during the present project.

Introduction

The LEX pretension mechanism is developed as a simple rotation lock. It is developed to simplify the installation of the wires inside the wind turbine blade. The lock makes it possible for the installer to easily buckle and lock the wire.

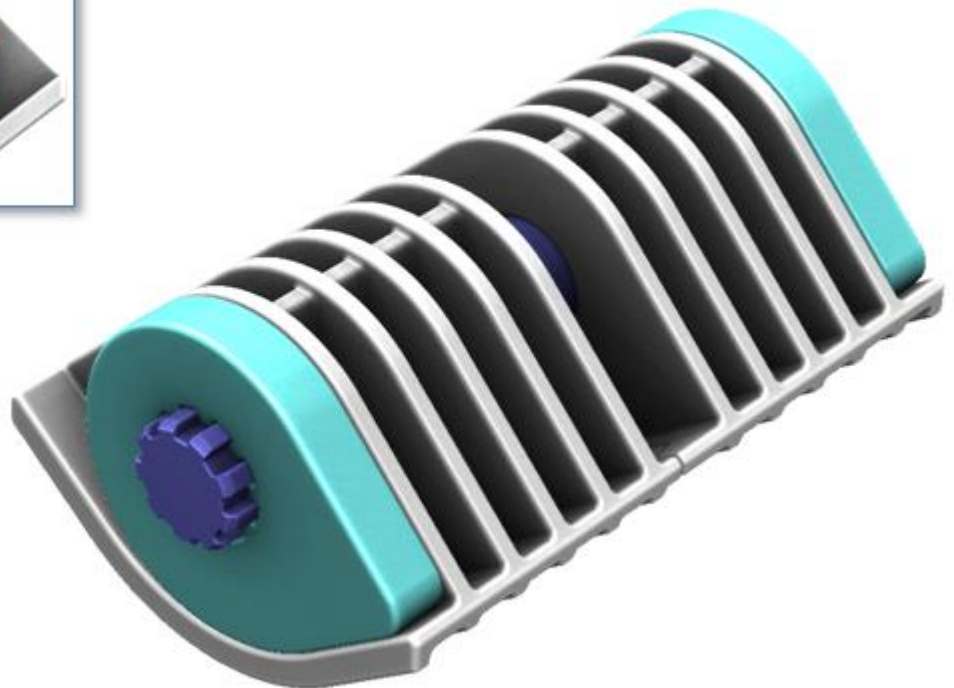


Figure 96: 3D model

The Product

The lock consists of six parts, the geometry for the lock is symmetric and consists of four different elements.

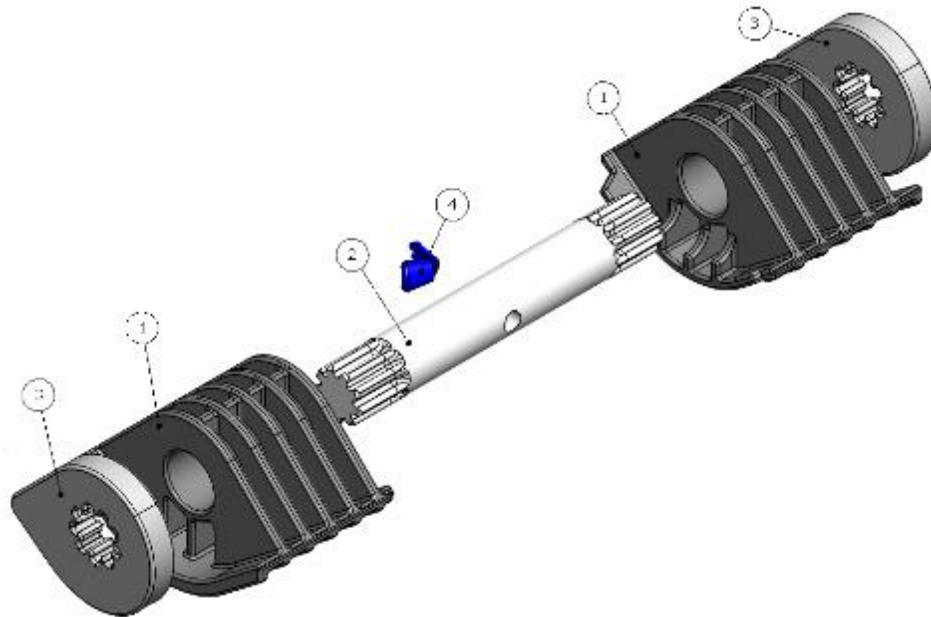


Figure 97: Exploded view

ITEM NO.	DISCRIPTION	PART NUMBER	QTV.
1	Base	1026034	2
2	Rod	1026035	1
3	Self-locking flanges	1026036	2
4	Conical Wire Lock	1026040	1

Item no. 1 and 2 (the base and the rod) is, from DIS, recommended to produce in a two component injection molded, e.g. Epoxy. Item no. 3 (the flanges) is recommended to be extruded or injection molded in a thermoplastic. Item no. 4 (the wire lock) is recommended to be injection molded in a thermoplastic.

The function

1. The base will be glued on the inside of the wind turbine blade.



Figure 98: Base

2. The wire is installed in a conical wire and inset in the rod. See Figure 99.

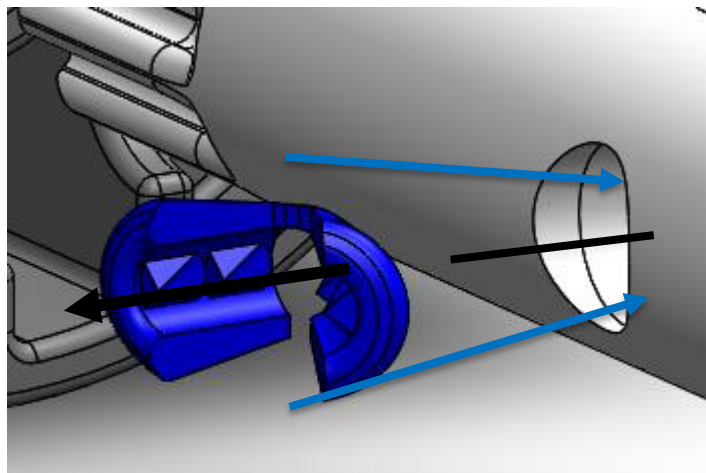


Figure 99: Conical wire lock

3. Use the tooling to tighten the wire, and place the flange/lock when you reach the wished force. See Figure 100.



Figure 100: Illustration of function

WP10 Market Entrance Barriers

WP responsible: Søren Horn Petersen from Boving Horn

Market Barriers

Closing delivery – Summary and conclusion

Introduction

The purpose of this note is three fold:

- a. To provide the formal closing delivery of work package 10 Market Entrance Barriers in the EUDP project 64013 – 0155 ” Torsional stiffening of wind turbine blades – mitigating leading edge damages” (LEX).
- b. To provide recommendations on which market barriers which still needs to be addressed in the future design and commercialisation work of the LEX pretension mechanism developed under this or future projects.
- c. To convey the overall conclusion of the work performed with recommendations for improvements for future projects.

References

The note summarizes the work done and presented in a number of other notes, viz.:

- d. Post note from blade Workshop held October 4th, 2013, noted dated December 25th, 2013.
- e. List of Market Barriers prioritised and forwarded for review by product developing team, dated May 2nd, 2014.
- f. Delivery 10.4.1: Map of Guide2Defect, dated May 30th, 2015
- g. Delivery 10.4.2: Full concept description of Guide2Defect, dated June 30th, 2015
- h. Review of Market Barriers, input to Søren dated June 10th, 2016.

Disclosure of Interest

The business model of Boving Horn is to partner up with innovators, who holds good ideas, but do not have the resources and/or competences to mature and commercialize them. Based on standard models and a wide network, Boving Horn evaluates, tests and matures the ideas; prepare bankable business plans including start-up plans; and execute the plans based on a business development agreement with the idea holder.

Boving Horn has used the work with Guide2Defect in conjunction with experiences

gained on other projects to develop the "Superman-model". This model is under commercialization through a partner driven company, CoGrow established in June, 2014, in which Boving Horn is co-founder and major shareholder.

Boving Horn has prior to starting up the work in the LEX project entered into a cooperation agreement with Bladena related to the maturing and commercialization of Guide2Defect, in which Boving Horn will be financially rewarded, when and if Guide2Defect generates income to Bladena. This agreement has materialised into the establishment of Guide2Defect Aps, in which CoGrow holds a large minority share and Bladena is the majority owner.

Market Barriers

i. Definition

In the project description, it was anticipated, partly based on past experience of introducing the D-String, that the market introduction of the retrofit stiffener would be very challenging, predominantly due to the plan of installing the retrofit stiffener inside in blades in operation, up tower and somehow attached to the load carrying and/or load transferring elements of the blade. It was thus an integrated part of the project and particularly the project start-up to clearly identify, understand, communicate and handle the barriers blocking the successful introduction of the retrofit stiffener into the market. In this project, these are the barriers referred to as Market Barriers.

The theoretical Definition of market barriers, by George Siegel, is:

...A cost of producing which must be borne by a firm which seeks to enter an industry, but is not borne by firms already in the industry.

On the kick-off workshop of the project held at DTU on October 4th, 2013, the definition of Market Barriers was evolved to:

...Any hindering – commercial, technical, regulative or legislative which prevents, threatens or delay the successful market introduction of the future LEX stiffener into the retrofit and new design blade market.

This is the definition, which has been applied for this project.

j. Project Assumptions

In the full project, two major assumptions related to market barriers were key for the establishment of this work package:

- i. *...we must prepare a substantiated cost/benefit model to support the financial justification (business case).*

- ii. *..We must identify and handle all technical objections, perceived as well as real, and implement the consequences in our design, documentation and communications.*

Hence, the work package 10 was split in two parts, i.e. a part working on identifying and handling market barriers and a part working specifically on providing a cost model based on statistical input from inspection report covering defects on blades.

k. Guide2Defect

Following the first assumption, and as part of the project it had already been decided that the work with establishing a business case for the installation of the Retrofit Stiffener should be included in the work with market barriers, and hence the development of the required tooling, data acquisition and application of the data has been given special attention under this work package as a pre-defined task 10.4: Preparation of substantiated cost-benefit model for the proposed product.

l. Brain Storm finding Barriers – Basis for the Work

At the abovementioned workshop, the process for identifying the relevant market barriers was agreed. First step was to have a brain storm at the work shop. The participants at the work shop represented all stake holders in the wind industry: Owners, OEM's (blade), research, design, certification (of blades and turbines), testing and servicing.

The brain storm gave the following results, see Figure 101: BrainstormFigure 101:



Figure 101: Brainstorm

m.

The brain storm and the identified potential market barrier established the platform for the remaining work on market barriers. Or listed in a more formal order:

- i. Worries: Risk, Approval from Management, Loss of performance, Problem (why), Does it work, Cost, Loads on blades/drive train.
- ii. Installation: Safety of installation and cost of installation
- iii. Justification: When, alternatives, competitive solutions
- iv. Technical Solutions: Consequential Issues, potential secondary damages, wear & tear, Life of LEX, can it be repaired? post installation inspection
- v. Certification / Formal requirements: Continued insurance/certification, is re-certification required for blade (repair or structural change), is re-certification required for turbine, re-testing of blade.
- vi. Warranty/liability: Will OEM transfer full engineering responsibility; must the turbine be out of warranty?

n. The Qualification Platform

Based on the brain storm, the work package manager compiled an overview of the potential market barriers and described them in more detail. This resulted in the below table covering a total of 23 market barriers to be addressed in 8 different categories:

Line	Theme	Barrier	Description
1	01 Technical Feasibility	Function	Does the product actually work?
2	01 Technical Feasibility	System Effects	Does it have any significant impacts on loads on blades or drive train?
3	01 Technical Feasibility	Functional Risk	Any potential secondary effects?
4	02 Formal Regulations	Certification of solution(s)	Does the solution require any form of certification to be implemented?
5	02 Formal Regulations	Re-certification of blade	Does the blade require recertification post installation of solution?
6	02 Formal Regulations	Re-testing of blade	Does the customer, DEM or certification body require re-testing of blade prior to certifying?
7	03 Justification	Can an interesting cost/benefit analysis be performed?	Taking all cost and benefits into consideration, can it be confirmed?
8	03 Justification	Management Approval	Is the initial cost of the performance loss during installation high for the local management to approve?
9	03 Justification	Can the pain be identified?	Is there any accepted need out in the real world and the pain clearly identified and verified?
10	03 Justification	Is there any competing solutions?	Are there any competing solutions and are they offering a better value proposition than the proposed solution?
11	03 Justification	Commercial Risk	Is the commercial risk acceptable for the customer taking performance loss, loss of face and market reacting into account?
12	04 Distribution	Any value proposition for the distribution chain?	Can a value chain be established, which satisfies the channels need for reward outmatching the effort?
13	05 Market Response	Will DEM ban the solution?	Will the DEM's fight the solutions, especially on the retrofit market?
14	06 Liabilities	Will there be any insurance issues?	Any insurance issues with the DEM's, sites, Bladena, Owners or distributors?
15	06 Liabilities	Transfer of liabilities, warranty	Will there be any warranty issues if installed as a retrofit solution?
16	06 Liabilities	Transfer of liabilities, engineering	Will the DEM's transfer parts of the whole engineering responsibility when installed in new blades?
17	06 Liabilities	Acceptance of liabilities	Can Bladena and/or the distribution channel accept the required liabilities?
18	07 Implementation	Can we find a suitable method of retrofit installation?	Considering cost, safety and standstill time, can we then find a suitable method to implement the solution?
19	08 Operation	Wear and tear	Will there be any direct or indirect wear & tear due to the implementation of the solution?
20	08 Operation	Consequential issues	Can there be any risks or issues elsewhere in the system caused by the implementation of the solution?
21	08 Operation	Secondary Damages	Can there be any secondary damages or issues elsewhere in the system caused by the implementation of the solution?
22	08 Operation	Maintainability	Can the solution be inspected and maintained after installation?
23	08 Operation	Loss of performance	Is there any loss of performance, fatigue life or power yield due to the installation of the solution?

The overview was tested in 3 iterations with the work package participants and their views and suggestions were incorporated.

The work package manager also formulated a prioritisation matrix as a tool for the work package participants to evaluate the market barriers on common criteria:

Relevance	Priority Values				
	10	8	6	4	2
Prevents	10	8	6	4	2
Threatens	8	6	4	2	1
Delays	6	4	2	1	0
Hampers	3	2	1	0	0
Ignorable	1	1	0	0	0
	1	3	6	8	10
	Low	Low	Medium	High	Extreme
	Cost To Overcome				

o. The Prioritisation of Market Barriers

The Market Barrier overview were then distributed to a number of stakeholders, and they were interviewed via telephone and hence each stakeholder score the each market barriers and hence prioritised the list. A total of 8 interviews were performed. An example of resume of an interview are below:

BOVING HORN

Market Barrier List Priority Summary

LEX Project Work Package 0.1
Version 2: January 26th, 2014

Line	Theme	Barrier	Description	Version 01		Sebastian, DEWI-OC	
				Relevance	Cost	Relevance	Cost
1	01 Technical Feasibility	Function	Does the product actually work?	10 Prevents	08 High	10 Prevents	08 High
2	01 Technical Feasibility	System Effects	Does it have any significant impacts on loads on blades or drive train?	8 Threatens	06 Medium	8 Threatens	06 Medium
3	01 Technical Feasibility	Functional Risk	Any potential secondary effects?	8 Threatens	06 Medium	8 Threatens	06 Medium
4	02 Formal Regulations	Certification of solution(s)	Does the solution require any form of certification to be implemented?	06 Delays	06 Medium	06 Delays	06 Medium
5	02 Formal Regulations	Re-certification of blade	Does the blade require recertification post installation?	06 Delays	06 High	06 Delays	08 High
6	02 Formal Regulations	Re-testing of blade	Does the customer, OEM or certification body require re-testing?	8 Threatens	06 High	8 Threatens	10 Extreme
7	03 Justification	Can an interesting cost/benefit analysis be performed?	Taking into account benefits to consideration, can it be done?	10 Prevents	03 Low	10 Prevents	03 Low
8	03 Justification	Management Approval	Is the initial cost in the performance loss during installation to high for the local management to approve?	8 Threatens	06 Medium	8 Threatens	06 Medium
9	03 Justification	Can the pain be identified?	Is there any accepted need but in the real world and the pain clearly be?	8 Threatens	08 High	8 Threatens	08 High
10	03 Justification	Is there any competing solutions?	Are there any competing solutions and are they offering a better value proposition than the proposed?	8 Threatens	08 High	8 Threatens	08 High
11	03 Justification	Commercial Risk	Is the commercial risk acceptable for the customer taking performance loss, loss of face and market reacting?	8 Threatens	06 Medium	8 Threatens	06 Medium
12	04 Distribution	Any value proposition for the distribution chain?	Can a value chain be established, which satisfy the channels need for?	8 Threatens	08 High	8 Threatens	08 High
13	05 Market Response	Will OEM ban the solution?	Will the OEM's fight the solutions, especially on the retrofit market?	03 Hampers	06 Medium	03 Hampers	06 Medium
14	06 Liabilities	Will there be any insurance issues?	Any insurance issues with the OEM's, sites, Bladena, owners or?	06 Delays	06 Medium	06 Delays	06 Medium
15	06 Liabilities	Transfer of liabilities, warranty	Will there be any warranty issues installed as part of the solution?	8 Threatens	06 Medium	8 Threatens	06 Medium
16	06 Liabilities	Transfer of liabilities, engineering	Will the OEM's transfer parts for the whole engineering responsibility when installed in the blades?	8 Threatens	06 Medium	8 Threatens	06 Medium
17	06 Liabilities	Acceptance of liabilities	Can Bladena and/or the distribution channel accept the required?	10 Prevents	08 High	10 Prevents	08 High
18	07 Implementation	Can we find a suitable method for retrofit installation?	Considering cost, safety and stand still time, can we then find a suitable method to implement the solution?	8 Threatens	08 High	8 Threatens	08 High
19	08 Operation	Wear and tear	Will there be any direct or indirect wear and tear due to the implementation?	06 Delays	06 Medium	06 Delays	06 Medium
20	08 Operation	Consequential Issues	Can there be any risks for issues elsewhere in the system caused by the implementation of the solution?	10 Prevents	10 Extreme	10 Prevents	10 Extreme
21	08 Operation	Secondary Damages	Can there be any secondary damages for issues elsewhere in the system caused by the?	10 Prevents	08 High	10 Prevents	08 High
22	08 Operation	Maintainability	Can the solution be inspected and maintained after installation?	06 Delays	06 Medium	06 Delays	06 Medium
23	08 Operation	Loss of performance	Is there any loss of performance, fatigue or power yield due to the?	8 Threatens	08 High	8 Threatens	08 High

Interview date: March 2, 2014
Interviewer: Søren Horn Petersen, Boving Horn
Interviewee: Sebastian Flores, DEWI-OC

Other Comments:
Data given from Sebastian's point of view focusing on the items relevant for the certification body. In point 2, Sebastian comments that the methods should be developed to handle this as part of the design process.

p. List of Market Barriers

After the analysis of the interviews a final list market barrier list was prepared, tested among the work package participants and eventually forwarded to the product development team to review and for inclusion in the development work:

Line	Theme	Barrier	Description	Pre-handling				
				Relevance	R-Score	Cost	C-Score	PriorityScore
23	08:Operation	Loss of performance	Is there any loss of performance, fatigue or power yield due to installation of the solution?	10:Prevents	10	08:High	8	80
4	02:Formal/Regulations	Certification of solution(s)	Does the solution require any form of certification to be implemented?	06:Delays	6	06:Medium	6	36
19	08:Operation	Wear and Tear	Will the be any direct or indirect wear & tear due to the implementation of the solution?	06:Delays	6	06:Medium	6	36
22	08:Operation	Maintainability	Can the solution be inspected and maintained after installation?	06:Delays	6	06:Medium	6	36
6	02:Formal/Regulations	Re-testing of blade	Does the customer, DEM or certification body require re-testing of blade prior to certifying?	08:Threatens	8	06:High	3	24
18	07:Implementation	Can we find a suitable method of retrofit installation?	Considering cost, safety and standstill time, can we find a suitable method to implement the solution?	10:Prevents	10	08:High	8	80
9	03:Justification	Can the pain be identified?	Is there any accepted need but in the real world and the pain clearly be identified and verified?	08:Threatens	8	08:High	8	64
12	04:Distribution	Any value proposition for the distribution chain?	Can a value chain be established, which satisfy the channels need for reward but matching the effort?	08:Threatens	8	08:High	8	64
10	03:Justification	Is there any competing solutions?	Are there any competing solutions and are they offering a better value proposition than the proposed solution?	08:Threatens	8	08:High	8	64
16	06:Liabilities	Transfer of liabilities, engineering	Will the DEM transfer parts of the whole engineering responsibility when installed in new blades?	08:Threatens	8	06:Medium	6	48
5	02:Formal/Regulations	Re-certification of blade	Does the blade require certifications post installation of solution?	06:Delays	6	06:High	3	18
8	03:Justification	Management approval	Is the initial cost of the performance loss during installation higher than the local management will approve?	03:Hampers	3	06:Medium	6	18
13	05:Market/Response	Will DEM ban the solution?	Will the DEM fight the solutions, especially on the retrofit market?	03:Hampers	3	06:Medium	6	18
7	03:Justification	Can an interesting cost/benefit analysis be performed?	Taking cost and benefits into consideration, can it be confirmed?	10:Prevents	10	03:Low	3	30
14	06:Liabilities	Will there be any insurance issues?	Any insurance issues with the DEM's sites, Bladena, owners or distributors?	06:Delays	6	06:Medium	6	36
1	01:Technical/Feasibility	Function	Does the product actually work?	10:Prevents	10	08:High	8	80
11	03:Justification	Commercial risk	Is the commercial risk acceptable for the customer taking performance loss, loss of face and market reacting into account?	08:Threatens	8	06:Medium	6	48
15	06:Liabilities	Transfer of liabilities, warranty	Will there be any warranty issues if installed as a retrofit solution?	08:Threatens	8	06:Medium	6	48
3	01:Technical/Feasibility	Functional risk	Any potential secondary effects?	08:Threatens	8	08:High	8	64
2	01:Technical/Feasibility	System effects	Does it have any significant impacts on loads on blades or drive train?	08:Threatens	8	06:Medium	6	48
17	06:Liabilities	Acceptance of liabilities	Can Bladena and/or the distribution channel accept the required liabilities?	10:Prevents	10	08:High	8	80
20	08:Operation	Consequential issues	Can there be any risks for issues elsewhere in the system caused by the implementation of the solution?	10:Prevents	10	10:Extreme	10	100
21	08:Operation	Secondary damages	Can there be any secondary damages or issues elsewhere in the system caused by the implementation of the solution?	10:Prevents	10	08:High	8	80

- q. Feed Back from the product development team
The Product Development Team has after design reviewed the list and commented each individual market entrance barrier and how it has been handled in the design work. Further the product development team has - based on the Market Barrier List and other commercial input - prepared the below SWOT analysis:

STRENGTH	WEAKNESS
<ul style="list-style-type: none"> ▪ Intuitive and logic solution ▪ IPR in main markets ▪ EUDP project development – product demonstrated ▪ Commercial Sub-component test done with OEM ▪ Technically proven in sub-component test ▪ Removes known failure mode ▪ Industry network involved in development ▪ Bladena technology already in the market ▪ Utilisation of current sales channels 	<ul style="list-style-type: none"> ▪ Missing demonstration in field and commercial reference ▪ Field measurements mainly done on medium size blades ▪ Complex product impacts blade structure ▪ Failure rate statistics does not exist ▪ Difficult to quantify the ROI ▪ Not yet any specific solution for new blade manufacturing, only retrofit
POSSIBILITIES	THREATS
<ul style="list-style-type: none"> ▪ Longer and more aerodynamic blades ▪ Blades and blade damages get more attention from WTO and OEM ▪ Failure mode known to OEMs ▪ Failure mode seen in field and test ▪ High focus on LCoE and lowering this ▪ Focus on blade life time and reliability ▪ O&M cost needs to be brought down ▪ Increase in offshore with higher risk and cost if failures occur ▪ Large flatbacks common in blade design ▪ Field test in a 83,5 m blade, EU/EUDP DemoWind project ▪ Development and test standards to include combined loading 	<ul style="list-style-type: none"> ▪ Competition for non IP solutions (less effective) ▪ Potential re-certification of the blades ▪ Failures in full scale test not public available ▪ Slow change in design at OEMs ▪ “Not invented here” syndrome at OEMs ▪ Reluctance from OEMs to use external technology ▪ Internally politics and structure at OEMs ▪ Confined space for retrofit installation ▪ Non successful field test ▪ Political interference in the market, less offshore, change in market conditions

This work package has reviewed the commented list and the SWOT analysis, and has re-evaluated the risk assessments and priority. The conclusion is incorporated in the below list.

Line	Theme	Barrier	Description	Feedback from Product Developing Team	Closing/Conclusion	Post-handling					Status			
						Pre-Test	Priority	Relevance	Post-R-Score	Cost		C-Score	Priority	
20	08 Operation	Consequential Issues	Can there be any risk for users if the system is used by the implementer on the solution?	This is the implementer's responsibility.	Given the high priority, we will document further. IDH will check the solution is maintained.	1	10	Prevents	10	10	Extreme	10	100	🔴
21	08 Operation	Secondary Damages	Can there be any secondary damage to the system if the implementer is not following the solution?	The tests have shown that the software might have effects on the blades through the test. The team is aware of this.	This is the implementer's responsibility. The team will be a stopper.	5	10	Prevents	10	10	Extreme	10	100	🔴
17	06 Liabilities	Acceptance of Liabilities	Can Bladena or other that distribute the solution be held responsible for the solution?	Considering the product is not selling at the moment, they will not be held responsible for the solution.	This is the implementer's responsibility. The team will be a stopper.	3	10	Prevents	10	08	High	8	80	🔴
3	01 Technical Feasibility	Functional Risk	Any potential secondary effects?	This is the implementer's responsibility.	Should be verified and if not, it should be difficult to become a secret.	7	08	Threatens	8	08	High	8	64	🔴
2	01 Technical Feasibility	System Effects	Does it have any significant impacts on the system if the solution is not followed?	A present system effects are known, but the effects that the solution will have on the system are not known.	This is the implementer's responsibility. The team will be a stopper.	11	08	Threatens	8	08	High	8	64	🔴
11	03 Justification	Commercial Risk	Is it commercially acceptable for the customer to take on the responsibility for the solution?	Yes, the responsibility for the solution is on the customer, although the customer is not responsible for the solution.	OK. The responsibility for the solution is on the customer.	12	08	Threatens	8	06	Medium	6	48	🔴
15	06 Liabilities	Transfer of Liabilities, warranty	Will there be any warranty issues if the solution is not followed?	No. Bladena will be responsible for the solution.	Not answered. Will the customer accept this?	13	08	Threatens	8	06	Medium	6	48	🔴
14	06 Liabilities	Will there be any insurance issues?	Any insurance issues with the OEM, the customer, or the distributor?	None is considered at the moment.	Should be verified.	16	06	Delays	6	06	Medium	6	36	🔴
7	03 Justification	Can it be interesting to consider if the solution is performed?	Taking into account the cost of the solution, is it interesting to consider if the solution is performed?	A cost-benefit analysis is being conducted. The solution is estimated to be profitable.	A cost-benefit analysis is being conducted. The solution is estimated to be profitable.	19	10	Prevents	10	03	Low	3	30	🔴
13	05 Market Response	Will it be a market solution?	Will the OEM sign the solution if the solution is not followed?	The OEM is relatively positive about the solution, but they are not sure if they will sign it.	Based on the feedback, the solution will be increased.	23	03	Hampers	3	08	High	8	24	🟡
1	01 Technical Feasibility	Function	Does the product actually work?	Preliminary tests show that the product is working, but more tests are needed.	This is the implementer's responsibility. The team will be a stopper.	2	06	Delays	6	03	Low	3	18	🟡
16	06 Liabilities	Transfer of Liabilities, engineering	Will the OEM transfer the responsibility for the solution to the customer?	No. Bladena will be responsible for the solution.	OK. The responsibility for the solution is on the customer.	14	06	Delays	6	03	Low	3	18	🟡
5	02 Format/Regulations	Re-certification of blade	Does the blade require re-certification for installation on the solution?	Yes, the blade requires re-certification for installation on the solution.	OK. The blade is certified for installation on the solution.	21	06	Delays	6	06	High	6	36	🟡
8	03 Justification	Management Approval	Is there any management approval needed for the solution?	No. The solution is approved by the management.	Awaiting the decision from Aeroblast. The team will be a stopper.	22	03	Hampers	3	06	Medium	6	18	🟡
10	03 Justification	Is there any competing solutions?	Are there any competing solutions to the solution?	Yes, there are competing solutions, but the solution is the most promising.	OK. The solution is the most promising.	9	03	Hampers	3	03	Low	3	9	🟡
18	07 Implementation	Can we find suitable methods for retrofit installation?	Considering the safety of the solution, is it possible to find suitable methods for retrofit installation?	The solution is suitable for retrofit installation.	Duty has been lowered. The team will be a stopper.	4	03	Hampers	3	01	Ignorable	1	3	🟢
9	03 Justification	Can the pain be identified?	Is there any pain identified in the solution?	Yes, there is pain identified in the solution.	OK. The pain is identified.	8	03	Hampers	3	01	Ignorable	1	3	🟢
12	04 Distribution	Any value proposition for the distribution?	Can the solution be distributed through the distribution channels?	The solution is suitable for distribution through the distribution channels.	Yes. However, the value proposition is not clear.	10	01	Ignorable	1	03	Low	3	3	🟢
23	08 Operation	Loss of performance	Is there any loss of performance in the solution?	No. The solution is suitable for operation.	OK. The solution is suitable for operation.	6	01	Ignorable	1	01	Ignorable	1	1	🟢
4	02 Format/Regulations	Certification of solution(s)	Does the solution require any certification for installation?	The solution is suitable for installation.	SoNo. No requirement.	15	01	Ignorable	1	01	Ignorable	1	1	🟢
19	08 Operation	Wear and Tear	Will there be any wear and tear in the solution?	No. The solution is suitable for operation.	OK.	17	01	Ignorable	1	01	Ignorable	1	1	🟢
22	08 Operation	Maintainability	Can the solution be inspected and maintained?	Yes, the solution is suitable for inspection and maintenance.	OK.	18	01	Ignorable	1	01	Ignorable	1	1	🟢
6	02 Format/Regulations	Re-testing of blade	Does the customer require re-testing of the blade?	The customer requires re-testing of the blade.	OK.	20	01	Ignorable	1	01	Ignorable	1	1	🟢

In general, most market barriers have been duly considered, but the meta-product (physical product + soft features around it) has not been fully established yet by the project development team. That said, the overall design of the product is very strong and definitely feasible for the application.

The re-evaluation has prompted a number of recommendations, as per the below:

Key recommendations:

- i. The consequences of in installation is existing blades (retrofit) as regards to secondary damagers, loads and buckling must be investigated further and the claim of the ability to handle all effects should be verified.
 - ii. Warranty and insurance issues are not handled in detail as this was not part of the project, and this should be done. Prior to begin marketing the question of who takes warranty of what, must be addressed. Also the impact on insurance all along the value chain must be addressed.
 - iii. A full cost/benefit model has been prepared based on the work performed under the Guide2Defect task, but the cost of installation the X-Stiffener has not yet been fully investigated. When done, this should be included in the cost benefit model.
2. Preparation of a substantiated cost-benefit model for the proposed product
- Following assumption i. of this work package, a major part this work package was to finalise the Guide2Defect program, acquire data for this and deliver statistics for the cost-benefit model developed by professor John Dalsgaard Sørensen from Aalborg University. The Guide2defect is a software, which based on agreed criteria categorise defects in a way, which enable subtraction of relevant statistical data for comparative analysis and cost/benefit analysis. The origin of the Guide2defect concept is the requirement from the D-string marketing experience obtained by Bladena for documenting the problem, which the product was solving. Currently, no such data is available on the market, and this opens up not only competitive advantages for Bladena, but also the opportunity to spin-out a separate by-product.
- a. Core of Guide2Defect
The core of Guide2defect is not the software itself, but the underlying conventions on how to categorise sites, blades and defects. To utilise the time of the work package participants most effective, it was decided to perform the work via 3 work outs, based on preparation and follow up by the work package manager, and using a power point presentation as log.
- The team has 3 workouts:
- i. Work Out I: May 29th, 2014
 - ii. Work Out II: June 10th, 2014

iii. Work Out III: November 6th, 2014

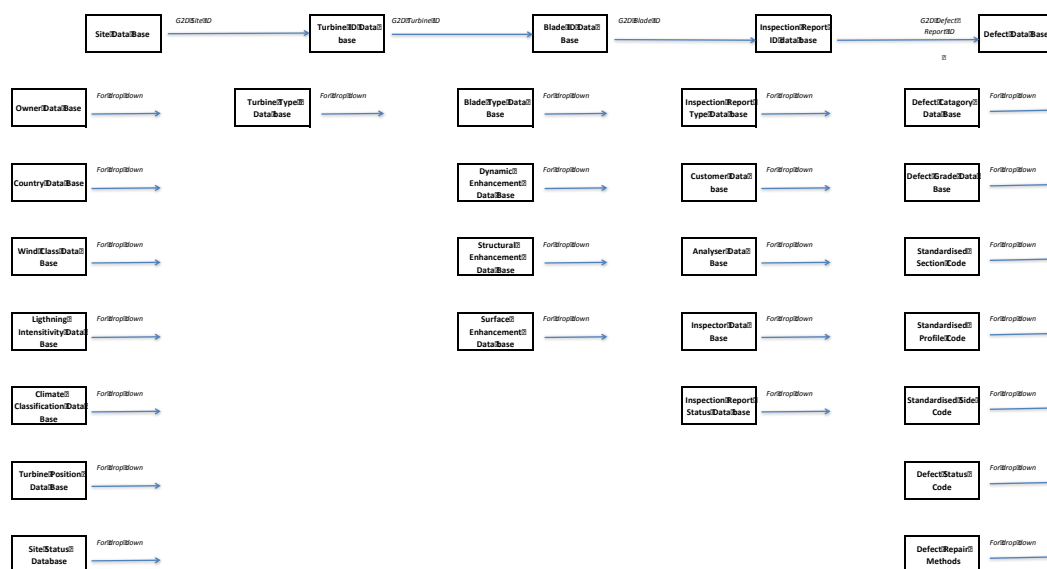
The work outs and the conclusion reached are documented in the PowerPoint log, and prior to closing the log, it was through two iterations among the participants to ensure full consensus. Further the final finding has been tested in other work shops under this project, and comments received has been incorporated.

Hence, there is now consensus of the Guide2defect core design.

The Core Design has 3 key elements: Overall Data Base map, The basic data (for sites) and the defect Tree.

b. Overall Data Base map

After consensus were reached, the work package manager work with the map, and designed the updated Guide2Defect database as per the following map:



c. The Basic Data

Further, the work package manager took the agreed basic data and organised this as follows:

- i. Site name, with GPS coordinates, Altitude turbine model & manufacturer, blade type & manufacturer, data of commissioning and site position.
- ii. Type, coverage, date and supplier of inspection.
- iii. Based on the GPS coordinates data for IEC Wind Class, Lighting Intensity Class, UV Class and Climate classification (Koppen)
- iv. Operational hours.
- v. Defect position (based on standardised position grid) on blade and radius.

d. Defect Tree

The defect tree defines the defect categories, and should in principle cover all potential defects. However, as a principle, if new defects are identified, they will be included in the defect tree.

The defect tree applied in the Guide2defects is as per below:

Group	Type	Category	Code		
Surface	Cracks	Longitudual	S-01-01		
		+/- 45 degrees	S-01-02		
		Transverse	S-01-03		
		TL Cracks	S-01-04		
	Appereance	Spider Web	S-02-01		
		Grazing	S-02-02		
		Pin Holes	S-02-03		
		Flaking	S-02-04		
		Pitting Holes	S-02-05		
		Bullet Hole	S-02-06		
		Burn Marks/lightning Damage	S-02-07		
		Contamination	S-02-08		
Auxillary Equipment	Auxillary Equipment	Lost Dynamic Enhancer	S-03-01		
		Lost Lightning Receptor	S-03-02		
		Damaged Dynamic Enhancer	S-03-03		
		Damaged Lightning Receptor	S-03-04		
		Damaged Leading Edge Foil	S-03-05		
		Drain Hole blocked	S-03-06		
		Debonding	Laminate	Bond Cap	D-01-01
				Ply no bonding	D-01-02
				White Area	D-01-03
			Adhesive Bonds	Transverse	D-02-01
				Open Tip	D-02-02
				Longitudual	D-02-03
In Laminate	In Laminate	Void/Air Pocket	L-01-01		
		Dry Spot	L-01-02		
		Wrinkles	L-01-03		
No Failure	No Failure Reported	No Failure	N-01-01		
Blade Replacement	Blade Replacement	Fire	R-01-01		
		Broken	R-01-02		
		Exploded/Very large piece missing	R-01-03		
		Large Parts missing	R-01-04		
		Turbine De-commissioned	R-01-05		
		Blade demounted for replacement	R-01-06		

e. Development of database and Establishment of Guide2Defect

The full development of the Guide2Defect data base has been documented in detail in three deliverables:

- i. Delivery 10.4.1: Map of Guide2Defect, dated may 30th, 2015

- ii. Delivery 10.4.2: Full Concept Description of Guide2Defect, dated June 30, 2015
- iii. Full Business and Roll-out plan for Guide2Defect Aps, accepted by Bladena in October 2015.

Following this, Guide2Defect Aps was established as a joint venture with CoGrow and as a subsidiary of Bladena Aps on January 6th, 2016 with registration number 3735 7979 with home base in Slagelse, Denmark.

Guide2Defect Aps has initiated the commercialisation of Guide2Defect and has – at the time of writing – compiled more than defects for partners and paying customers. Guide2Defects Aps has finalised the full design and implementation of the data base, and are using an online database programmed in the Knack.com environment.

3. Cost-Benefit Model

The process for the cost-benefit model is that Guide2defect provides statistical data for the cost model developed by Professor John Dalsgaard Sorensen from Aalborg University under this work package.

a. Data

during the project, this work package has entered defects from 923 defects reports covering a total of 1870 blades and 4913 defects. The inputs are summarised below:

Guide2Defect

Overview based on November 30th, 2015

				Total Population	
				Numbers	Hours to detect
Base Data:					
Number of Sites				33	
Number of Blades				1870	
Number of Inspection Reports				923	
Number of Defects				4913	
Defect per blade				2,6	
Defect per inspection reports				5,3	
Defect Categories:					
Surface	Cracks	Longitudual	S-01-01	518	68.961
		+/- 5 degrees	S-01-02	212	64.380
		Transverse	S-01-03	380	62.175
		TL Cracks	S-01-04	0	0
	Apperance	Spider Web	S-02-01	167	71.623
		Grazing	S-02-02	37	64.897
		Pin Holes	S-02-03	282	62.602
		Flaking	S-02-04	1098	63.707
		Erosion	S-02-05	1662	63.638
		Bullet Hole	S-02-06	160	62.944
		Burn Marks/lightning damage	S-02-07	11	39.433
		Contamination	S-02-08	15	59.863
		Heather Grey	S-02-09	4	41.940
		Bulge	S-02-10	87	35.547
	Auxiliary Equipment	Lost Dynamic Enhancer	S-02-11	0	0
		Lost Lightning Receptor	S-02-12	0	0
		Damaged Dynamic Enhancer	S-02-13	0	0
		Damaged Lightning Receptor	S-02-14	220	59.787
Debonding	Laminate	Bond Cap	D-01-01	0	0
		Ply no Bonding	D-01-02	32	64.688
	Adhesive Bonds	Transverse	D-02-01	0	0
		Open Tip	D-02-02	0	0
		Longitudual	D-02-03	5	49.664
In Laminate	In Laminate	Void/Air Pocket	L-01-01	0	0
		Dry Spot	L-01-02	0	0
		Wrinkles	L-01-03	0	0
No Failure	No Failure Reported	No Failure	N-01-01	23	30.959
Blade Replacement	Blade Replacement	Fire	R-01-01	0	0
		Broken	R-01-02	0	0
		Exploded/Very large piece missing	R-01-03	0	0
		Large Parts Missing	R-01-04	0	0
		Turbine De-commissioned	R-01-05	0	0
		Blade Remounted for replacement	R-01-06	0	0
total				4913	63.419
Blade Section:					
Root Section		First 5% of blade length	R	114	59.391
Transition Zone		5,1% to 10% of blade length	Z	78	64.328
Max Chord Section		10,1% to 3,3% of blade length	C	497	66.362
Mid Section		33,4% to 66,6% of the blade length	M	1.511	64.894
Tip Section		66,7% to 97,5% of blade length	T	1.794	62.427
Blade Tip		97,6% to 100% of blade length	B	919	61.760
Total				4.913	63.419

b. Specific Data for cost model

The mitigation path (the defects, on which the product has a positive effect) has been analysed based on input from Bladena. The result has been submitted for application in the cost model. The improvements percentages given in the mitigation path can be applied in simple cost models, and just be used for justification for the D-string. The Mitigation path is below:

Defect Category				Defects as in Guide 2 Defect (November 30th, 2015)							Mitigation percentage by installation as given by Bladena							Theoretical Defects in Installation					Summary				
Group	Type	Category	Code	D-Stiffener							D-Stiffener							D-Stiffener					D-Stiffener				
				Root Section	Transition Zone	Max Chord	Mid Section	Tip Section	Blade Tip	Root Section	Transition Zone	Max Chord	Mid Section	Tip Section	Blade Tip	Root Section	Transition Zone	Max Chord	Mid Section	Tip Section	Blade Tip	% blades	% blades	Improvement, %	Improvement, %	Average Defects/	Time to detection
Surface	Cracks	Longitudual	S-01-01	10	6	47	167	140	35	0%	20%	80%	30%	0%	0%	10	5	9	117	140	35	22%	17%	5%	22%	1.28	68.961
		+/- degrees	S-01-02	0	2	34	93	47	11	0%	10%	60%	30%	0%	0%	0	2	14	65	47	11	10%	7%	3%	26%	1.13	64.380
	Transverse	Cracks	S-01-03	22	19	98	113	41	9	0%	20%	80%	50%	0%	0%	22	15	20	57	41	9	16%	9%	7%	46%	1.26	62.175
		TL Cracks	S-01-04	0	0	0	0	0	0	0%	0%	0%	0%	0%	0%	0	0	0	0	0	0	0%	0%	0%	0%	0.00	0
	Appearance	Spider Web	S-02-01	2	0	5	17	58	45	0%	0%	0%	0%	0%	2	0	5	17	58	45	7%	7%	0%	0%	1.31	71.623	
		Grazing	S-02-02	4	5	6	4	10	4	0%	0%	0%	0%	0%	4	5	6	4	10	4	2%	2%	0%	0%	1.12	64.897	
		Pinholes	S-02-03	6	4	24	74	76	27	0%	0%	0%	0%	0%	6	4	24	74	76	27	11%	11%	0%	0%	1.34	62.602	
		Flaking	S-02-04	26	15	94	221	274	192	0%	0%	0%	0%	0%	26	15	94	221	274	192	44%	44%	0%	0%	1.34	63.707	
		Erosion	S-02-05	10	14	85	356	489	195	0%	0%	0%	0%	0%	10	14	85	356	489	195	61%	61%	0%	0%	1.45	63.638	
	Auxiliary Equipment	Auxiliary Equipment	Bullet Hole	S-02-06	0	0	0	0	0	0	0%	0%	0%	0%	0%	0	0	0	0	0	0	0%	0%	0%	0%	0.00	62.944
Burn Marks			S-02-07	0	1	0	0	38	88	0%	0%	0%	0%	0%	0	1	0	0	38	88	7%	7%	0%	0%	1.26	39.433	
Contamination			S-02-08	1	0	0	3	0	7	0%	0%	0%	0%	0%	1	0	0	3	0	7	1%	1%	0%	0%	1.00	59.863	
Heather Grey			S-02-09	0	0	0	8	4	0	0%	0%	0%	0%	0%	0	0	0	8	4	0	1%	1%	0%	0%	1.25	41.940	
Bulge			S-02-10	0	0	0	0	3	0	0%	0%	0%	0%	0%	0	0	0	0	3	0	0%	0%	0%	0%	1.33	35.547	
Lost Dynamic Enhancer			S-02-11	0	0	0	33	37	16	0%	0%	0%	0%	0%	0	0	0	33	37	16	5%	5%	0%	0%	1.01	0	
Lost Lightning Receptor			S-02-12	0	0	0	0	0	0	0%	0%	0%	0%	0%	0	0	0	0	0	0	0%	0%	0%	0%	0.00	0	
Damaged Dynamic Enhancer			S-02-13	0	0	0	0	0	0	0%	0%	0%	0%	0%	0	0	0	0	0	0	0%	0%	0%	0%	0.00	0	
Damaged Lightning Receptor			S-02-14	0	1	0	6	29	137	0%	0%	0%	0%	0%	0	1	0	6	29	137	9%	9%	0%	0%	1.27	59.787	
Debonding			Laminate	Bond Cap	D-01-01	0	0	0	0	0	0	0%	30%	80%	50%	0%	0%	0	0	0	0	0	0%	0%	0%	0%	0.00
	Ply Debonding	D-01-02		5	5	3	4	8	3	0%	0%	0%	0%	0%	5	5	3	4	8	3	1%	1%	0%	0%	1.14	64.888	
	Transverse	D-02-01		0	0	0	0	0	0	0%	0%	0%	0%	0%	0	0	0	0	0	0	0%	0%	0%	0%	0.00	0	
In Laminate	In Laminate	Open Tip	D-02-02	0	0	0	0	0	0	0%	0%	0%	0%	0%	0	0	0	0	0	0	0%	0%	0%	0%	0.00	0	
		Longitudual	D-02-03	0	0	0	0	2	3	0%	0%	0%	0%	0%	0	0	0	2	3	0%	0%	0%	0%	1.00	49.664		
		Void/Air Pocket	L-01-01	0	0	0	0	0	0	0%	0%	0%	0%	0%	0	0	0	0	0	0	0%	0%	0%	0%	0.00	0	
No Failure	No Failure reported	Dry Spot	L-01-02	0	0	0	0	0	0	0%	0%	0%	0%	0%	0	0	0	0	0	0	0%	0%	0%	0%	0.00	0	
		Wrinkles	L-01-03	0	0	0	0	0	0	0%	0%	0%	0%	0%	0	0	0	0	0	0	0%	0%	0%	0%	0.00	0	
		No Failure	N-01-01	23	0	0	0	0	0	0%	0%	0%	0%	0%	23	0	0	0	0	0	1%	1%	0%	0%	1.00	30.959	
Blade Replacement	Blade Replacement	Fire	R-01-01	0	0	0	0	0	0	0%	0%	0%	0%	0%	0	0	0	0	0	0	0%	0%	0%	0%	0.00	0	
		Broken	R-01-02	0	0	0	0	0	0	0%	20%	40%	20%	0%	0	0	0	0	0	0	0%	0%	0%	0%	0.00	0	
		Exploded Very Large Piece Missing	R-01-03	0	0	0	0	0	0	0%	0%	0%	0%	0%	0	0	0	0	0	0	0%	0%	0%	0%	0.00	0	
		Large Parts Missing	R-01-04	0	0	0	0	0	0	0%	0%	0%	0%	0%	0	0	0	0	0	0	0%	0%	0%	0%	0.00	0	
		Turbine De-commissioned	R-01-05	0	0	0	0	0	0	0%	0%	0%	0%	0%	0	0	0	0	0	0	0	0%	0%	0%	0%	0.00	0
		Blade Remounted for replacement	R-01-06	0	0	0	0	0	0	0%	0%	0%	0%	0%	0	0	0	0	0	0	0	0%	0%	0%	0%	0.00	0

c. Cost Model

Aalborg University has developed a generic cost model which is linked to the information in the Guide 2 Defect (G2D) database. The model can be used to formulate a damage model with 6 categories and hence form basis for informed choice between several options, with the extremes being no action and stop of operation. The model is thoroughly described Under work package 1 in this Document.

The findings has been presented in a number of workshops by John Dalsgaard Sørensen of Aalborg University, often immediately after G2D has been presented. Below is the summary of the example typically used at the work shops:

Example



Defect type considered in G2D: "Root – Surface – Cracks – Longitudinal"

6 stages:

- Stage 1: Length 0 to 50mm (Category 1)
- Stage 2: Length 50 to 200mm (Category 2)
- Stage 3: Length 200 to 500mm (Category 2)
- Stage 4: Length 500 to 1000mm (Category 3)
- Stage 5: Length 1000 to 3000mm (Category 4)
- Stage 6: Above 3000mm (Category 5)

Table 1: Number of longitudinal surface cracks with a given size.

Size	0-50mm	50-200mm	200-500mm	500-1000mm	1000-3000mm	>3000mm
Number	6	15	34	53	23	18

4. Work Process

The chosen work method of using a combination of intensive work-outs combined with one-to-one dialogue and email communication all coordinated with a strong project manager has proven to be very effective and has beating the "calendar-death-issue". This method has allowed a wide range of stake holders taking actively part of the work providing valuable input and knowhow but not delaying progress, but no shows and long planning horizons. Hence this working method is highly recommendable for similar work packages.

The dialogue with other work packages has been more challenging, and particular has the original team behind the project development work package failed to see the value of the work package, and has not responded in due time to the market entrance list. The result is a strong mechanical product, but no considerations for the meta-product and the non-objective reservations at customers. The strong recommendation for future similar projects is thus to ensure full buy-in from the product development team in the commercial angle towards product development and to have an improved and more formal dialogue between the commercial and the product development work package. If Boving Horn should lead a similar work package in future projects, a specific work out with the product development team would be included in the planning.

5. Results

This work package has delivered what it should, visible a full commercial Guide2defect spun out in a separate subsidiary and under commercialisation; input for the costing model based on empiric data acquired via the initial version of Guide2Defect; a cost model developed by Aalborg University ready to be applied in the marketing effort; a list of market

barriers and finally a full evaluation of the handling of the market barriers. The work package has thus provided value to the overall project as well as to the participants, and maybe as important – has resulted in a new by-product spun out in a separate company.

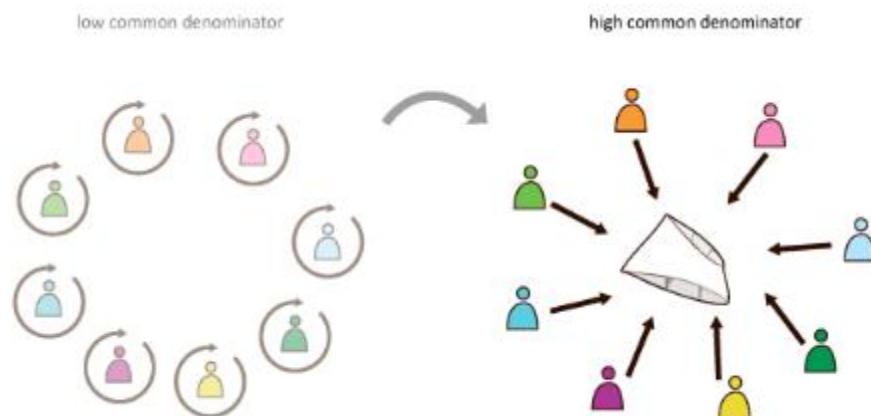
6. Closing

Based on the above, the work package is thus considered as delivered as planned and is closed.

WP11 Visualization and Logging

WP responsible: Rune Kirt, Mads Thomsen, Jonas Bentzen, Sanne Fredin Christensen from Kirt Thomsen

Partners: KIRT x THOMSEN, Bladena (+ input from DTU Wind Energy, AAU, Total Wind Blades, DTU Mech., Vattenfall, EON)



Introduction

To meet the challenges of having various partners with different backgrounds, using different technical nomenclatures and terms, and having different focus areas this work package have added a new “tool” to the development process by creating a visual foundation for logging of ideas, conclusions and challenges. KIRT x THOMSEN has developed this into a further commercialized service product – a visual handbook – that helps clarify, verify and accelerate R&D projects in industry. Further, the work package has included a number of individual meetings, study trips and lecture attendance where input from partners has been collected and used to highlight the key aspects of the hypothesis using the visualization as a tool for dialogue, of technical conclusions and results and logging of progress.

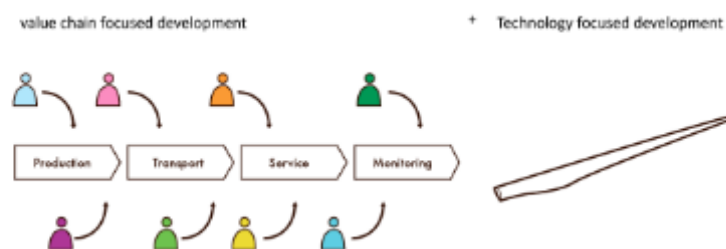
The focus has still the same in the overall description. However, this work package was thought as hosting several workshops (work-out), task 11.2-11.10, along the development process of WP9 among others. This focus seemed of less value compared to the development of the ‘program visualization/logging tool’ which focus is to create the same results as task 11.2-11.10. In other words, instead of collecting all knowledge from arranging workshops/work-outs we have arranged individual meetings, went on study trips and attend lectures.

Finally, the project has experienced a much higher the complexity of hypothesis (loads, twisting, aerodynamics, etc.) therefore WP11 has focused on visualizing the key aspects of the deformations in a way all external and internal stakeholders can grasp.

Purpose

The purpose is divided into three main focus areas:

- Create a common **visual platform** for communication between all of the 18 diversified project partners
- Communicate the high complexity** of the hypothesis of leading edge damages in an easy comprehensible way
- Visualize and bring focus on the **industry value chain in product development**, mainly processes about installation, service/maintenance and decommissioning.



Work performed

Work performed in WP11 can be grouped into following main areas.

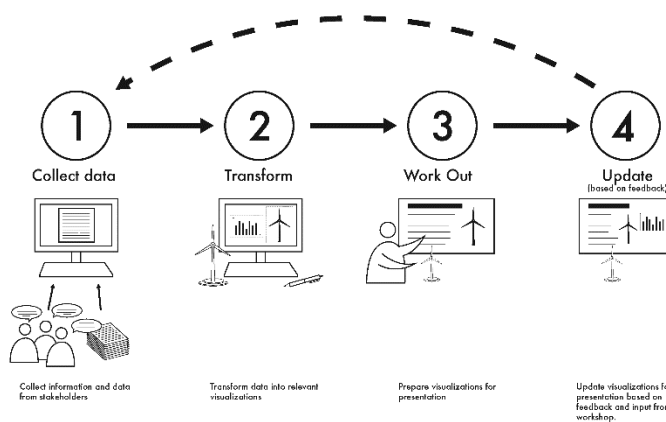
- Develop extensive visualization package for use at kickoff and rest of project time
- Acquire knowledge about hypothesis for leading edge damages
- User/Field research about work conditions
- Integrate new subjects in handbook
- Build up 3D and prepare blade movements
- Learn and adapt new animation techniques

Results

Following models and visualizations - digital or physical - has been developed in the work package.

- Visual platform
- Visual logging tool (handbook)
- Animation (deformations)
- Product development (storyboarding-consulting)
- NGIR templates
- Photocard

KIRT x THOMSEN has worked by an iterative method, starting the process by asking who is the audience (target group) to receive the output information and what are they interested in. With this as backbone knowledge, the process of collecting information/data/input through meetings/lectures/user research has been initiated (1). Step two (2) has been to transform the input into a format (animation, model, etc.), which will explain the meaning in the best way to the given audience. Third step (3) was to present the material at a workshop/meeting/email and get feedback of how to improve and correct the content. Last step (4) was to update the material. And then repeating the process again over and over again till content and output is acceptable.



Visual tools for R&D

The media can and will vary based who is the audience - what is the use and purpose of it, and how will it be used afterwards.

KIRT x THOMSEN works with all sorts of visualization tools. For this work package, we have developed a visual toolkit to fit the best to the project’s purpose. Animation is a key tool to visualize and understand the complex nature of hypothesis’ mix of structural deformation forces and aerodynamics.



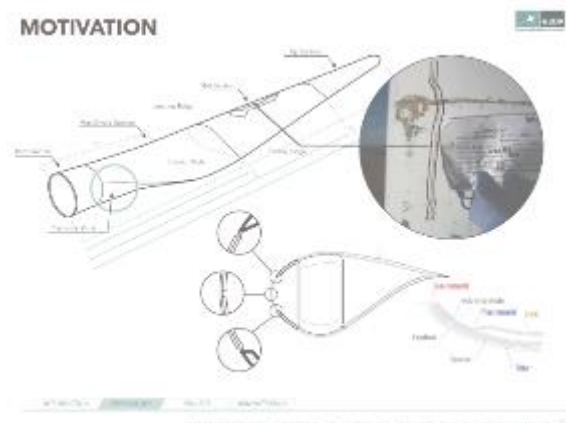
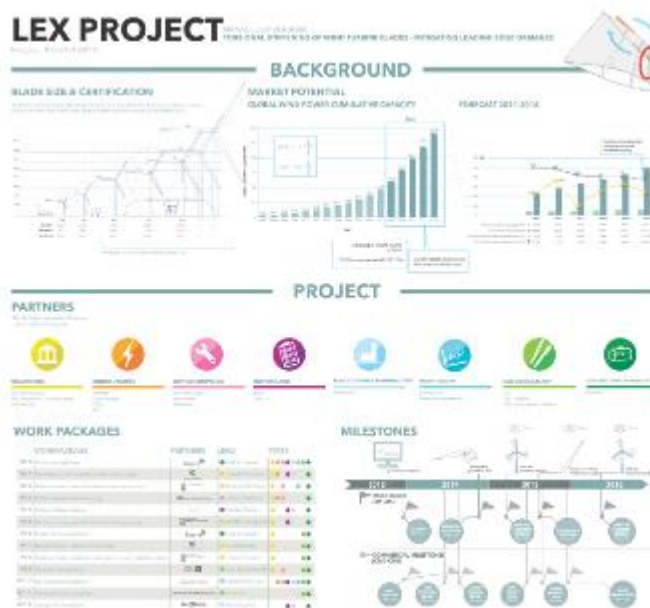
1. Visual platform

To meet to need of a common technical understanding among all stakeholders we have developed a visual package that should create a clear understanding of the technical part of

the project as well as the project setup itself. The complex information was transformed into visualizations in:

- Presentation, ppt
 - PowerPoint presentation layout and content design (kickoff)
- Boards
 - 2x A1 boards printed w. project setup and technical focus
- Partner/WP/timeline overview
 - A4 Milestone and partner overview printed
- 3D printed models
 - 3x 3D printed model of WTG, scale 1:100
 - 1x 3D printed model of test-rig, scale 1:100
 - 4x handmade models of blade section
- Blade visualizations
 - 32x illustrations

All in a way, that created a clear understanding and a verification of the project to create basis for discussion of the deformation hypothesis.

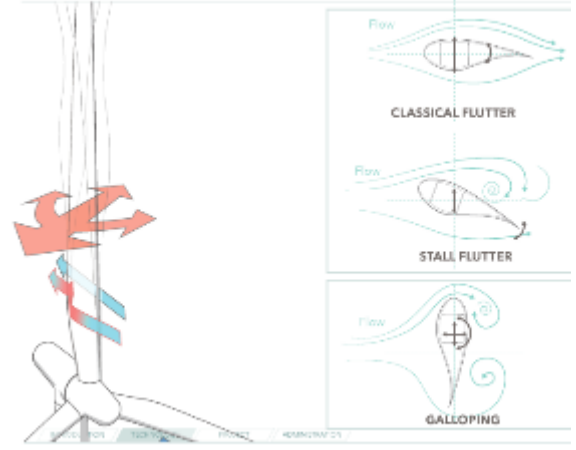


LEX PARTNERS

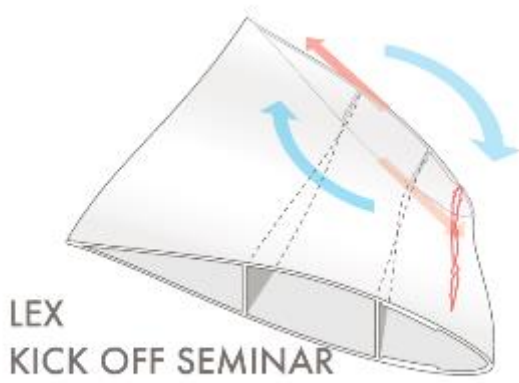


LEX PROJECT | TORSIONAL STIFFNESS OF WIND TURBINE BLADES - MITIGATING LEADING EDGE DAMAGES

AEROELASTIC INSTABILITIES



LEX PROJECT | TORSIONAL STIFFNESS OF WIND TURBINE BLADES - MITIGATING LEADING EDGE DAMAGES

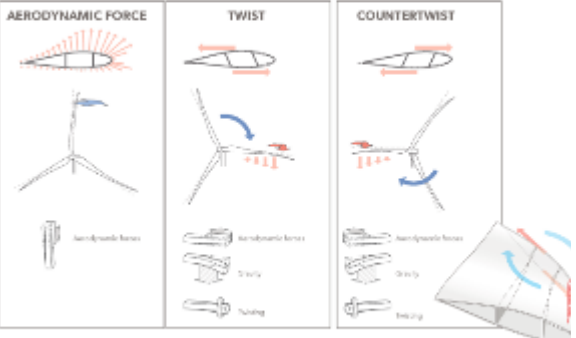


LEX KICK OFF SEMINAR

TORSIONAL STIFFNESS OF WIND TURBINE BLADES - MITIGATING LEADING EDGE DAMAGES



COMPLEX LOAD SCENARIOS



LEX PROJECT | TORSIONAL STIFFNESS OF WIND TURBINE BLADES - MITIGATING LEADING EDGE DAMAGES



A scaled 3D print model of a wind turbine was developed in 3D software and printed and assembled in a scale 1:100. Three copies were produced to be used as a reference model when having workshop, meetings, discussion or other dialogue in the daily work. First time they were used at the kickoff workshop in oct 2013. Afterwards one was handed over to Bladena as the project key holder, one to E.On to be used to discuss about the wind turbines topic in their organization and in the industry and one was kept by KIRT x THOMSEN to be used as reference for the coming visualizations and dialogue/meetings/workshops to come in the project.

The turbine model is flexible enough to bend the blades and the rotor has the ability to pitch each blade. We have looked into other 3D printing materials and in the future they might be able to produce a selected blade section with higher “rubber” flexibility if expenses allow it.



2. Visual logging tool (handbook)

To create a red line and a common language through the project we came up with the idea of creating a visual dictionary - or handbook as it has been named in the project. First edition of the handbook was developed for the kickoff meeting. Second edition was updated for the annual meeting in nov 2014 with input from WP1, WP7, WP8 about standardization, beam theory and aerodynamics. Further the handbook will be updated with input from WP3, WP5 with input service crew work and testing.



The final edition was ready by winter 2015/16. The final edition has been printing in 200 hard copies with flat back and 200 with stapled binding. A large amount of these prints have already been handed out to internal project partners, as well as to external stakeholders, such as Vestas R&D among others.

The feedback has been very positive both from university for purpose of education as well as blade manufactures for the design team of the future blades.

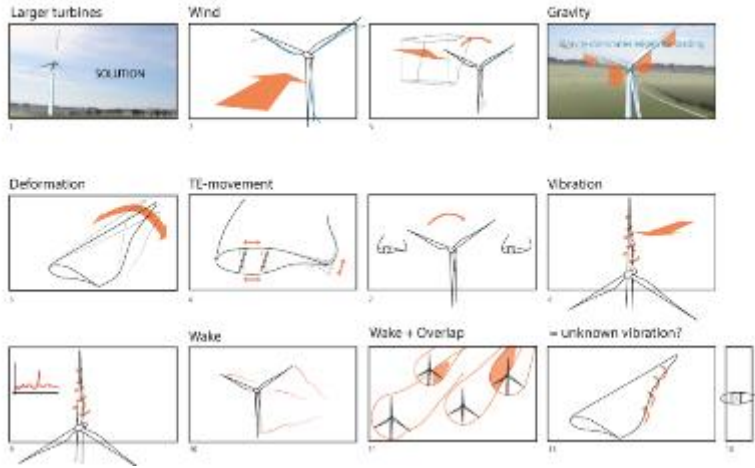
3. Animation (deformations)

An animation is developed based on a sketched out storyline. The animation is showing the deformation of the blades by wind forces, gravity and rotation – on a rotor view and from a single blade perspective. The wake is initiated by experimentation with particle animation.

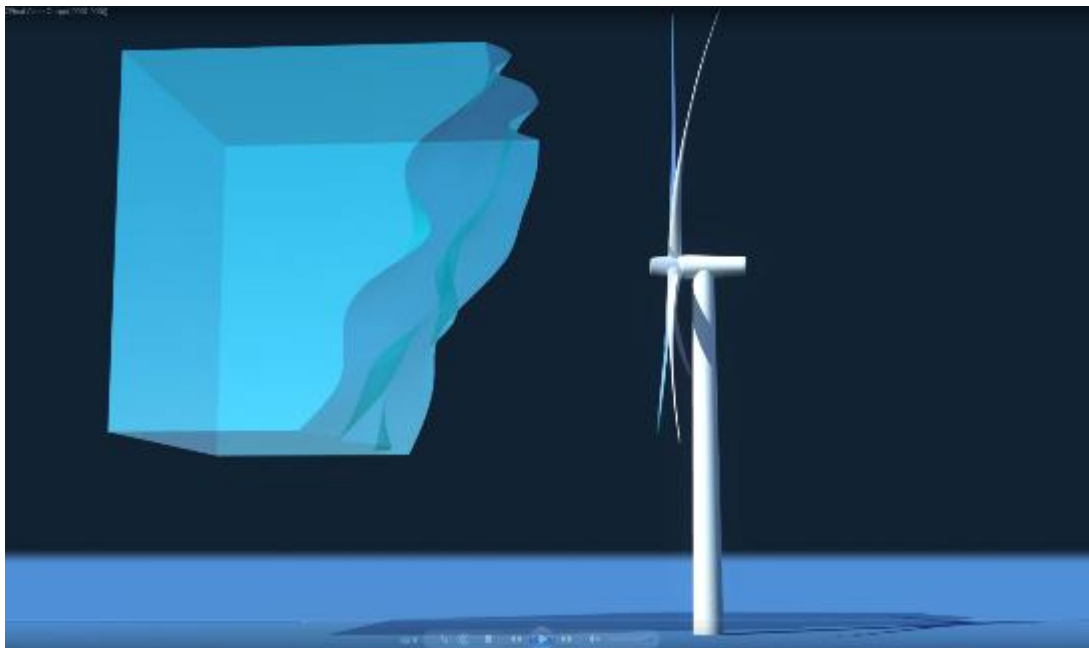
LEX Animation - Animatic.

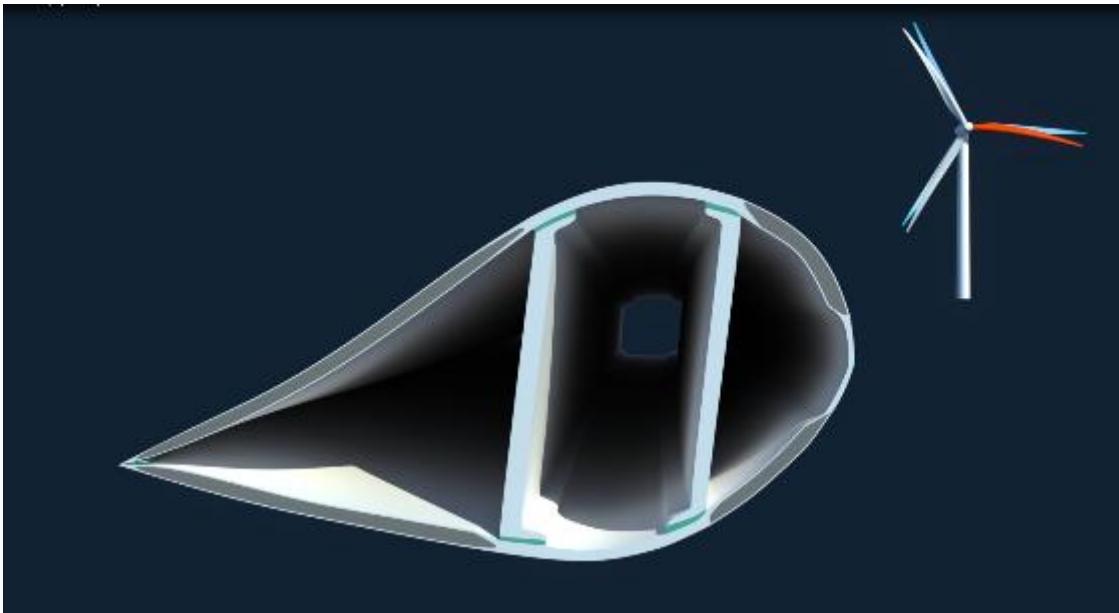
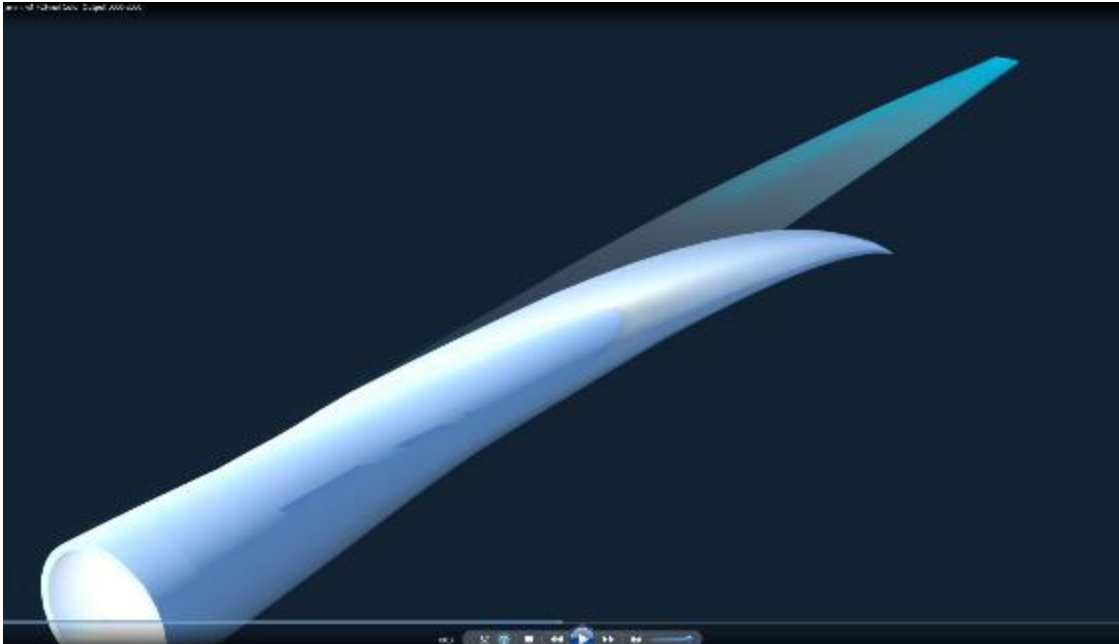
Storyboard v2

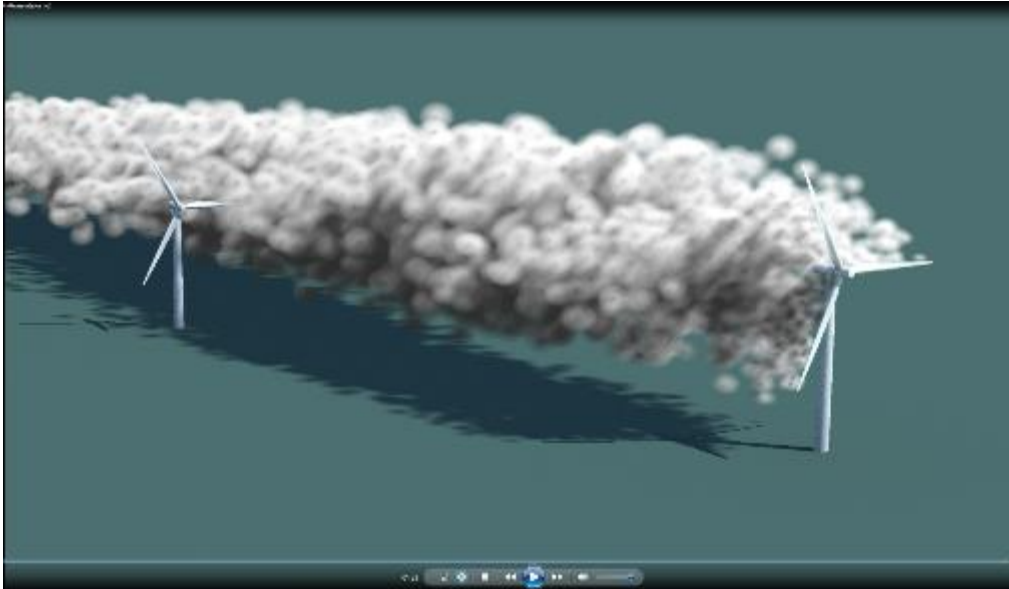
EMPHATIC (EMPHATIC) 2014-2015
EMPHATIC (EMPHATIC) 2014-2015
EMPHATIC (EMPHATIC) 2014-2015



The animation is uploaded online by the end of LEX project.



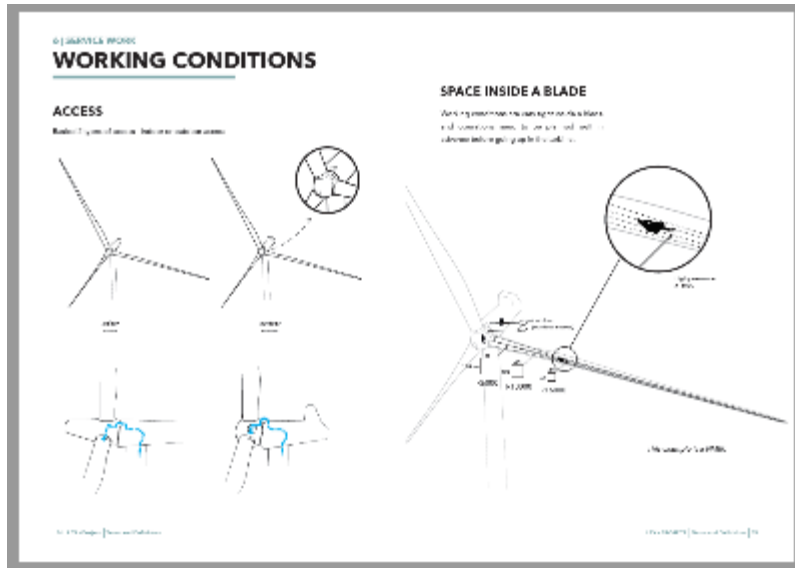




4. Product development (user research)

Two field trips were initiated – one trip to Total Wind Blades in Brande to see various blade types and one trip to Tjæreborg to get up into a working wind turbine. Both trips have given input to work procedures and access dimensions, weather conditions and as a whole a real life insight which could not have been achieved at the office.

This knowledge input and meetings with Total Wind Blades, has been transformed into visualizations which are featured in the handbook and have been used actively in the design process of the X-Stiffener.



Trip to Brande

Study the blade working conditions at Total Wind in Brande.



Test turbine, Tjæreborg (Esbjerg)

Study the very tight access options through the spinner and nosecone in a working turbine. And the attachment of wires, and other equipment.



5. NGIR templates

NGIR is Next Generation Inspection Reports. Today inspections reports look very differently from service companies to energy utilities. The work of NGIR was to generate of common standard of inspection report and which terms to use when inspecting.

The starting idea of this task was to create one Instruction (guide of how to do the work) and one Report (an empty word document to fill out). As input was collected from meeting, it turned out 7 documents in total was needed.

Therefore, we created a visual guideline with icons, colours, header, and fonts to make in simple for the reader/user to navigate in.

Visual guideline:



Skrifttype: DIN Alternate Light

OVERSKRIFT - DIN ALTERNATE MEDIUM

Bredtaket i callibri regular.
 Utpe non mīdīe mēna que que per-
 cōdi ad que conem et quōtā dōle ad
 dolōstīvum, que non res autem de a
 callīcōpūle sumet ut.
 Bo. Ecturīsqūant lobōre ad cōstītas
 quōtā vertīte solo quāvante quā plū
 ut aut letīstēm perīvū ut dūm quā-
 perīo etur, si cūptatōm et adīc tem
 nōtū tū dīlī mōdō cōnsequ dāndē

Farver

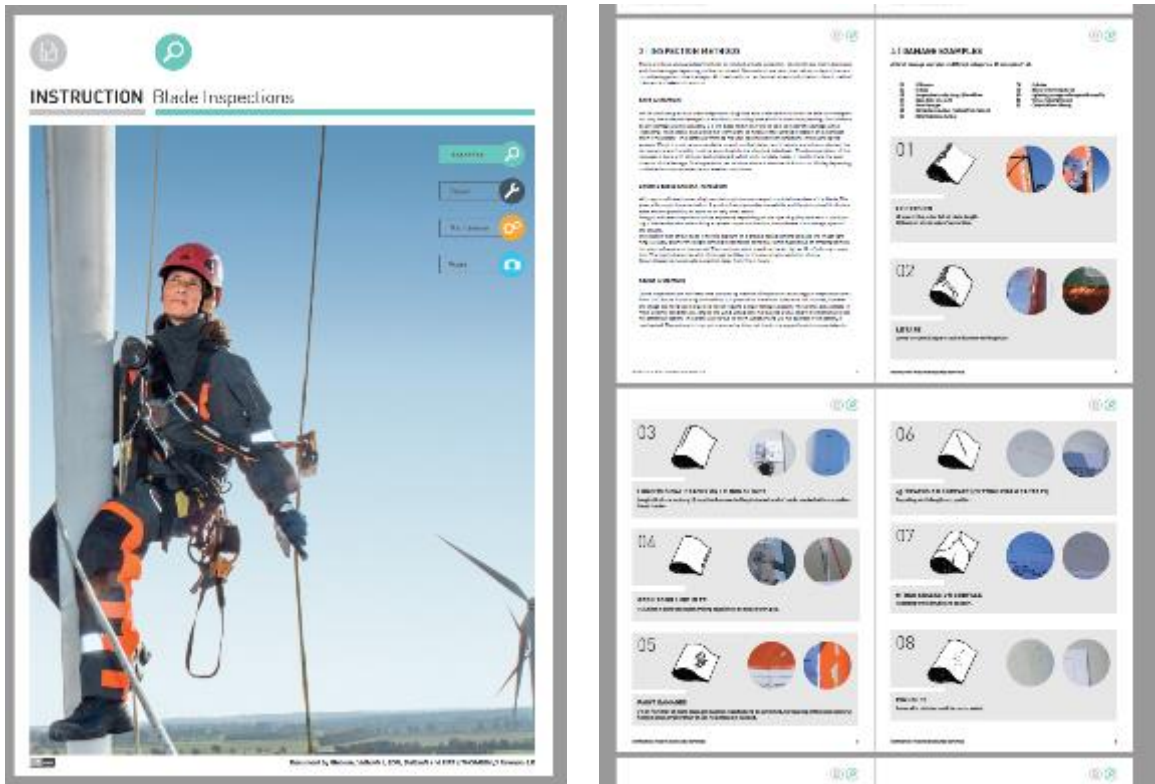


Ikoner

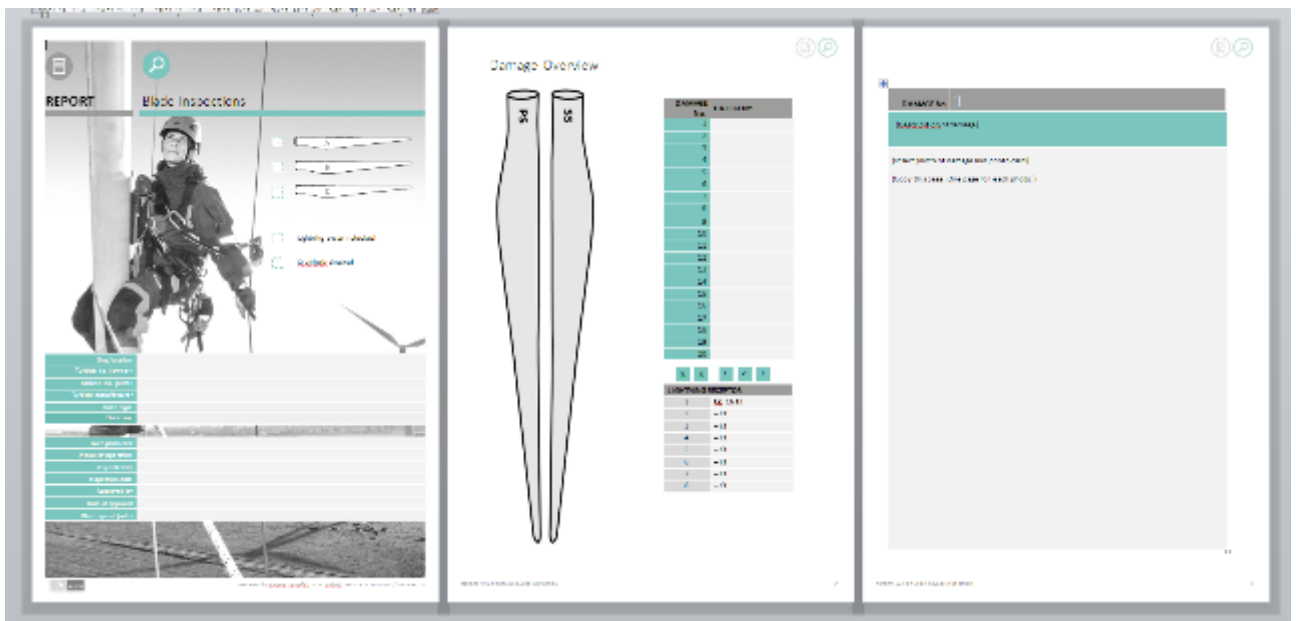


Content to Instructions and Reports have been collected by Bladena from the industry partners Vattenfall, E.on, and Statkraft. From that we have updated the documents.

See Instruction on next page.



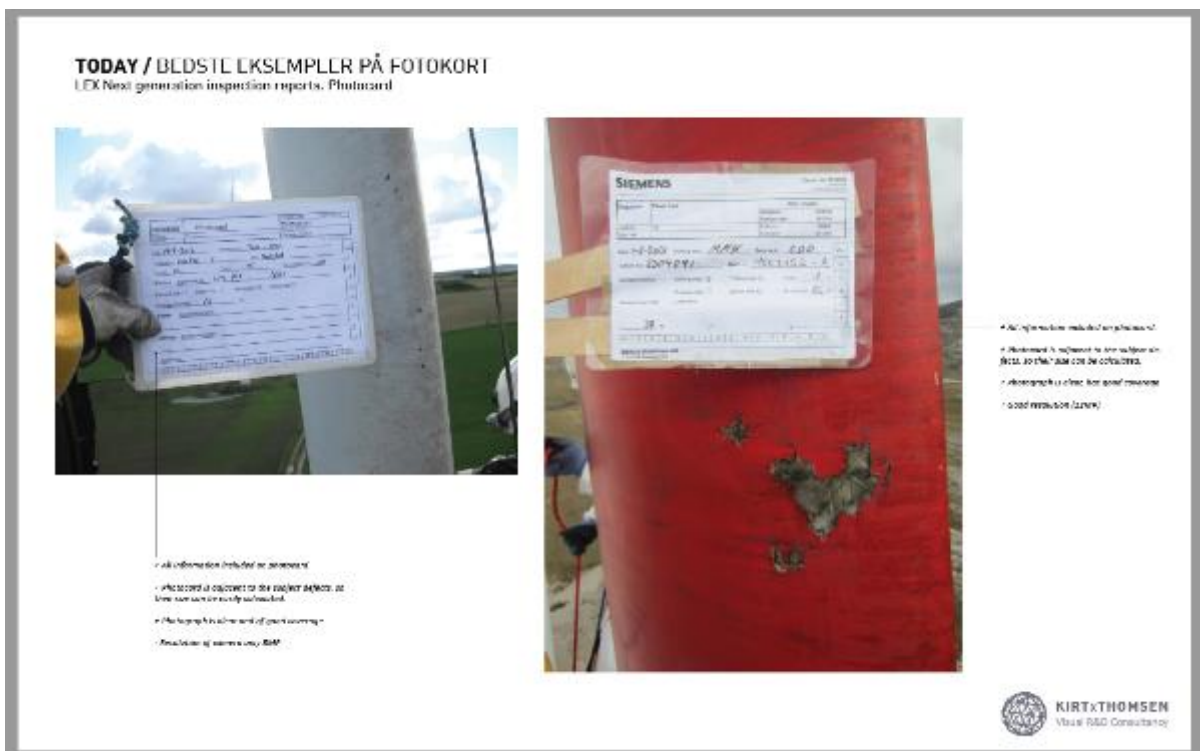
Report:



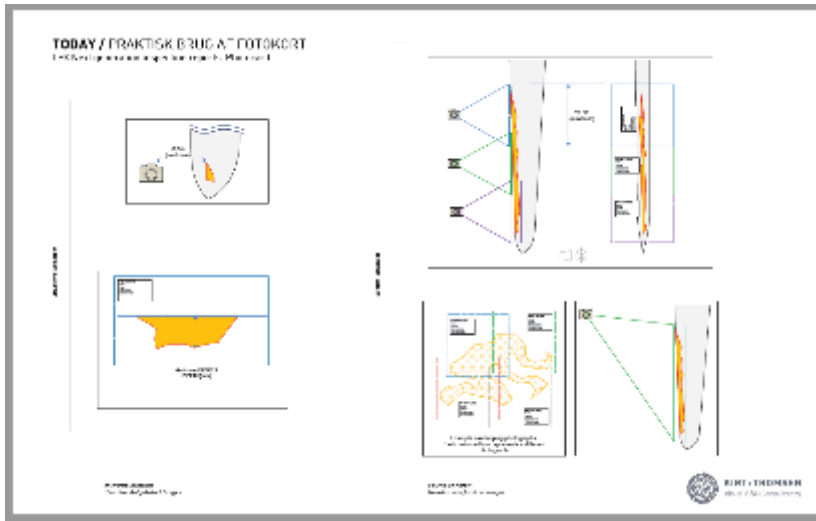
6. Photocard

The aim was to design and create a new standard of photocard to be used across wind industry. E.on, Vattenfall and DONG have been industry partners in the process, along with Bladena as blade experts.

Input from industry partners was collected, in order to highlight existing work method and problems related to existing photocards.

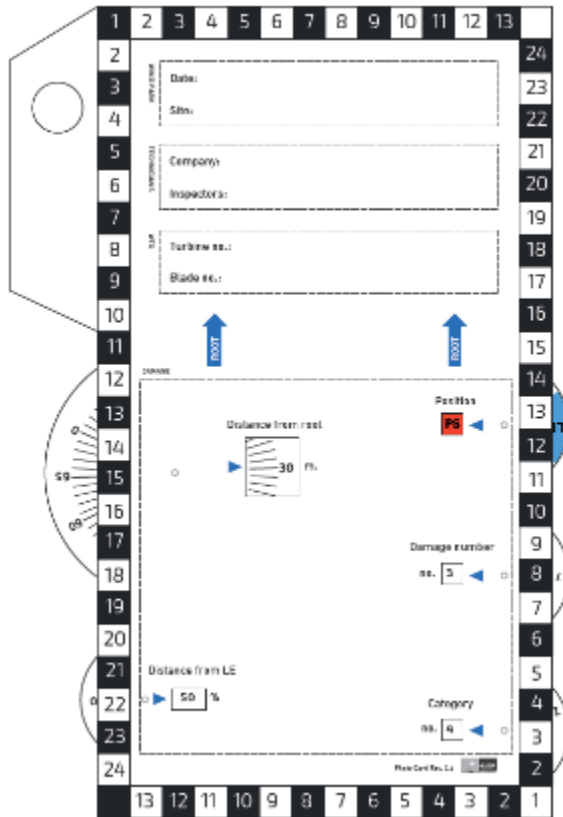




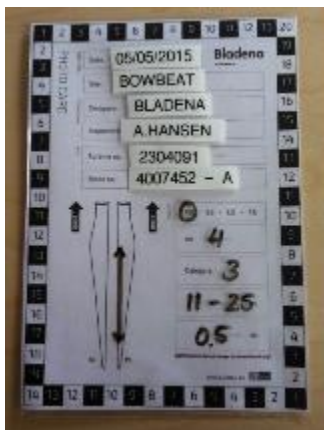


Based on the research a development process was conducted to create the new common card. The final design draws lines to the photocard which Dong Energy already is using today. Optimizing and adjustments to the size, content and handling have been modified.

First prototype of this new card has been used by Vattenfall and E.on during Q3-Q4 2015.



One of the designs from the design process, and testing of adding information:



WP12 Design of new blade

WP responsible: Pedro Muñoz de Felipe from Aeroblade

Introduction to WP

Under operational conditions wind turbine blades are exposed to different loads which produce high stresses in their structures. Along their operational life, it can be seen that several damages appear at the blades structures (visible or not from the surface) causing high costs of maintenance and raising the price of the wind turbine.

Due to that, it can be ensured that nowadays the wind turbine international standards are not covering all relevant structural related failures. In order to improve the strength of blades and increase their life time (decreasing maintenance costs) Bladena has developed different structural enhancement technologies.

One of the main purposes of Aeroblade is to evaluate these enhancements based on structural reinforcements using FEM techniques that allow, in terms of structural integrity, detailed analyses.

The second target of this WP is to evaluate the impact of the Bladena's devices in the Levelized Cost of Energy (LCOE).

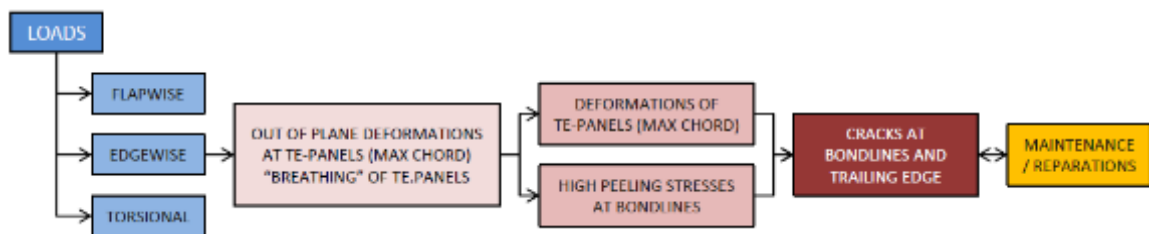


Figure 102: Wind blade operational conditions scheme - Loads applicable to wind blades and stresses, deformations and damages that occur as a consequence.

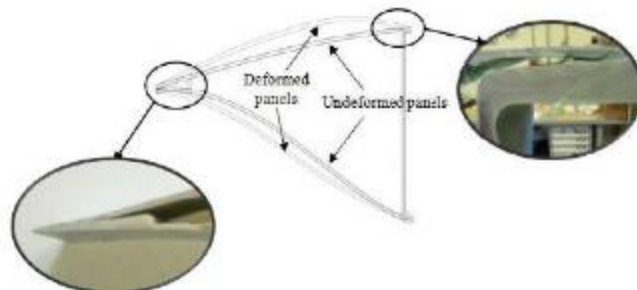


Figure 103: Breathing of TE panels – Out of plane deformations that occur at T.E panels located at Max Chord area.

Scope

The aim of this work package is to design a large (60m) light weight blade based on some of the patented technology from Bladena. When the blade is designed a discussion with the owners in the refurbishment project will be set-up and the outline including the budget for producing these blades will be presented.

Although cross reinforcement may not be optimal for a new design, it is applicable in case of retrofit. A comparison has been performed between an existing blade design and a new one consisting of the previous one retrofitted with the X-Stiffeners.

The comparison includes cost aspect, e.g. manufacturing cost, by introducing the new technology. The 60m blade has been analyzed with and without this technology in order to see whether is attractive for large blades e.g. for offshore installation. Final FEM models have been analyzed by means of a non-linear solver and 3D solid elements have been used.

Aeroblade's 60m blade design has been used as a baseline, the analysis includes additional design criteria consisting of loads combination, evaluation of cross-sectional distortion and the generated strains.

AB6X rotor blade

The main features of the AB6X blade, which has been taken as the analysis baseline are as follows.

Main Dimensions:

- Length: 57500mm
- Max. Chord: 3802mm(at STA 12500mm)
- Root diameter: 2921mm



Figure 104: Main features of AB6X blade – AB6X edgewise and flapwise views.

Structural Configuration:

- Mainly composed by two shells (pressure shell and suction shell)
- Shells are bonded to each other at leading and trailing edges and to inner span wise shear webs
- Shells include pre-cured caps (integrated solid laminate)
- Shells and shear webs define the central box
- Closed shells withstand torsion loads
- Integrated caps withstand moments in flap direction
- LE and TE reinforcements contribute to the blade stiffness necessary to withstand moments in edge direction
- Webs withstand shear loads

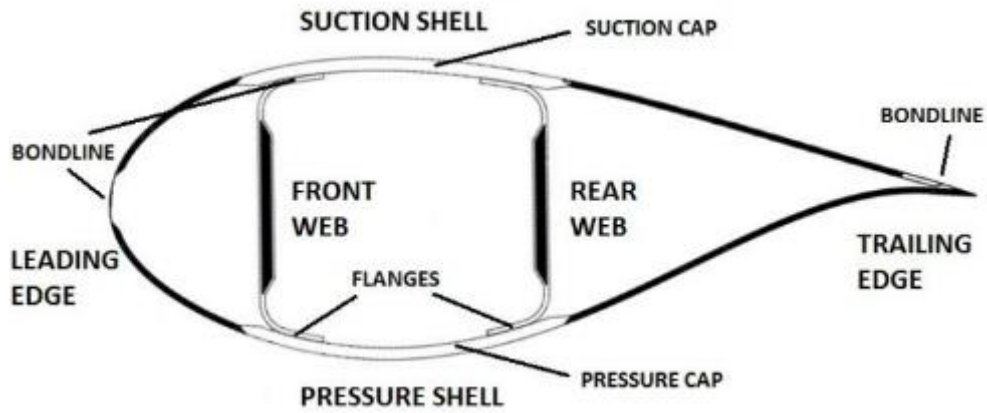


Figure 105: Blade structural configuration – Blade structure main parts.

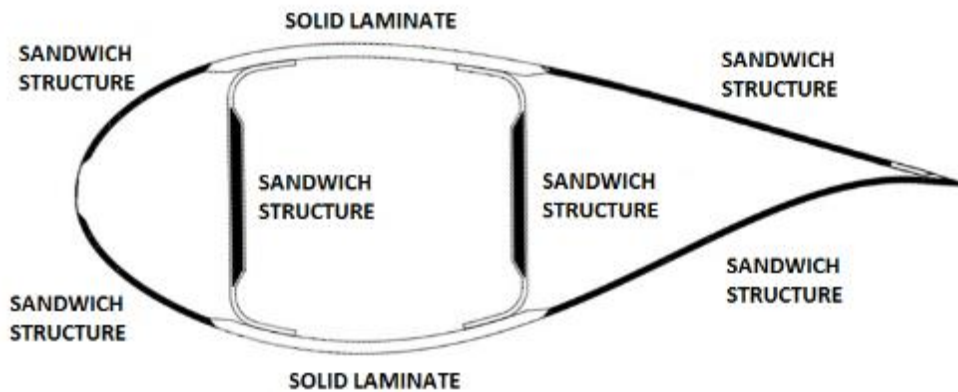


Figure 106: Blade structural configuration – Nature of Blade structure main parts.

Blade finite element models

The main features of the FE models that have been developed within the project are listed below:

- Structural components modeled with 2D (basis for the 3D elements models) and 3D elements.
- Two principal model versions have been developed, a 2D model (with conventional shell elements) and a 3D model (with continuum shell elements). The 2D model has provided the basis for the 3D FE modeling.

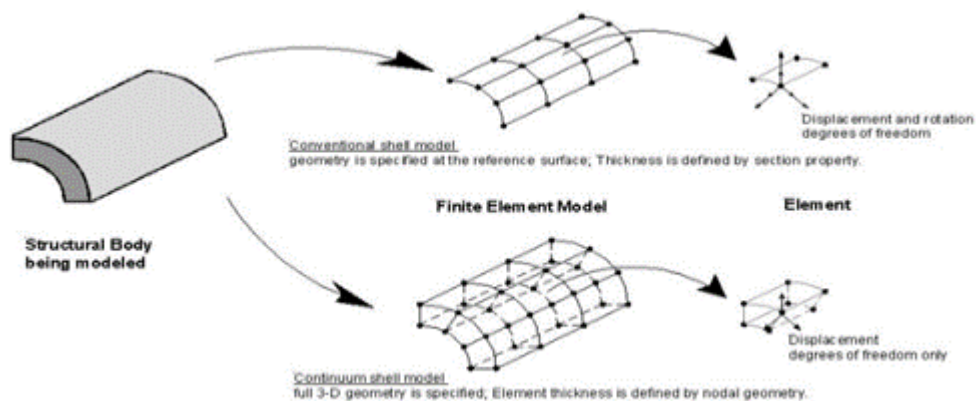


Figure 107: Differences between conventional and continuum shell models.

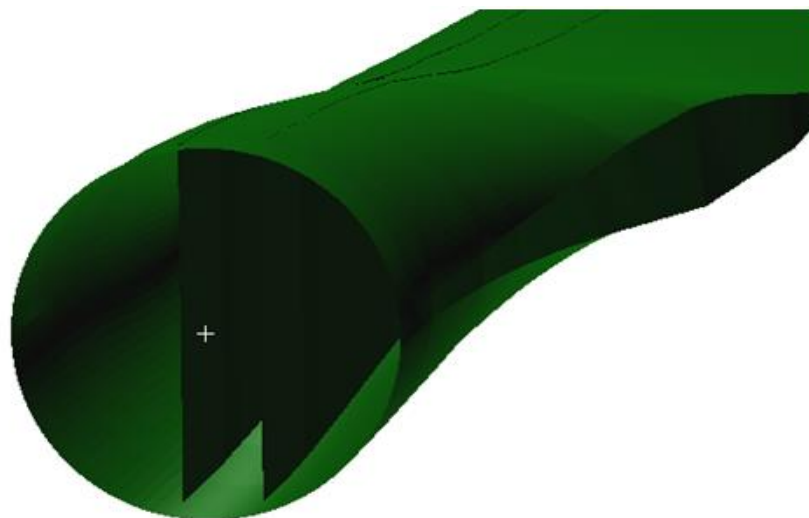


Figure 108: 2D Finite element model -



Figure 109: 3D Finite element model

- 2D orthotropic material properties and the corresponding orientation for each structural component are considered
- Individual plies are defined
- Blade is clamped at the root section
- Covering the most critical load for the cap, positive flap moment (MFlapPos) load case is simulated
- On the basis of the initial 3D model (3Dv01) two refined 3D FE model has been developed (3Dv02 and 3Dv03).

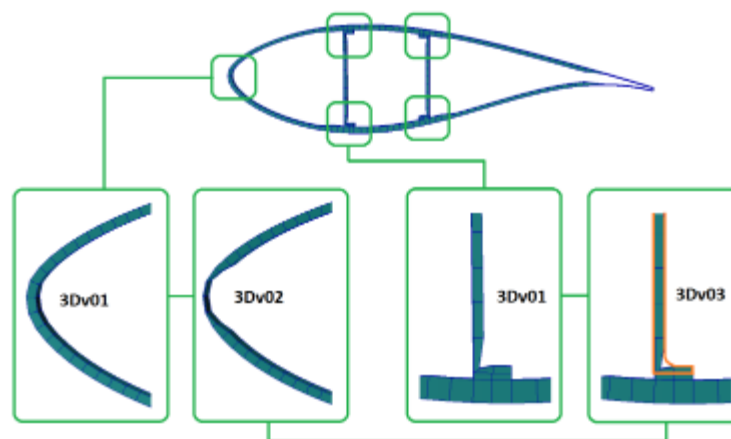


Figure 110: Refined 3D Finite element models

- The 3Dv03 model has provided the basis for the development of additional 3D FE models, used to evaluate the X-Stiffener performance within the blade structure.
- Aerodynamic loads are applied at different sections and performed in 2 steps:

- 1st step: blade loaded flapwise causing a deflection in this direction
- 2nd step: blade loaded (additionally) in edgewise direction

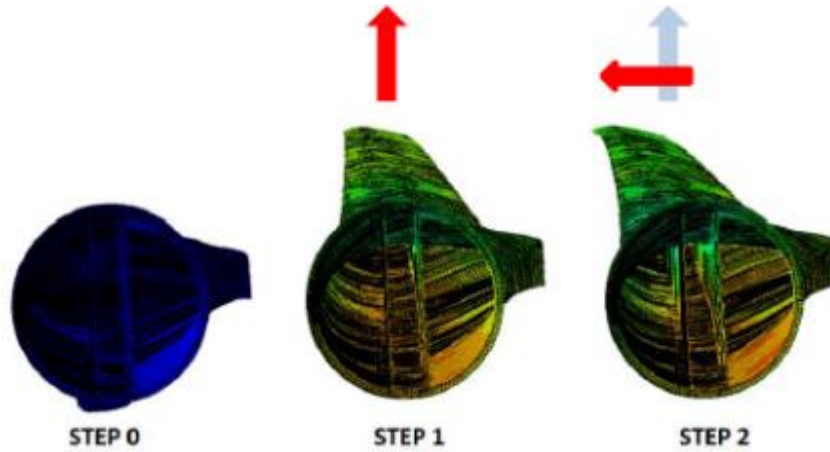


Figure 111: Aerodynamic loads –Application steps.

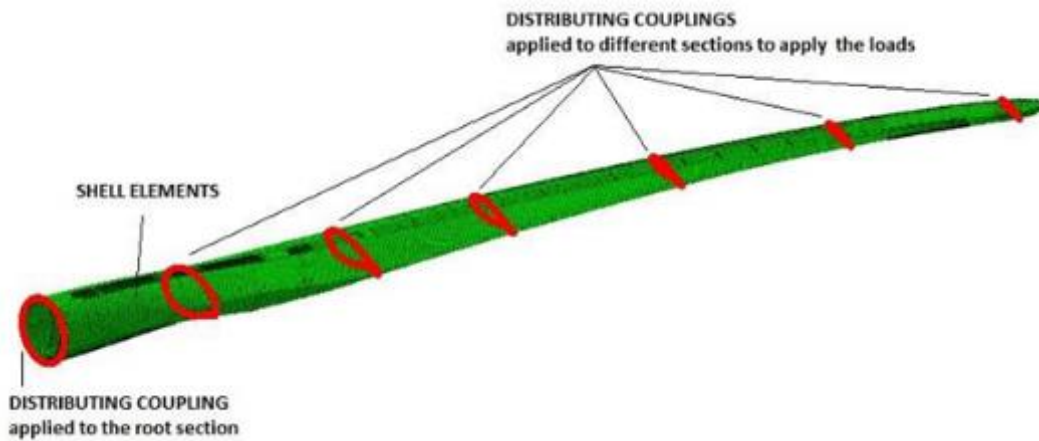


Figure 112: Aerodynamic loads –Application sections.

Modelization of Bladena X-Stiffeners:

The X-Stiffeners are strings that work as tension elements (not compression). Which are implemented among the points located at the corner between caps and shear webs. In the FE models X-Stiffeners have been modeled by means of bar elements between two nodes located near the points explained above. The attachment among these nodes and the nodes that belong to the shells and webs has been modeled by means of kinematic coupling constraints.



Figure 113: X-Stiffener implementation within blade structure.

```
*MATERIAL, NAME=STIFFENER_MAT
*ELASTIC
20000.,0.01
*NO COMPRESSION
**
*ELEMENT, TYPE=B31, ELSET=STIFF_3900
3900,3901,3902
*BEAM SECTION, ELSET=STIFF_3900, MATERIAL=STIFFENER_MAT, SECTION=CIRC
5.
0.,0.,-1
```

Figure 114: X-Stiffeners FE modelization.

3D FE models

In order to verify the X-Stiffeners performance, a comparison has been done among the results obtained from the FE models listed below. Although additional 3D FE models have been performed throughout the WP12 development, those were considered to be which best represented the improvement, in terms of blade cross-sectional shear distortion, of X-Stiffeners implementation within the blade.

The table below shows the differences among such FE models.

PARAMETERS	FEM MODELS		
	3Dv03	3Dv03 LEX-X5 AEROBLADE	3Dv03 LEX-X BLADENA
NUMBER OF LEX-X STIFFENERS	NONE	Every 500 mm	Every 500mm
STIFFENERS PROPERTIES	NA	E=57 GPa; R= 5mm	E=57 GPa; R= 5mm
COUPLINGS EXISTENCE	NA	NO	NO
CONSIDERATION OF LEX-X STIFFENERS COMPRESSION	NA	NO	YES

Table 17: Characteristic of the most representative FE models

FE models results

Due to web's corners displacements are directly related to blade cross-sectional shear distortion, and as a consequence to X-Stiffeners performance, such values have been under study over the above listed FEM models.

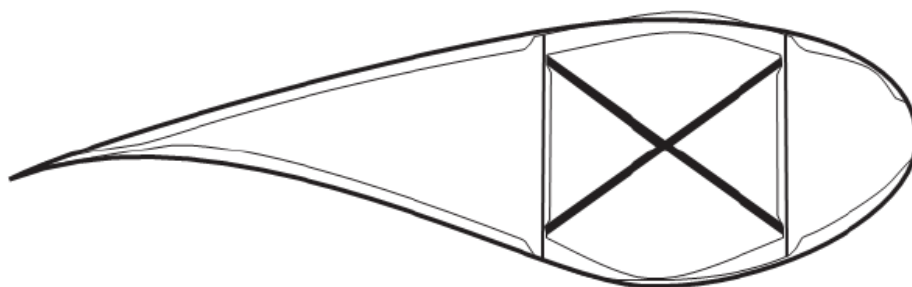


Figure 115: X-Stiffener configuration – Location within the blade structure.



Figure 116: Webs' FE mesh, node location. FFU-FRL and FFL-FRU distances definition.

The graphics below show the results obtained from the FEM models commented above, regarding web distance variations. Such values have been depicted for STEP1, where MFlap load is applied and during STEP2, where both MFlap and MEdge loads combined are applied.

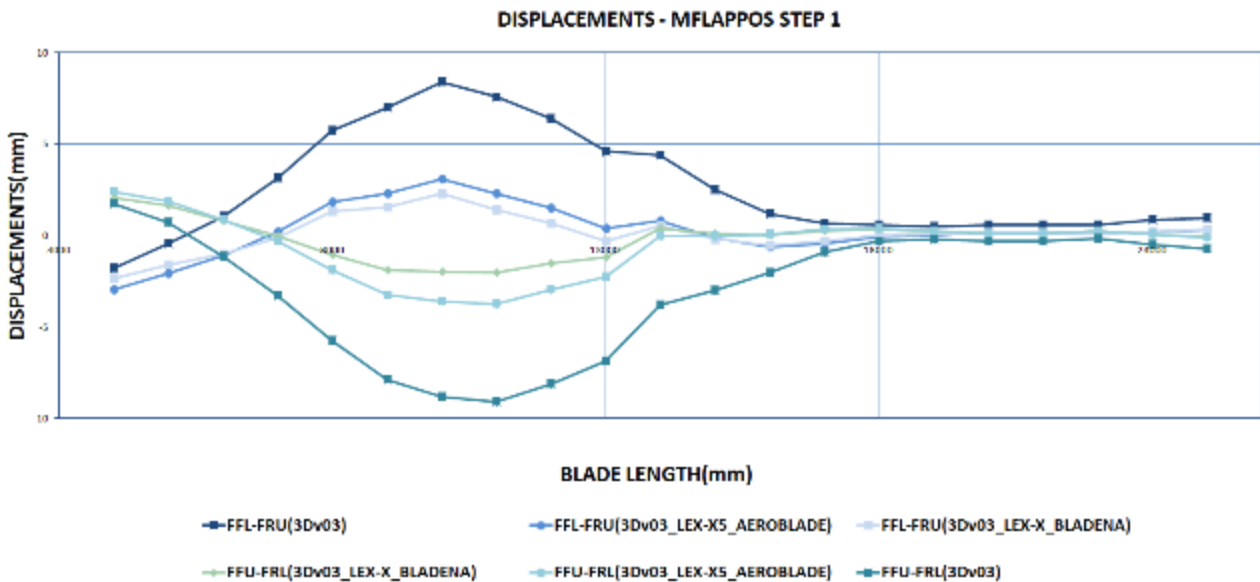


Figure 117: FFU-FRL and FFL-FRU distances variation. Variation measured at Step 1 for the 3D FE models listed above.

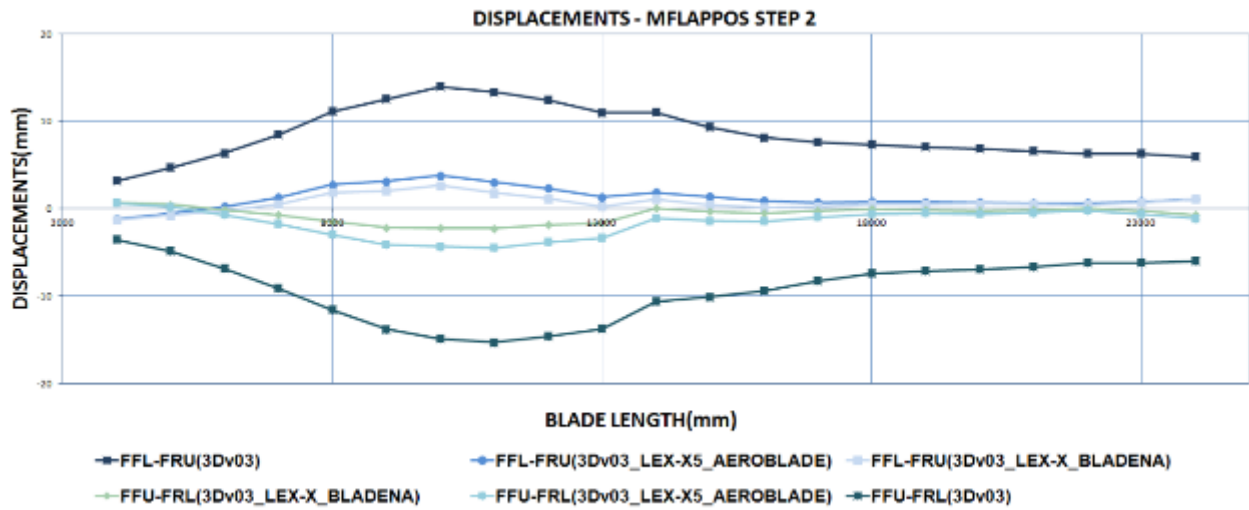


Figure 118: FFU-FRL and FFL-FRU distances variation. Variation measured at Step 2 for the 3D FE models listed above.

Table 18: Stiffeners axial stress values for 3Dv03 LEX-X BLADENA and 3Dv03 LEX-X5 AEROBLADE models.

3Dv03 LEX-X BLADENA				3Dv03 LEX-X5 AEROBLADE			
ELEMENT	S_{11} (N/mm ²)	ELEMENT	S_{11} (N/mm ²)	ELEMENT	S_{11} (N/mm ²)	ELEMENT	S_{11} (N/mm ²)
3900	16.85	14100	43.02	3900	13.64	14100	78.91
4100	-27.43	14400	-4.71	4100	0.00	14400	0.00
4400	13.51	14600	29.50	4400	8.97	14600	61.28
4600	-24.23	14900	-13.79	4600	0.00	14900	0.00
4900	8.68	15100	18.88	4900	2.28	15100	0.00
5100	-18.55	15400	-17.50	5100	0.00	15400	0.00
5400	3.99	15600	13.85	5400	0.00	15600	0.00
5600	-14.32	15900	-25.89	5600	0.00	15900	0.00
5900	-3.77	16100	5.32	5900	0.00	16100	0.00
6100	-8.77	16400	-14.41	6100	6.60	16400	0.00
6400	-11.04	16600	11.22	6400	0.00	16600	41.67
6600	-1.41	16900	-16.92	6600	18.37	16900	0.00
6900	-17.24	17100	10.25	6900	0.00	17100	35.11
7100	7.99	17400	-11.54	7100	32.30	17400	0.00
7400	-29.67	17600	16.11	7400	0.00	17600	40.22
7600	21.44	17900	-4.77	7600	52.93	17900	0.00
7900	-39.19	18100	22.55	7900	0.00	18100	42.26
8100	42.85	18400	-9.45	8100	74.21	18400	0.00
8400	-55.22	18600	20.97	8400	0.00	18600	0.00
8600	46.16	18900	-4.53	8600	79.92	18900	0.00
8900	-60.83	19100	23.68	8900	0.00	19100	40.92
9100	51.54	19400	-11.16	9100	90.65	19400	0.00
9400	-65.84	19600	25.09	9400	0.00	19600	40.26
9600	61.42	19900	-15.40	9600	105.94	19900	0.00
9900	-62.27	20100	27.12	9900	0.00	20100	41.42
10100	76.25	20400	-14.35	10100	118.81	20400	0.00
10400	-67.69	20600	28.38	10400	0.00	20600	40.41
10600	70.05	20900	-12.19	10600	111.21	20900	0.00
10900	-75.09	21100	27.80	10900	0.00	21100	37.82
11100	58.89	21400	-9.80	11100	102.68	21400	0.00
11400	-69.33	21600	24.08	11400	0.00	21600	34.16
11600	53.29	21900	3.38	11600	97.18	21900	0.00
11900	-65.88	22100	23.96	11900	0.00	22100	35.61
12100	42.34	22400	-8.90	12100	84.86	22400	0.00
12400	-60.98	22600	25.52	12400	0.00	22600	40.71
12600	31.92	22900	-18.21	12600	70.72	22900	0.00
12900	-65.08	23100	34.20	12900	0.00	23100	53.00
13100	10.39	23400	-28.45	13100	52.62	23400	0.00
13400	-37.02	23600	46.04	13400	0.00	23600	65.76
13600	22.78	23900	-49.69	13600	71.39	23900	0.00
13900	12.12	24100	58.18	13900	0.00	24100	73.05

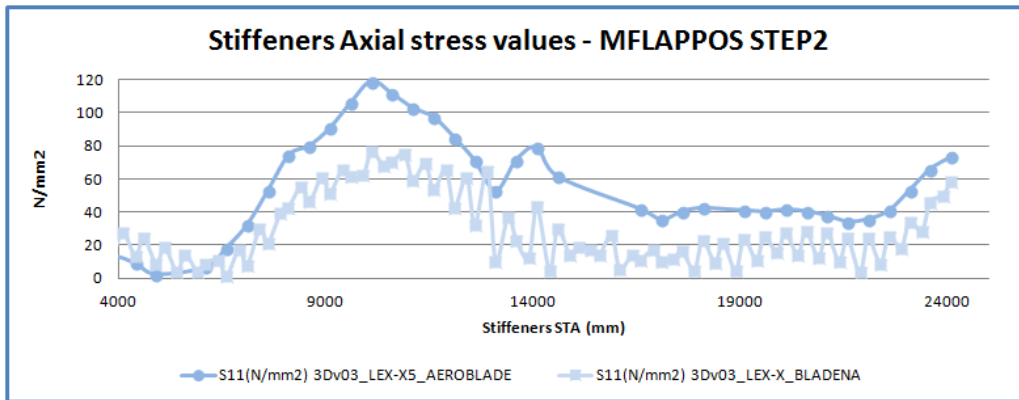


Figure 119: Stiffeners axial stress values for 3Dv03 LEX-X BLADENA and 3Dv03 LEX-X5 AEROBLADE models. Null values have not been depicted for clarification purposes.

COST MODEL: IMPACT OF BLADENA'S DEVICES

Apart from the work related to the FE Modelization (presented in previous section), AeroBlade has developed a cost model in order to take into consideration the effect in the Levelized Cost of Energy (LCOE) of the implementation of some Bladena Devices in a blade. This model uses parameters like:

- Location of the WTG
- Nominal Power
- Maturity of the WTG (or Wind Farm)
- Blade's main Material
- Annual Equivalent Hours
- WTG's Lifetime
- New Blade or Retrofit

That combined with real data gathered from AeroBlade's experience (own developments, information from partners and recognized sources):

- Second level Cost Breakdown Structure (CBS)
 - Influence in the BOM
 - Influence in the processes
- Standard Capex Ranges (by continents)
- Standard Opex Ranges (by continents)
- Type of defects to be addressed

gives a good first overview in order to analyze the convenience of the investment in Bladena's devices.

Determination of CAPex

Assumptions that have been used: Wind turbine generator ONSHORE

Cost Breakdown:

- Wind turbine generator installed without blade cost
- Blade cost baseline for the two principal types of wind blade as function of material: E-glass and Carbon. These figures are based in AeroBlade's internal knowledge and in international reports.
- CBS depend on the country/location (Asia, Europe and America). Percentage of total cost of wind blade (blade materials, consumables, labor and overheads). The numbers of this section are based in AeroBlade's internal knowledge and in international reports.
- Implementation of Bladena devices will have an impact in the manufacturing costs (either negative, less cost, due to potential reduction of the bill of material or positive,

cost increase, because the installation of the devices can suppose extra time and/or materials). The percentages applied in this part are derived from Aeroblade's manufacturing experience and from the FEM Model that has been developed in this project.

Depending on the devices to be implemented, the main reinforcement of the blade and the manufacturing place, the impact in the total CAPex will be different.

Determination of OPex

OPex costs can be differentiated in two main groups:

- Operational cost
- Maintenance cost

Assumptions that have been used: Operational and inspection cost will not be affected by the Bladena's devices.

From the maintenance cost, only a percentage is due to the blade (other effects on different components have not been taken into account for the moment), and that cost is the one that can be reduced with the implementation of Bladena's devices.

The devices developed by Bladena are oriented to correct several common defects, the prevalence of those defects among those affecting the blades is extracted from Aeroblade's records, but it is a configurable parameter that can be adapted to the reality of each wind turbine owner.

The installation of the devices could theoretically solve part of those problems and that is precisely the part of the cost that will be saved. These parameters will be adjusted with the field track record and the own experience of each operator.

Conclusion on WP12

On the one hand it shall be concluded that the implementation of X-Stiffeners within the blade structure leads to a significant decrease of the blade cross sectional shear distortion. Indeed, from the comparison of 3Dv03 and 3Dv03 LEX-X5 AEROBLADE FE models shall be stated that the FFU-RFL and FFL-RFU distances have been reduced by more than 80%.

On the other hand the axial stress values obtained for X-Stiffeners at 3Dv03 LEX-X BLADENA FE model, lead to conclude that X-Stiffeners modelling shall take into account that such elements are only able to take tension forces. Otherwise, stiffeners would work not only in tension but also in compression and this is a non conservative assumption.

Summary of the Project results

The partners of the project have come to the common understanding that the geometric non-linear phenomena cross-sectional shear distortion is a severe issue for modern long wind turbine blades, more than 60m. Advanced finite element simulations performed by Bladena and Aeroblade have come to the same conclusion, namely that cross-sectional shear distortion is an issue which needs to be addressed.

The current commercially available aero elastic simulation tools do not include this topic. In this project two solutions for this shortage were developed:

- The first one concerns updating the DTU Wind energy aero elastic code HAWC2 with new capabilities. This approach considers more details of the blade during aero elastic simulations, therefore the results are expected to be more accurate, e.g. including cross-sectional shear deformations.
- The second method couples the aero elastic and FEM computations in a number of steps that ensure that key nonlinear aspects of the blade structure are captured in the overall analysis.

It has also been concluded that blades with large flat-backs are more prone to cross-sectional shear distortion due to the lack of support in the TE area. The finite element simulations have confirmed the reduction of cross-sectional shear distortion magnitude when the X-Stiffener technology is used.

During the project, field measurements were carried out on two relative small turbines. As expected, the small blades have shown little cross-sectional shear distortion (CSSD) magnitude. Furthermore, the wind conditions during both field tests were low, which resulted in low cross-sectioned shear distortion behaviour. It has been shown in FEM-models that the cross-section shear distortion is dominated by the flapwise load which is very much weather depended. The field tests have been very useful to both calibrate the small FEM blade models. This confirmed that very stiff blades and box bar construction blades with a circular geometry in the 8-10m radius, such as the V80 are not to prone to cross-sectional shear distortion.

The FEM simulations performed by both Bladena and Aeroblade have confirmed that when the blades scale up in size, the cross-sectional shear distortion becomes of major importance. A comparison of small and large FEM blade models revealed that both the magnitude of the cross-sectional shear distortion and the peeling stresses in the adhesive bondlines connecting the main structural parts of the blade together, increases when the blades increase in size.

The peeling stresses in the bondlines increase with the length of the blade, whereas the strength of the glue has not increased during the same “blade evolution” period. As blades with large flat-backs have a higher CSSD magnitude, the stress level is even higher. The X-Stiffener technology is a simple and yet effective way to address the cross-sectional shear

distortion by eliminating the root cause. Thus, the X-Stiffener reduces the fatigue loads in the bondlines to non-critical levels – achieving the overall objective of obtaining long term stable turbine profiles.

The technology was tested on sub-component level and large scale test at Technical University of Denmark (DTU) and it was proven to work without compromising the integrity of the tested blades. FEM simulations and “full-scale” tests show similar behaviour with and without the X-Stiffener.

A large number of FEM studies were carried out each one focusing on individual topics, e.g. difference between different load cases, variation of the blade design, flat-back and no flat-back designs, the influence of blade length on the CSSD magnitude, etc. FEM was used extensively in order to understand the blades behaviour and to create the premises for the testing campaign. Furthermore, the communication content related to blade behaviour (movies, sketches, etc.) is based on FEM simulations.

During the project, due to the novelty of the technology some of the tools used in the simulation process needed to be upgraded in order to capture cross-sectional shear distortion. DTU Wind has made a major improvement in the commercially available code HAWC2 which is now capable of using a more advanced structural blade model in a time simulation. This means that the accuracy of the simulations has increased and more reliable results can be achieved. Furthermore, Bladena was trained to use the aero elastic code HAWC2.

Advancements in structural simulations of the blade were carried out as well where different ways of simulating loads on a blade were performed including a wind distribution approach, this being the “real” load distribution a blade sees during normal operation.

The technical work involved a large number of partners with different backgrounds and technical understanding, therefore good communication was essential. Within the project a good collaboration was achieved between partners including exchange of technical data, e.g. technical files in different formats, etc. The process was supported by utilizing professional communication tools such as 3D printed models and table models, explicit movies and sketches. A handbook with terms and definitions was compiled with input from partners of the project with advanced relevant knowledge. The handbook is available for download and was printed in a high number of copies and distributed among the partners and to industry and academia. Feedback from industry revealed that they use the handbook on a regular basis during day to day business.

A number of students and academic personnel was put in contact with industry partners where they were able to get an insight on the industry demands and requirements. This helped academia to further understand the needs of the industry and pave the path for further advances and research within wind energy. Similarly, the industry was able to get an insight where the academia is heading and what to expect in the coming years.

During the project, the NGIR reports and photo-card has been developed. In close contact with the needs of the WTO, the reports have a uniform visual identity and approach, where they communicate in a generalized and easy-to-understand way. The NGIR reports secure a specific standard of inspecting and documenting blade damages and repairs, and are at the same time easy to use for service providers.

During the project the X-Stiffener technology was developed from patent to a functioning product. The development process went through different stages. During each development stage different features were tested, validated and/or improved. This required a large number of sub-component testing at DTU, see examples in Figure 120 & Figure 121 below.



Figure 120 – Component testing of initial prototype



Figure 121 – Component testing of final prototype

The final prototype, see Figure 123, as well as installation method was tested in a small sub-component test, which showed that the product could withstand the required loads. After this, a small number of prototypes was manufactured and installed in the 15m blade section for further testing (See Figure 122). The final prototype has been manufactured from machining or 3D-printing, however each component has been designed with rapid prototyping in mind for cost efficiency.



Figure 122 – Installation of X-Stiffener in 15m section



Figure 123 – Final prototype

The large scale test of the 15m blade section was developed at DTU Mechanical with the purpose of introducing torsional loads to the blade section and to show the effect of the developed X-Stiffener prototype. A new test rig and load introduction method was developed. The load application system was developed to be able to introduce both combined edgewise and torsional loads and pure torsional load. The aim of the large-scale testing was to apply the loads in order to introduce CSSD and to verify the effects of the X-Stiffener prototype when installed in the blade. Results showed that the CSSD was reduced significantly by installing the X-Stiffener. Furthermore, the numerical FEM studies of the CSSD matched very well with the measurements from the large scale test.

During the project, the three wind turbine owners within the project, E.On, Vattenfall and DONG Energy took initiative to form a working-group called Nordic Blade Group. The collaboration has now expanded to consist of 20 European wind turbine owners. The group has only focus on blades and in this project the focus has mainly been on full-scale testing and standardization. During the project a number of workshops and seminars have also been held by the research institutions and Bladena. At DTU Mechanical one with focus on full-scale testing which also had participants from all five European blade test centres, certification bodies, DNV GL, DEWI OCC and manufactures e.g. Siemens and Envision. One was held by DTU Wind with focus on loads and aerodynamic. Another was held by AAU Aalborg on reliability and cost. And finally one by AAU Esbjerg on FEM and structural theory.

Next step towards commercialization of the X-Stiffener technology

During the time the LEX project was running, Bladena was involved in a commercial project where the X-Stiffener technology was used. A 60m blade range with a large flat-back design developed cracks during the final stages of design, in the full-scale test facility. A Root-Cause

analysis carried out by Bladena identified the cross-sectional shear distortion phenomenon as the root-cause of the cracks.

FEM simulations and full-scale test measurements performed on the commercial 60m blade range confirmed the scaling studies carried out within the LEX project where it was found that large blades with a large flat-back design have an increased cross-sectional shear distortion magnitude. In the 60m blade range case, the CSSD lead to blade failure during the full-scale test. Extensive FEM studies, subcomponent and full-scale testing were carried out in order to address this issue. In Figure 124, a snapshot from the commercial sub-component testing is illustrated.



Figure 124: Sub-component test of the rear box of the 60m blade range with the X-Stiffener technology.

This commercial reference was a good opportunity to validate the usage of the X-Stiffener technology in large blades, thus confirming the assumptions taken within the LEX project.

Next step towards commercialisation is to have the X-Stiffener technology installed in a large turbine with 60m + blades. Bladena together with a European partner applied for a EU-DemoWind project where a 7MW offshore turbine with 83,5m blades. Hopefully this project will be accepted by EU+EUDP, so the next important steps can be made towards commercialisation.

References

- [1]. Larsen TJ, Aagaard Madsen H, Larsen GC, Hansen KS. Validation of the dynamic wake meander model for loads and power production in the Egmond aan Zee wind farm. *Wind Energy*. 2013;16(4):605-624. 10.1002/we.
- [2]. Larsen TJ, Larsen GC, Aagaard Madsen H, Petersen SM. Wake effects above rated wind speed. An overlooked contributor to high loads in wind farms. In *Scientific Proceedings. EWEA Annual Conference and Exhibition 2015*. European Wind Energy Association (EWEA). 2015. p. 95-99.
- [3]. Luis Alberto Gonzales Seabra. Life time equivalent fatigue load analysis of a SSP 34m blade. DTU Wind Energy Report-1. August 2014
- [4]. Pedersen J. T., 1990, "Kinematic Nonlinear Finite Element Model of a Horizontal Axis Wind Turbine, part 1", Risoe National Laboratory
- [5]. Pedersen J. T., 1990, "Kinematic Nonlinear Finite Element Model of a Horizontal Axis Wind Turbine, part 2", Risoe National Laboratory
- [6]. Taeseong Kim, Anders M. Hansen, Kim Branner. Development of an anisotropic beam finite element for composite wind turbine blades in multibody system. *Renewable Energy* 59 (2013)
- [7]. Blasques, J. P., Bitsche, R. D., Fedorov, V., & Lazarov, B. (2015). Accuracy of an efficient framework for structural analysis of wind turbine blades. *Wind Energy*. doi:10.1002/we.1939
- [8]. Larsen T, Hansen A. How 2 HAWC2, the user's manual. Denmark. Forskningscenter Risø. Risø-R, Risø National Laboratory, 2007
- [9]. Bak C, Zahle F, Bitsche R, Kim T, Yde A, Henriksen LC, Natarajan A, Hansen M. Description of the DTU 10 MW reference wind turbine. *Wind Energy* 2014; To be accepted.
- [10]. The DTU 10MW reference wind turbine data repository. <http://dtu-10mw-rwt.vindenergi.dtu.dk>. 13.
- [11]. EDP renewables offline turbine database, August 2013
- [12]. Dinwoodie, Iain Allan; Endrerud, Ole-Erik; Hofmann, Matthias; Martin, Rebecca; Bakken Sperstad, Iver. *Wind Engineering*, Vol. 39, No. 1, 01.02.2015, pp. 1-14.
- [13]. NORCOWE Reference Wind Farm: www.norcowe.no
- [14]. F. Mølholt Jensen. K. Branner, 2013. *Advances in wind turbine blade design and materials*, Chapter 1.
- [15]. F. Mølholt Jensen, J. Dalsgaard Sørensen, M. McGugan, J. Plauborg, C. Berggreen, A. Buliga, L. Damkilde, T. Juul Larsen, L. Egedal Kirchhoff, S. Horn Petersen, R. Kirt, P. Munez de Felipe, 2014, "Torsional Stiffening of Wind Turbine Blades – Mitigating leading edge damages"
- [16]. A. Buliga, 2016, "SSP34 blade – Support to large sub-component test", *Bladena*
- [17]. A. Buliga, 2016, "SSP 15m measurement plan V.3", *Bladena*
- [18]. A.M.Hansen, 2007, "Detailed Nacelle Dynamics", In: *Research in Aeroelasticity EFP-2006*, pp. 91-100, Risoe-R-1611(EN), Risoe National Lab. NORCOWE Reference Wind Farm: www.norcowe.no
- [19]. A.M.Hansen, 2016, "Super elements in HAWC2 based on general 3D FEM models", DTU Wind Energy Report E-0127, Department of Wind Energy, DTU.
- [20]. A.M.Hansen and T.J.Larsen, 2009, "Gear Dynamics", In: *Research in Aeroelasticity EFP-2007-II*, pp. 134-142, Risoe-R-1698(EN), Risoe National Lab. EDP renewables offline turbine database, August 2013

Appendix A: Additional findings and papers

A new approach regarding coupling of aero elastic analysis with FEM computations on wind turbine blade calculations has been developed. It is one of the results of WP6,7 and 8 working together. The approach is a method of overcoming the shortages of certification bodies rules by utilizing the available tools in a smart way.

In summary it consists of a number of steps to follow when a blade is designed:

1. Structural properties are extracted from a detailed FEM model of a blade and exported in a format that can be used for aero elastic analysis.
2. A number of standard aero elastic analyses are performed.
3. Key analyses cases are picked from the ones performed at step 2, concerning different loading scenarios of the blade. E.g. parked position, yaw misalignment in high wind, etc. and loads are being generated.
4. Non-linear FEM analyses are performed based on the cases specified at point 3 having as input data generated by the same step 3, e.g. loads.

These steps ensure that key nonlinear aspects of the blade structure are captured in the overall analysis. They were to be missed if the final step, geometrically non-linear FEM analysis, was not performed.

The overall numerical process should be seen as an update by adding the final extra step.

Appendix B: Workshops and seminars during the LEX project

- Market Barrier and Cost Workshop: October 2013. Location: DTU Mech, Lyngby, arranged by John Dalsgaard Sørensen, AaU-Aalborg and Søren Horn Petersen, BovingHorn: 14 companies attending.
- Workshop on Cost & Reliability and Guide2Defect database: Marts 2014. Location: Fredericia, arranged by John Dalsgaard Sørensen, AaU Aalborg and Søren Horn Petersen.
- Three workshops on Guide2Defect, Marts 2014. Arranged by Søren Horn Petersen, BovingHorn.
- Workshop on Loads and Aerodynamics: August 2014. Location: DTU Wind, Roskilde, arranged by Torben J. Larsen, DTU Wind.
- FEM Workshop: December 2014, Location: Ringsted, arranged by Lars Damkilde, AaU Esbjerg.
- Test and Standardization Seminar: June 2015. Location: DTU Mechanical, Lyngby, arranged by Find Mølholt Jensen, Bladena. - 22 companies were attending representing the whole value chain.
- FEM Workshop: June 2016. Location: Ringsted, arranged by Pedro Muñoz de Felipe, AeroBlade and Find Mølholt Jensen, Bladena.

In addition to the above listed workshops and seminars, a large number of meetings between partners and work packages has taken place.

Appendix C: FEM modelling and analysis

FEM approach

The FEM approach in this phase of the project is to study the principle rather than actual facts. This is due to the multiple assumptions that needs to be taken into account and the lack of aeroelastic simulations. The V100 FEM blade model has shown similar behaviour when different series of accelerations were used within the provided data.

Solver

The commercial finite element package MSC software is used for pre-processing and solving of FEM models. MSC Nastran is applied as the solver in all analysis. Using Sol400 advanced problems as non-linear static, normal modes, buckling and transient dynamic analysis can be solved. In this phase of the project non-linear geometric analyses and non-linear transient dynamic analyses were used.

FEM model

MSC Patran together with the Blade Modelling Tool (BMT) are used for pre-processing of the FEM models. The BMT tool is capable of generating accurate geometries of wind turbine blades. The BMT also generates various layout, sandwich panels and adhesive joints. The blade structure and composite panels are modelled with 8-noded layered 3D solid elements.

The BMT tool generates volume geometry according to the blade data. The blades varying profiles are described with points creating a number of cross sections. These sections are connected with splines and geometry can be seen in Figure 125.

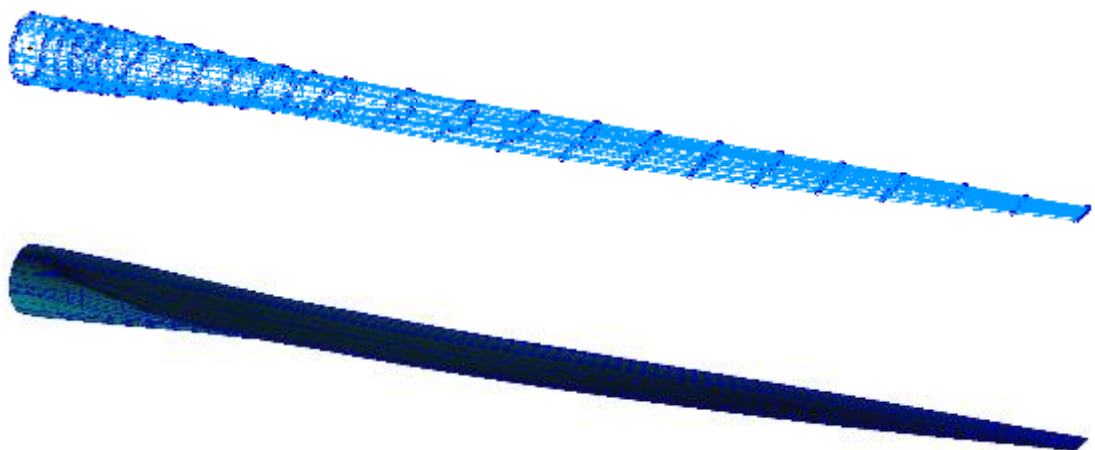


Figure 125: Top: Points and splines that are used to define the blade geometry can be seen. Bottom: The spline “skeleton” has been filled out with geometry (volumes) and are ready to be meshed.

The BMT tool is also used to define the material for each layer throughout the blade creating the composite characteristics and for adjusting and generating a mesh on the blade. The composite layup typically has 15-90 plies though the thickness and composite properties are assigned to continuum elements.

The BMT tool has a number of capabilities that gives the freedom to perform different sensitivity studies in order to fully understand different blade characteristics and the impact on the overall structure, such as:

1. Scaling of the model in three separate dimensions and for each section using well-known and documented scale up algorithms available in the literature.
2. Changing geometry, e.g. of the curvature of the aerodynamic shell.
3. Opening and shortening of the TE panels to create a flat-back.
4. Layup adjustment, e.g. the number of layers, materials and layer thickness.
5. The option of creating flanges and bondlines along the shear webs. This can be used to good effect together with the contact method.

Appendix D: Data from WP5

Strain measurements acquired in the single actuator configuration. The strain gauge readings with and without the retrofitted X-Stiffeners in section A are given in the following:

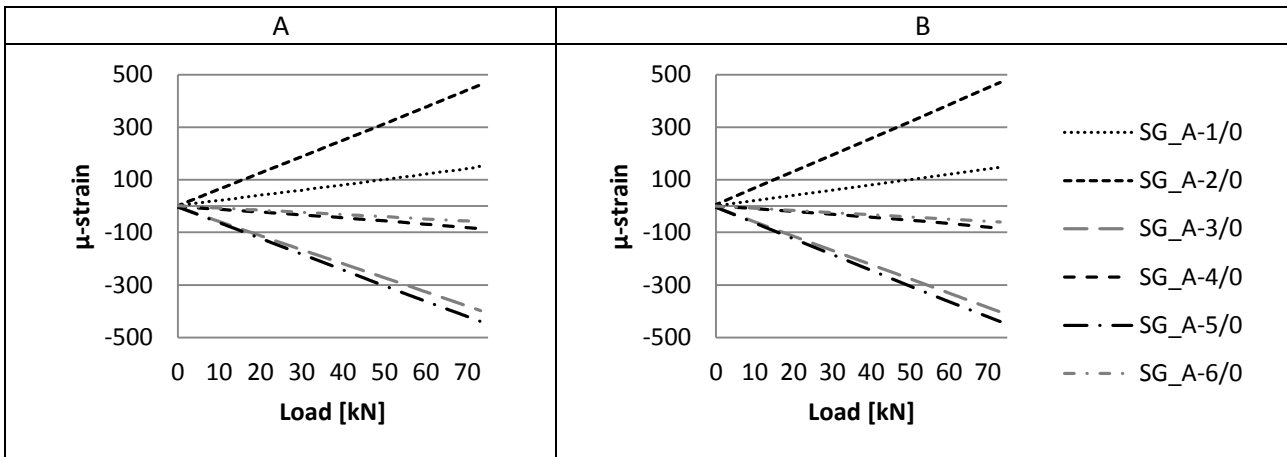


Figure 126: Strain in section A in the 0 degree direction including: a) without X-Stiffener and b) with X-Stiffener

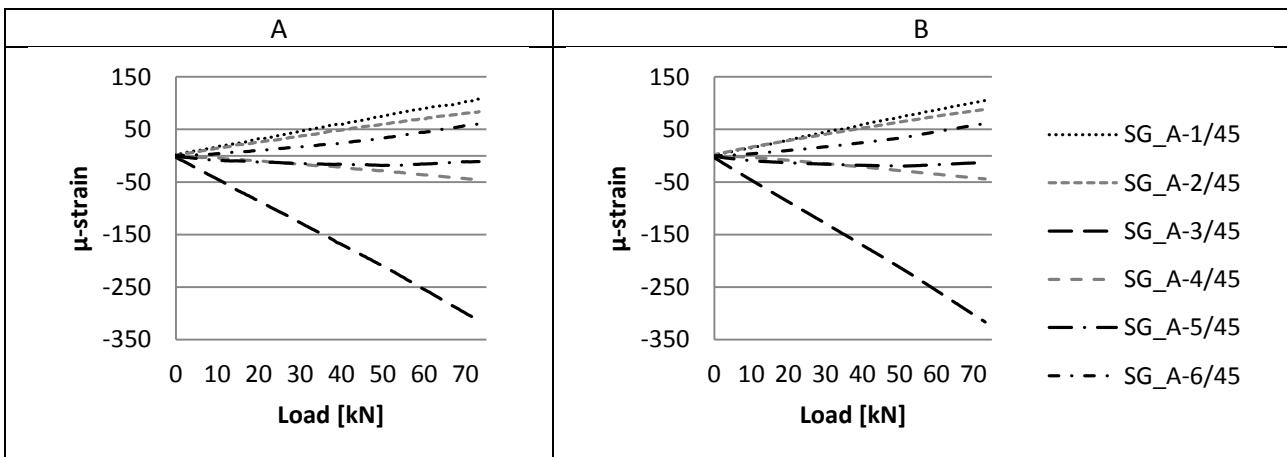
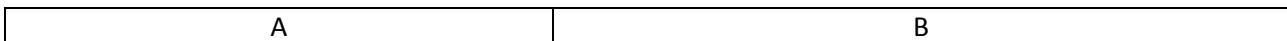


Figure 127: Strain in section A in the 45 degree direction including: a) without X-Stiffener and b) with X-Stiffener



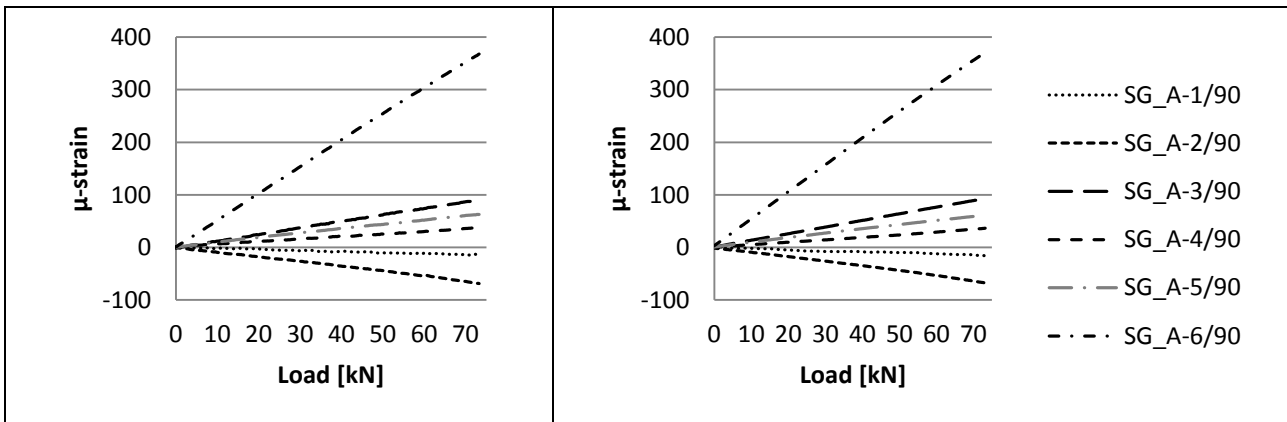


Figure 128: Strain in section A in the 90 degree direction including: a) without X-Stiffener and b) with X-Stiffener

Table 19: Peak strain in section A

SG nr. [-]	Without X-Stiffener		With X-Stiffener		Dev. [%]	Without X-Stiffener		With X-Stiffener		Dev. [%]
	Strain in 0 degree [μ ϵ]		Strain in 45 degree [μ ϵ]			Strain in 90 degree [μ ϵ]				
1	151.0	147.8	2.12	108.2	105.3	2.72	-14.6	-15.9	-8.93	
2	461.9	470.6	-1.89	83.7	88.1	-5.29	-68.8	-67.6	1.81	
3	-397.4	-402.2	-1.21	-314.5	-316.4	-0.60	90.0	92.9	-3.18	
4	-85.7	-85.3	0.44	-45.2	-44.0	2.67	38.2	36.5	4.37	
5	-439.6	-439.5	0.04	-18.6	-19.6	-5.40	63.1	61.3	2.87	
6	-59.6	-60.0	-0.67	61.2	61.2	-0.06	368.0	371.1	-0.86	

The strain gauge readings with and without the retrofitted X-Stiffeners in section B are given in the following:

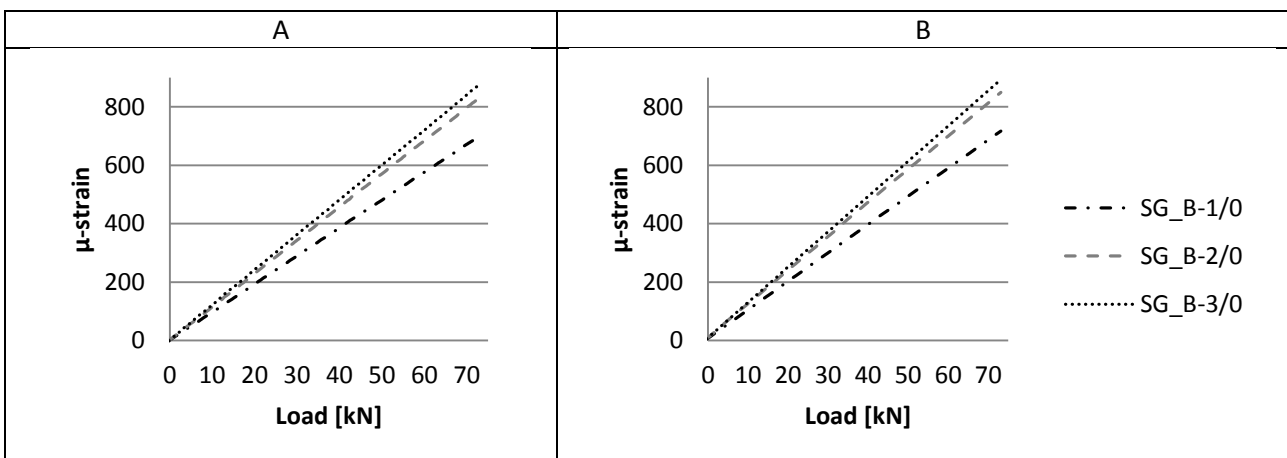


Figure 129: Strain in section B in the 0 degree direction including: a) without X-Stiffener and b) with X-Stiffener

A	B
---	---

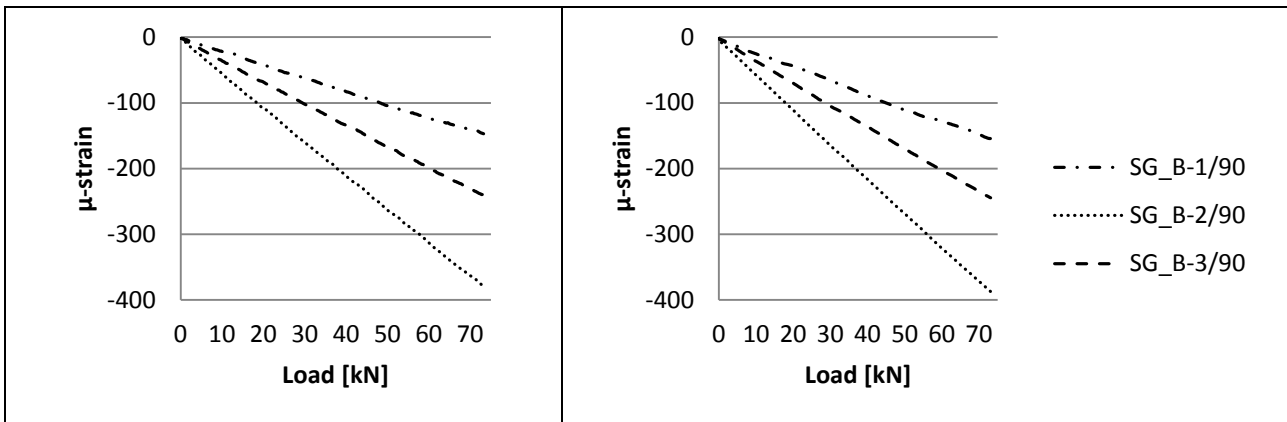


Figure 130: Strain in section B in the 90 degree direction including: a) without X-Stiffener and b) with X-Stiffener

Table 20: Peak strain in section B

	Without X-Stiffener	With X-Stiffener		Without x-stiffener	With x-stiffener	
SG nr. [-]	Strain in 0 degree [μ ϵ]		Dev. [%]	Strain in 90 degree [μ ϵ]		Dev. [%]
1	702.5	717.4	-2.11	-147.1	-154.4	-4.95
2	834.5	850.3	-1.89	-379.0	-387.0	-2.10
3	879.4	893.8	-1.65	-240.5	-244.3	-1.59

The strain gauge readings with and without the retrofitted X-Stiffeners in section C are given in the following:

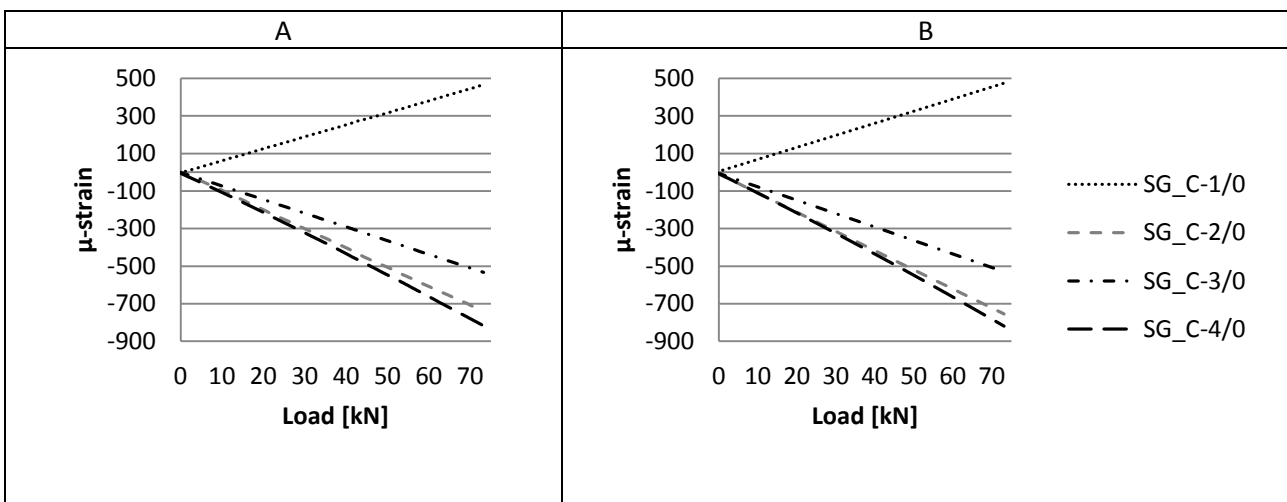


Figure 131: Strain in section C in the 0 degree direction including: a) without X-Stiffener and b) with X-Stiffener

A	B
---	---

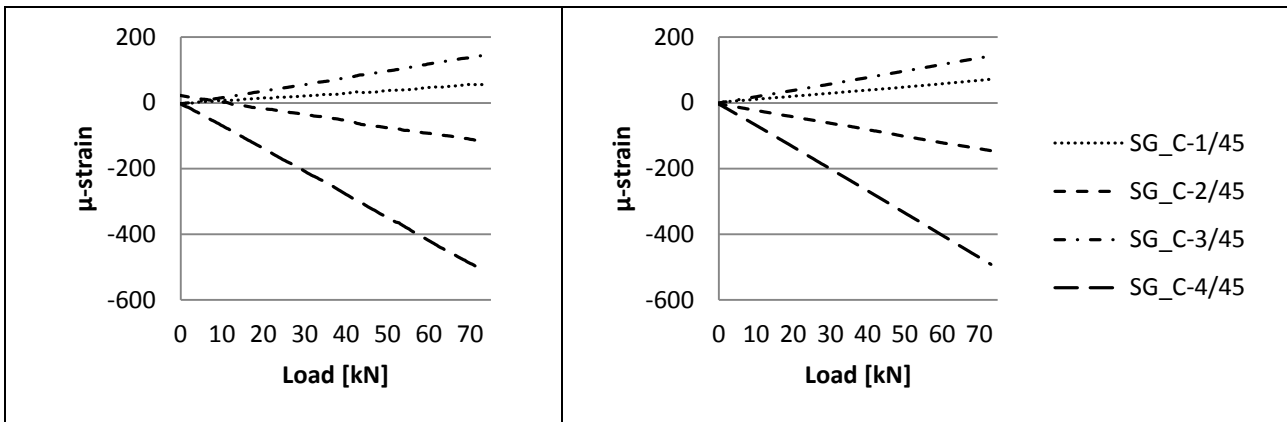


Figure 132: Strain in section C in the 45 degree direction including: a) without X-Stiffener and b) with X-Stiffener

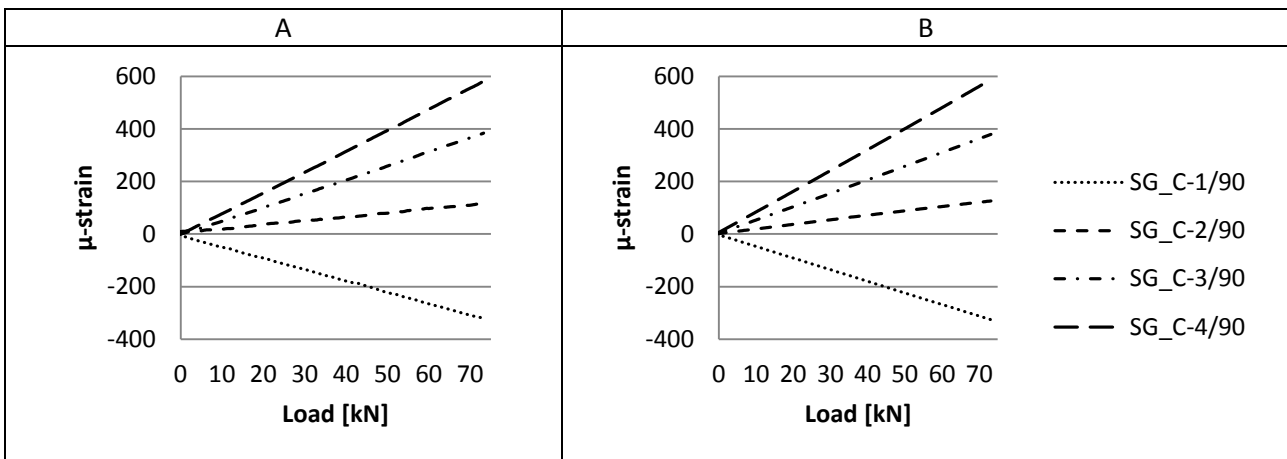


Figure 133: Strain in section C in the 90 degree direction including: a) without X-Stiffener and b) with X-Stiffener

Table 21: Peak strain in section C

SG nr. [-]	Strain in 0 degree [με]		Dev. [%]	Strain in 45 degree [με]		Dev. [%]	Strain in 90 degree [με]		Dev. [%]
	Without X-Stiffener	With X-Stiffener		Without X-Stiffener	With X-Stiffener		Without X-Stiffener	With X-Stiffener	
1	466.6	473.9	-1.56	55.9	71.4	-27.71	-321.4	-326.1	-1.46
2	-742.7	-754.4	-1.58	-119.4	-146.1	-22.35	115.0	125.5	-9.10
3	-533.2	-528.9	0.81	144.9	142.3	1.77	383.7	379.5	1.10
4	-817.0	-819.7	-0.32	-511.1	-491.5	3.84	581.4	588.0	-1.15

Strain measurements acquired in the double actuator configuration. The strain gauge readings with and without the retrofitted X-Stiffeners in section A are given in in the following:

A	B
---	---

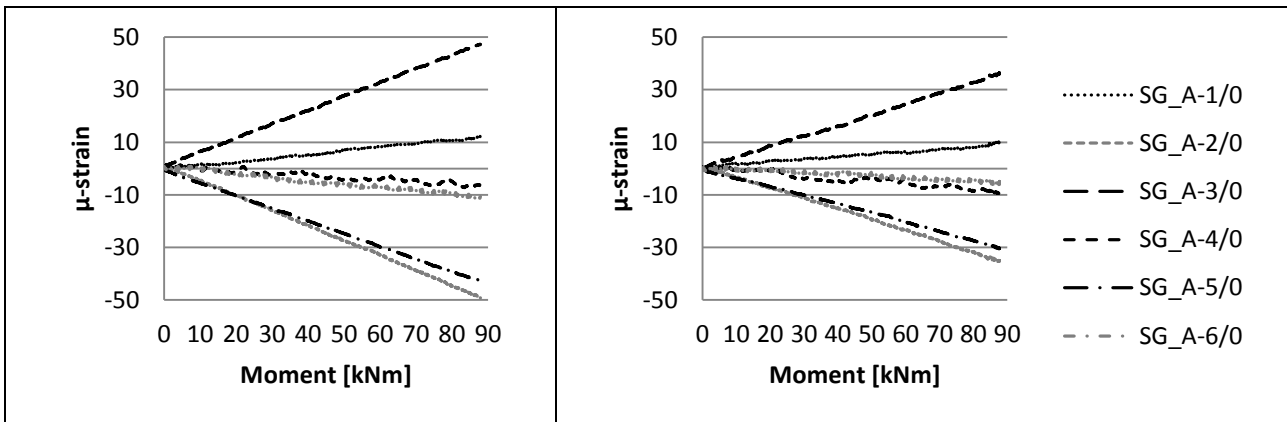


Figure 134: Strain in section A in the 0 degree direction including: a) without X-Stiffener and b) with X-Stiffener

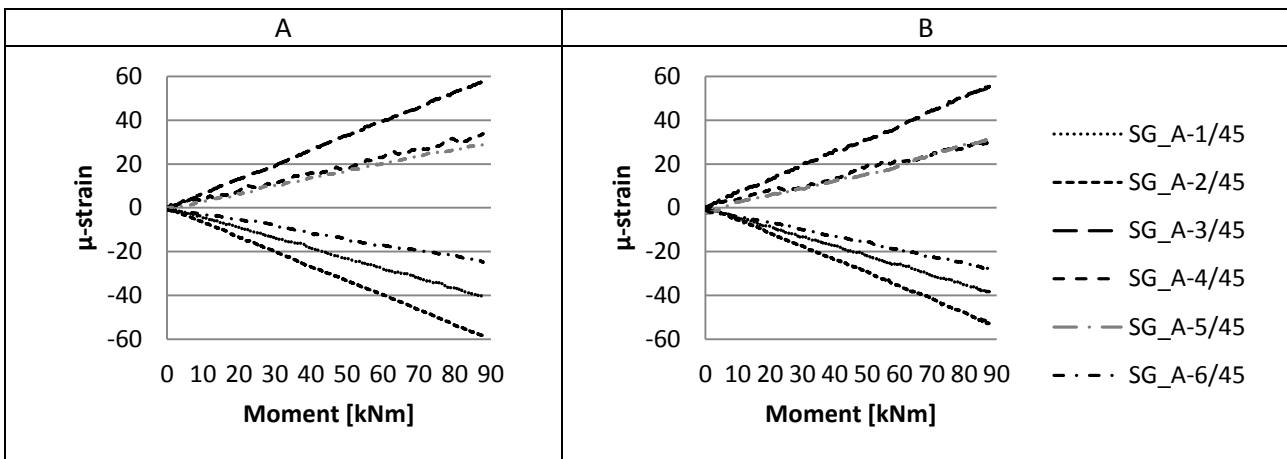


Figure 135: Strain in section A in the 45 degree direction including: a) without X-Stiffener and b) with X-Stiffener

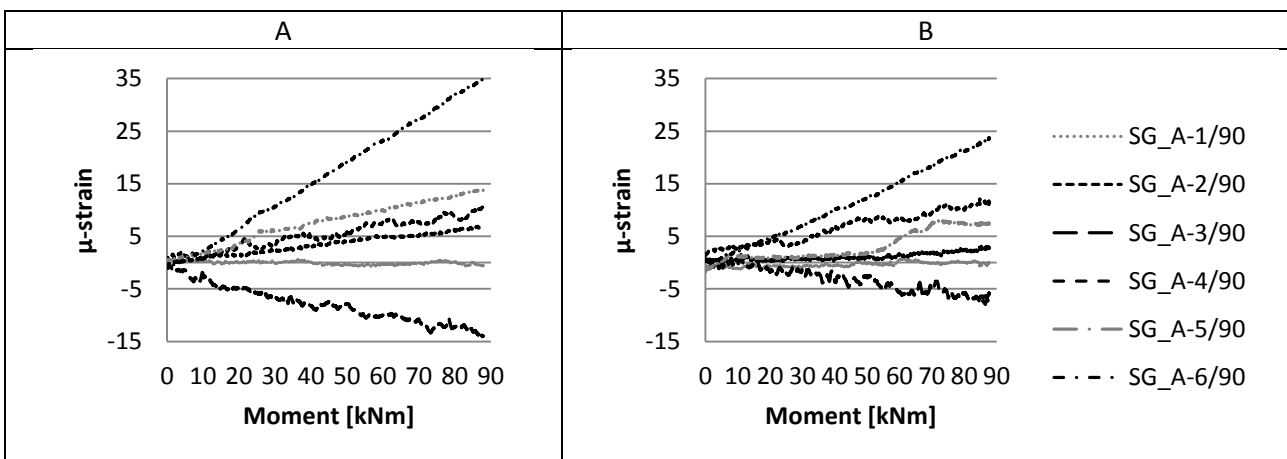


Figure 136: Strain in section A in the 90 degree direction including: a) without X-Stiffener and b) with X-Stiffener

Table 22: Peak strain in section A

	Without X-Stiffener	With X-Stiffener		Without X-Stiffener	With X-Stiffener		Without X-Stiffener	With X-Stiffener	
--	---------------------	------------------	--	---------------------	------------------	--	---------------------	------------------	--

SG nr. [-]	Strain in 0 degree [$\mu\epsilon$]		Dev. [%]	Strain in 45 degree [$\mu\epsilon$]		Dev. [%]	Strain in 90 degree [$\mu\epsilon$]		Dev. [%]
1	12.9	10.4	17.6	-40.7	-38.7	4.89	-0.84	-1.37	-63.5
2	-49.2	-35.5	27.9	-58.4	-52.9	9.37	7.04	3.15	55.2
3	47.3	36.4	23.1	57.7	55.4	3.90	-14.1	-7.97	43.5
4	-7.25	-9.92	-36.5	33.8	30.0	11.2	10.6	12.11	-14.2
5	-42.7	-30.5	28.6	28.8	31.2	-8.52	13.9	8.24	40.8
6	-11.3	-6.38	43.7	-24.9	-28.0	-12.6	34.8	23.7	31.8

The strain gauge readings with and without the retrofitted X-Stiffeners in section B are given in in the following:

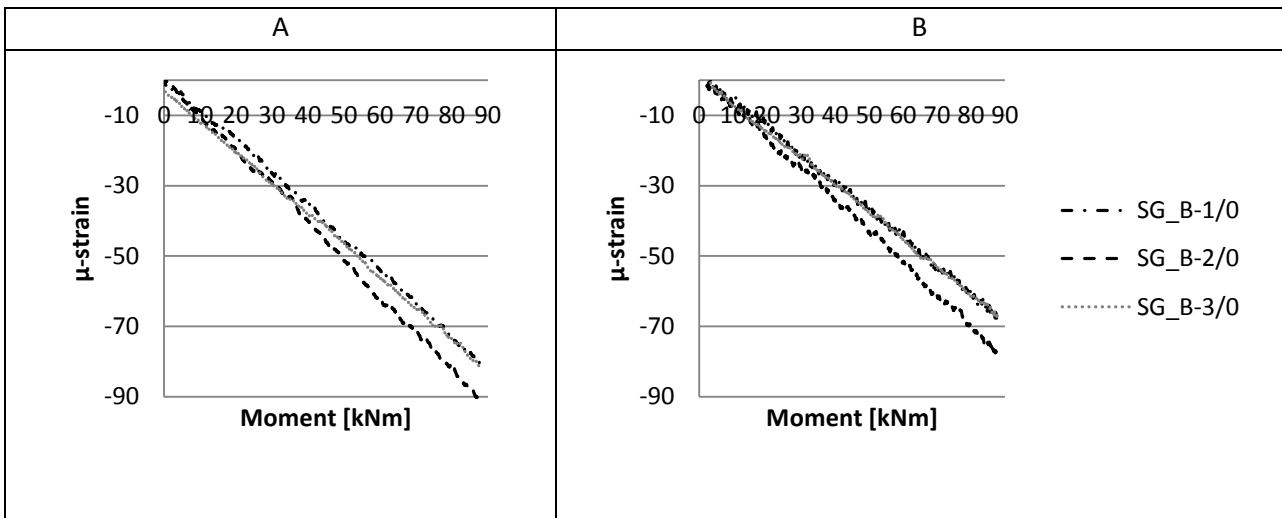


Figure 137: Strain in section B in the 0 degree direction including: a) without X-Stiffener and b) with X-Stiffener

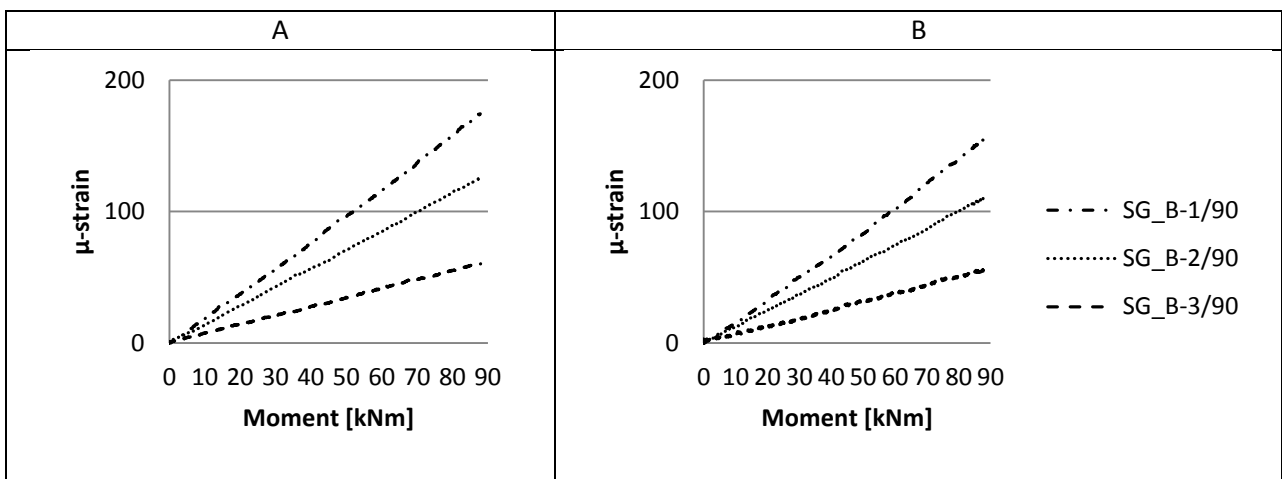


Figure 138: Strain in section B in the 90 degree direction including: a) without X-Stiffener and b) with X-Stiffener

Table 23: Peak strain in section B

SG nr. [-]	Without X-Stiffener	With X-Stiffener	Dev. [%]	Without x-stiffener	With x-stiffener	Dev. [%]
	Strain in 0 degree [$\mu\epsilon$]			Strain in 90 degree [$\mu\epsilon$]		
1	-80.5	-68.3	15.2	174.3	154.8	11.2
2	-91.1	-77.9	14.5	125.4	110.6	11.8
3	81.7	-67.3	17.6	60.3	56.5	6.30

The strain gauge readings with and without the retrofitted X-Stiffeners in section C are given in in the following:

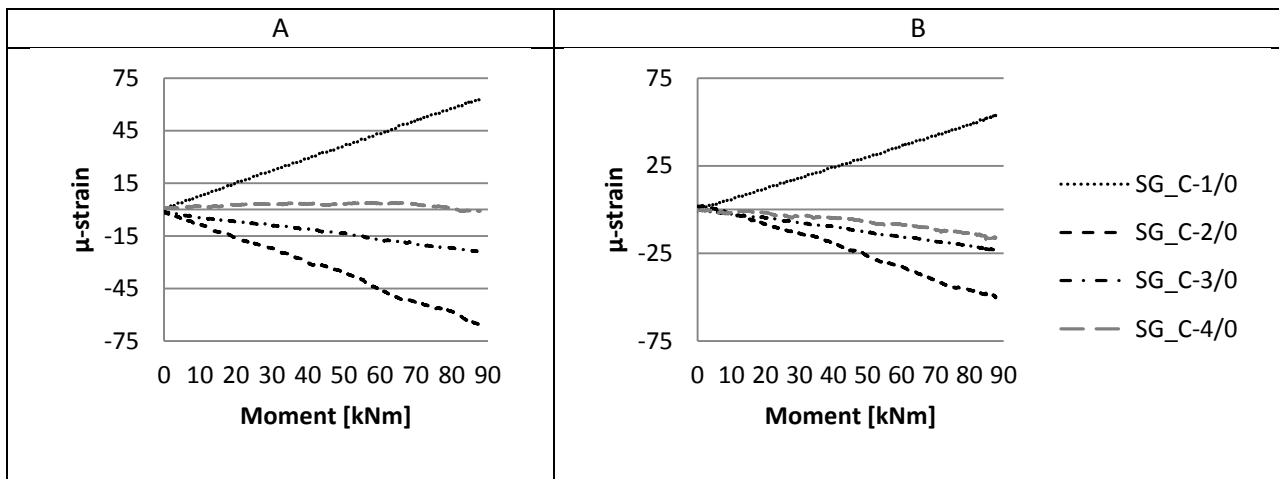


Figure 139: Strain in section C in the 0 degree direction including: a) without X-Stiffener and b) with X-Stiffener

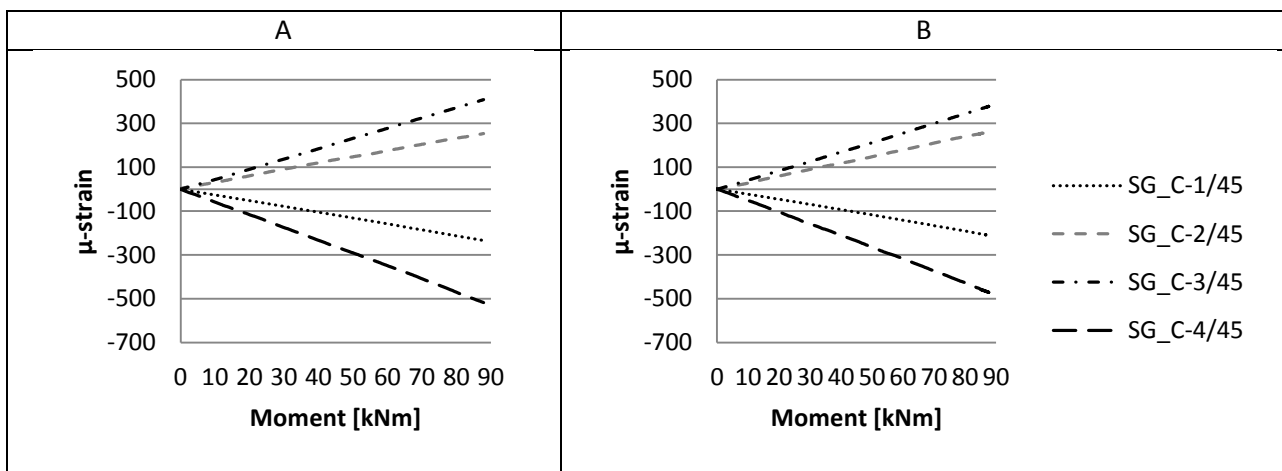


Figure 140: Strain in section C in the 45 degree direction including: a) without X-Stiffener and b) with X-Stiffener

A	B
---	---

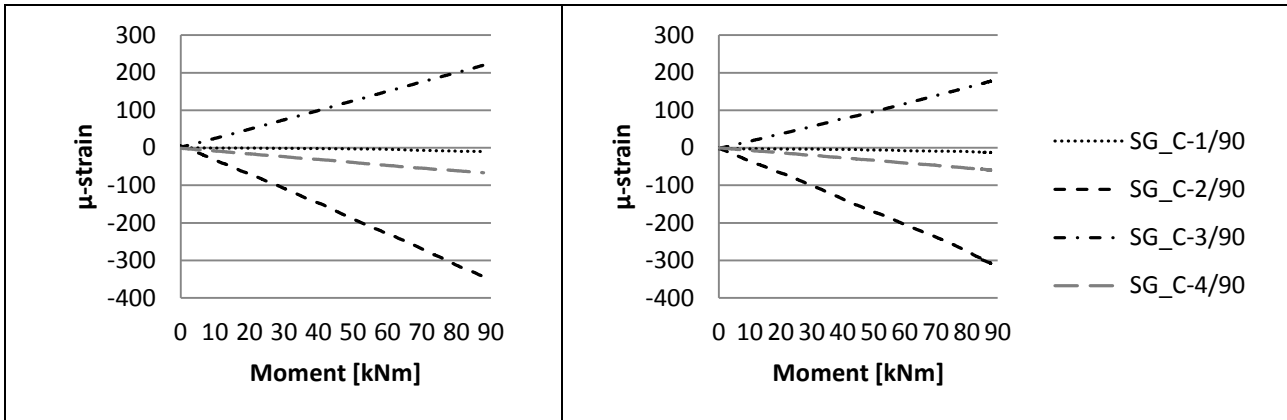


Figure 141: Strain in section C in the 90 degree direction including: a) without X-Stiffener and b) with X-Stiffener

Table 24: Peak strain in section C

	Without X-Stiffener	With X-Stiffener		Without X-Stiffener	With X-Stiffener		Without X-Stiffener	With X-Stiffener	
SG nr. [-]	Strain in 0 degree [$\mu\epsilon$]		Dev. [%]	Strain in 45 degree [$\mu\epsilon$]		Dev. [%]	Strain in 90 degree [$\mu\epsilon$]		Dev. [%]
1	63.2	53.9	14.8	-234.2	-211.1	9.84	-9.83	-12.7	-29.5
2	-65.6	-50.4	23.3	253.7	261.8	-3.19	-307.4	-307.4	10.4
3	-24.6	-23.1	5.97	408.5	378.8	7.26	177.6	177.6	19.3
4	4.20	-16.6	499.5	-517.5	-471.3	8.92	-59.5	-59.5	10.6

Appendix E: Data from WP5 part 2

DIC measurements acquired in the single actuator configuration. For zone 1 the following data is acquired:

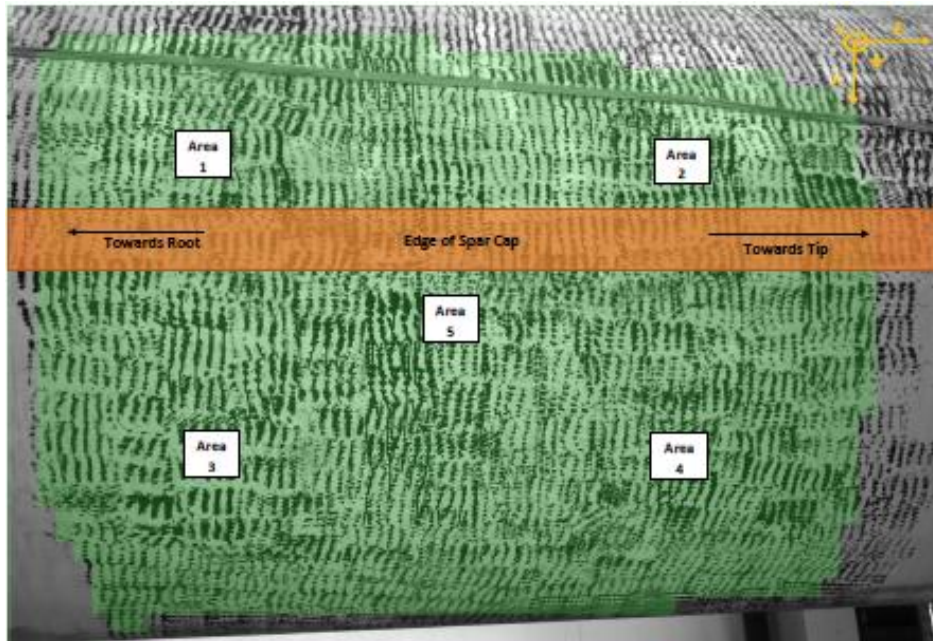


Figure 142: Location and labelling of the full field measurement in zone 1

Out-of-plane deformations in zone 1 are presented in Figure 143.

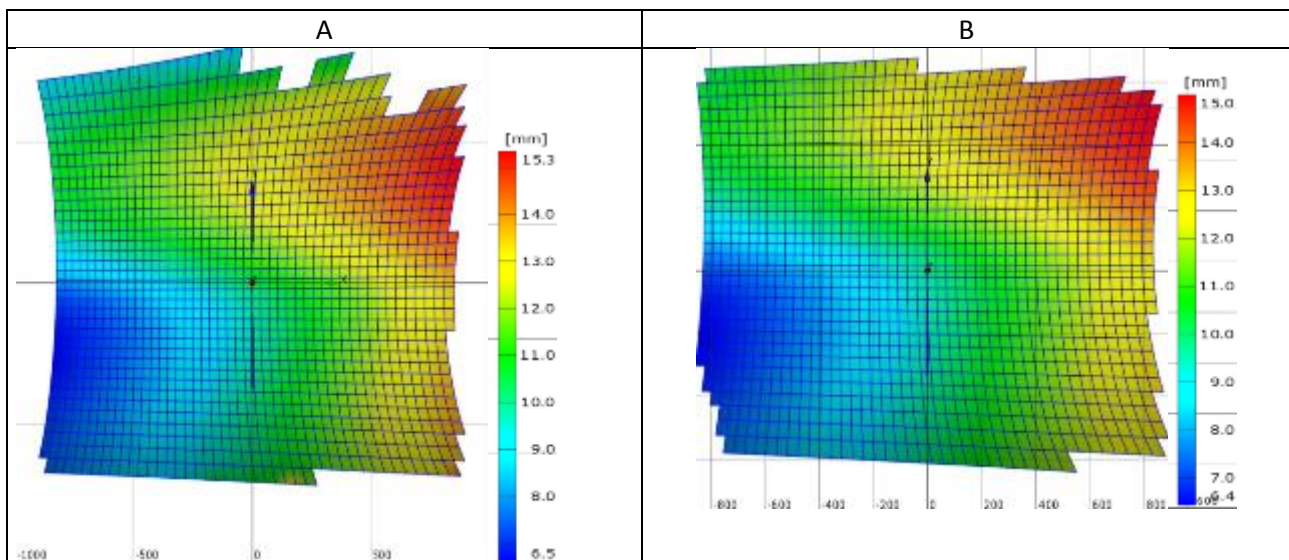


Figure 143: Full field measurement of the out-of-plane deformation: a) without X-Stiffener and b) with X-Stiffener

Table 25: Peak strain in area 1-5 within zone 1

Area nr. [-]	Without X-Stiffener		Dev. [%]	With X-Stiffener		Dev. [%]	Without X-Stiffener		Dev. [%]
	Strain in 0 degree [$\mu\epsilon$]	Strain in 45 degree [$\mu\epsilon$]		Strain in 0 degree [$\mu\epsilon$]	Strain in 45 degree [$\mu\epsilon$]				
1	-184.8	-71.12	61.5	-71.12	-141.6	-130	217.4	217.4	0.00
2	-94.64	-94.64	0.00	-148.6	-146.5	1.41	57.31	57.31	0.00
3	-866.6	-866.6	0.00	-476.9	-476.9	0.00	310.8	310.8	0.00
4	-641.4	-641.4	0.00	-352.8	-352.8	0.00	223.1	223.1	0.00
5	-516.1	-516.3	-0.04	-141.6	-184.8	-30.5	378.7	378.7	0.00

Strain gauge measurements in area 1-5 as a function of load is presented in Figure 144 - Figure 146.

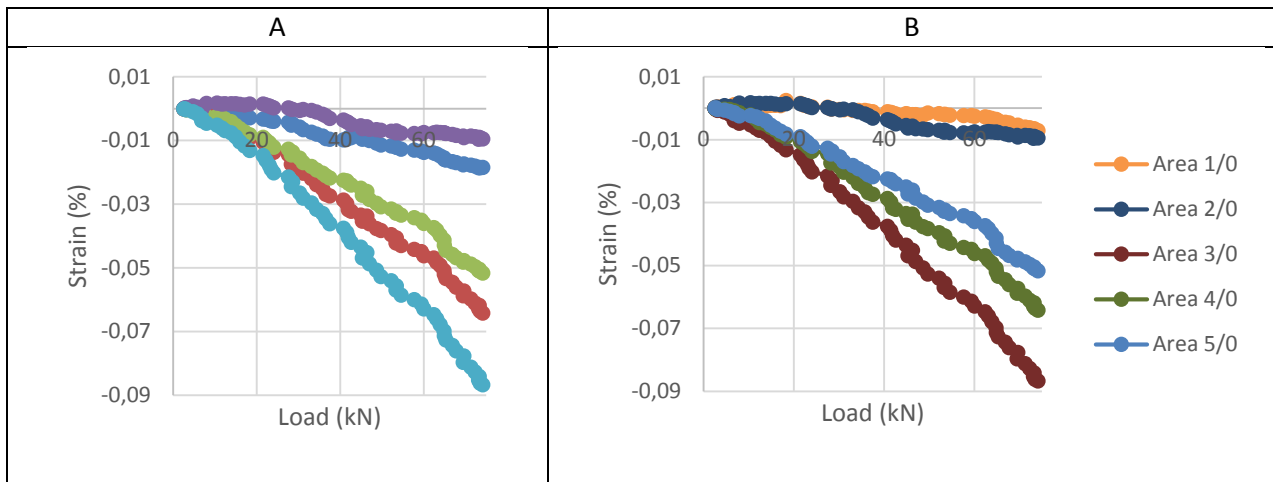


Figure 144: Strain in the 0 degree direction including: a) without X-Stiffener and b) with X-Stiffener

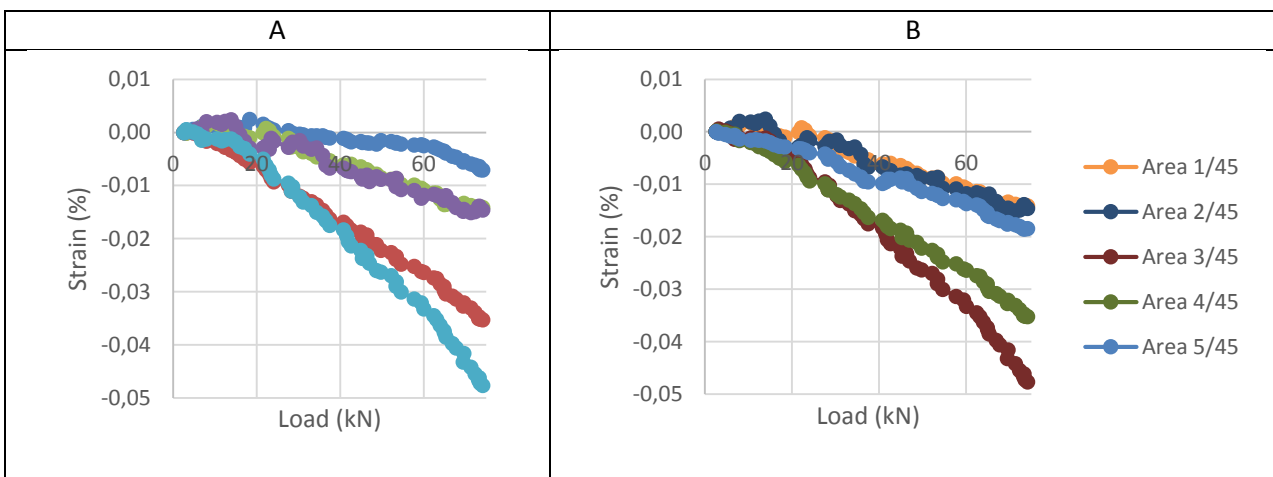


Figure 145: Strain in the 45 degree direction including: a) without X-Stiffener and b) with X-Stiffener

A	B
---	---

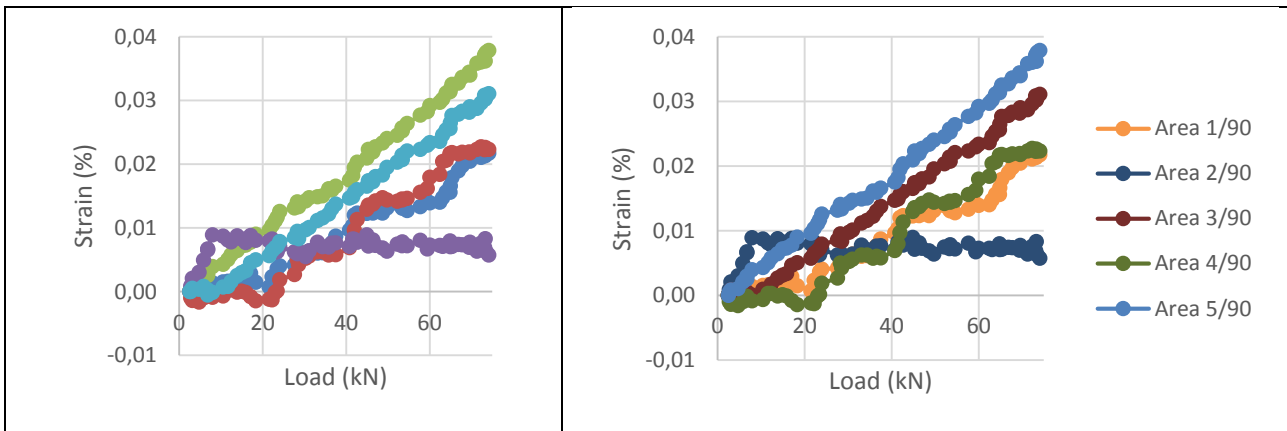


Figure 146: figure x: Strain in the 90 degree direction including: a) without X-Stiffener and b) with X-Stiffener

For zone 2 the following data is acquired.

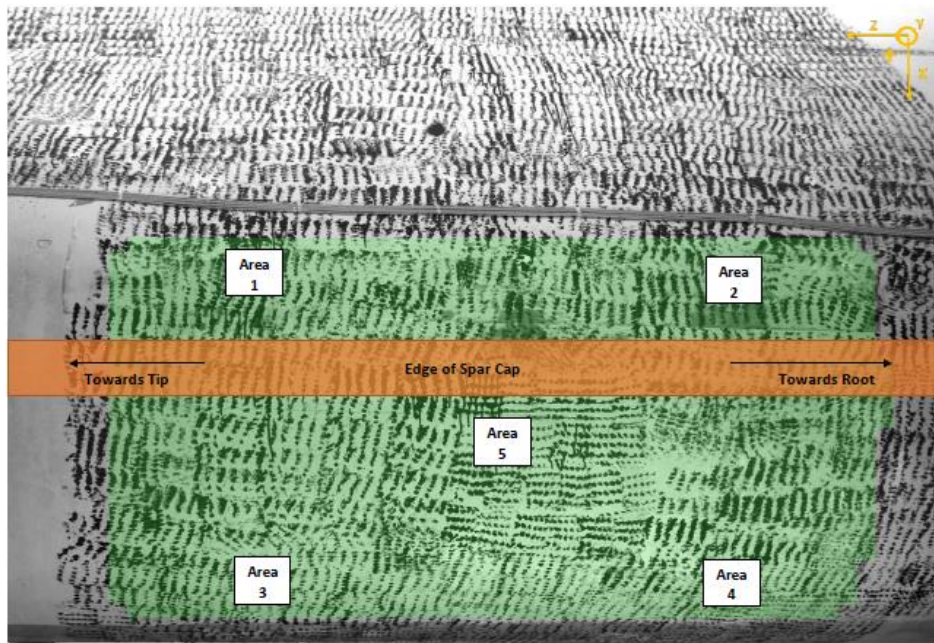


Figure 147: Location and labelling of the full field measurement in zone 2

Out-of-plane deformations in zone 2 are presented in Figure 148.

A	B
---	---

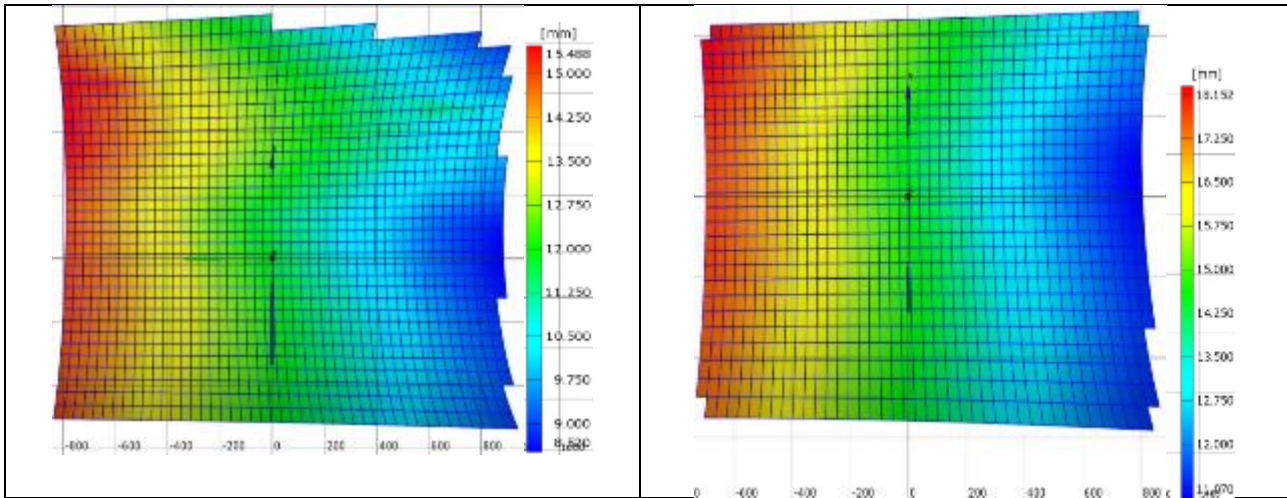


Figure 148: Full field measurement of the out-of-plane deformation: a) without X-Stiffener and b) with X-Stiffener

Table 26: Peak strain in area 1-5 within zone 2

Area nr. [-]	Without X-Stiffener		With X-Stiffener		Dev. [%]	Without X-Stiffener		With X-Stiffener		Dev. [%]
	Strain in 0 degree [$\mu\epsilon$]	Strain in 45 degree [$\mu\epsilon$]	Strain in 0 degree [$\mu\epsilon$]	Strain in 45 degree [$\mu\epsilon$]		Strain in 0 degree [$\mu\epsilon$]	Strain in 45 degree [$\mu\epsilon$]			
1	-457.3	-415.3	9.18	263.6	-49.29	81.3	280.1	240.7	14.1	
2	-360.8	-862.8	-139	165.9	20.45	87.7	576.7	343.3	40.5	
3	-943.4	-650.2	31.1	-334.3	20.27	93.9	300.5	194.6	35.2	
4	-806.7	-640.7	20.6	-167.4	-56.22	66.4	361.9	181.9	49.7	
5	-635.2	-954.6	-50.3	61.64	-143.5	-133	211.8	610.6	-188	

Strain gauge measurements in area 1-5 as a function of load is presented in Figure 149 - Figure 151.

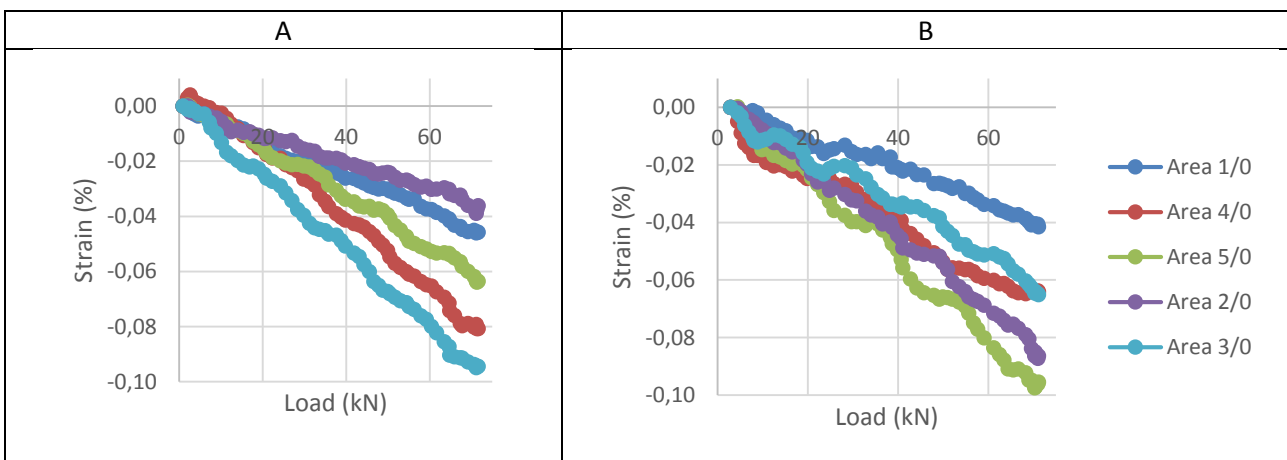


Figure 149: Strain in the 0 degree direction including: a) without X-Stiffener and b) with X-Stiffener

A	B
---	---

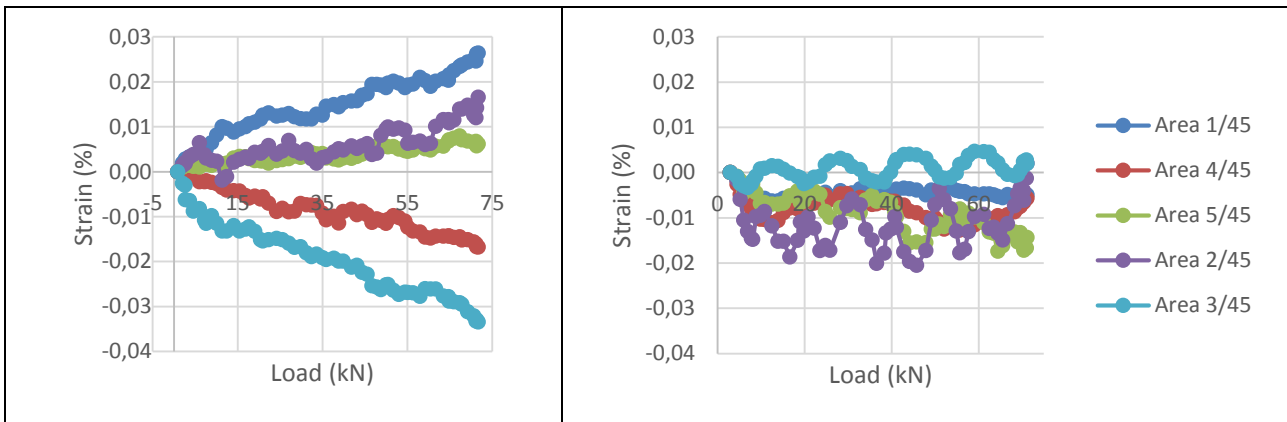


Figure 150: Strain in the 45 degree direction including: a) without X-Stiffener and b) with X-Stiffener

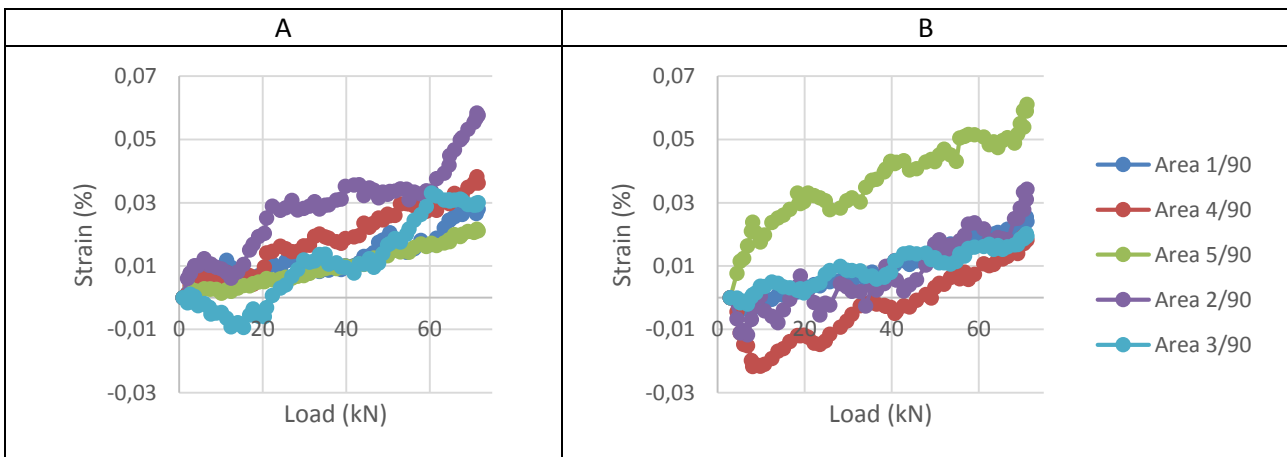


Figure 151: Strain in the 90 degree direction including: a) without X-Stiffener and b) with X-Stiffener

For zone 3 the following data is acquired.

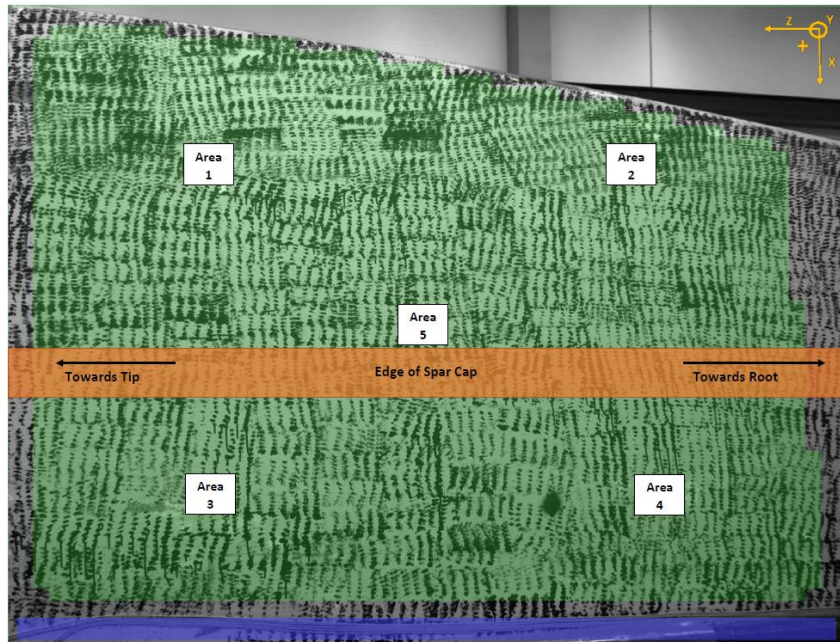


Figure 152: Location and labelling of the full field measurement in zone 3

Out-of-plane deformations in zone 3 are presented in Figure 153.

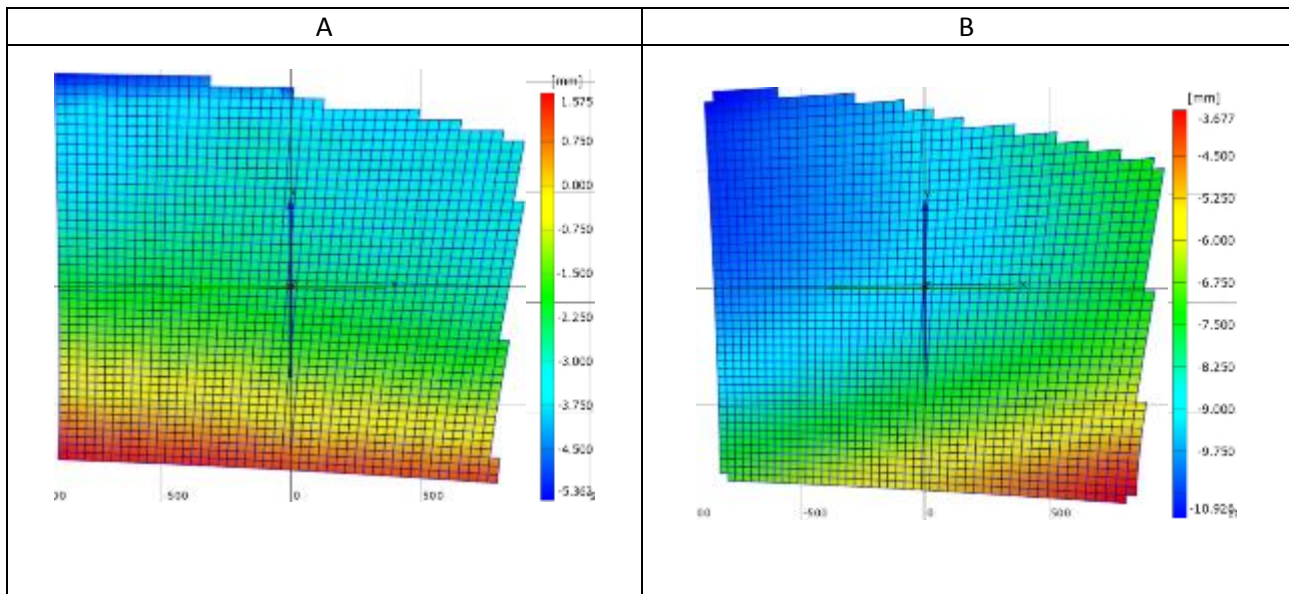


Figure 153: Full field measurement of the out-of-plane deformation: a) without X-Stiffener and b) with X-Stiffener

Table 27: Peak strain in area 1-5 within zone 3

Area nr. [-]	Without X-Stiffener		With X-Stiffener		Without X-Stiffener		With X-Stiffener		Dev. [%]
	Strain in 0 degree [$\mu\epsilon$]	Dev. [%]	Strain in 45 degree [$\mu\epsilon$]	Dev. [%]	Strain in 90 degree [$\mu\epsilon$]	Dev. [%]			
1	526.1	-13.4	208.6	57.1	76.82	-566	596.4	-89.48	-511.3

2	577.1	-40.69	92.9	-47.45	-18.14	61.8	-230.7	-234.2	-1.52
3	83.79	293.5	-250	-23.06	-64.36	-179	-155.9	-388.9	-149
4	22.84	550.6	-	-21.67	-73.10	-237	-259.0	-303.3	-17.1
5	288.2	38.27	86.7	-60.63	13.64	77.5	-512.4	-198.2	61.3

Strain gauge measurements in area 1-5 as a function of load is presented in Figure 154 - Figure 156.

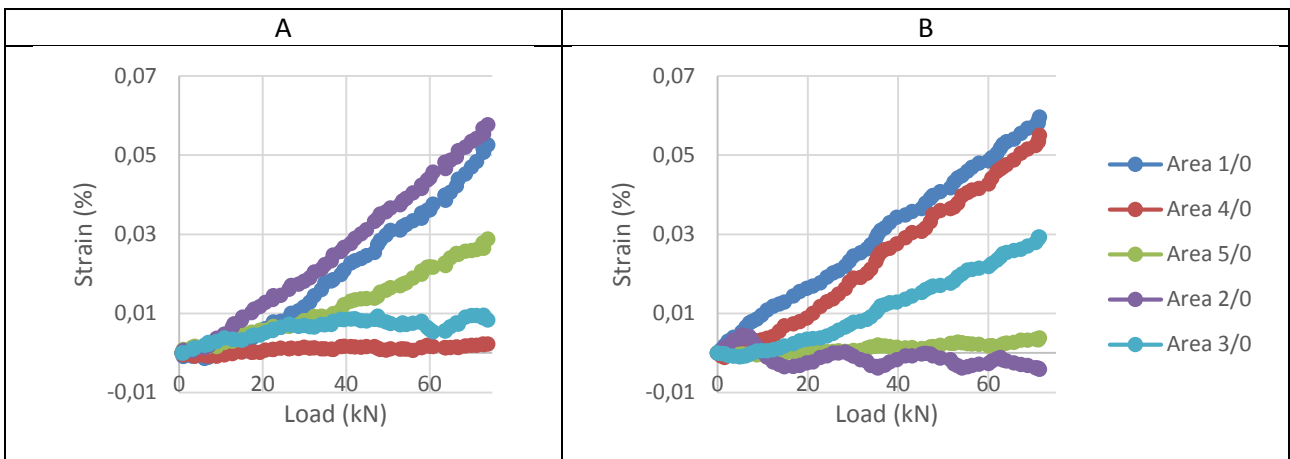


Figure 154: Strain in the 0 degree direction including: a) without X-Stiffener and b) with X-Stiffener

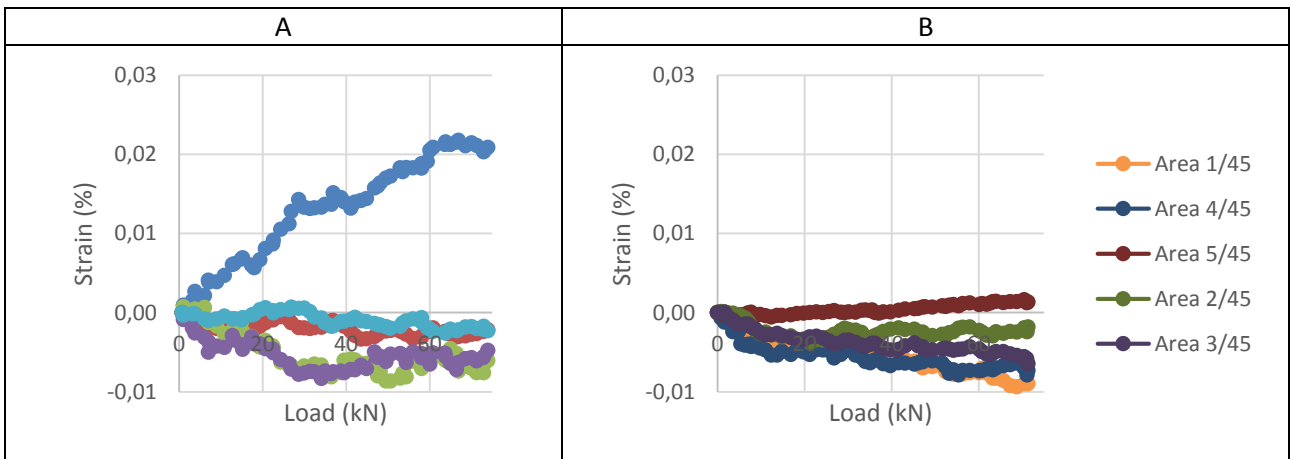
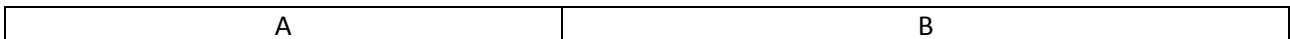


Figure 155: Strain in the 45 degree direction including: a) without X-Stiffener and b) with X-Stiffener



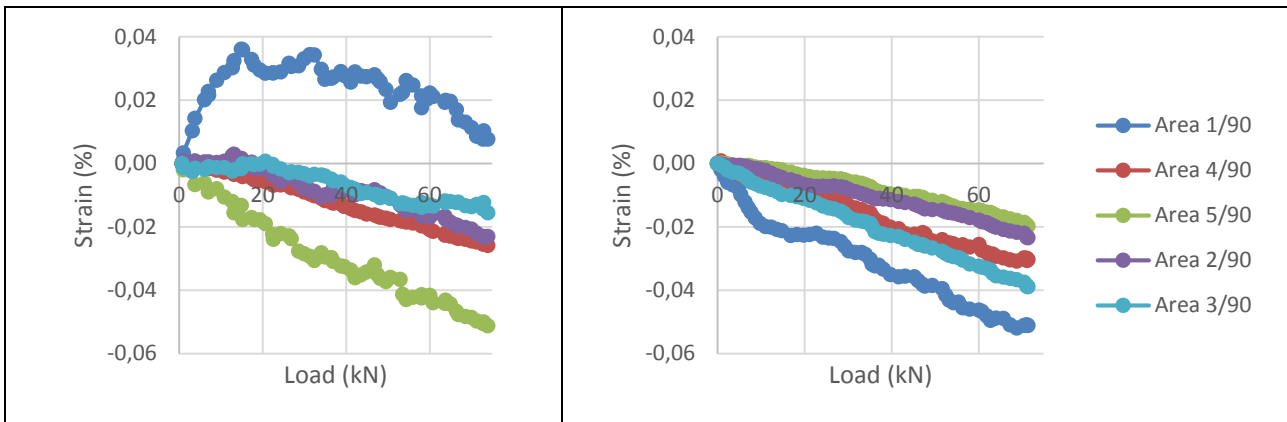


Figure 156: Strain in the 90 degree direction including: a) without X-Stiffener and b) with X-Stiffener

For zone 4 the following data is acquired.

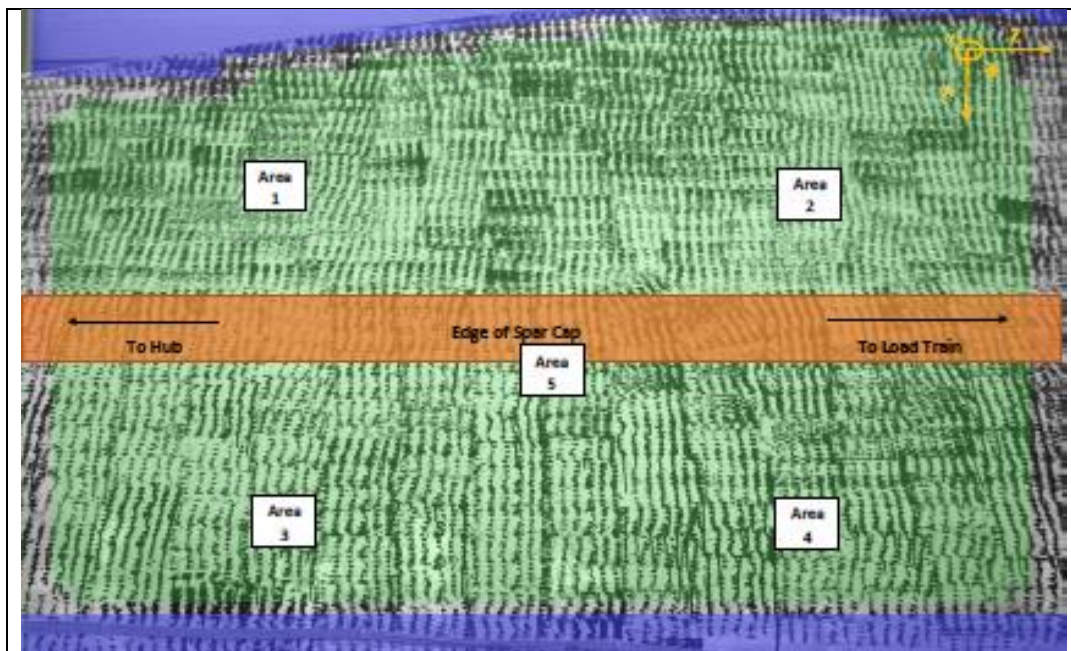
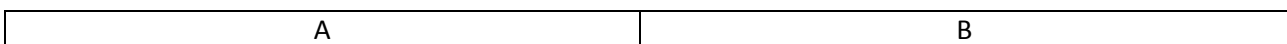


Figure 157: Location and labelling of the full field measurement in zone 4

Out-of-plane deformations in zone 4 are presented in Figure 158.



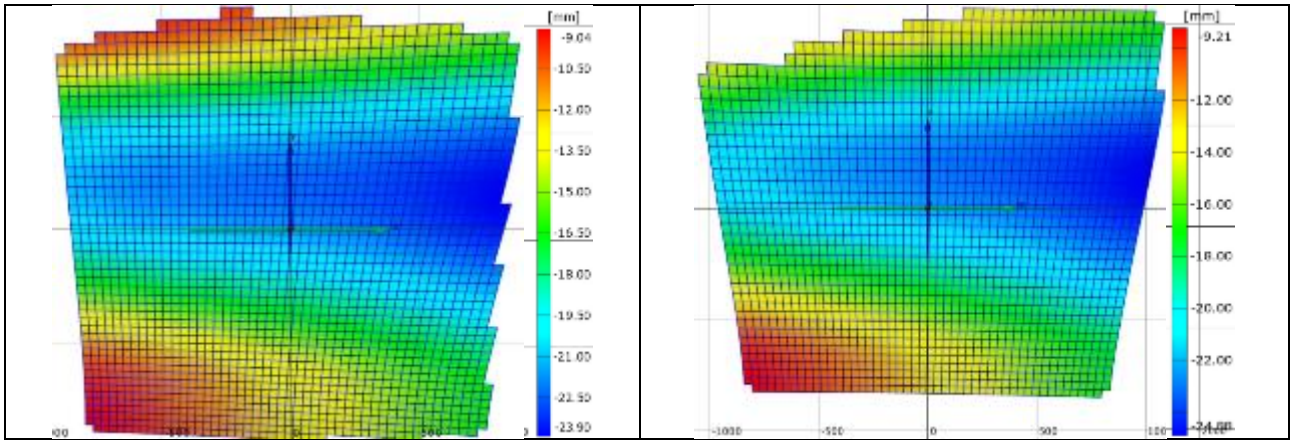


Figure 158: Full field measurement of the out-of-plane deformation: a) without X-Stiffener and b) with X-Stiffener

Table 28: Peak strain in area 1-5 within zone 4

Area nr. [-]	Without X-Stiffener		Dev. [%]	With X-Stiffener		Dev. [%]	Without X-Stiffener		Dev. [%]
	Strain in 0 degree [$\mu\epsilon$]			Strain in 45 degree [$\mu\epsilon$]			Strain in 90 degree [$\mu\epsilon$]		
1	603.1	548.6	9.04	17.66	-311.5	-	-523.1	151.2	71.1
2	544.7	544.9	-0.04	-210.9	-358.4	-69.9	-606.4	-803.0	-32.4
3	278.8	284.8	-2.15	-310.2	-406.6	-31.1	-308.1	-253.6	17.7
4	206.2	-451.4	-119	-342.2	-647.5	-89.2	-307.0	423.1	-37.8
5	454.8	-909.7	-100	-514.2	-329.6	35.9	-1184	-1001	15.5

Strain gauge measurements in area 1-5 as a function of load is presented in figure x-x.

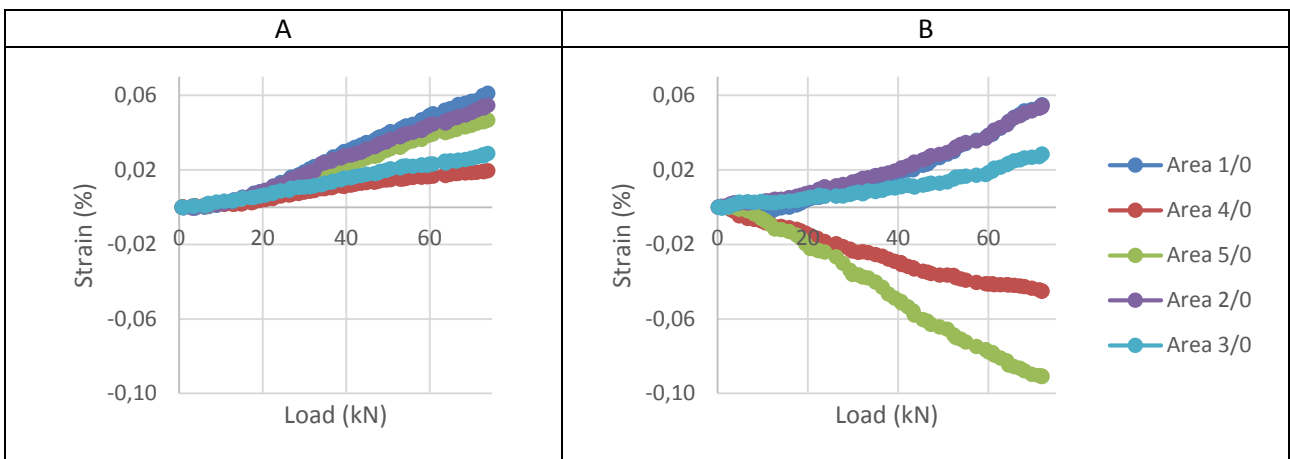


Figure 159: Strain in the 0 degree direction including: a) without X-Stiffener and b) with X-Stiffener

A	B
---	---

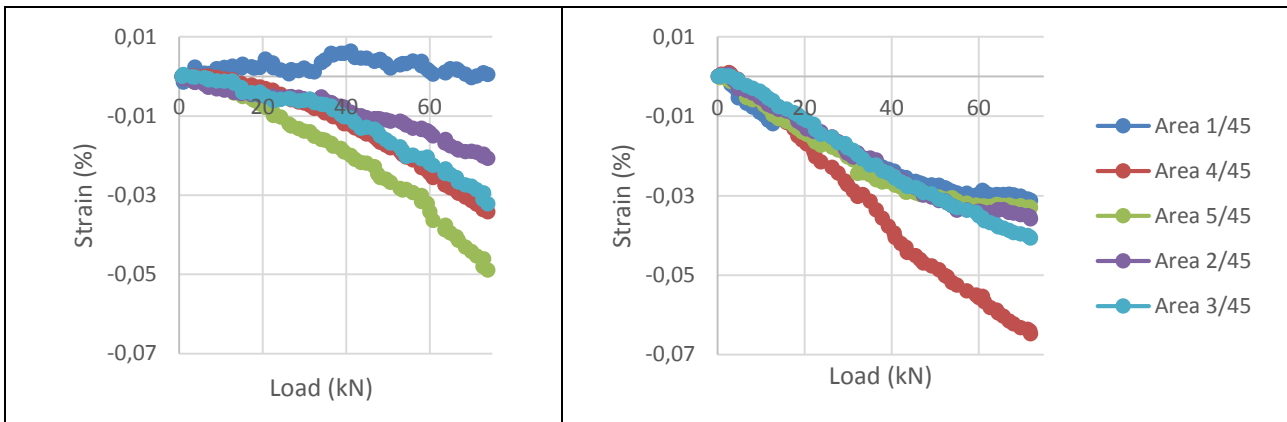


Figure 160: Strain in the 45 degree direction including: a) without X-Stiffener and b) with X-Stiffener

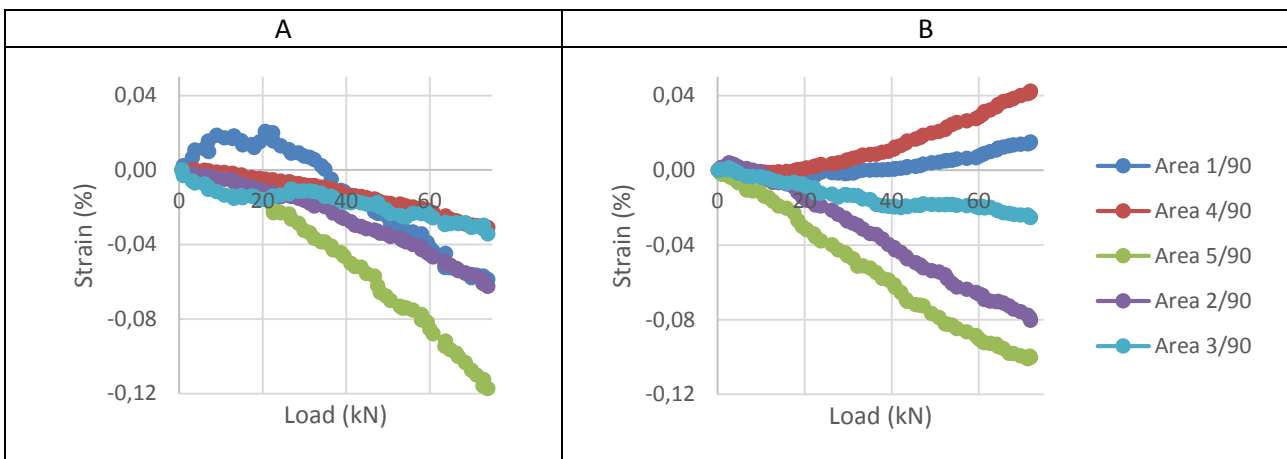


Figure 161: Strain in the 90 degree direction including: a) without X-Stiffener and b) with X-Stiffener

Note: no DIC measurements are acquired in the double actuator configuration.